UNIVERSITY OF READING

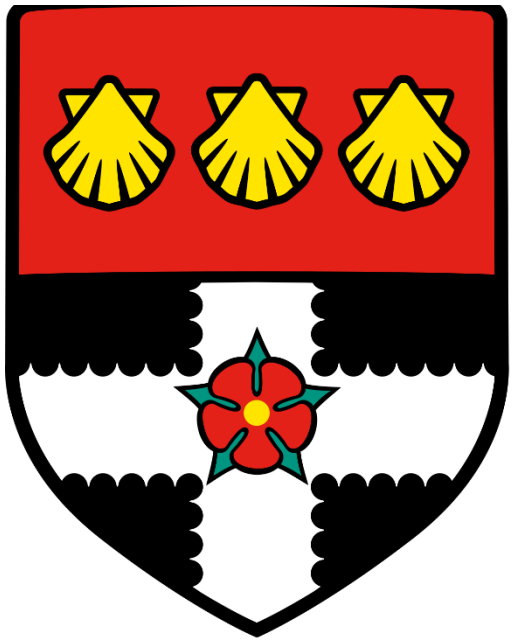

Investigating the role of HSP47 in megakaryocyte and platelet function

A thesis submitted for the degree of Doctor of Philosophy

Gemma Little

School of Biological Sciences

June 2022

Declaration

I confirm that this is my own work and the use of all material from other sources has been properly and fully acknowledged.

Signed: Gemma Little

Date: 6th June 2022

Acknowledgments

Firstly, I would like to thank my supervisor Jon, for the constant support throughout the last four years. Your encouragement is second to none, thank you for being patient and dealing with my constant chattiness.

Chris, you laid the initial foundations for my love of research and platelets and for that I am extremely thankful. I wouldn't have started my PhD in Reading if it wasn't for you, thank you for your support throughout.

Alice and Craig, thank you for always being there to answer questions no matter how small and always being at the end of line when I needed some help. Craig you are a fantastic encouragement, whether in the lab or when we've been running laps of campus – the stress release was often needed and always appreciated. Alice, thank you for being my examiner to finish my PhD with an interesting discussion about HSP47 and how it all fits together. Also, a big thankyou to Nick Pugh, my external examiner.

To everybody in the Reading Platelet group, past and present, thank you for your friendship and all the laughs throughout my PhD. Trips to the pub have made even the toughest weeks thoroughly enjoyable. To Paru, thank you for holding my hand and guiding me into the wonderful world of collagen toolkit peptides. Tanya, thank you for making trips into the windowless BRU a little brighter with your presence. To Alex, thank you for always being there to help with the microscopes, the many beers drunk and CRP diluted…eventually. To Amanda and Renato, even after you left Reading you continued to be both great friends and a huge support and for that I will always be grateful. To Neline, Zannah, Kirk, Alex S, Marcin, Eva, Carly, Safa, Ilaria, Daniel and everybody else in the lab and Wayne and the rest of the BRU team, it has been my pleasure to spend so much time learning from you, exploring ideas with you and laughing at the mistakes in-between. To Jo, you were a fab lab mate but an even better friend and housemate, thank you for being there to talk science at midnight, and occasionally suggesting it was time to stop worrying about it over the weekend. Sophie and Charlie, my ladies who lunch during incubations, my biggest cheerleaders and best friends, I wouldn't have wanted to be on this journey with anybody else.

Mum and Dad, Ian and Chris, I have finally finished education and still have no idea about my next steps. Forever the indecisive one. Words cannot explain how grateful I am for all of your support. To my grandparents, your support has been immense and I can't wait to celebrate with you. To my brothers, thanks for always keeping me grounded. Alisanne, my big sister and

best friend, always at the end of the phone or appearing outside when things were tough, thank you for always being there to hold my hand, and the many many drinks buffets.

Jamie, I couldn't have done this without you - you know more about platelets and chaperone proteins than I could have ever expected. Thank you for always being a smiling face to get home to and for always encouraging me to try again when experiments went wrong. You're a true golden egg.

Finally, to my grandad, Dr Malcolm Coward. I know you won't be here for Graduation but seeing how proud you were when I had eventually submitted my thesis was the best Christmas present a granddaughter could ask for. Thank you for holding my hand tight when things were tough and your unwavering confidence in me. I did it.

Abstract

HSP47, a collagen specific chaperone protein, has been identified within the platelet and has been shown to influence the ability of platelets to respond to collagen and initiate haemostasis. Megakaryocytes, which produce platelets, mature in the bone marrow (BM) but also secrete extracellular matrix factors that support the BM environment. We aimed to understand the role HSP47 plays in megakaryocyte maturation, proplatelet formation and collagen synthesis. We also aimed to determine whether HSP47 acts as a platelet surface receptor.

Using a megakaryocyte lineage-specific transgenic HSP47 gene-deficient mouse, we identified that megakaryocyte ploidy and proplatelet formation was not altered in MKs from HSP47 deficient mice ($P>0.05$) however collagen production from the MKs was reduced ($P<0.05$) suggesting that HSP47 plays no role in MK maturation but is involved in the maintenance of the BM environment.

Using peptide sequences identified to enable HSP47-collagen interactions, we identified that human platelets are able to adhere and spread on these sequences, however they do not support granule release, aggregation or thrombus formation. We also identified, using the HSP47 binding sequences, that HSP47 is able to modulate platelet-collagen interactions that result in platelet aggregation and activation but not thrombus formation.

Finally, we confirm the presence of additional chaperone proteins within the platelet, and identify using inhibitors, that Endoplasmin may be involved in collagen receptor-mediated aggregation and thrombus formation on collagen, and that BiP may be implicated in TRAP6 stimulated aggregation and thrombus formation on collagen.

Deletion of HSP47 from MKs suggests that HSP47 may be a therapeutic target to prevent fibrosis of the BM. Investigations using HSP47 binding sequences identified that HSP47 has dual functionality within the platelet, both supporting platelet adhesion in addition to modulating platelet collagen receptor-collagen interactions. Confirmation of additional chaperone proteins add to the increasing understanding that ER proteins regulate platelet function and can be targeted using inhibitors.

Publications and presentations

Publications: Published/ under review:

Müller-Reif JB, Thienel M, Zhang Z, Ehreiser V, Huth J, Shchurovska K, Kilani B, Schweizer L, Geyer PE, Novotny J, Lüsebrink E, Strecker J, Little G, Orban M, Nemr SE, Spannagl M, Kindberg J, Arnemo JM, Mach O, Vogel M, Dueck A, Polzin Amin, Stark K, Gibbins JM, Maier D, Limper L, Frobert O, Mann M, Massberg S, Petzold T. An evolutionary conserved, immobility associated antithrombotic mechanism. (Under review – Nature)

Cai H; Sasikumar P; **Little G**; Bihan D; Hamaia S; Zhou A; Gibbins JM; Farndale RW. (2021) Identification of HSP47 Binding Site on Native Collagen and Its Implications for the Development of HSP47 Inhibitors. *Biomolecules*, 11 (7).

Gaspar RS; Sage T; **Little G**; Kriek N; Pula G; Gibbins JM. (2021) Protein disulphide isomerase and NADPH oxidase cooperate to control platelet function and are associated with cardiometabolic disease risk factors. *Antioxidants*, 10, 497.

Taylor K; **Little G**; Gibbins JM. (2021) Mind the gap: connexins and pannexins in platelet function. *Platelets*.

Needs SH; Bull SP; Bravo J; Walker S; **Little G**; Hart J; Edwards AD. (2020). Remote video link observation of model home sampling and home testing devices to simplify usability studies for point-of-care diagnostics*. Wellcome Open Research*.

Publications: Manuscript in preparation:

Little G; Sage T; Sasikumar P; Farndale RW; Gibbins JM. Identification of the binding sequences within collagen that allow HSP47 to regulation platelet signalling and activation (*In preparation)*

Little G; Bye AP; Sage T; Gibbins JM. HSP47 is essential for megakaryocyte maturation and differentiation and may be a target for bone marrow fibrosis in myeloproliferative neoplasms (*In preparation*)

Mitchell JL; **Little G**; Bye AP; Gaspar R; Unsworth AJ, Stainer AR; Sangowawa D; Morrow GB; Kriek N; Sage T; Gibbins JM; Desborough MJ; Mutch NJ; & Jones CI. Platelet FXIII-A plays novel roles in platelet function and clot retraction (*In preparation*)

Sasikumar P; Gaspar RS; **Little G**; Bye AP; Gibbins JM. The post translational modification SUMOylation regulates platelet function (*In preparation*)

Mitchell JL; Unsworth AJ; Kriek N; Sage T; **Little G**; Whitworth P; Jones CI; Gibbins JM; Desborough MJ; Bye AP. (*In preparation*) Recombinant von Willebrand Factor (Vondendi) reverses platelet dysfunction caused by antiplatelet agents in vitro.

Presentations:

Oral Presentation and Scientist in Training prize winner: **HSP47 regulates collagen structure and synthesis by megakaryocytes.** British Society of Haemostasis and Thrombosis Annual Scientific Meeting. January 2022.

Oral Presentation: **The collagen-binding chaperone HSP47 modulates platelet responses to collagen: identification of HSP47-binding sequences within type II and III collagens.** University of Reading School of Biological Sciences PhD Symposium. June 2020

Oral Presentation: **The collagen-binding chaperone HSP47 modulates platelet responses to collagen: identification of HSP47-binding sequences within type II and III collagens.** First Platelet Society Meeting, Jesus College, Cambridge. September 2019.

POSTER: **Identification of HSP47 collagen binding sequences that impact platelet function**. GRC: Cell Biology of Megakaryocytes and Platelets. Texas, February 2019

POSTER: **Identification of HSP47 collagen binding sequences that impact platelet function**. GRS: Cell Biology of Megakaryocytes and Platelets. Texas, February 2019

POSTER: **Identification of HSP47 collagen binding sequences that support platelet function**. European Platelet Network (EUPLAN) Conference. Bruges, September 2018

POSTER: **Characterisation of Molecular Chaperones in Platelets.** First Platelet Society Early Career Researcher Meeting. Manchester, July 2018

POSTER: **Characterisation of Molecular Chaperones in Platelets.** University of Reading School of Biological Sciences PhD Symposium. June 2018

Abbreviations

5HT - serotonin

AC - adenylyl cyclase

ACD - Acid citrate dextrose

ADP - adenosine diphosphate

AFT6 - Activating Transcription Factor 6

ATP - adenosine triphosphate

AUC - area under curve

BiP - Binding immunoglobulin Protein

BM - bone marrow

BSA - Bovine serum albumin

Btk - Brunton's tyrosine kinase

CAB - collagen assay buffer

cAMP - cyclic adenosine monophosphate

COVID-19 - coronavirus disease 2019

CRP-XL - cross-linked collagen-related peptide

CVD - cardiovascular disease

DAG – diacylglycerol

ddH_2O – double distilled H_2O

DIC - differential interference contrast

DiOC6 - 3,3’-Dihexyloxacarbocyanine Iodide

DMS - Demarcation membrane system

dNTP - deoxyribonucleotide triphosphates

DTS - dense tubular system

ECM - extra cellular matrix

EDTA - ethylenediaminetetraacetic acid

eIF2 - eukaryotic initiating factor 2

EMT - epithelial-mesenchymal-transition

ER - Endoplasmic reticulum

ET - essential thrombocythemia

FAK - focal adhesion kinase

FBS - fetal bovine serum

Fc Receptor γ-chain - FcR γ-chain

FS - Formal saline

GC - guanylyl cyclase

GM-CSF - Granulocyte-macrophage colony-stimulating factor

GP - glycoprotein

GPCR - G-protein coupled receptors

GRP170 - glucose regulated protein 170

GVHD - Graft-Versus-Host-Disease

HSC - Haematopoietic stem cells

HSP - heat shock protein

IP3 - inositol 1,4,5-trisphosphate

IRE1 - Inositol-requiring enzyme 1

ITAM - Immunoreceptor tyrosine-based activation motif

JAK – Janus kinase

KDEL-R – KDEL receptor

KO - knock-out

LDL - low density lipoprotein

LTA - light transmittance aggregometry

MFI - median fluorescence intensity

MI - myocardial infarction

MK - Megakaryocyte

MPN - Myeloproliferative neoplasm

n.s. - non-significant

NBD - nucleotide binding domain

NO - nitric oxide

OCS - open cannicular system

ON - osteoblastic niche

P13 – PU-WS13, Endoplasmin inhibitor

P4H - Prolyl 4-hydroxylase

PBA - plate based aggregometry

PBS - Phosphate buffered saline

PDI - Protein disulphide isomerase

PF4 - platelet factor 4

PFA - paraformaldehyde

PFT - Pifithrin-μ, BiP inhibitor

PGI2 - prostacyclin

PH - pleckstrin-homology domain

PI - propidium iodide

PI3K - PI 3-kinase

PIP2 - phosphatidylinositol 4,5-bisphosphate

PIP3 - phosphatidylinositol 3,4,5-trisphosphate

PKA - protein kinase A

PKC - protein kinase C

PKG - protein kinase G

PLC - phospholipase-C

PPF - proplatelet formation

PPP - Platelet-poor plasma

PRP - Platelet-rich plasma

PTM - post-translational modification

PVDF - polyvinylidene difluoride

RBC - Red blood cell

rHSP47 - recombinant HSP47 protein

RIAM - Rap1-GTP-interactive adaptor molecule

ROI - region of interest

ROS - reactive oxygen species

RT - Room temperature

SBD- substrate binding domain

SDS - sodium dodecyl sulphate

SH3 - Src homology 3

sHSPs - small Heat Shock Proteins

siRNA - small interfering RNA

SMIH -Small molecule inhibitor of Hsp47

Sp1 - Specificity protein 1

SPDP - succinimidyl 3-(2-pyridyldithio) propionate

TAE - tris-acetate-EDTA

TBS-T - Tris buffered saline with Tween 20

TGS - Tris/Glycine/SDS buffer

TLR - toll-like receptor

TP - Thromboxane receptor

TPO – thrombopoietin

TRAP6 – thrombin receptor activating peptide 6

UPR - unfolded protein response

VN - vascular niche

vWF - von Willebrand Factor

WT - Wild type

αHSP47 – Inhibitory antibody against Hsp47

Table of Contents

List of Figures

List of Tables

Chapter 1 - Introduction

1.1 General introduction

Platelets are the smallest cells in the blood but play a vital role in the balance between haemostasis and thrombosis (von Hundelshausen and Weber, 2007). Haemostasis maintains the normal function of our circulation, however thrombosis is a pathological situation that occurs when clots form in incorrect locations or grow to be excessively large. Platelets respond to a number of stimuli, maintaining a resting state in circulation but activate and aggregate in response to damaged blood vessels. The ability of platelets to respond to damage to the endothelium and 'plug' the break in order to prevent haemorrhage and maintain haemostasis has been widely documented and their role in disease states such as diabetes, cancer, inflammation and Alzheimer's disease is becoming increasingly recognised (Santilli et al., 2015, Karachaliou et al., 2015, Franco et al., 2015, Catricala et al., 2012). Platelets also play a role in foetal development, with Bertozzi et al initially identifying the role of platelets in vascular and lymphatic development (Bertozzi et al., 2010).

Platelets have a range of receptors on their surface which respond to their respective ligands and activate a range of signalling pathways. These lead to activation, aggregation and clot formation to maintain haemostasis, forming a clot when required. Collagen is a potent platelet agonist and a number of collagen receptors exist on the platelet surface including glycoprotein (GP)VI, and integrin α2β1 (Moroi et al., 1989, Gibbins et al., 1997, Nieuwenhuis et al., 1985, Santoro, 1986). HSP47, a collagen specific molecular chaperone, is usually found in the endoplasmic reticulum (ER) and enables collagen to form its correct triple helical structure (Ishida and Nagata, 2011, Kaiser et al., 2009). HSP47 plays a role in platelet function, identified by the use of HSP47 inhibitors and knock out mice, although the mechanism by which it does this is not yet understood (Sasikumar et al., 2018).

Antiplatelet drugs play a major role in the prevention cardiovascular events, with treatments involving antiplatelet medication resulting in a 20-25% reduction of these events in people with established cardiovascular disease (CVD) or those at a high risk of developing CVD (2002). A greater understanding of the mechanisms of the individual platelet signalling pathways, including that of HSP47, will allow the development of more targeted anti-platelet therapeutics.

1.2 Haematopoiesis

All blood cells derive from multipotent haematopoietic stem cells (HSCs). Through responses to growth factors and stimulants, this single cell type can differentiate into all the blood cell

types present within the circulation (Spangrude et al., 1988). During foetal development, before formation of mature marrow, extramedullary haematopoiesis occurs with haematopoiesis occurring in the foetal liver and spleen (Kim, 2010). In adults, differentiation of HSCs occurs mainly in the bone marrow, however it can also occur in liver and spleen (Kim, 2010, Ho et al., 2015). In the presence of a number of cytokines and growth factors including granulocyte-macrophage colony-stimulating-factor (GM-CSF) and thrombopoietin (TPO), HSCs differentiate initially into common myeloid progenitors, then into megakaryocytes (MKs) which produce platelets (Robinson et al., 1987, Kaushansky et al., 1994, Szalai et al., 2006).

1.3 Megakaryocytes and megakaryopoesis

Megakaryocytes are large (50-100µm in humans, up to 50µm in mice) rare cells which account for ~0.01% of nucleated cells in the bone marrow and their primary function is to produce platelets (Nakeff and Maat, 1974). Megakaryocytes are mainly found in the bone marrow, however, have also been identified in the lung and in the periphery (Lefrançais et al., 2017, Garg et al., 2019). Each MK can produce approximately 10^4 platelets, with the adult human producing 1 x 10^{11} platelets per day and increasing with demand (Long, 1998, Branehög et al., 1975).

Growth and maturation of MKs from HSCs is driven by TPO binding its MK specific receptor, c-Mpl, leading to the MK becoming polyploid by endomitosis. This results in the MK becoming 64n or larger as repeating cycles of DNA replication are not followed by cell division and the DNA resides in a single nucleus (Kaushansky et al., 1994, Kuter et al., 1994, Zimmet and Ravid, 2000). TPO interacting with c-Mpl also induces expansion of the cytoplasm, increased expression of cytoskeletal proteins, and the development of the demarcation membrane system (DMS) (Solar et al., 1998, Long et al., 1982, Behnke, 1968). The MK DMS, a structure continuous with the cell surface, eventually forms the plasma membrane of future platelets. Upregulation of transcription factors, such as GATA1, FOG1 and FLI1 lead to expression of MK markers CD41, CD42b and GPIX respectively. Also upregulated within the megakaryocyte is platelet factor 4 (PF4), a protein which is packaged into platelet granules and released during activation (Broekman et al., 1975). The promotor for the PF4 gene has since been manipulated with transgenes to control expression of proteins within the megakaryocyte lineage, a tool which has been widely used in the 14 years since it was first reported (Tiedt et al., 2006). Previously, PF4-Cre murine models have been used to undertake research into platelet function, furthering the understanding of the role of protein disulphide isomerase (PDI) and HSP47 (Kim et al., 2013a, Wu et al., 2012a, Sasikumar et al., 2018).

The bone marrow contains a number of extracellular matrix proteins which allow the HSC to develop into MKs. The bone marrow, in terms of HSC to MK maturation, is generally split into two different areas. In the osteoblastic niche (ON), the region closest to the bone, collagen I is the most abundant protein (Reddi et al., 1977). This is the region where HSCs are generally found, and the presence of type I collagen inhibits proplatelet formation, ensuring HSCs differentiate into mature MKs but don't produce platelets in this location (Balduini et al., 2008) (Sabri et al., 2004, Sabri et al., 2006, Arai and Suda, 2007, Pallotta et al., 2009). Polyploid MKs migrate towards the centre of the marrow, also known as the vascular niche (VN). This migration is regulated by upregulation of the cytokine SDF-1 and its receptor, CXCR4. Here, MKs find an increase in extracellular proteins such as collagen IV, fibrinogen and von Willebrand Factor (vWF) which allow for the later stages of maturation (Avecilla et al., 2004). Upon maturation, once MKs have produced sufficient internal membranes, granules and organelles, cytoskeletal rearrangement allows MKs to extend long branching processes, pro-platelets, into sinusoidal spaces and allow newly formed platelets to be released into the circulation, as demonstrated in Figure 1 (Tablin et al., 1990, Italiano et al., 1999).

Recently, Lefrancais *et al* published data suggesting that large, mature MKs migrate out of the bone marrow towards the lungs where approximately 50% of platelets are produced. (Lefrançais et al., 2017). They also identified populations of haematopoietic progenitors and immature MKs in extravascular spaces of the lungs, capable of reconstituting platelet counts following challenge to the bone marrow.

In vitro culture of MKs also produce platelets, suggesting that the bone marrow environment itself is not required for MK development and maturation, however this is a process that is extremely inefficient compared to *in vivo* with MKs in culture producing ~20-400 platelets per MK, a significantly lower yield than the estimated *in vivo* release of ~10,000 platelets per MK (Takayama et al., 2008, Lu et al., 2011, Ono et al., 2012, Kaufman et al., 1965). This suggests that the microenvironment within the bone marrow plays a vital role in proplatelet, and in turn platelet, production.

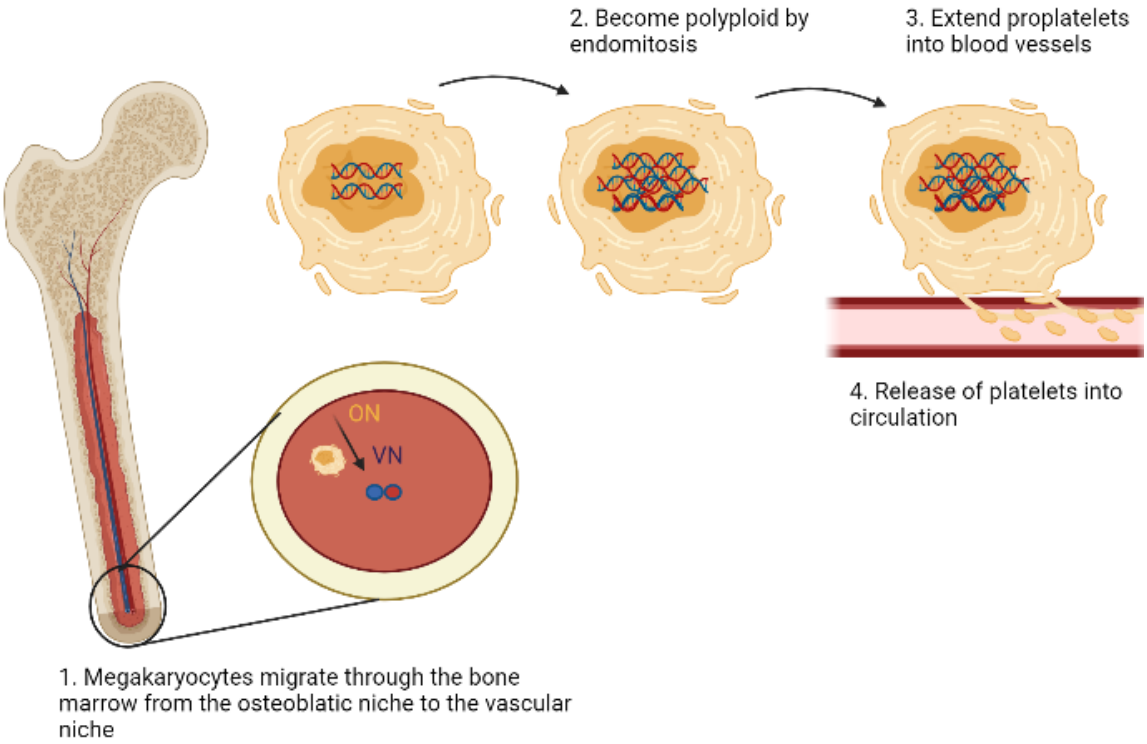

Figure 1. Megakaryocyte maturation and platelet formation
Megakaryocytes mature in the bone marrow from HSCs. During maturation they migrate through the bone marrow from the osteoblastic niche (ON) to the vascular niche (VN). During maturation, MKs undergo endomitosis resulting in polyploid nuclei and increased cytoplasmic content. In the vascular niche, MKs encounter an increased concentration of extracellular proteins including collagen IV, fibrinogen and vWF. MKs then undergo a cytoskeletal arrangement to extend proplatelets into the circulation and allow for the release of platelets. Created in BioRender.com.

1.4 Platelet structure

Platelets are the smallest constituents of the blood, measuring 2-5µm in size when resting. The platelet membrane contains a number of glycoproteins such as GPIb-IX-V and integrin αIIbβ3, both of which are essential for the interaction of platelets with injured vessel walls, platelet activation, aggregation and clot retraction (White et al., 1995, Huang et al., 2019). The platelet submembrane is rich in actin filaments, with actin estimated to account for 15-20% of the total protein and is required for platelet shape change and translocation of receptors (White, 1969, Smyth et al., 2015, Bearer et al., 2002).

Platelets contain several different secretory organelles including α granules, dense granules, lysosomes and mitochondria, as shown in Figure 2. The average human platelet contains 50 to 80 α-granules, with each α-granule containing, vWF, integrins, GPVI, GPIb-IX-V, P-selectin and thrombospondin (Sixma et al., 1989, Maynard et al., 2007). A number of these proteins such as GPVI, GPIb-IX-V and integrin αIIbβ3 already exist on the platelet surface however α-granule content release following activation results in increased surface expression (Niiya et al., 1987). Other proteins, such as P-selectin, are exclusively expressed on the surface of activated platelets and can be used as a marker of activation (Hsu-Lin et al., 1984). Dense granules are smaller and less numerous than a-granules and contain adenosine triphosphate (ATP) and adenosine diphosphate (ADP), serotonin (5HT) and calcium (White, 2008). Lysosomes are a store for glycohydrolases which degrade glycoproteins, glycolipids and glycosaminoglycans which are released following activation (Ciferri et al., 2000). Healthy platelets contain 5-8 mitochondria which regulate metabolism, activation and ATP production for cell viability (Hayashi et al., 2011, Kholmukhamedov and Jobe, 2019). Mitochondria also control the platelet lifespan, with the mitochondrial lifespan within each platelet determining turnover (Jobe et al., 2008). It has also been reported that platelets contain peroxisomes and T granules. Peroxisomes contain catalyse, and T granules contain toll-like receptor (TLR) 9 transcripts after upregulation during proplatelet production (Thon and Italiano, 2012, Thon et al., 2012).

Platelets also contain a number of membrane systems, including the open canalicular system (OCS) and the dense tubular systems (DTS). The OCS is an extension of the platelet surface membrane that extends towards the centre of the platelet and acts as a channel for the granule content releasate (Breton-Gorius, 1975, Behnke, 1967, White and Krumwiede, 1987, Fogelson and Wang, 1996). The OCS membrane can also be evaginated and provides the additional membrane required when platelets undergo shape change and spreading, a process

which can increase the platelet surface area up to 4 times that of the resting platelet (Escolar et al., 1989, White, 2005). The DTS comes from the smooth ER of a MK and exists in platelets as random channels throughout the cytoplasm (Behnke, 1967).

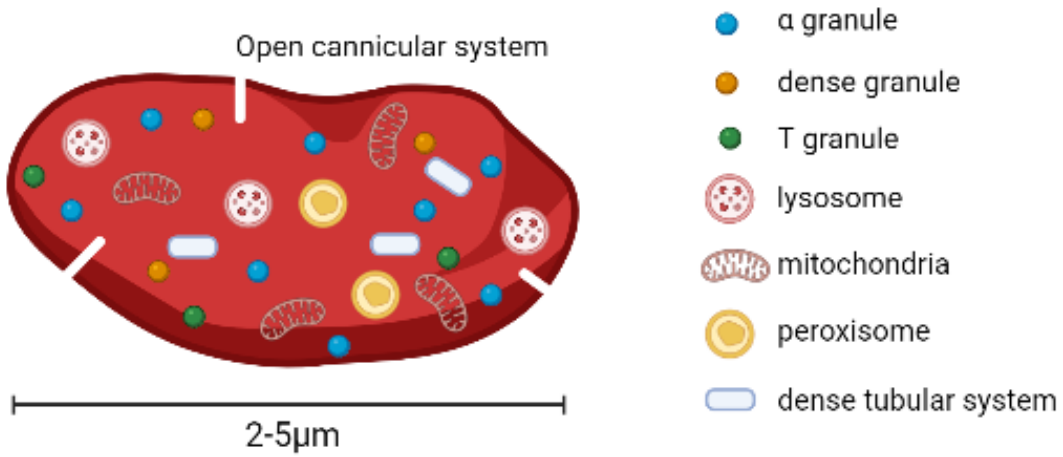

Figure 2. Platelet ultrastructure
Platelets, 2-5µm in size, contain α granules, containing vWF, integrins, GPVI, GPIb-IX-V, P-selectin; dense granules containing adenosine triphosphate (ATP) and adenosine diphosphate (ADP), serotonin (5HT) and calcium; T granules containing toll-like receptor 9 transcripts; lysosomes, mitochondria and peroxisomes. Platelets also have an open cannicular system, channel like projections into the centre of the platelet acting as a channel for granule content release, and the dense tubular system – random channels in the cytoplasm that contains proteins known to play a role in platelet function.

1.5 Platelets in haemostasis and thrombosis

Platelets' primary function is to maintain the integrity of the vascular system, or haemostasis by plugging injury to the vasculature and preventing bleeding, a process which has been identified to occur in three main stages (Scharf, 2018). The high pressure of the vascular system and the small size of platelets results in them being marginalised to the edge of the blood vessels in the circulation (Aarts et al., 1988). In normal healthy blood vessels, platelets are found in a quiescent state, prevented from activation by the production and release of nitric oxide (NO) and prostacyclin (PGI_2) from healthy endothelial cells (Mellion et al., 1981, Dutta-Roy and Sinha, 1987). When the blood vessel is damaged, the endothelial layer breaks exposing the underlying layers, the tunica intima and basement membrane, and also results in loss of localised NO and PGI_2. The tunica intima contains collagens which enable the platelets to adhere via vWF initially, as shown in Figure 3 and then more stable interactions can occur (Ruggeri, 1997). This is stage one of the process: initiation or tethering of the platelets. The collagen-vWF-platelet interaction initiates multiple activatory mechanisms resulting in shape change, activation and aggregation. This is stage two of the process. Finally, a growing thrombus is stabilised by an insoluble fibrin mesh in order to block the breakage and maintain a constant blood flow, a process which is essential to prevent excessive loss of blood and finalises the three-stage process (Ni et al., 2000).

Thrombosis can occur when platelets are activated at an inappropriate time or place, often due to a pathological condition such as the presence of atherosclerotic plaques in the vasculature. Atherosclerosis is the underlying cause for most cases of coronary artery disease and peripheral arterial disease and many cases of stroke (Badimon et al., 2012). High plasma levels of low density lipoprotein (LDL) cholesterol result in entry and retention of the LDL into the subendothelial layer, where LDLs become modified and induce endothelial cells to secrete chemotactic substances and adhesion receptors (Tabas et al., 2007). These receptors increase recruitment and adhesion of leukocytes into the arterial wall (Badimon et al., 2012). These cells then release pro-thrombotic and pro-inflammatory mediators into the circulation, and add to the interruption of NO and PGI_2 release, allow platelets to roll on the endothelium even under high shear and therefore support firm adhesion of platelets to the surface (Huo et al., 2003). Rupture of these plaques can also result in the exposure of the extracellular matrix proteins of the vessel proteins leading to platelet activation and formation of a thrombus. This thrombus may occlude an already narrowed vessel causing an ischemic stroke or myocardial infarction (Libby, 2002).

Thrombosis is a common complication of Cancer but can also be caused by chemotherapy. Both arterial and venous thrombosis are associated with malignancy, though the link connecting arterial thrombosis has only been recently recognised even though it is thought these patients account for up to 25% of cases (Blann and Dunmore, 2011). Patients with cancer experience a high burden of thromboembolic disease, with the incidence of arterial thromboembolic events, myocardial infarction (MI) or stroke at 6 months after cancer diagnosis increasing from 2.2% in the healthy population to 4.7% (Navi et al., 2017). In these patients circulating thrombi or rupture of upstream plaques result in MI and therefore myocardial arrest due to hypoxia. (Blann and Dunmore, 2011)

Patients infected with SARS-CoV-2 and the resulting coronavirus disease 2019 (COVID-19) are more likely to progress to a severe disease state if they have pre-existing cardiovascular complications, with evidence suggesting that activated platelets, endothelial cells, macrophages and neutrophils, in addition to an activated coagulation system can be found in critically ill patients (Klok et al., 2020, Tang et al., 2020, Middeldorp et al., 2020, Bye et al., 2021). While thrombosis is a common complication in COVID-19 patients, there has also been reports of rare cardiovascular side effects after immunisation with SARS-CoV-2 vaccines (Shiravi et al., 2021). The Oxford-AstraZeneca vaccine, a DNA vaccine delivered using a vector based system, has been suggested to result in an increase of platelet-activating antibodies against PF4 leading to immune thrombotic thrombocytopenia, though these complications are much rarer than those associated with COVID-19 infection (Voysey et al., 2021, von Hundelshausen et al., 2021, Mehta et al., 2021, Scully et al., 2021).

1.6 Platelet receptors and their ligands

Platelets contain multiple surface receptors, including a range of integrins (α2β1, αIIbβ3 and others); G-protein coupled receptors (GPCRs) such as the thrombin receptors PAR-1 and PAR-4, purinergic receptors $P2Y_1$ and $P2Y_{12}$ and the thromboxane receptor (TP); immunoglobulin super family receptors such as GPVI and FcγRIIA and many others. Whilst many of these receptors are present on other cell types, others, such as GPVI, are platelet specific. Interactions of activatory platelet surface receptors with their specific ligands result in the initiation of a range of signalling cascades which all eventually lead to common platelet activation processes such as shape change, spreading and clot formation. Thromboxane A2 and thrombin bind to $G_{12/13}$ coupled GPCRs. Thrombin, in addition to 5-HT and ADP also bind to G_q coupled GPCRs, activating phosopholipase-C (PLC) β and supporting the conversion of phosphatidylinositol 4,5-bisphosphate (PIP_2) to inositol 1,4,5-trisphosphate (IP_3) and protein

kinase C (PKC), which both in turn increase intracellular calcium. ADP also binds to $P2Y_{12}$, a G_i coupled GPCR which supports the phosphorylation of PIP_2 to phosphatidylinositol 3,4,5-trisphosphate (PIP_3) by PI-3-kinase (PI3K). G_i coupled and G_z coupled GPCRs also inhibit adenylyl cyclase (AC), which converts ATP to cyclic adenosine monophosphate (cAMP), with cAMP inhibiting platelet activation. Binding of laminin, fibronectin, collagen, fibrinogen and vitronectin to their respective integrins, α6β1, α5β1, α2β1, αIIbβ3 and αvβ3 all result in the activation of PLCγ2 which again supports the conversion of PIP_2 to IP_3 and an increase in intracellular calcium. Collagen is able to bind both α2β1 and GPVI-FcR γ chain complex which also result in the activation of PLCγ2. Increase in intracellular calcium is an essential step in the activation of a platelet and results in shape change, secretion and activation, as demonstrated in Figure 4.

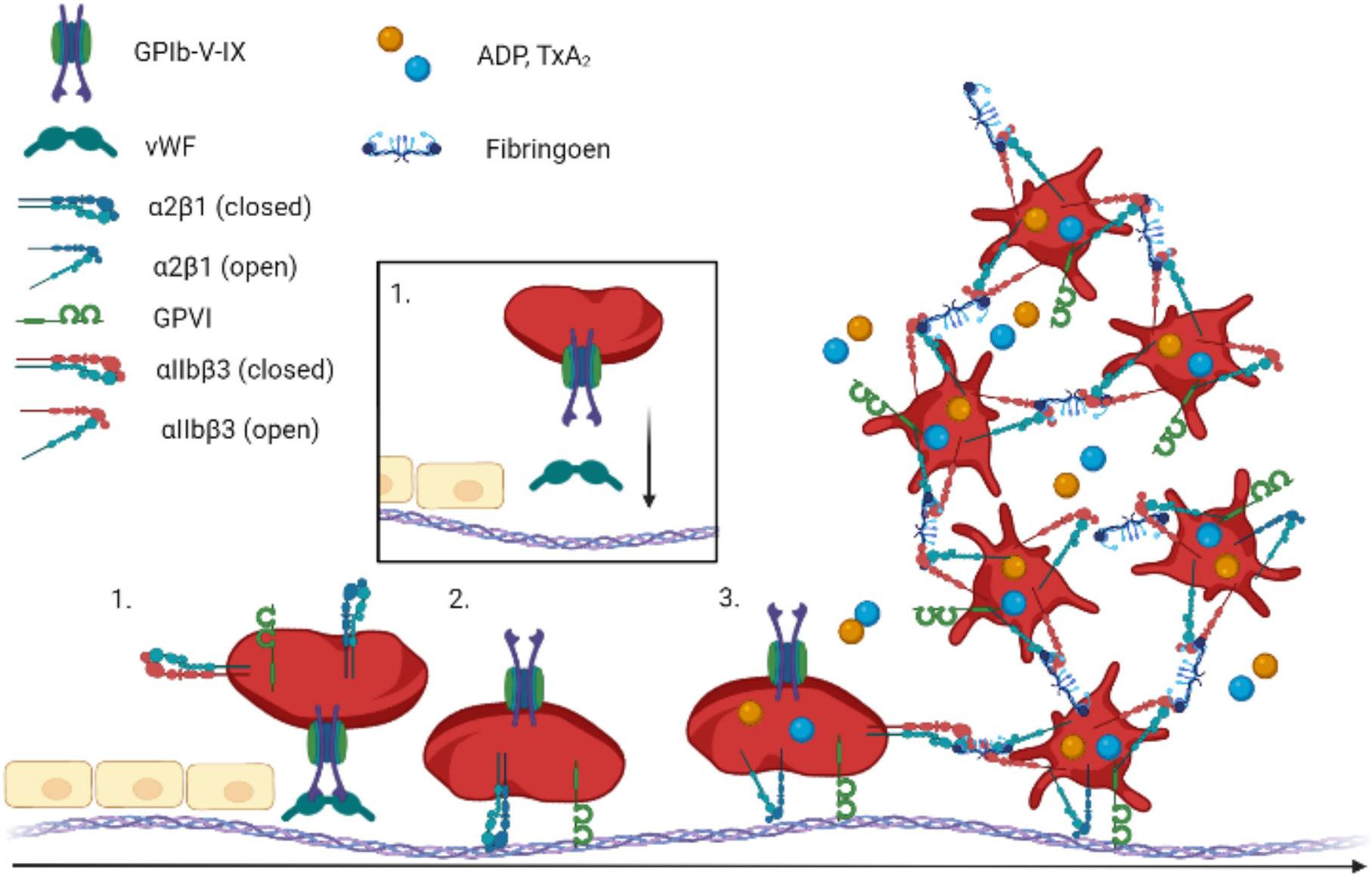
GPIb-V-IX
ADP, TxA2
vWF
Fibringoen
α2β1 (closed)
α2β1 (open)
GPVI
αIIbβ3 (closed)
αIIbβ3 (open)
1.
1.
2.
3.

Figure 3. Thrombus formation on collagen.
1. Injured endothelium exposes collagen, presenting a binding site for von Willebrand Factor (vWF). vWF is also able to bind to platelet surface receptor GPIb-V-IX allowing for the initial tethering of the platelet to the injured endothelium. This interaction slows platelets down, allowing for the more stable binding of α2β1 and GPVI (2). Intracellular signalling cascades result in the release of secondary messengers adenosine diphosphate (ADP) and thromboxane A_2 (TxA_2), which activate localised platelets resulting in the activation of αIIbβ3 (3). Upon activation of αIIbβ3, fibrinogen binds two molecules on different platelets resulting in the formation of a thrombus. Created in BioRender.com

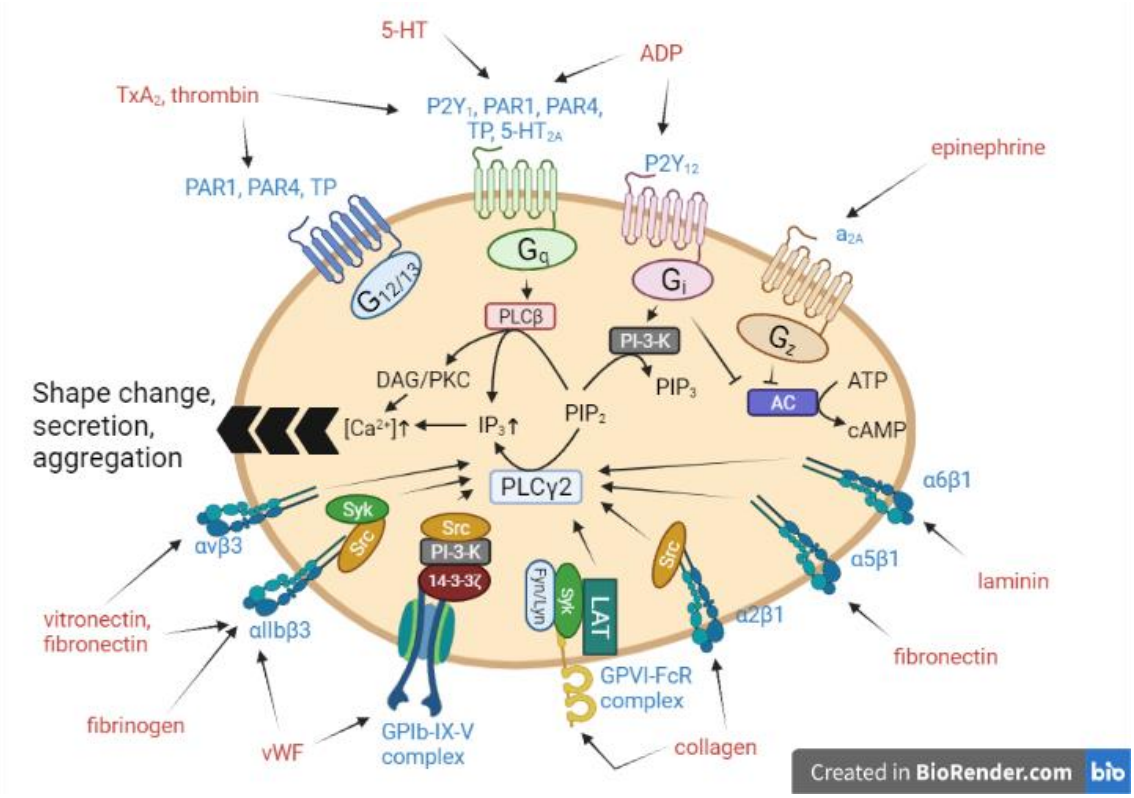

Figure 4. Platelet surface receptors and their ligands

Platelets contain a number of surface receptors (text in blue), which allow for signal transduction and platelet activation upon ligand (text in red) binding. Activation of GPCR's coupled to $G_{12/13}$, G_q and G_i result in the activation of enzymes which convert $PIP_{2\ into}$ PIP_3, IP_3 and PKC .Activation of GPCRs coupled to G_i and G_z inhibit the activation of AC, blocking the conversion of ATP into cAMP, a platelet inhibitor. Activation of integrins and the GPVI-FcR complex result in the activation of PLCγ2 which also converts $PIP_{2\ into}$ PIP_3. PKC and IP_3 result in the release of calcium from stores, increasing the intracellular concentration and resulting in shape change, secretion and aggregation.

PIP_2 =phosphatidylinositol 4,5-bisphosphate, PIP_3 = phosphatidylinositol 3,4,5-trisphosphate, IP_3 = inositol trisphosphate, PKC = protein kinase C, AC = adenylyl cyclase, ATP = adenosine triphosphate, cAMP = cyclic adenosine monophosphate, PLCγ2 = phospholipase C γ2. Created in BioRender.com

1.7 Inhibitory platelet mechanisms

The ability of platelets to activate and aggregate in order to trigger haemostasis is essential, however platelets also require inhibitory mechanisms in order to keep platelets in the circulation resting. Inhibitory mechanisms are also required at sites of injury where platelet aggregates are forming in order to prevent mass thrombus formation and vessel occlusion. Healthy endothelial cells work to keep platelets in a non-adhesive, non-aggregatory state by releasing PGI_2 and NO, as demonstrated in Figure 5 (de Nucci et al., 1988). PGI_2 interacts with the prostacyclin GPCR (IP-R) on the platelet surface, leading to the dissociation of Gβγ and Gαs. Gαs stimulates AC, which in turns stimulates the conversion of ATP to cAMP which then leads to the activation of protein kinase A (PKA) (Narumiya et al., 1999). NO is cell permeable, so passes into the platelet and binds soluble guanylyl cyclase (GC) eventually resulting in the activation of protein kinase G (PKG) (Hanafy et al., 2001). Activation of both PKA and PKG result in the phosphorylation and subsequent inhibition of multiple proteins required for platelet activation.

1.8 Platelet-collagen signalling

In high shear conditions, such as those found within arteries, platelets initially adhere to collagen via an interaction between the platelet surface GPIb-V-IX and circulating vWF (Ruggeri, 1997). Collagen provides a binding site for the vWF, allowing a transient interaction (tethering) between the platelet and the endothelial surface as shown in Figure 3 (Vasudevan et al., 2000). The interaction of these proteins is not strong enough for the platelet to adhere to the surface of the endothelium and requires the presence and activation of other surface proteins. The formation of the GPIb-V-IX-vWF complex does however reduce the velocity at which platelets are moving and increases the likelihood of direct interactions to occur including the interaction of collagen with the collagen receptors GPVI and integrin α2β1 (Dopheide et al., 2002). Activation of GPVI and α2β1 result in signalling cascades which eventually activate integrin αIIbβ3 leading to a confirmation change allowing for high affinity interactions with its ligands, fibrinogen, vWF and fibronectin (Gibbins et al., 1997, Jarvis et al., 2004, Watson et al., 2005).

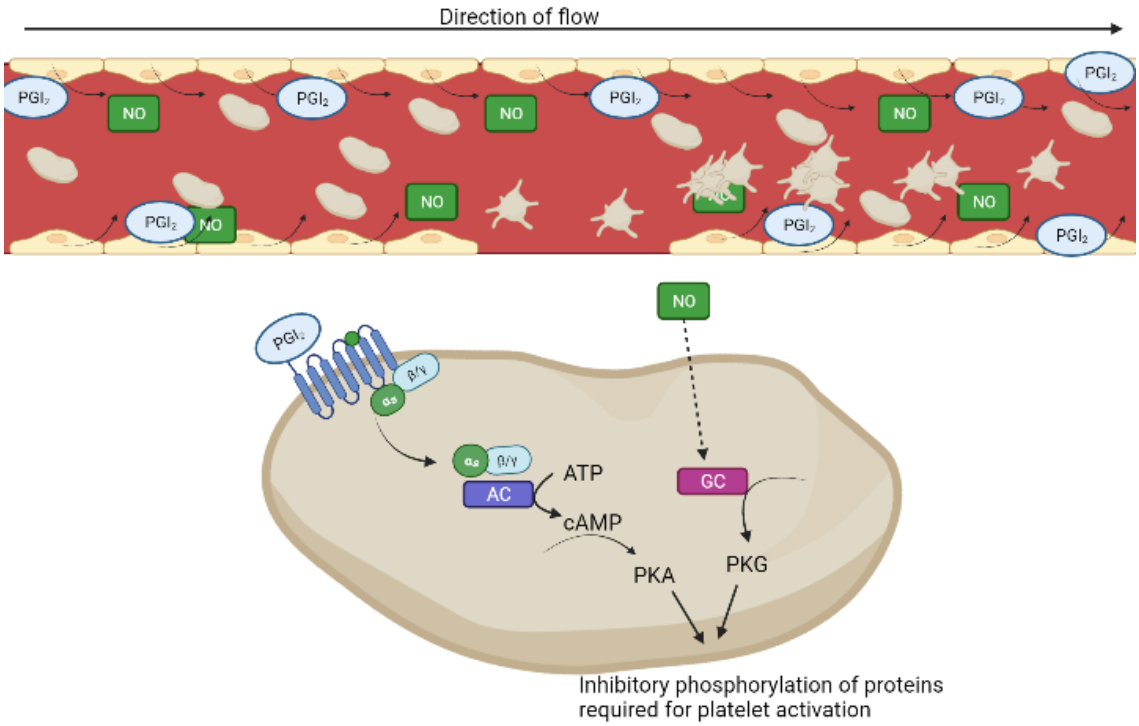

Figure 5. Endothelial inhibition of platelets
Within the circulation platelets remain in a quiescent state, assisted by the release of PGI_2 and NO from healthy endothelial cells. PGI_2 binds to the prostacyclin GPCR (IP-r) on the platelet surface leading to the dissociation of Gβγ and Gαs.Gαs stimulates adenylyl cyclase (AC) resulting in the conversion of adenosine triphosphate (ATP) into cyclic adenosine monophosphate (cAMP) which in turn activates protein kinase A (PKA). Nitric oxide (NO) is cell permeable so passes into the platelet, binding to soluble guanylyl cyclase (GC) which results in the activation of protein kinase G (PKG). Both PKA and PKG result in the phosphorylation and subsequent inhibition of proteins required for platelet activation. In the absence of PGI_2 and NO release from endothelial cells platelets activation is not inhibited and therefore platelets can be activated within circulation. Created in Biorender.com.

1.9 Integrins

Integrins are a large family of transmembrane adhesion receptors which consist of an α and a β subunit, and are able to control cell adhesion in numerous cell types which is essential for migration, survival, proliferation and differentiation (Hynes, 2002). Each subunit consists of an extracellular domain which contributes to ligand binding, a transmembrane domain and a smaller cytoplasmic tail which allows signalling proteins and cytoskeletal proteins to bind. α-chains consist of four or five extracellular domains, and β-chains seven, and there are a number of regions which allow for interdomain flexibility, these allow for confirmational changes within the subunit which regulate the affinity of integrin-ligand binding (Campbell and Humphries, 2011).

Platelets carry five different integrins on their surface: αIIbβ3, α2β1, α5β1, α6β1 and αVβ3, with αIIbβ3 being the most abundantly expressed at an average of 80,000 copies per platelet and its function is the most understood (Burkhart et al., 2012). αIIbβ3 binds a number of ligands including fibrinogen, fibrin, vWF and fibronectin – all proteins containing an arginine-glycine-aspartic acid (RGD) sequence. α2β1, α5β1 and α6β1 all support platelet adhesion to the ECM via their ligands collagen, fibronectin and laminin respectively (Staatz et al., 1989, Piotrowicz et al., 1988, Ill et al., 1984).

1.9.1 Inside-out and outside-in signalling

As previously mentioned, activation of GPVI and integrin α2β1 stimulate signalling cascades that lead to the activation of αIIbβ3. Initiation of inside-out signalling occurs following PLC activation, a downstream effector of the GPVI and α2β1 signalling cascades, that hydrolyses PIP_2 into diacylglycerol (DAG) and IP_3, and IP_3 induces Ca^{2+} release (Geue et al., 2017, Suzuki-Inoue et al., 2003, Varga-Szabo et al., 2009). DAG and Ca^{2+} activate CalDAG-GEF1 and PKC, leading to the conversion of Rap1-GDP to Rap1-GTP (Cifuni et al., 2008). Lee *et al* suggested that Rap1-GTP and Rap1-GTP-interactive adaptor molecule (RIAM) forms a complex with talin which then interacts with the β3 subunit, however this was disputed by Stritt *et al* who generated RIAM-null mice and showed that platelets from these mice have unaltered integrin αIIbβ3 and α2β1 activation (Lee et al., 2009, Stritt et al., 2015). The mechanism of talin-1 recruitment to the integrin is still unknown, however the association disrupts a salt bridge between the αIIb and the β3 subunit, activating the integrin and resulting in a conformation change from the bent (closed) state to the extended (open) state (Petrich et al., 2007, Nieswandt et al., 2007).Upon activation of the integrin by inside-out signalling, fibrinogen is able to bind to αIIbβ3 and trigger outside-in signalling (Huang et al., 2019). Integrin clustering

then occurs and promotes Src activation (Senis et al., 2014). Calpain cleaves the β3 tail, dissociating partially active Src which then phosphorylates and activates a number of signalling molecules including focal adhesion kinase (FAK), Syk kinase, RhoGAP and PI3K (Li et al., 2010). Activation of the integrin also results in actin polymerisation, and together with the signalling molecules result in cytoskeletal reorganisation, spreading, granule release and irreversible activation of platelets (Huang et al., 2019).

1.10 GPVI signalling cascade

GPVI is a transmembrane surface receptor protein composed of 319 amino acids (Human GPVI) that associates with the Fc Receptor γ-chain (FcR γ-chain) in platelets (Gibbins et al., 1997). The extracellular region contains two immunoglobulin-like domains and a Ser/Thr-rich region allowing GPVI to extend from the platelet surface (Clemetson et al., 1999). The 51 amino acid cytoplasmic region shows no homology to other receptors and contains two unique sequences, an acid-rich region close to the transmembrane domain and a Proline-rich region in the middle of the cytoplasmic domain which is thought to bind selectively to the Src homology 3 (SH3) domain of Src family tyrosine kinases Fyn and Lyn (Moroi and Jung, 2004, Suzuki-Inoue et al., 2002). GPVI binds to collagen and results in the clustering of FcR γ-chains and subsequently the activation of a tyrosine kinase linked signalling cascade. Immunoreceptor tyrosine-based activation motifs (ITAM) within the cytoplasmic tails of the clustered FcR γ-chains become phosphorylated by Fyn and Lyn providing a binding site for Syk and the recruitment of SLP-76 and LAT (Suzuki-Inoue et al., 2002, Ezumi et al., 1998, Gross et al., 1999, Pasquet et al., 1999). As demonstrated in Figure 6, SLP-76 and LAT allow for recruitment and accumulation of PI3K and Brunton's Tyrosine Kinase (Btk) and eventually lead to the phosphorylation and activation of PLCγ2. PLCγ2 activation results in the cleavage of PIP_2 to IP_3 and DAG. IP_3 mediates the release of the second messenger Ca^{2+} from intracellular stores, increasing cytosolic concentrations and activating PKC whilst DAG directly activates PKC (Jackson et al., 2003, Bye et al., 2016). PI3K, PLC and PKC mediate platelet activation via multiple pathways and are essential for the secretion of secondary mediators from α and dense granules within the platelet and activation of the integrin αIIbβ3 (Harper and Poole, 2010, Watson et al., 2005). Integrin activation is essential in order to bridge adjacent platelets together via fibrinogen, with one fibrinogen monomer binding two integrin αIIbβ3 receptors on neighbouring platelets.

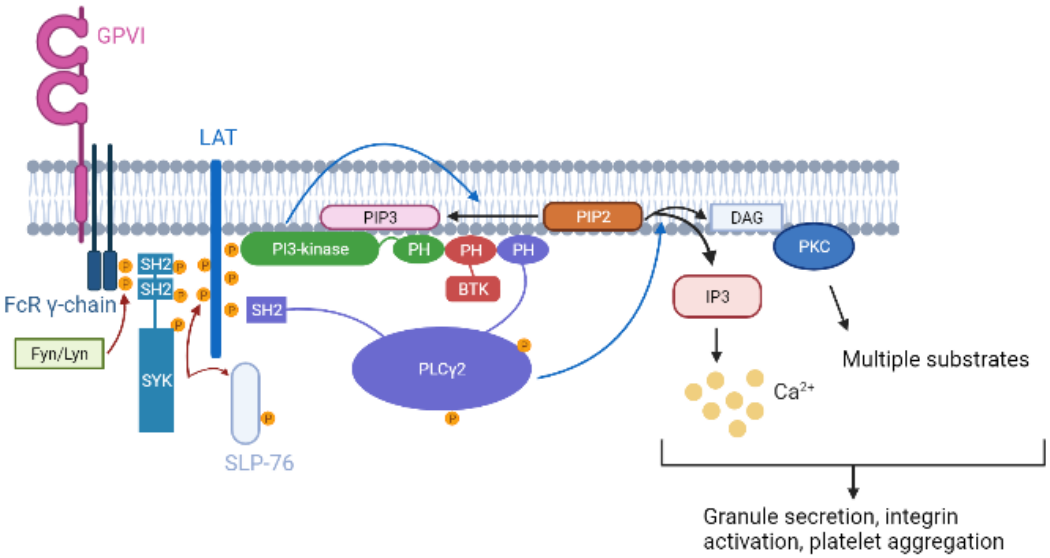

Figure 6. GPVI signalling cascade

The collagen receptor GPVI signals through its coupled Fc Receptor (FcR) γ-chain. The FcR γ-chain contains an Immunoreceptor Tyrosine based motif (ITAM) that is phosphorylated at tyrosine sites by Src family kinases Fyn and Lyn and leads to activation of the tyrosine kinase Syk. Phosphorylation of Syk initiates a signalling cascade: phosphorylation of LAT and SLP-76 activate PLCγ2 resulting in cleavage of PIP_2 to DAG and IP_3. DAG activates PKC, and IP_3 release initiates downstream mobilisation of intracellular calcium, both essential for granule secretion and integrin activation. Red arrows indicate tyrosine phosphorylation and blue arrows indicate enzyme-catalysed conversion. SH2 = Src-homology 2 domain, PLCγ2 = phospholipase C γ2, PH = pleckstrin-homology domain, BTK = Bruton's tyrosine kinase, PIP_3 = phosphatidylinositol 3,4,5-trisphosphate, PIP_2 = phosphatidylinositol 4,5-bisphosphate, DAG = diacylglycerol, IP3 = inositol trisphosphate, PKC = protein kinase C. P = phosphorylation sites.

In addition to GPVI, collagen also binds to integrin α2β1. α2β1 is the second most abundant integrin on the platelet surface behind αIIbβ3, with each platelet carrying between 2,000 and 4,000 copies compared to 80,000 integrin αIIbβ3 copies (Burkhart et al., 2012). The α2 subunits are able to bind to the amino acid sequence GFOGER found within collagen, specifically types I and IV (Zutter and Santoro, 1990, Knight et al., 2000). Platelet adherence to collagen through α2β1 is stronger than the GPIb-V-IX interaction, tethers platelets, and allows for thrombi to build and prevent bleeding after damage to the endothelium, as shown in Figure 3. α2β1 is essential for platelets to spread on collagen, however it also requires signalling through GPVI for this to occur (Suzuki-Inoue et al., 2001).

Until recently, GPVI and α2β1 were considered to be the only activatory collagen receptors expressed on platelets (Clemetson et al., 1999). Recent investigations however, exploring the recruitment and roles of peripheral membrane proteins that temporarily associate with proteins in the lipid bilayer or the lipids themselves, identified a range of chaperone proteins that have been shown to play a role in the regulation of platelet function such as the thiol isomerase PDI and of particular interest the collagen binding protein heat shock protein (HSP) 47.

1.11 Heat Shock proteins

Heat shock proteins (HSPs) are ubiquitous intracellular proteins that respond to cellular stress to promote survival and were initially identified when an increase in heat caused chromosomal puffs in the salivary glands of Drosophila (Peterson et al., 1979). This mechanism was later identified to be a universal and ancient mechanism which is observed in both eukaryotes and prokaryotes (McAlister and Finkelstein, 1980, Lemaux et al., 1978, Kelley and Schlesinger, 1978). In cells containing HSPs, change in heat can cause internal stress within the cell and fluctuation of only a few degrees can cause protein unfolding, entanglement and aggregation. This change in tertiary structure of proteins triggers the heat shock response (Courgeon et al., 1984). The heat shock response can also lead to cytoskeleton rearrangements including the formation of stress fibres and the collapse of actin and tubulin networks; disturbance in subcellular localisation; fragmentation of the ER and Golgi; and a decrease in the number of mitochondria and lysosomes (Welch and Suhan, 1985). In addition to this the heat shock response can also result in the formation of stress granules in the cytosol that contain non translating mRNA, translation initiation components and other proteins affecting mRNA function leading to a decrease in translation (Buchan and Parker, 2009). The heat shock response can also result in a change in cellular morphology as a change

in the ratio of proteins to lipids leads to higher fluidity, enhanced permeability and a drop in cellular pH (Kruuv et al., 1983, Vigh et al., 2007, Coote et al., 1991, Piper et al., 2003). This combination of cytoskeletal rearrangements, reduced translation and a change in membrane morphology leads to halting of the cell cycle, growth and proliferation and in extreme circumstances, cell death. Heat shock proteins are highly conserved molecules that are upregulated during cell stress to prevent apoptosis and promote survival. There are seven classes of heat shock proteins with the predominantly expressed class known as the molecular chaperones (Ellis et al., 1989). This class is comprised of five major families grouped mainly by their size – small heat shock proteins (sHSPs), HSP60s (around 60kDa in size), HSP70s (around 70kDa in size), HSP90s and HSP100s. These molecular chaperones work to fold newly synthesised proteins and refold misfolded proteins reducing the likelihood of non-folded proteins aggregating (Gragerov et al., 1991, Kerner et al., 2005).

1.12 Chaperone proteins

There are an estimated 25,000 proteins responsible for humans to be biologically functional that are synthesized as linear chains of amino acids and require the correct secondary and tertiary structure to serve their purpose (Kim et al., 2013b). Whilst some newly translated proteins can fold spontaneously, the majority require molecular chaperones to assist in de novo folding (Kerner et al., 2005, Hartl, 1996). Chaperones also work to prevent protein aggregation and mark terminally misfolded proteins for degradation (Kim et al., 2013b). Chaperone proteins contain a C-terminal tetra peptide KDEL sequence or similar sequences such as RDEL, KVEL and KNDEL (Kelly, 1990). This motif acts as a retention/retrieval sequence, keeping chaperone proteins within the ER or for those that remain bound to nascent proteins until they reach the Golgi, targeting them to return back to the ER where protein production occurs. Multiple KDEL containing proteins have been identified on the platelet surface but how these proteins are secreted, and their roles are not fully understood.

Thiol isomerases, a family of enzymes recognised for their function in protein synthesis and contain a KDEL sequence at their C terminal, catalyse the formation and modification of disulphide bonds between cysteine residues (Hatahet and Ruddock, 2009). Multiple members of the thiol isomerase family and are stored and released in platelets including PDI, ERp5, ERp57 and Erp72 (Chen et al., 1992, Chen et al., 1995, Cho et al., 2008, Holbrook et al., 2010, Holbrook et al., 2018). PDI can be found on the surface of resting platelets, is secreted from activated platelets and is required for stable thrombus formation but not haemostasis in mice (Essex et al., 1995, Chen et al., 1995, Chen et al., 1992, Kim et al., 2013a). A homologue to PDI, Erp57 is also expressed on the platelet surface and plays a role in platelet aggregation (Wu et

al., 2012b). Other thiol isomerases, such as Erp5 and Erp72 are also thought to play a role in thrombosis as genetic knockouts and inhibition of these proteins lead to a reduction in platelet function (Passam et al., 2015, Holbrook et al., 2018).

1.13 HSP47

HSP47 is a highly conserved 47kDa glycoprotein which was identified bound to Type I collagen in chick embryo fibroblasts and has since been identified in a range of animals from zebrafish to humans (Nagata et al., 1986, Pearson et al., 1996, Ikegawa et al., 1995). HSP47 is translated as a single peptide and after cleavage consists of 418 amino acids (Clarke and Sanwal, 1992). The precursor contains a signal molecule at the N terminus which targets the protein to the ER, and an ER retention sequence (RDEL) at the C terminus (Hirayoshi et al., 1991). Within the ER, HSP47 acts as a collagen-specific molecular chaperone, an interaction which is essential for the development of murine embryos, as homozygous HSP47 deficient embryos did not survive past 11.5 days after gestation and were severely deficient in αI collagen structures in mesenchymal tissues (Nagai et al., 2000).

1.13.1 Expression of HSP47

HSP47 is transcribed from the 6 exons and 5 introns of the SERPINH1 gene on chromosome 11q13 (Hosokawa et al., 1993, Ikegawa et al., 1995). Within mice, HSP47 is transcribed from a gene of ~7.8kb in length which also consists of 6 exons and 5 introns. HSP47 is the only heat inducible chaperone present in the ER of mammalian cells (Nagata et al., 1986). Following heat shock, heat shock factor 1 binds a heat shock element -180bp from the HSP47 transcription initiation site and leads to the synthesis of HSP47 mRNA. Whilst heat shock can induce HSP47 expression, collagen is the most abundant protein in mammals making up a third of the total protein and therefore requires a constitutively expressed level of HSP47 transcription in order to support collagen production (Neuman and Logan, 1950, Ito and Nagata, 2019). Binding of Specificity protein 1 (Sp1) to a binding site at-210bp allows for this constant expression of collagen, and a 500-bp segment in the first intron of HSP47 is the site responsible for cell type-specific expression of HSP47 in skin, chondrocytes and bone precursors (Hirata et al., 1999).

1.13.2 HSP47 as a collagen chaperone

HSP47 is known to specifically bind to procollagens, unlike other HSP's involved in collagen production that also have additional client proteins (Bose and Chakrabarti, 2017). HSP47 is expressed in all collagen producing cells, and its expression levels strictly correlate with the amounts of collagen synthesis being synthesised. Members of the collagen family tend to follow a strict amino acid structure with numerous -(Gly-Xaa-Yaa)$_x$– repeats to ensure triple

helical structure, supported by the glycine backbone. HSP47 has been identified to bind to collagens where Xaa and Yaa are proline and arginine, respectively (Koide et al., 2002, Koide et al., 2006, Tasab et al., 2002).

Type I collagen is formed from two αI chains and one α2 chain, with both types of chain synthesized as pro-α-chains and co-translationally transported into the ER. Once synthesized, a number of chaperone proteins including HSP47, BiP, Endoplasmin, Prolyl 4-hydroxylase (P4H) and PDI bind procollagen to prevent incorrect folding until all three α chains are assembled (Lamande and Bateman, 1999, Hendershot and Bulleid, 2000, Wilson et al., 1998). Once the chains have been assembled and aligned, the three α chains form a triple helical structure following the formation of disulphide bonds in the C terminus and proceeding to the N terminus in a zipper like movement. During the progression of the triple helical zipping, PDI and P4H dissociate from the procollagen and chaperones such as HSP47 will bind as HSP47 preferentially associates with the triple helical procollagen structure (Myllyharju, 2003). Once correctly assembled, procollagen is transported out of the ER, through to the Golgi where HSP47 dissociates due to a change in pH (ER pH ~7.4, Golgi pH ~6.3) and is recycled back to the ER via its RDEL retention sequence (Satoh et al., 1996, Paroutis et al., 2004, Nagata, 2003). In acidic conditions, like that found in the Golgi, the KDEL-receptor (KDEL-R) has a greater affinity for KDEL (or similar) sequences so proteins bind to the receptor (Wilson et al., 1993). Upon ligand binding, the KDEL-R triggers phosphorylation of Src family kinases which are required for Golgi-to-plasma-membrane transport (Capitani and Sallese, 2009). KDEL proteins are then packaged into COPI vesicles for return to the ER (Orci et al., 1997).

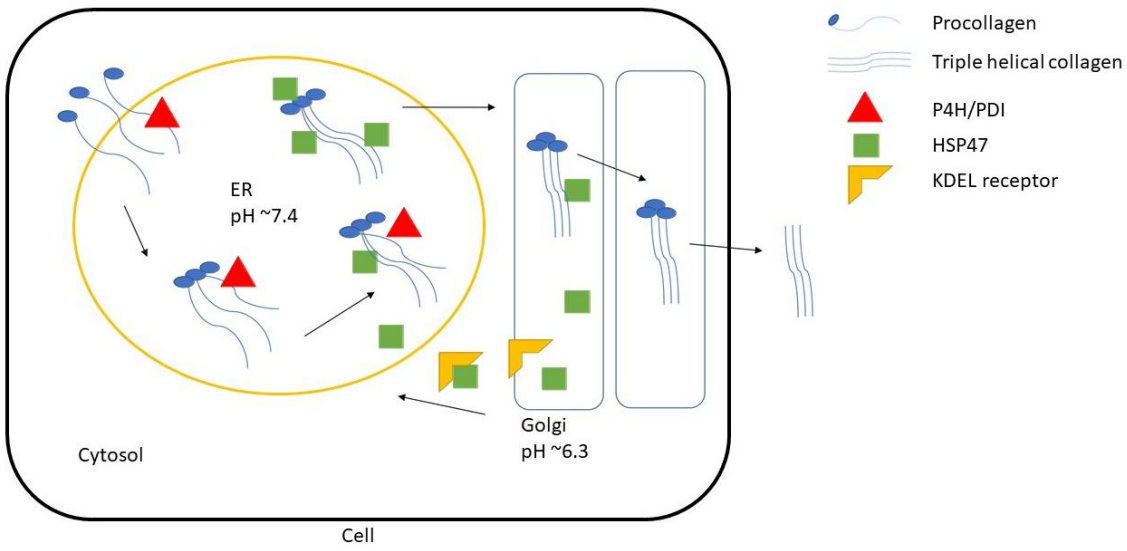

Figure 7. HSP47 as a collagen chaperone
Nascent procollagen chains are transported into the ER upon where P4H/PDI (red triangle) bind and being the process of forming triple helix' in a zipping process. HSP47 (green square) preferentially binds triple helical procollagen, allowing the dissociation of P4H and PDI. HSP47 then transports procollagen from the ER to the Golgi, where the increase in acidity results in HSP47 dissociating. Procollagen is cleaved to produce collagen and exists the cell, but HSP47 binds to the KDEL-receptor (yellow) and transports HSP47 back to the ER.

1.13.3 HSP47 in megakaryocytes and platelets

HSP47 was identified on the platelet surface during a proteomic investigation into proteins associated with the plasma membrane (Kaiser et al., 2009). The initial study identified that inhibition of HSP47 abolished collagen stimulated aggregation, but only partially reduced or had no effect on platelet aggregation stimulated by other agonists. This was further investigated by Sasikumar *et al.* and AlOuda *et al.* who identified that the HSP47 in platelets comes from the platelet precursor, the megakaryocyte (Sasikumar et al., 2018)(AlOuda *et al.,* Under review*)*. Platelet HSP47 was shown to interact with collagen fibrils, and a HSP47 inhibitory molecule was able to reduce the interaction between platelet GPVI and collagen fibrils suggesting that HSP47 influences platelet-collagen interactions. Inhibition of HSP47 resulted in reduced dense granule secretion and calcium mobilisation, and a reduction in PLCγ2 phosphorylation, all suggesting that HSP47 modulates platelet function. Localisation studies identified that HSP47 colocalises with other chaperone proteins including calreticulin and RabGDI, and also associates with lipid rafts in platelets. More recently, it has been identified that HSP47 interacts with the collagen receptor GPVI, supporting its dimerization, regulates its signalling pathway and contributes to platelet-collagen interactions (AlOuda *et al.,* Under review). Development of a megakaryocyte lineage specific knock out mouse model enabled a closer examination of the role of platelet HSP47 specifically in platelet regulation (Sasikumar et al., 2018). In an experimental model of thrombosis, after laser injury to the cremaster muscle, less stable thrombi were formed *in vivo* in HSP47 knockout (KO) mice or when wild type (WT) mice samples were treated with an inhibitor. An *in-vitro* thrombus formation underflow model also showed that either knockout platelets, or those treated with an inhibitor were less able to form thrombi (Sasikumar et al., 2018). Platelet counts in these animals were normal, while their bleeding times were extended, suggesting that HSP47 plays a role in haemostasis and thrombosis and requires further understanding of its mechanism.

1.13.4 Clinical relevance of HSP47

As a molecular chaperone that specifically binds procollagen, and is essential for collagen synthesis, it is unsurprising that HSP47 is associated with collagen-related diseases such as fibrosis and osteogenesis imperfecta (Masuda et al., 1994, Razzaque et al., 1998a, Honzawa et al., 2014, Marshall et al., 2016, Christiansen et al., 2010, Essawi et al., 2018). Fibrotic diseases are characterised by accumulation of the extra cellular matrix (ECM) components, including collagen, leading to disruption of structure and matrix integrity and finally disrupting the physiological function of the organ (Ito and Nagata, 2019). In a streptozotocin induced model of myocardial fibrosis, overexpression of HSP47 increased the area of myocardial cells,

increased mRNA expression of multiple cardiac hypertrophic markers and increased the fibrotic index (level of scarring) seen in murine hearts (Xie et al., 2020). Interestingly, increased HSP47 expression can also be the result of fibrosis rather than the cause. Both HSP47 and collagen expression are increased following the chemical initiation of liver fibrosis, idiopathic pulmonary fibrosis, intestinal fibrosis and glomerulonephritis (Masuda et al., 1994, Razzaque et al., 1998a, Honzawa et al., 2014). An *in-vivo* model of chronic Graft-Versus-Host-Disease (GVHD) in the lacrimal gland identified an increase in HSP47 expression correlated with presence of abnormal fibroblasts (Yamane et al., 2018). These spindle shaped fibroblasts were able to produce excessive ECM and cause lacrimal gland dysfunction.

Recently, a small number of patients have presented with Osteogenesis Imperfecta but do not overmodify collagen chains (Christiansen et al., 2010). Of these patients, nine have been identified instead to have mutations in the HSP47 SERPINH1 gene. The cases were identified in young children and the children did not survive past 5 years. One of these cases allowed researchers to identify, using patient cells, that HSP47 monitors the integrity of the type I procollagen triple helix at the ER-Golgi boundary and the lack of HSP47 resulted in an increase in transit rate of proteins with a compromised triple helical structure (Christiansen et al., 2010).

Multiple studies have also identified a link between HSP47 and cancer. In healthy cells, HSP47 forms a complex with IRE1α and Binding immunoglobulin Protein (BiP). Release of this complex due to ER stress leads to IRE1α activation; increase of intracellular reactive oxygen species (ROS) and impaired cell growth, however, in cancerous cells ER stress signals are faulty, HSP47-IRE1α-BiP complexes remain and cancer cells survive and grow (Yoneda et al., 2020). Increased HSP47 expression has also been shown to impact on cancer metastasis via epithelial-mesenchymal-transition (EMT) and may enhance cancer cell-platelet interactions increasing cell colonisation potential (Xiong et al., 2020, Yamada et al., 2018) . The role of HSP47 in EMT may be, in part, due to its ability to bind and stabilise discoidin domain receptor 2 (DDR2), a protein which plays a crucial role in EMT and regulates membrane dynamics (Chen et al., 2019). *In-vitro* renal cell overexpression of HSP47 was associated with poor prognosis and reduced survival with Qi *et al.* suggesting HSP47 expression levels could be used a predictor of unfavourable prognosis in carcinoma patients (Yamada et al., 2018, Qi et al., 2018). Additionally, HSP47 has been shown to play a role in tumour progression particularly in bladder cancer by promoting angiogenesis in an ERK- and CCL2-dependent mechanism (Ma et al., 2021). In contrast, a laryngeal squamous cell carcinoma model showed that HSP47 expression is markedly reduced when compared to adjacent non-cancerous tissues and low

HSP47 expression correlated with poor prognosis. Upregulation of HSP47 in this model resulted in reduced proliferation, promotion of apoptosis and G1 phase arrest (Song et al., 2017).

1.13.5 Targeting HSP47 therapeutically

With HSP47 expression shown to be implicated in multiple conditions, it has been targeted for the development of new therapeutics. Small interfering RNA (siRNA) against HSP47, delivered by liposomes, has been successful in ameliorating effects of fibrotic conditions and in some cases prophylactic use prevented onset. This method has been used to treat chronic GVHD, vocal fold mucosal fibrosis and pulmonary fibrosis (Ohigashi et al., 2019, Kishimoto et al., 2019, Otsuka et al., 2017, Liu et al., 2021). In the vocal fold mucosal fibrosis model, sustained knockdown of HSP47 using siRNA was also able to reverse scar-associated collagen accumulation, and in two pulmonary fibrosis models treatment using anti-HSP47 siRNA displayed improved lung function (Kishimoto et al., 2019, Liu et al., 2021). A chemical compound library identified a molecule AK778, its cleavage product Col003 competitively inhibited the interaction between HSP47 and procollagen, de-stabilizing the collagen triple helix presenting as an alternative therapeutic tool for fibrosis (Ito et al., 2017).

The recent development of a photoactivatable HSP47, that allows regulation of collagen biosynthesis in mammalian cells using light, may also provide an additional therapeutic tool (Khan et al., 2019). A tyrosine mutation at Tyr383 of HSP47 to a light-responsive tyrosine renders the protein inactive. This inactive protein is reported to be easily taken up into cells via retrograde KDEL receptor-mediated uptake, accumulates in the ER due to the KDEL-receptor pathway, and upon light exposure the modified HSP47 becomes functional in-situ, increasing the intracellular HSP47 expression and stimulating collagen secretion.

In collagen-based skin conditions, where patients present with chronic wounds and blistering, exogenous application of HSP47 upregulated deposition of fibrillar collagen types I, III and V in certain cell types. Collagen IV was also increased in some cells, offering an additional use of therapeutic HSP47 as inhibition HSP47 may reduce the ability of collagen to lay down new fibrils (Khan et al., 2020).

1.14 Hypothesis

HSP47 modulates collagen production within the megakaryocyte without impacting other aspects of megakaryocyte function. HSP47, a collagen chaperone protein, also acts as a receptor on the platelet surface. Like HSP47, additional chaperone proteins exist within the platelet and regulate platelet function.

1.15 Aims

Collagen mis-production is known to be implicated in a number of pathologies, and megakaryocytes, the platelet precursors, produce collagen. The objectives of the research carried out in this project was therefore to identify whether HSP47 is able to modulate production of MK collagen and the impact that has on MK function. Previous work has shown that HSP47 impacts platelet function, in a collagen specific manner as it has no impact on thrombin stimulated responses. We aimed to identify whether HSP47 is able to act as a receptor on the platelet surface and initialise functional platelet responses. We also aimed to identify if additional KDEL proteins exist within the platelet proteome and regulate platelet function.

1.16 Research Objectives

1) Use megakaryocyte lineage HSP47 knock out mice to measure MK function.

2) Use HSP47 binding sequences, identified from within the collagen toolkits, to determine if HSP47 acts as a receptor on the platelet surface and is capable of supporting platelet function.

3) Investigate the role of additional chaperone proteins within the platelet to determine if it is a general paradigm that these proteins are involved in platelet function.

Chapter 2 - Materials and Methods

2.1 Materials

Collagen-related peptide (CRP-XL), GFOGER, Collagen toolkit peptides (Collagen II peptides 13, 14, 20 and 33, Collagen III peptide 5a) and collagen toolkit peptide flanking sequence (GPP_{10}) were purchased from Cambcol (Cambridge, UK). Collagen (Kollagen Reagens HORM Suspension) was purchased from Takeda (Austria).

96 well, clear bottom half area plates were purchased from Greiner bio-one (Gloucestershire, UK). Unless stated, all other materials were of chemical grade and purchased from Sigma (Dorset, UK) or Fisher Scientific (Loughborough, UK).

2.1.1 Antibodies

Table 1. Primary antibodies used in this study

Antibody	Species	Application	Dilution	Source and catalogue number
anti - HSP47	Rabbit	Immunocytochemistry	1:500	Abcam, Ab109117 (ERP4217)
anti - tubulin	Mouse	Immunocytochemistry	1:500	Protein tech, 66031-1
anti - Grp170	Mouse	Immunoblotting	1:500	Santacruz, sc-398224 (A-3)
		Flow cytometry	1:500	
		Immunocytochemistry	1:100	
anti - Endoplasmin	Rat	Immunoblotting	1:500	Santacruz, sc-32249 (9G10)
		Flow cytometry	1:500	
		Immunocytochemistry	1:100	
anti - BiP	Mouse	Immunoblotting	1:500	Santacruz, sc-376768 (A-10)
		Flow cytometry	1:100	
		Immunocytochemistry	1:100	
anti - Calreticulin	Rabbit	Flow cytometry	1:250	Merck, 06-661
		Immunocytochemistry	1:100	
anti - aIIbB3	Goat	Immunocytochemistry	1:250	Santacruz, sc-6602
anti - 6x His	Rabbit	Protein binding assay		Abcam, Ab137839

Table 2. Directly conjugated antibodies used in this study

Antibody	Species	Application	Dilution	Source and catalogue number
FITC anti CD41	Rat	Flow cytometry	1:200	BD Pharmingen, 553848
		Immunocytochemistry	1:250	
PE anti CD62P (P-selectin)	Mouse	Flow cytometry	1:100	BD Pharmingen, 555524
FITC anti fibrinogen	Mouse	Flow cytometry	1:100	Dako, F0111

Table 3. Secondary antibodies in this study

Antibody	Species	Application	Dilution	Source and catalogue number
Alexa Fluor 488 anti-Goat IgG	Donkey	Immunocytochemistry	1:500	Life Technologies, A11055
Alexa Fluor 488 anti-Rat IgG	Chicken	Immunoblotting	1:4000	Life Technologies, A21472
		Flow cytometry	1:200	
		Immunocytochemistry	1:500	
Alexa Fluor 647 anti-Mouse	Donkey	Immunoblotting	1:4000	Life Technologies, A31571
		Flow cytometry	1:200	
		Immunocytochemistry	1:500	
Alexa Fluor 647 anti-Rabbit	Donkey	Flow cytometry	1:200	Life Technologies, A31573
		Immunocytochemistry	1:500	
Alexa Fluor 568 anti-Rabbit	Goat	Immunocytochemistry	1:500	Life Technologies, A11036
HRP anti Rabbit	Goat	Protein binding assay		Abcam, ab6721

2.1.2 Inhibitors

Small molecule inhibitor of HSP47 (SMIH, compound IV, RH00007SC) was purchased from Maybridge, UK). HSP47 inhibitory polyclonal rabbit antibody (αHSP47) was purchased from LSBiosciences, USA. Grp94 inhibitor, PU-WS13 was purchased from MerckMillipore (Watford, UK).

2.2 Methods

2.2.1 Megakaryocyte isolation and function

2.2.1.1 Isolation of primary megakaryocytes

Mice were terminated using CO_2 and cervical dislocation in accordance with Schedule 1 of the Animals (Scientific Procedures) Act 1986. Femora and tibiae were collected using scissors and forceps. Clean femora and tibiae were cut open at the knee side using a razor blade. Bones were then placed in a 0.6mL microcentrifuge tube with a hole from an 19G needle in the bottom. The 0.6mL microcentrifuge tube was then placed in a 1.5mL microcentrifuge tube containing with 100µL DMEM with 100 U/mL penicillin and 50mg/mL streptomycin (DMEM with P/S) in it. This was centrifuged at 2500g for 1 minute to flush the bone marrow into the media. Marrow was resuspended in an additional 1mL of media approximately10 times using a P1000 before filtering through a 70µm cell strainer. The cell strainer was rinsed using 2mL media before cells were counted using a Countess II (Invitrogen) then pelleted at 300g for 5 minutes. Supernatant was removed and cells were resuspended for use in further assays.

2.2.1.2 Analysis of megakaryocyte ploidy

Cells were resuspended in 450µL 1:1 CATCH buffer (25mM HEPES; 3mM ethylenediaminetetraacetic acid (EDTA); 3.5% (w/v) bovine serum albumin (BSA) in phosphate buffered saline (PBS)) and PBS with 5% (v/v) fetal bovine serum (FBS). $2x10^6$ cells were stained with FITC-CD41 or FITC-IgG for 20 minutes on ice in the dark. Additional samples for non-stained controls were also included in analysis. Samples were topped up to 1mL with PBS, then cells pelleted by centrifugation at 300g for 5 minutes. Cells were fixed in 500µL PBS containing 1% (w/v) paraformaldehyde (PFA) and 0.1% EDTA for 10 minutes on ice before addition of 500µL PBS and pelleted at 300g for 10 minutes. Cells were permeabilised in 500µL PBS containing 0.1% (v/v) triton for 10 minutes on ice before addition of 500µL PBS and pelleted at 300g for 10 minutes. Cells were stained using 0.05µg/mL propidium iodide (PI) containing RNase A (100µg/mL final) in PBS for either 1 hour at RT in the dark or at 4°C overnight. RNase A was added to degrade RNA and ensure PI only bound to DNA. Samples were analysed using a BD Accuri C6 Plus flow cytometer through FL1 and FL3 channels with the standard filters (533/30 and 670LP, respectively).

2.2.1.3 Culture of primary megakaryocytes

Cells were resuspended in 1mL DMEM with P/S and 10% (v/v) FBS (complete media) then incubated with anti-rat antibodies against CD3; Ly6G/Ly6C; CD11b; CD45 and TER-119/Erythroid (all Biolegend, 1.5µg antibody/animal) to remove all other bone marrow cells. Cell depletion antibodies were incubated with cells for 20 minutes at 4°C on a roller. Cells were washed with 1mL complete media to remove unbound antibody before being resuspended in 800µL complete media with 200µL washed anti-rat IgG magnetic beads. Cells and beads were incubated on a roller at RT for 15 minutes before being gently vortexed, briefly pulsed to remove any media from the top of the tube then placed in a magnetic holder for 3 minutes. The supernatant was then removed, cells in the supernatant counted using a Countess II (Invitrogen), pelleted at 300g for 5 minutes and resuspended at $3x10^6$ cells/mL in complete media containing 50ng/mL TPO and 10U/mL hirudin. TPO and hirudin are added to cells to encourage efficient maturation of megakaryocytes (Avecilla et al., 2004, Strassel et al., 2012). Cells were incubated for 2 days at 37°C in 5% CO_2, then 50% of the media was removed and replaced with fresh complete media containing TPO. On day 5, cells were collected, pelleted at 300g for 5 minutes then resuspended in 2mL complete DMEM. Mature MKs were enriched by a two-step BSA gradient (4mL 3% (w/v) BSA, 4mL 1.5% (w/v) BSA, 2mL cells in complete DMEM) allowing the cells to separate over 45 minutes at room temperature (RT). Larger, heavier, more mature cells (lower fraction) were used on the day for proplatelet formation, and the smaller less mature cells (upper fraction) were centrifuged at 300g for 5 minutes and resuspended at $1x10^6$ cells/mL in complete DMEM containing 50ng/mL TPO and 10U/mL hirudin. Cells were incubated for an additional 4 days to allow further differentiation.

2.2.1.4 Proplatelet formation (PPF)

Cells from the mature MK fraction were pelleted at 300g for 5 mins and resuspended in complete DMEM at $3x10^6$ cells/mL. Cells were diluted 1:8 in CO_2 independent media (Gibco) containing pen/strep, L-glutamine, 2.5% (w/v) HEPES pH7 and 10% (w/v) FBS supplemented with 50ng/mL TPO and 10U/mL hirudin. CO_2 independent media supports cell survival without the need for a CO_2 supply. After two hours, cells were transferred to Ibidi 8 well µ-slides coated with 0.01% poly-l-lysine. PPF was imaged for 24 hours at 37°C on a Nikon Ti2 using a 40X differential interference contrast (DIC) objective with images taken every 15 minutes.

2.2.1.5 Immunocytochemistry

13mm coverslips were coated with Matrigel (Corning) diluted 1:6 in complete DMEM for 1 hour at 37°C. Coverslips were washed 3x with ice cold PBS then mature megs were seeded onto coverslips and left for 2 days at 37°C with 5% CO_2. Cells were fixed using an equal volume

of 8% (w/v) PFA for 10 minutes at RT before being washed 3x with PBS then permeabilised using 0.1% (v/v) triton X-100 in PBS for 5 minutes. Samples were stained using FITC-CD41, anti-HSP47 and anti-tubulin or respective IgG controls in 1% (w/v) BSA in PBS for 1 hour at RT before being washed 3x with PBS and secondary antibodies applied in 1% BSA in PBS for 1 hour at RT. Samples were washed 3x PBS then mounted using hydromount. Samples were imaged on a Nikon Ti-A1 confocal system using a 100x oil objective and NIS-Elements image acquisition 3.1 software.

2.2.1.6 Analysis of collagen synthesis

Soluble collagen was extracted from spent cell culture media after cells had been cultured in supplemented DMEM containing 50ng/mL TPO and 10U/mL hirudin using a Soluble Collagen Assay from Abcam (Cambridge, UK). Cells were collected and pelleted, then the media containing newly synthesized collagen was collected. Media was spun at 10,000g for 15 minutes at 4°C to pellet any debris then the clarified supernatant was transferred to a new tube. 20µL of clarified cell media was added to two parallel wells then 60µL Collagen Assay Buffer (CAB) was added to each. Standards were produced using Collagen stock concentration diluted in double-distilled H_2O (dd)H_2O and 80µL of each was added to the 96 well plate. 20µL diluted Collagenase Enzyme mix was then added to standards and one of the two cell culture samples, with 20µL CAB added to the other culture samples – these are now the sample background controls. The 96 well plate was then incubated at 37°C for 60 minutes in the dark. 75µL detection reaction solution (Peptide labelling stock diluted in detection reaction buffer) was then added to each sample and incubated in the dark at 37°C for 5 minutes. 25µL developer solution (concentrated developer solution diluted in ddH2O) was added to all samples then incubated at 37°C in the dark, gently shaking at 200rpm on a plate shaker for 15 minutes. Finally, fluorescence was measured of all samples with excitation at 376nm and emission at 468nm. Blanks were subtracted from their relevant samples, a standard curve was fitted to the standards and total soluble collagen produced was calculated.

2.2.2 Human Platelet Preparation

Blood samples were taken from drug free, consenting volunteers on the day of the experiment according to the methodology approved by the University of Reading Research Ethics Committee. Briefly, blood was drawn into 3.8% (w/v) sodium citrate vacutainers. 7.5mL acid citrate dextrose (ACD) (85mM sodium citrate, 71mM citric acid, 100mM glucose) was added to 50mL citrated blood before isolation of platelets by differential centrifugation. Platelet-rich plasma (PRP) was prepared by centrifugation of whole blood at 100g for 20 minutes at RT and

carefully aspirated so as not to disturb the buffy layer of leukocytes, then platelets were pelleted from PRP at 1400g for 10 minutes at room temperature in the presence of 10µL PGI_2 (stock is 125µg/mL, solubilised in ethanol). The platelet pellet was re-suspended in 25mL modified Tyrode's-HEPEs buffer (134mM NaCl, 2.9mM KCl, 0.34mM Na_2HPO_4, 12mM $NaHCO_3$, 20mM HEPES, 1mM $MgCl_2$ and 5mM glucose, pH 7.3 at (RT) in the presence of 3mL ACD and 10µL PGI_2. Platelets were re-pelleted at 1400g for 10 minutes before resuspension in 1mL modified Tyrode's-HEPES buffer. The platelet count was determined using Sysmex XP-300 haematology analyser (Sysmex UK, Milton Keynes) and the cells adjusted to $4x10^8$ by the addition of modified Tyrode's-HEPES buffer. Platelets were rested for 30 minutes at 30°C to allow the effects of PGI_2 to wear off and platelet responses to recover.

Where PRP was used for experiments, citrated whole blood was centrifuged at 100g for 20 minutes without the addition of ACD. PRP was then aspirated as previously described and used immediately.

2.2.3 Platelet aggregation assays

Light Transmission Aggregometry

225µL washed platelets ($4x10^8$ platelets/mL), or 225µL PRP were added to Helena aggregometer cuvettes containing a magnetic stirrer. Each aggregometer channel in a Helena AggRam aggregometer (Helena BioSciences) was blanked using modified Tyrode's-HEPES, or platelet rich plasma (PPP) in cases where aggregation was measured in PRP. Channels were allowed to run for 20 seconds to create a baseline before 25µL 10X agonist was added to each tube and aggregation was measured for 300 seconds. Where inhibitors were used, these were incubated with platelets/PRP as described in results and figure legends, before samples were stimulated.

Plate based aggregometry

45µL washed platelets ($4x10^8$ platelets/mL), or 45µL PRP were incubated in a 96-well half area, flat bottomed plate for 5 minutes at 37°C using a plate shaker (Quantifoil Instruments). 5µL 10X agonist was then added to each well and the plate was shaken at 1200rpm for 5 minutes at 37°C using a plate shaker. Resting washed platelets and modified Tyrode's-HEPES buffer was then added to empty wells in the plate and absorption of light at 405nm was measured using a Flexstation 2 (Molecular Devices, Winnersh). Absorbance was converted to light transmittance using the equation: $LT = 10^{-Absorbance}*100$ and percentage aggregation determined by using the mean of 3x Tyrode's-HEPES values as 100% aggregation and the mean of 3x resting washed

platelet values as 0% aggregation.
Where inhibitors were used, these were incubated with platelets/PRP as described in results and figure legends, before samples were stimulated. Where PRP was used for aggregation experiments, percentage aggregation was determined by using the mean of 3x PPP values (obtained by centrifugation of 500µL PRP at 17,000g for 3 minutes to pellet the platelets) defined as 100% aggregation and the mean of 3x PRP values as 0% aggregation.

2.2.3 Immunoblotting

2.2.3.1 Preparation of platelet lysates (human and murine)

Washed human platelets ($4x10^8$ cells/mL) were treated with an appropriate volume of 6X sample buffer in reducing conditions (12% (w/v) Sodium Dodecyl Sulphate (SDS), 30% (v/v) glycerol, 0.15M Tris-HCl (pH 6.8), 0.001% (w/v) Brilliant Blue R, 30% (v/v) β-mercaptoethanol). Samples were boiled at 95°C for 10 minutes before storing at -20°C until use.

2.2.3.1 SDS-PAGE/Immunoblotting

Proteins were separated by SDS-PAGE, as previously described by Laemmli, using 10% mini PROTEAN TGX precast gels (Bio-Rad, CA, USA)(Laemmli, 1970). Precision Plus Protein Dual Colour (BioRad, CA, USA) molecular weight standards were also included to estimate protein size. Gels were loaded in a Mini-PROTEAN tetra vertical electrophoresis cell and were run in the presence of Tris/Glycine/SDS buffer (TGS) (25mM Tris, 192mM glycine, 0.1% SDS, pH 8.3) for 90 minutes at a constant voltage of 150V.
After protein separation, proteins were transferred to a polyvinylidene difluoride (PVDF) membrane using a Trans-Blot SD semi-dry transfer cell (Bio-Rad, CA, USA). One piece of PDVF soaked in methanol was placed below the resolving gel, above 4 sheets of 3mm filter paper soaked in anode buffer (300mM Tris-base, 20% (v/v) methanol; pH 10.4) and below 4 sheets of 3mm filter paper soaked in cathode buffer (25mM Tris-base, 40mM 6-amino-n.hexanoic acid; pH 9.4) placed between the electrodes of the semi-dry blotter. Proteins were transferred from the resolving gel onto the PVDF for 90 minutes at 170V (constant voltage).
PVDF membranes were then transferred into a 2% (w/v) BSA solution dissolved in TBS-T (Tris buffered saline with Tween 20: 20mM Tris, 140mM NaCl, 0.1% (v/v) Tween, pH 7.6) to block the membrane for 1 hour at RT. Primary antibodies were diluted to concentrations as mentioned previously in 2% (w/v) BSA in TBS-T and incubated overnight at 4°C on a roller. Blots were then washed for 5 minutes three times with TBS-T. Species specific secondary antibodies conjugated to Alexa fluorophores were added 1:5000 to 1% (w/v) BSA in TBS-T and

incubated in the dark for 1 hour at RT. PVDF membranes were washed for 5 minutes 3 times in TBS-T. PVDF membranes were then imaged using a Typhoon FLA 9500 fluor-imager (GE Biosciences, Amersham, UK).

2.2.4 Platelet function assays

2.2.4.1 Spreading

Glass coverslips were coated with 100µg/mL collagen for 1 hour at RT, washed three times with PBS before blocking with 5mg/mL heat deactivated 0.2µm filter sterilised BSA for 1 hour at RT and washed again three times with PBS. 300µL of $2x10^7$cells/mL platelets were allowed to adhere and spread for 45 minutes at 37°C. Non-adhered platelets were then removed, and coverslips carefully washed three times with PBS before fixing with 0.2% Formal saline (FS) (0.17% w/v NaCl, 0.8% v/v formaldehyde) for 10 minutes, washed three times again with PBS then permeabilised with 0.1% (v/v) Triton-X100 for 5 minutes. Platelets were washed three times again then stained for F-actin using Alexa-488 tagged Phalloidin (diluted 1:500 in PBS) for 30 minutes at RT. Platelets were washed three times again then mounted onto coverslips using Gold anti-fade mounting media. Samples were stored at 4°C in the dark overnight and imaged using Nikon Ti-confocal system 100x oil objective and NIS-Elements image acquisition 3.1 software. Three randomly selected fields of view per image were captured for image analysis. Images were analysed using ImageJ (NIH, USA) to determine number of cells adhered and surface area coverage.

2.2.4.2 Flow cytometry

Washed platelets ($4x10^7$ cells/mL) or PRP were stimulated with CRP-XL, thrombin receptor activating peptide (TRAP6) or collagen toolkit peptides in the presence of 0.5µL PE-Cy5 mouse anti-human CD62P antibody (to measure P-Selectin exposure, a measure of alpha granule release) and 0.5µL FITC rabbit anti-human anti-fibrinogen antibody (as a surrogate marker of integrin αIIbβ3 activation) for 20 minutes at RT in the dark. Samples were then fixed with 0.2% formal saline (FS) and analysed using a BD-Accuri C6 Plus Flow Cytometer (BD, Winnersh, UK). Data was collected from 5,000 events per sample and analysed using inbuilt BD Accuri C6 plus software. Where inhibitors were used, platelets or PRP were incubated as described in results and figure legends before samples were stimulated.

2.2.4.3 In vitro thrombus formation under flow

Channels of Vena8 Fluoro+ Cellix Chips (World Precision Instruments, Hitchin, UK) were coated with 100µg/mL Collagen or Collagen toolkit peptides for 1 hour at room temperature before

being washed with Modified Tyrode's-HEPES buffer. Whole blood, containing 3.8% citrate was stained 1:250 with DiOC6 (3,3'-Dihexyloxacarbocyanine Iodide) (4µg/mL final). Using a Cellix pump attached to a Nikon A1R confocal microscope, blood was perfused through the chip at 1000^{s-1} in a temperature-maintained environment at 37°C and visualised using a 20X objective lens. Frames were captured at a rate of one frame per 2 seconds for 8 minutes.

2.2.4.4 Immunocytochemistry

Washed platelets ($2x10^8$ cells/mL) were either resting or activated with TRAP6 in the presence of 4µg/mL eptifibatide to allow activation but inhibit aggregation under stirring conditions for 3 minutes at 37°C before fixation with 4% final (v/v) PFA for 15 minutes. Platelets were pelleted at 950g for 10 minutes then re-suspended in 1mL 15% (v/v) ACD in PBS twice. Platelets were finally re-suspended in 250µL 1% (w/v) protease free BSA in PBS before adhering 90µL to poly-l-lysine coated glass coverslips at 37°C for 90 minutes. Coverslips were washed three times for 5 minutes each with PBS and blocked with 1% (w/v) protease free BSA in PBS before staining. Primary antibodies were diluted to concentrations described previously in filtered permeabilisation buffer containing 1% (w/v) protease free BSA, 0.2% (v/v) Triton X-100 and 2% (v/v) donkey serum and left at 4°C overnight. Samples were washed three times for 5 minutes each with PBS before staining using species specific secondary antibodies raised in donkeys. Secondary antibodies 1:500 (v/v) in lysis buffer were left for 1 hour at RT in the dark. Samples were fixed with 4% final (v/v) PFA for 5 minutes before washing three times in PBS and mounting on slides using Gold anti-fade mounting media. Samples were imaged as described previously. Images were analysed using ImageJ (NIH, USA).

2.2.5 Peptide cross linking

Collagen toolkits peptides Coll II 13, 14, 20, 26 and 33; Coll III 5a and peptide flanking sequence GPP_{10} were cross-linked using a modification of a previously established method (Morton et al., 1995). In brief, Peptides were dissolved in water (adjusted to pH 8.3) and then 1.5 molar equivalents of the cross-linking agent succinimidyl 3-(2-pyridyldithio) propionate (SPDP) dissolved in dry ethanol (dried using molecular sieve 3A) was added under a flow of nitrogen. Peptides were rotated at room temperature for 1 hour to allow for cross linking before being transferred to a Slide-a-Lyzer dialysis cassette and dialysed against 2 litres 0.01M acetic acid at 4°C three times for ≥2 hours each with constant stirring. Volume of peptide before and after cross linking was measured and used to determine recovery, this was usually 100%.

2.2.6 Protein binding assays

100µg/mL type I collagen was heated to RT, 40°C or 60°C for 20 minutes using a heat block before adding 100µL to wells of 96 well, flat bottom plate for 1 hour before being blocked with 175µL 5% (w/v) BSA in Modified Tyrode's-HEPES for 1 hour. Three x 5minute washes with 200µL 0.05% (v/v) Tween in PBS were followed by 100µL 10µg/mL His-tagged HSP47 (kindly gifted by Dr Aiwu Zhou, Shanghai JiaoTong University School of Medicine) for 1 hour. A further 3 PBS washes were carried out, before incubating with 100µL 1:4000 rabbit polyclonal antibody to 6xHis for one hour. A further 3 PBS washed were carried out, before incubating with 100µL 1:1000 HRP conjugated goat anti rabbit IgG for 30 minutes. A final 3x PBS washes were carried out before addition of 50µL of TMB substrate solution. 50µL stop solution was added after 150 seconds and absorbance was read at 450nm using a Flexstation2 (Molecular Devices, Winnersh, UK)

2.2.7 Image Analysis

All microscopy files were analysed using FIJI, ImageJ (NIH, USA). For in vitro thrombus formation, a region of interest (ROI) was drawn around the channel. Total fluorescence was measured for each frame. Each frame was also converted to a binary image using the Li thresholding method, with the background in black and thrombi in white (Li and Lee, 1993, Li and Tam, 1998). (Li and Lee, 1993, Li and Tam, 1998). Percent surface coverage within the ROI was calculated for each frame.

2.2.8 Statistical Analysis

Statistical testing as described in figure legends and results sections, but generally using students t-test for 2-grouped comparisons, and one-way ANOVA with Dunnett's multiple comparisons where multiple groups were assessed. All data are presented as mean ± SD and $P<0.05$ was considered statistically significant. Statistical analyses were conducted using GraphPad Prism software 9.0 (GraphPad, San Diego, CA).

Chapter 3 – Role of HSP47 in megakaryocyte collagen synthesis and function

3.1 Introduction

Collagen accounts for 30% of total protein mass in the human body. HSP47 is known to be a collagen chaperone, preferentially binding to procollagen and escorting it out of the ER to the Golgi where the ends are cleaved off. Megakaryocytes, the platelet precursor, are found in the bone marrow, and are known to secrete other ECM proteins including type IV collagen, fibronectin and laminin in order to maintain the bone marrow environment (Malara et al., 2014). Overproduction of megakaryocytes and collagen overproduction/mis-production are associated with a number of a different pathologies, ranging from osteogenesis imperfecta to the myeloproliferative disorders, primary myelofibrosis and, essential thrombocythemia (Wilkins et al., 2008, Malara et al., 2018, Sam and Dharmalingam, 2017).

The treatment options for these pathologies are often not specific for the respective disease-causing mechanism. An example of this is essential thrombocythemia (ET) patients are often treated using aspirin to inhibit their platelet function and/or chemotherapy in order to reduce their platelet count in the circulation (Patrono et al., 2013, Barbui et al., 2018). Chemotherapy in particular, however, comes with a number of associated side effects including a further reduction of the patients already reduced white blood cell count. HSP47 is a systemic collagen chaperone protein, and we are hypothesizing that it may be a suitable therapeutic target for pathologies involving megakaryocyte and collagen overproduction however its role in megakaryocytic collagen synthesis and structure regulation has not been assessed.

To investigate this, we used a megakaryocyte lineage HSP47 knockout mouse model and isolated megakaryocytes to determine if knockout MKs were still functional and had similar characteristics. Megakaryocytes have a number of functions, including their ability to mature and increase their copies of DNA; migrate through the bone marrow; form proplatelets, and in turn platelets.

3.2 Methods

3.2.1 Generation of megakaryocyte lineage HSP47 deficient mice

HSP47 is essential for collagen production, and therefore a systemic knockout in mouse models is embryonically lethal at 11.5 days post coitus (Nagai et al., 2000). In order to investigate the role of HSP47 in megakaryocytes, a lineage specific knockout was created by Prof. Nagata (Kyoto Sangyo University, Japan). On a C57/BL6 background, HSP47 was mutated to contain a loxP recombination site flanking either side of exon 6. Transgenic mice containing the floxed HSP47 allele were then crossed with transgenic mice containing the cre recombinase under a Pf4 promoter, the PF4-Cre model (Jackson Labs, Maine, USA), resulting in HSP47 gene deletion in the MK line only due to restricted PF4 promotor activation in these cells (Sasikumar et al., 2018). Activation of PF4 promoter drives Cre-recombinase expression which in turn catalyses recombination at loxP sites, resulting in deletion of the DNA between these sites in megakaryocytes.

Breeding HSP47$^{flox/+}$ with PF4-Cre mice results in four possibilities, as displayed in Figure 8:

1) HSP47$^{+/+}$, PF4-Cre negative (-ve)

2) HSP47$^{+/+,}$ PF4-Cre positive (+ve)

3) HSP47$^{flox/+}$, PF4-Cre -ve

4) HSP47$^{flox/+}$, PF4-Cre +ve

Breeding HSP47$^{flox/+}$, PF4-Cre +ve (4) mice together resulted in six possibilities:

1) HSP47$^{+/+}$, PF4-Cre negative (-ve)

2) HSP47$^{+/+,}$ PF4-Cre positive (+ve)

3) HSP47$^{flox/+}$, PF4-Cre -ve

4) HSP47$^{flox/+}$, PF4-Cre +ve

5) HSP47$^{flox/flox}$, PF4-Cre -ve : control animals, “wild-type (WT)”

6) HSP47$^{flox/flox}$, PF4-Cre +ve : experimental animals, “knockouts (KO)”

Sasikumar *et al.* confirmed that mice in the control category were PCR positive for floxed HSP47, PCR negative for PF4-Cre and immunoblotting identified presence on HSP47 within platelets (Sasikumar et al., 2018). They also confirmed that mice in the experimental category were PCR positive for floxed HSP47, PCR positive for PF4-Cre and immunoblotting confirmed the absence of HSP47 within platelets.

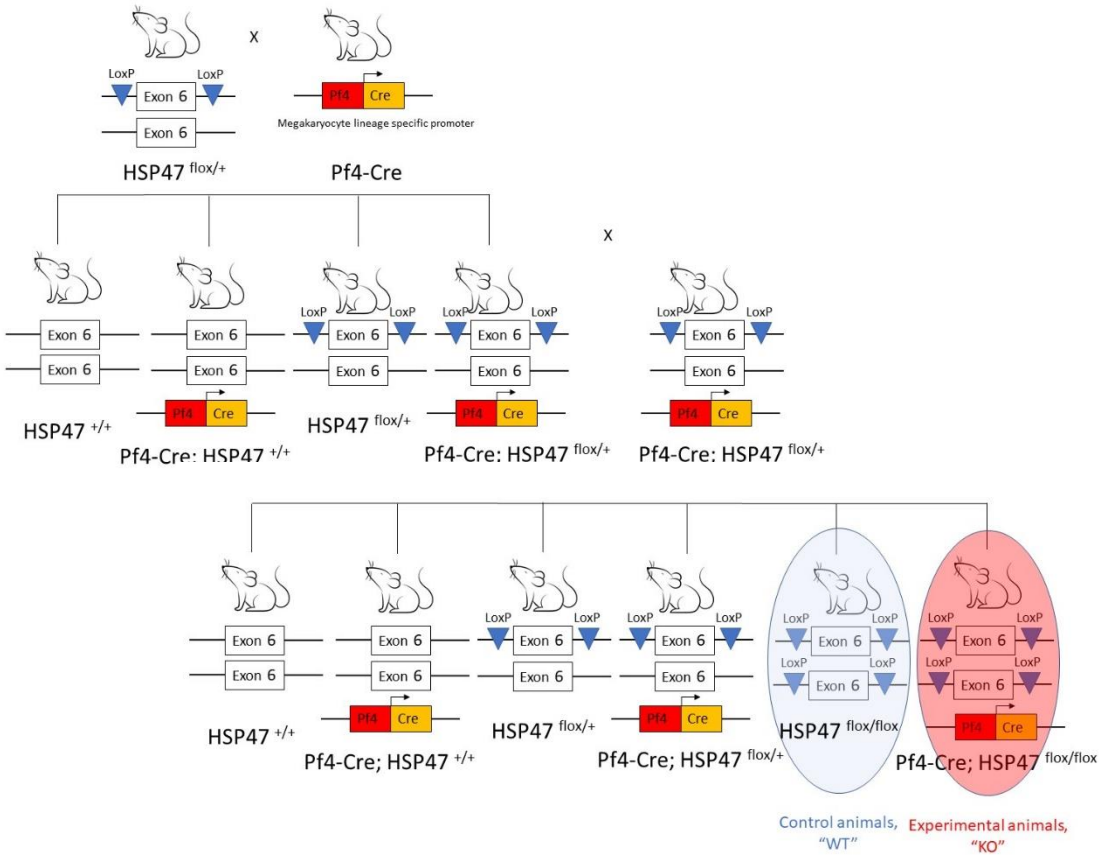

Figure 8. HSP47 knockout mice breeding strategy.
Mice containing one allele of the floxed HSP47 was crossed with a PF4-Cre positive mouse model resulting in four different outcomes. PF4-Cre+, HSP47 $^{flox/+}$ were bred together resulting in 6 different outcomes. Those which were homozygous for floxed HSP47 but PF4-Cre negative were designated the control, wild-type (WT) animals. Those which were homozygous for floxed HSP47 and PF4-Cre positive are the experimental knock-out (KO) animals.

3.2.2 Genotyping procedure

In order to establish the breeding colony described in Figure 8, PCR analysis of genomic DNA taken from an ear clipping was performed to identify the presence/absence of PF4-Cre and the size of HSP47, as the floxed gene presents with a slightly increased size (from 350bp to ~450bp, an increase of ~100bp). To isolate DNA, ear clippings were heated to 95°C in 300µL 1mM EDTA and 1mM NaOH for 10 minutes. DNA was then added to a DNA master mix, as shown in Table 4, containing 5µL 2X DreamGreen (cocktail of DNA polymerase, Taq, deoxyribonucleotide triphosphates (dNTPs) and $MgCl_2$) (Thermofisher, UK), $MgCl_2$, 10µM primers (as described in Table 5), 2µL of DNA and topped up to 10µL with nuclease free H_2O. DNA was amplified using the cycles optimised for detection of floxed HSP47 and PF4-Cre, as listed in

Table ***6***, before being visualised on a 1% agarose gel containing SYBR Safe in Tris-Acetate-EDTA (TAE). Bands were visualised following separation at 120V for 30 minutes using a GE Healthcare Typhoon, as shown in **Figure *9***.

Table 4. DNA Master mix contents

Reaction mix	HSP47	PF4-Cre
	For 10µL mix:	For 10µL mix:
2x DreamGreen containing:	5µL	5µL
-DreamTaq DNA polymerase		
-DreamTaq Green buffer		
-dNTPs		
-MgCl2		
MgCl2	0.2µL	0.3µL
10µM primer (forward and reverse)	0.2µL	0.2µL
DNA samples	2µL	2µL
Nuclease free H2O	2.6µL	2.5µL

Table 5. PCR Primers

	Primers	PCR products
HSP47	Forward primer: 5'-GAGTGGGCTGAGCCCTCTCAAGAAAATCC-3' Reverse primer: 5'-CTTCGGTCAGGCCCAGTCCTGCCAGATG-3'	Wild type -350bp Flox - 450bp
PF4-Cre	Forward primer: 5'-CCCATACAGCACACCTTTTG-3' Reverse primer 5'-TGCACAGTCAGCAGGTT-3'	450bp

Table 6. PCR cycles

HSP47		
Step	**Temperature (°C)**	**Time**
1. Initial denaturation	94	10 minutes
2. Denaturation	94	30 seconds
3. Annealing	60	60 seconds
4. Extension	77	30 seconds
5. Repeat steps 2-4 for 32 cycles		
6. Hold	4	
PF4-Cre		
Step	**Temperature (°C)**	**Time**
1. Initial denaturation	94	10 minutes
2. Denaturation	94	30 seconds
3. Annealing	52	60 seconds
4. Extension	72	30 seconds
5. Repeat steps 2-4 for 40 cycles		
6. Hold	4	

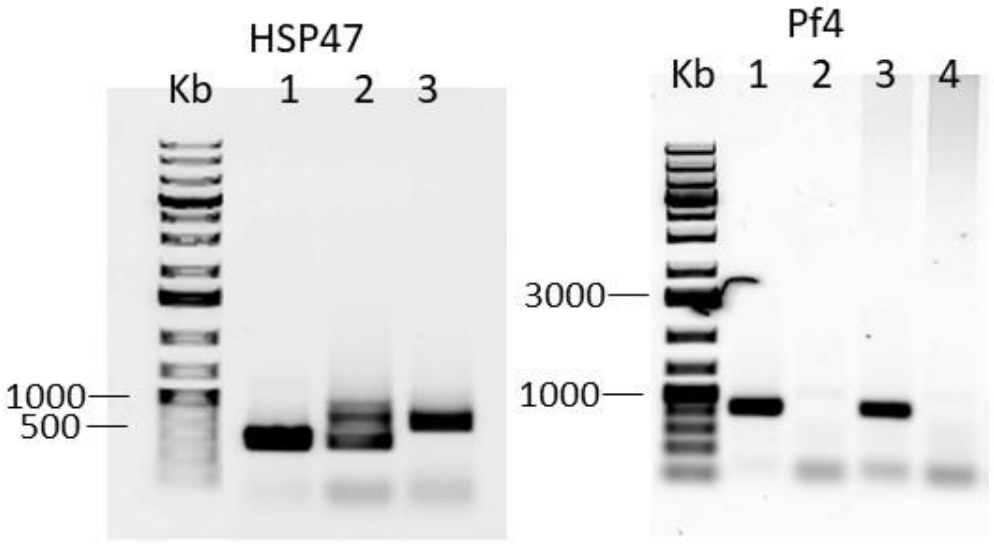

Figure 9. Agarose gel of PCR products following amplification by primers for HSP47 and Pf4-cre.

DNA, isolated from mice ears using 1mM EDTA and 1mM NaCl, was amplified using primers targeted at HSP47 and Pf4-cre as listed in Tables 4, 5 and 6. Amplified DNA was loaded onto a 1% (w/v) agarose gel in TAE containing SyberSafe and run at 120V for 90 minutes before being visualised using a GE-Typhoon 9500 fluroimager. On the HSP47 gel, lane 1 = WT/WT, lane 2 = WT/Flox, lane 3 = Flox/Flox. On the Pf4 gel, lane 1 = Pf4-Cre positive; lane 2 = Pf4-Cre negative, lane 3 = Pf4-Cre positive, lane 4 = Pf4-Cre negative.

3.3 Results

3.3.1 HSP47 is present in WT but not KO megakaryocytes

Following the generation of lineage-specific HSP47 deficient mice, the deletion of expression in megakaryocytes was confirmed using immune-fluorescence confocal microscopy.

To do this, isolated and cultured mature megakaryocytes were allowed to settle on Matrigel coated coverslips for 48 hours. Samples were then fixed, permeabilised and stained for CD41 (αIIb subunit of integrin αIIbβ3, a megakaryocyte surface marker), tubulin and HSP47. Samples were then mounted onto coverslips and imaged using a 100X oil objective on a Nikon A1 Confocal microscope.

Figure 10 shows representative images of 4 different experiments. In the WT sample, it is possible to see HSP47 distributed throughout the megakaryocyte, including in its projections away from main cell body.

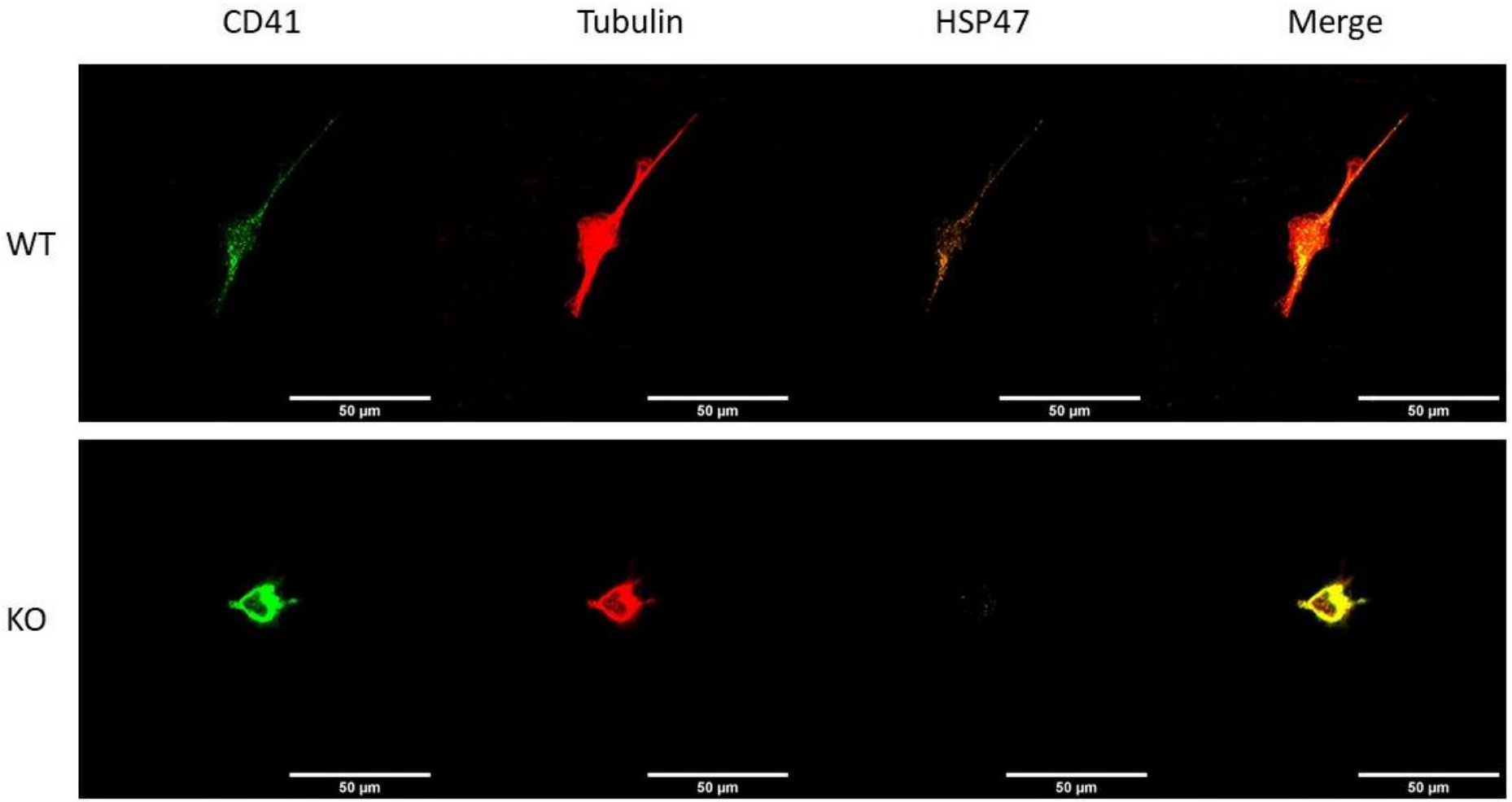
CD41
Tubulin
HSP47
Merge
WT
KO
50 µm

Figure 10. HSP47 is present in WT but not KO megakaryocytes
Megakaryocytes from WT and HSP47 KO mice were isolated, cultured for 5 days then allowed to adhere to Matrigel coated coverslips for 48 hours at 37°C in 5% CO2. Samples were then fixed in 4% PFA, permeabilised in 0.1% triton X-100 in PBS and stained using antibodies against CD41, tubulin and HSP47. Samples were stained with secondary antibodies then imaged using a 100X oil objective using a Nikon A1 confocal microscope. Representative images of 4 repeats. Scale bar = 50μm.

3.3.2 MK-specific HSP47 deficient mice present similar blood counts

The bone marrow is the primary site of haematopoiesis in adults producing the majority of the cellular components of blood and blood plasm, though at the foetal stage of development, haematopoiesis occurs in the foetal yolk sac, liver and spleen (Long et al., 1982, Gordon et al., 1990, Morita et al., 2011, Kim, 2010). The structure of the bone marrow is known to be important in the production of hematopoietic cells with its microenvironment providing factors for cellular proliferation, differentiation and maturation (Travlos, 2006, Weiss and Geduldig, 1991). We have hypothesised that HSP47 impacts the production of collagen from megakaryocytes which may in turn alter the microenvironment of the bone marrow and therefore haematopoiesis.

To identify if there are any haematopoietic differences between WT and KO mice, blood was drawn into sodium citrate (3.8% (w/v) final concentration) using cardiac puncture then full blood counts were taken from four animals per group. Using a Sysmex XP300 haematology analyser measurements for A) white blood cell count, B) platelet count, C) red blood cell (RBC) count, D) haematocrit, E) haemoglobin concentration, F) mean corpuscular volume, G) mean corpuscular haemoglobin and H) mean corpuscular haemoglobin concentration (Figure 11). For all parameters measured, there was no difference identified between control (WT) and HSP47 deficient (KO) samples ($P>0.05$) suggesting that knock-out of HSP47 in megakaryocytes has no impact on haematopoiesis.

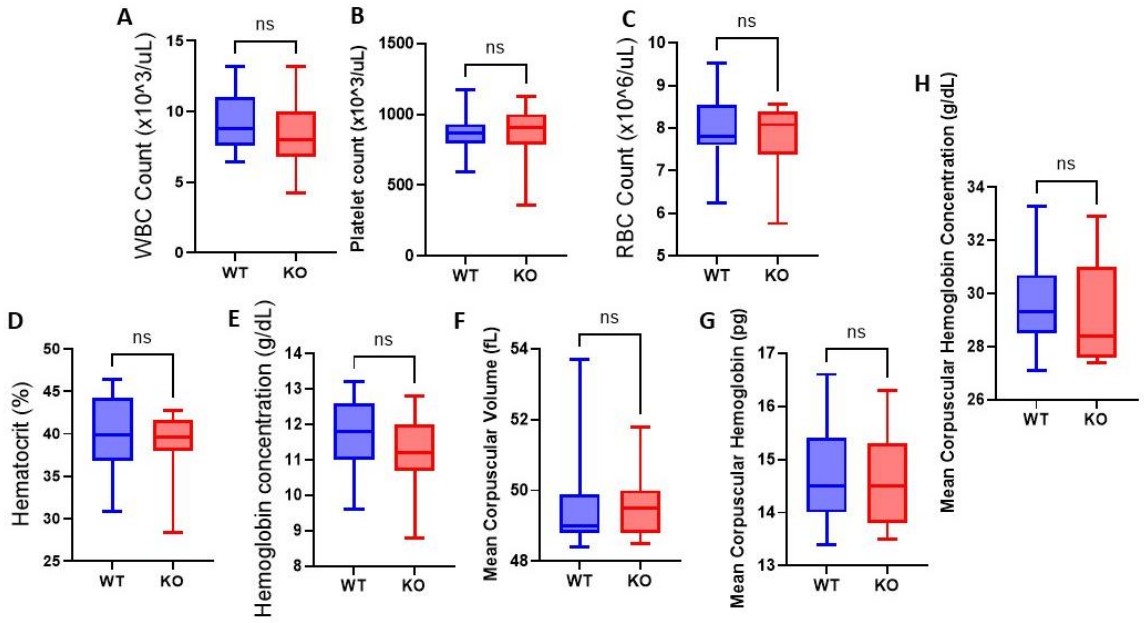

Figure 11. Full blood counts show haematopoiesis in WT and KO mice is un-altered
Full blood counts were taken following cardiac puncture immediately after bleeding and measured using a Sysmex XP300 haematology analyser. A) White blood cell count, B) Platelet count, C) Red blood cell count, D) Hematocrit, E) Hemoglobin concentration, F) Mean corpuscular volume, G) Mean corpuscular hemoglobin, H) Mean corpuscular hemoglobin concentration. Data represented as box and whisper plots showing mean, min and max values. Students t-test, ns = non significant ($P>0.05$), n=4.

3.3.3 Deletion of HSP47 in MKs does not alter ploidy

Megakaryocytes undergo a process of endomitosis, where each cell progresses through the cell cycle and undergoes repeated cycles of DNA replication without undergoing mitosis in order to become polyploid (Ebbe, 1976, Gurney et al., 1994). This results in the MK accumulating an increased DNA content. At this time the amount of protein and lipid synthesis within the megakaryocyte increases, and the cell increases its cytoplasmic content (Machlus and Italiano, 2013).

To measure whether HSP47 plays a role in the maturation of MKs, cells were observed whilst in culture in the presence of TPO, the ligand for the c-Mpl receptor which promotes MK growth and maturation (Kaushansky et al., 1994, Kuter et al., 1994). MKs were also cultured in the presence of recombinant hirudin, following Strassel *et al* identifying that hirudin increases the efficiency of culture *in vitro* to be more comparable of that *in vivo* (Strassel et al., 2012). DNA content was measured using Propidium iodide a dye which intercalates between DNA base pairs and is measured via flow cytometry.

Cells in culture, were grown in the presence of TPO and hirudin and were observed at 0, 2 and 5 days post isolation by DIC (Figure 12, A). In both control (WT) and HSP47 deficient (KO) cells at day 0, it is possible to see a large number of smaller cells. In both WT and KO samples it is also possible to see a number of larger cells, though there are more of the large cells in the WT sample. At day 2, it is possible to see more of the larger cells distributed through both WT and KO populations. At day 5, these larger cells are more abundant, and the smaller cells have also started to grow.

Propidium iodide was used to measure the ploidy number of megakaryocytes. Cells were isolated from the bone marrow then megakaryocytes were stained for CD41 before being fixed and permeabilised. Cells were then incubated with propidium iodide in the presence of RNase A, used to ensure PI binding to DNA as PI can also bind to RNA (see Section 2.2.2 for in depth protocol details). Cells were analysed using a BDAccuri C6Plus flow cytometer, where CD41 was used to gate for megakaryocytes and 5,000 cells were counted in this population per sample. B) shows the number of megakaryocytes within each polyploid state, and C) shows the mean ploidy of the total population measured. There is no significant difference between the control and HSP47 deficient MKs suggesting that HSP47 does not impact on MK maturation as determined by ploidy ($P>0.05$).

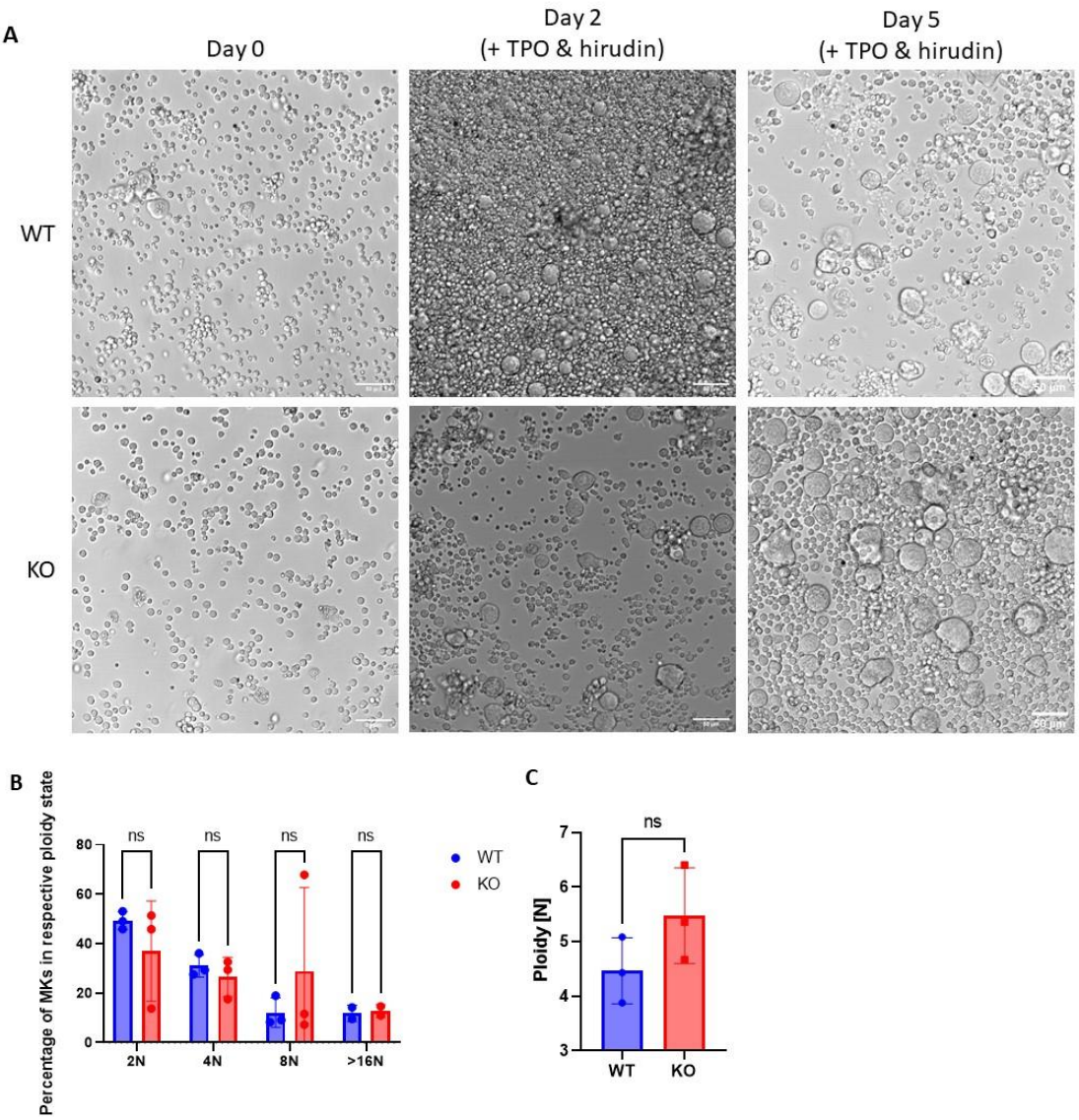

Figure 12. HSP47 deficient MKs become polyploid at a similar rate to control MKs.
A) Differential interference contrast microscope images of *wild type (*WT*) (MKs from WT mice)* and *knock out (*KO*) (MKs from KO mice)* megakaryocytes in culture after 0, 2 and 5 days in the presence of TPO and hirudin. Scale bar = 50µm. B&C) Cells were stained with FITC-CD41 and propidium iodide to determine the ploidy distribution via flow cytometry measured using a BD Accuri C6Plus. B) Percentage of MKs in each ploidy state. C) Average ploidy for each animal. Each data point is one animal, data is presented as mean ± SD. Students t-test, ns= non-significant (P>0.05), N=3.

3.3.4 Knockout of HSP47 has no impact on proplatelet formation

Megakaryocytes produce platelets in a multistep process that involves their migration from the centre of the bone marrow, the osteoblastic niche, to the vascular niche, nearer the sinusoidal blood vessels of the bone marrow (Machlus and Italiano, 2013). Tubulin drives cytoskeletal reorganisation, where cellular contents of the MK, including organelles and granules can be passed into proplatelets extending into the sinusoidal vessel and eventually into platelets in the circulation following release, as shown in Figure 1 (Hartwig and Italiano, 2006, Thon et al., 2010).

To identify the role of HSP47 in proplatelet formation, MKs were cultured for 5 days in the presence of TPO and hirudin. MKs were then separated using a BSA gradient involving gently prepared layers of 3% (w/v) BSA beneath 1.5% (w/v) BSA. Cells in complete DMEM were then gently placed on top of the 1.5% (w/v) BSA layer and allowed to settle using gravity, with larger more mature, heavier cells settling in the lower fractions. The larger, more mature cells were then incubated with a CO_2 independent medium (Gibco, CA, USA) which maintains the cellular environment without the need of a CO_2 incubator. MKs were imaged using a DIC microscope with a 40X objective over 24 hours at 37°C every 15 minutes in an Ibidi µ-well slide that had first been coated with 0.1% poly-lysine for 1 hour at RT before being washed once with ddH2O. Images were analysed by counting the number of proplatelet forming MKs present and determining the mean number of proplatelet forming MKs in each randomly selected field of view over 24 hours.

DIC microscopy images show MKs from control (WT) and HSP47 deficient (KO) mice producing proplatelets (Figure 13 A-D, A & B control, C & D HSP47 deficient mice, white box identifies zoomed in region). It is possible to see “string” like projections from cells, identified with white arrows, with “bead” like platelets forming along the string like extensions, identified with blue arrows (Figure 13 B.D). Tracking the percentage of proplatelet forming MKs at each timeframe shows that production from MKs from both control and HSP47 deficient mice is a dynamic process (Figure 13 E) and area under the curve (AUC) analysis identifies no significant difference in the AUC between the proplatelet formation by MKs from control and HSP47 deficient mice ($P>0.05$) (Figure 13 E). Quantification of the mean number of MKs forming proplatelets over 24 hours identified no difference when comparing MKs from control mice to those from HSP47 deficient mice ($P>0.05$) (Figure 13 G). This data suggests that HSP47 plays no role in proplatelet formation.

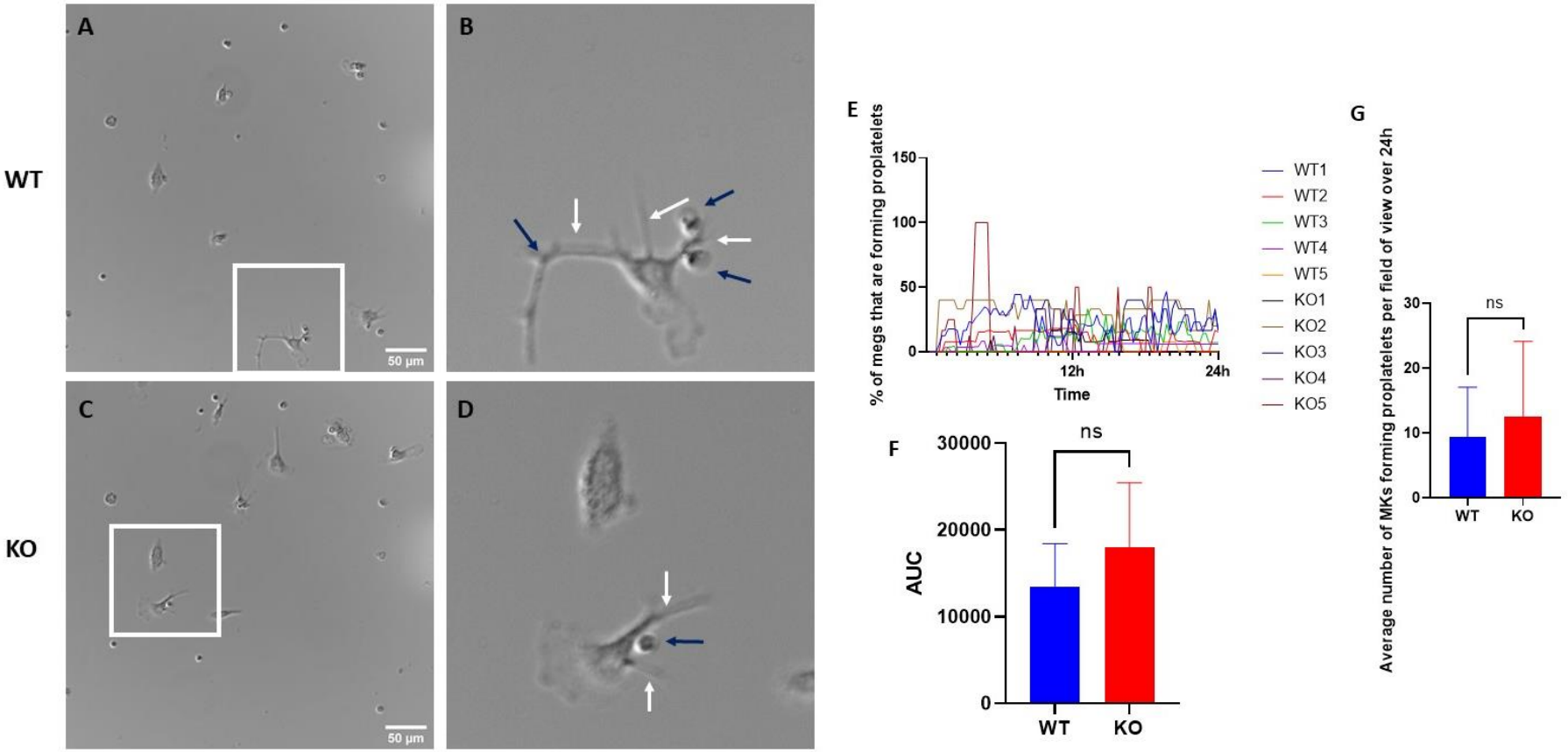
WT
KO
A
B
C
D
50 µm
50 µm
E
% of megs that are forming proplatelets
150
100
50
0
12h
24h
Time
WT1
WT2
WT3
WT4
WT5
KO1
KO2
KO3
KO4
KO5
F
AUC
30000
20000
10000
0
ns
WT
KO
G
Average number of MKs forming proplatelets per field of view over 24h
30
20
10
0
ns
WT
KO

Figure 13. HSP47 WT and KO megakaryocytes produce a similar yield of proplatelets
Megakaryocytes were allowed to mature for 5 days in the presence of 50ng/mL TPO and 10U/mL hirudin before being passed through a BSA gradient to separate the large, mature MKs from the smaller, less mature MKs. Mature MKs were resuspended in a CO_2 independent media to maintain a cellular environment without the need for a CO_2 incubator. Cells were imaged using a Nikon Ti2 differential interference contrast (DIC) microscope with a 40X objective every 15 minutes over 24 hours at 37°C in an Ibidi µ-well slide first coated with poly-lysine. A-D show representative DIC images of proplatelet formation, and zoomed in regions identified by the white box, of control (wild type – WT) (A, zoom = B) and HSP47 deficient (knock out – KO) (C, zoom = D) MKs. White arrows identify "string" like projections from the MK with blue arrows identifying "bead" like platelet structures on the strings. E) Percentage of proplatelet forming MKs per field of view over 24 hours. F) Area under the curve analysis of E. G) Average number of MKs forming proplatelets over 24hours. Data presented as mean ±SD. Students t-test, ns = non-significant (P>0.05), N=5

3.3.5 Collagen production is reduced from HSP47 deficient megakaryocytes

Collagen makes up an essential part of the extracellular matrix, where a network of proteins and macromolecules form a stable structure and contribute to the environment (Yue, 2014). The bone marrow (BM) environment has been shown to regulate MK maturation, migration, and function, with increased BM stiffness improving MK maturation and the presence of type I collagen in the osteoblastic niche inhibiting proplatelet formation (Aguilar et al., 2016, Reddi et al., 1977). Whilst the BM environment modulates MKs, MKs also support the bone marrow by releasing type IV collagen, fibronectin and laminin for the ECM, and also modulating other cells within the bone marrow due to the release of soluble factors from MKs regulating the quiescence of HSCs and migration of neutrophils within the marrow (Malara et al., 2014, Maximilian et al., 2020). Bone marrow fibrosis is characterized by increased deposition of reticulin fibres, formed of type III collagen, and in some cases increased deposition of collagen fibres, formed of type I collagen fibres (Kuter et al., 2007, Malara et al., 2018). Presence of collagen fibres are characteristic of advanced phases of myeloproliferative neoplasms (MPNs) therefore, our next step was to investigate whether in the absence of HSP47, MK production of collagen was reduced and would provide a therapeutic target for MPNs.

To investigate this, after cells ($3x10^6$ cells/mL) had been in culture in the presence of 50ng/mL TPO and 10U/mL hirudin for 5 days at 37°C in 5% CO_2, 2mL cell culture media was collected and newly synthesized, soluble collagen within the media was quantified. This process involved enzymatic degradation of collagen into glycine-rich oligopeptides which are quantified using a fluorogenic reagent and developer solution that selectively reacts with the N-terminal fragments (Abcam, Cambridge, UK).

MKs from control mice produced 1.5µg collagen, compared to 0.94µg collagen from HSP47 deficient MKs, a 37.6% reduction ($P<0.05$) suggesting that deficiency of HSP47 results in a reduction of collagen synthesis from MKs (Figure 14)

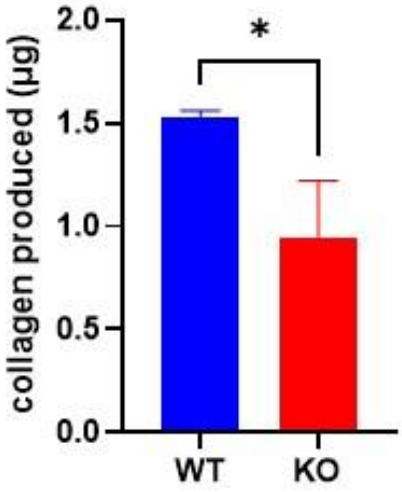

Figure 14. HSP47 deficiency reduces MK collagen production .
Spent media was collected from isolated control (wild-type, WT) and HSP47 deficient (knock-out, KO) megakaryocytes ($3x10^6$ cells/mL) cultured for 5 days in complete DMEM in the presence of 50ng/mL TPO and 10U/mL hirudin at 37°C in 5% CO_2. Newly synthesized, soluble collagen was quantified using a soluble collagen assay (Abcam, Cambridge, UK). Data presented as mean ±SD. Students t-test, * = P<0.5, N=4

3.3.6 Denaturation of collagen reduces the ability of platelets to form thrombi

Collagen is recognised to possess a triple helical structure, however the amount of triple helix present varies depending on the type of collagen. 96% of Collagen I comprises of triple helical structure, however they make up less than 10% of Collagen XII. The role of denatured collagen on platelet activation has never been investigated, even though there are a large number of collagen receptors on the platelet surface and collagen is one of the most potent platelet agonists. Clinically, tissues are heated as a treatment method for a number of diseases and injuries ranging from atherosclerotic plaques to menorrhagia and Parkinson's disease (Wright and Humphrey, 2002). Heating collagen to 54°C results in thermally induced structural changes, though whether this damage is reversible or not is a disputed topic (Sun et al., 2006). Genetic mutations in collagen can also result in a less stable structure, which plays a role in osteogenesis imperfecta (Kuivaniemi et al., 1991, Beck et al., 2000). Burns patients and wound healing may also be altered, leading us to question whether denaturing collagen impacts the ability of platelets to respond to collagen and activate.

To investigate the impact of heat denatured collagen on platelet recruitment and thrombus formation, T1 collagen was heated to RT (Native), 40°C and 60°C then 100µg/mL was coated onto Cellix Vena8fluro+ chips for one hour at RT before citrated whole blood stained with DiOC6 was perfused across at 1000^{s-1} (arterial shear rate) for 6 minutes at 37°C over a 20X objective on a Nikon A1 confocal microscope. Images were captured every 2 seconds, and then analysed using ImageJ to determine median fluorescence intensity and surface coverage of the field of view using a thresholding technique. Heat denatured collagen was also imaged using a Differential Interference Contrast (DIC) microscope.

DIC microscopy visualisation of native collagen, and collagen heated to 40 and 60°C (Figure 15 A, B, and C, respectively). In A and B it is possible to see long fibrils crossing the entire field of view however in C the fibrils are a lot shorter and it is possible to see where they have aggregated. After 6 minutes of thrombus growth, the median fluorescence intensity (MFI) was measured per frame (Figure 15 D), and the maximum fluorescence intensity measured in the field of view was calculated. Collagen heated to 40°C resulted in no change in platelet adhesion, measured by fluorescence, when compared to that of native collagen, but heating to 60˚C resulted in a ~75% reduction in fluorescence intensity, when compared to native ($P<0.05$). Platelet adhesion to collagen was also determined using a thresholding method, and similarly to when measuring MFI, collagen heated to 40°C resulted in no change in surface area covered by platelets when compared to that of native collagen. Heating collagen to 60°C resulted in a 75% reduction in surface coverage of platelets ($P<0.01$).

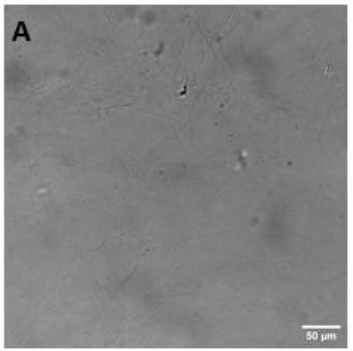
A
50 µm

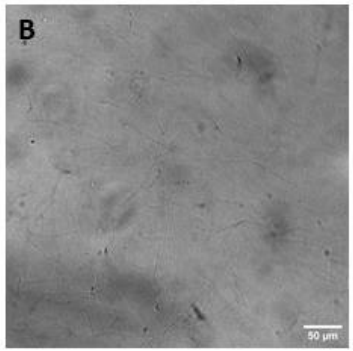
B
50 µm

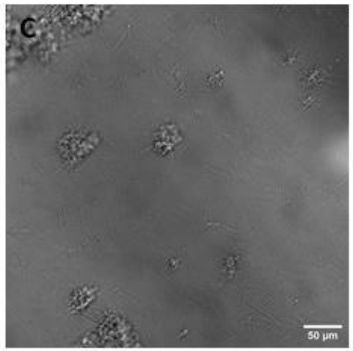
C
50 µm

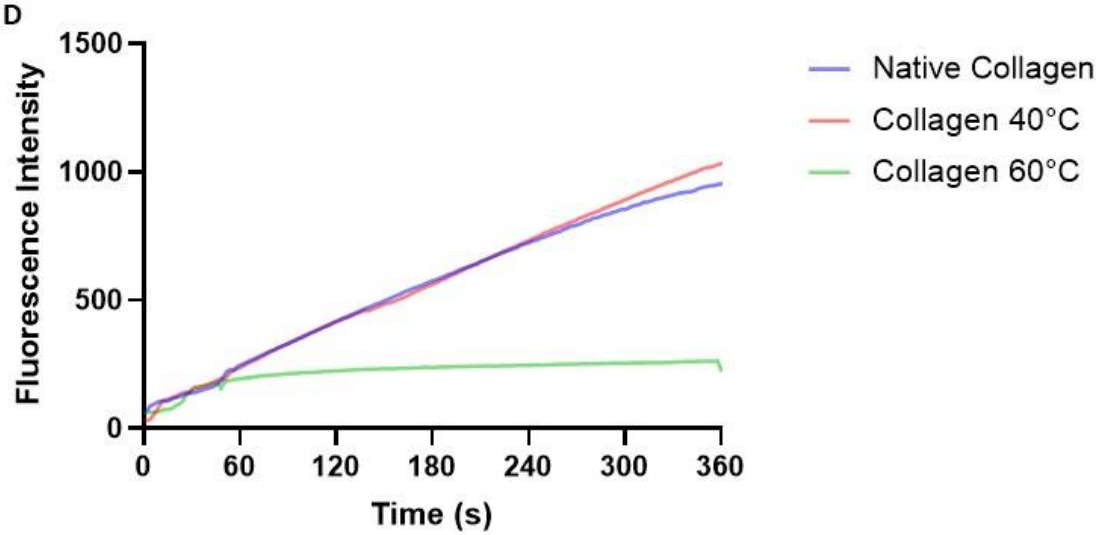
D
Fluorescence Intensity
1500
1000
500
0
0
60
120
180
240
300
360
Time (s)
Native Collagen
Collagen 40°C
Collagen 60°C

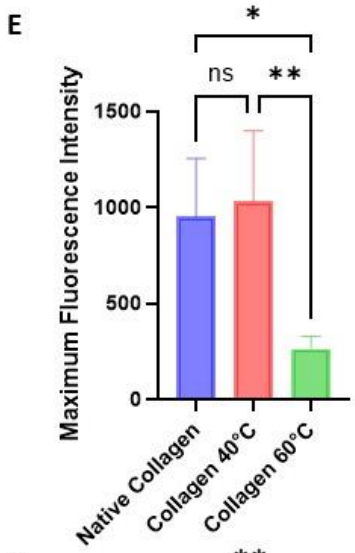
E
*
ns
**
Maximum Fluorescence Intensity
1500
1000
500
0
Native Collagen
Collagen 40°C
Collagen 60°C

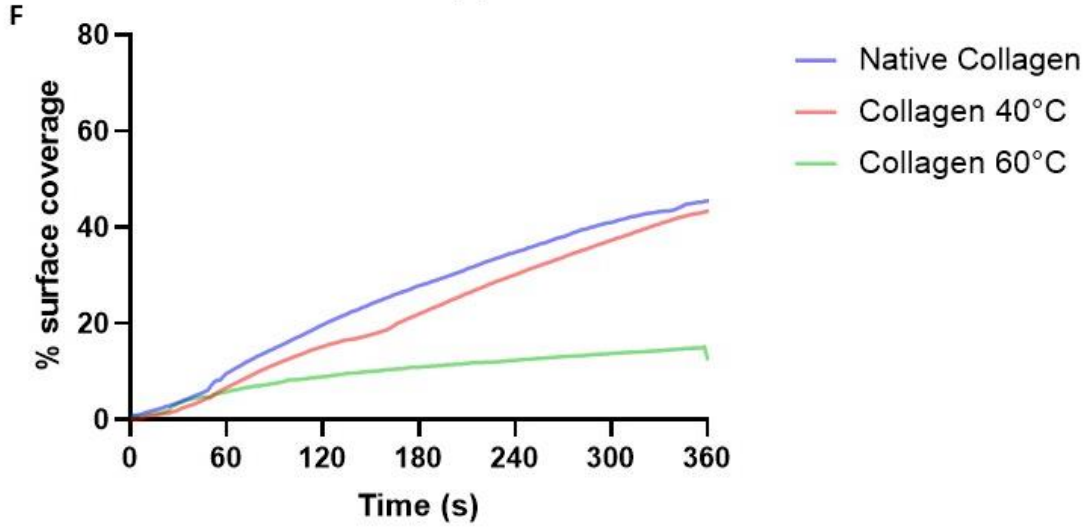
F
% surface coverage
80
60
40
20
0
0
60
120
180
240
300
360
Time (s)
Native Collagen
Collagen 40°C
Collagen 60°C

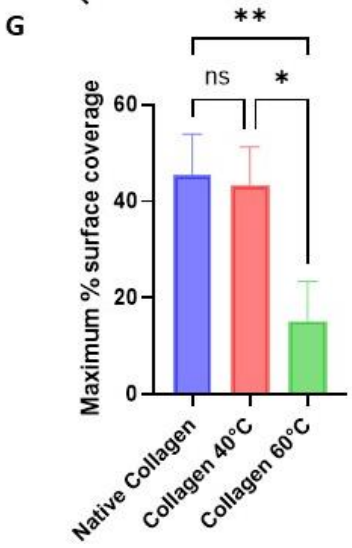
G
**
ns
*
Maximum % surface coverage
60
40
20
0
Native Collagen
Collagen 40°C
Collagen 60°C

Figure 15. Denaturing collagen fibrils impacts its ability to form thrombi
Heating collagen fibrils to 60°C for 10 minutes denatures fibrils and their ability to form thrombi. A-C) Differential interference contrast (DIC) microscope images of T1 collagen fibrils after 10 minutes of heating to RT (A), 40°C (B) and 60°C (C), scale bar = 50µm. Cellix Vena8 Fluoro+ channels were coated with 100µg/mL T1 Collagen which had been heated to RT (Native), 40°C or 60°C for one hour. Whole blood stained with DiOC6 was then perfused over the channel at 1000^{s-1} at 37°C for 6 minutes and imaged using a Nikon A1 Confocal microscope using a 20X objective. Microscope images were then analysed to determine the fluorescence intensity of the image and a thresholding method was used to determine the area of surface covered by adhered thrombi. D & E) Mean and maximum median fluorescence intensity. F & G) Mean and maximum percent surface coverage. D&F) Data presented as mean. E&G) Data presented as mean ±SD. One-way Anova with Sidak's multiple comparisons, ns = non-significant, P>0.05, * = P<0.5, ** = P<0.01, N=3.

3.3.7 HSP47 modulates collagen structure and its ability to support thrombus formation

Following the identification that denaturing collagen reduced the ability of platelets to form thrombi, and the knowledge that HSP47 binds to incorrectly folded collagen fibrils to prevent protein aggregates forming, we were interested to determine if HSP47 was able to modulate denatured collagen and support thrombus formation to be re-gained.

To investigate this, T1 collagen was heated to RT (Native), 40°C and 60°C then incubated with recombinant HSP47 (rHSP47) for 20 minutes at RT before being coated onto a Cellix chip for one hour at RT. Citrated whole blood stained with DiOC6 was then perfused across at 1000^{s-1} for 6 minutes at 37°C over a 20X objective on a Nikon A1 confocal microscope.

Using median fluorescence intensity (MFI) as a measure of platelet adherence and thrombi formation, we tracked the MFI per frame (every 2 seconds) and quantified the maximum fluorescence intensity over 6 minutes (Figure 16 A and B). As previously shown in Figure 15, collagen heated to 60˚C resulted in a 75% reduction in thrombus adhesion when compared to native collagen, an effect that was then reversed following the addition of rHSP47 to denatured collagen ($P<0.01$). Percent surface coverage was also calculated using a thresholding technique as an additional measure of platelet adhesion to collagen, quantifying per frame and the maximum percentage surface coverage over six minutes. Percent surface coverage also identified a 75% reduction in thrombus formation following denaturing of collagen at 60°C which was reversed following the addition of rHSP47 ($P<0.05$)

These results suggest that the addition of rHSP47 post collagen denaturation is able to modulate the structure of collagen and potentially return it to a structure capable of supporting thrombus formation.

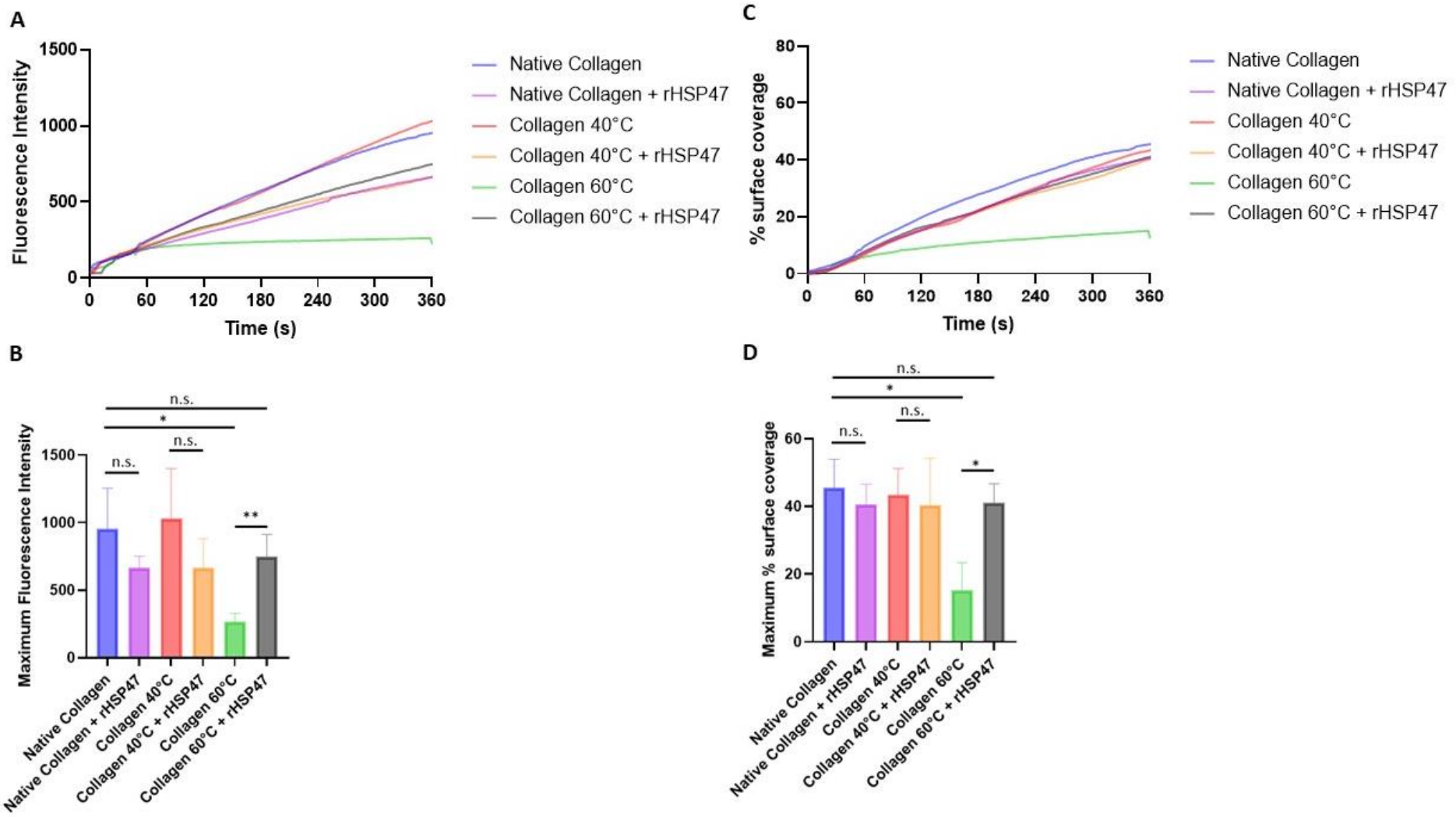
A
Fluorescence Intensity
1500
1000
500
0
0
60
120
180
240
300
360
Time (s)
Native Collagen
Native Collagen + rHSP47
Collagen 40°C
Collagen 40°C + rHSP47
Collagen 60°C
Collagen 60°C + rHSP47
C
% surface coverage
80
60
40
20
0
0
60
120
180
240
300
360
Time (s)
Native Collagen
Native Collagen + rHSP47
Collagen 40°C
Collagen 40°C + rHSP47
Collagen 60°C
Collagen 60°C + rHSP47
B
Maximum Fluorescence Intensity
1500
1000
500
0
n.s.
*
n.s.
n.s.
**
Native Collagen
Native Collagen + rHSP47
Collagen 40°C
Collagen 40°C + rHSP47
Collagen 60°C
Collagen 60°C + rHSP47
D
Maximum % surface coverage
60
40
20
0
n.s.
*
n.s.
n.s.
*
Native Collagen
Native Collagen + rHSP47
Collagen 40°C
Collagen 40°C + rHSP47
Collagen 60°C
Collagen 60°C + rHSP47

Figure 16. HSP47 reverses the impact of denatured collagen fibrils and its ability to form thrombi
Heating collagen fibrils to 60°C for 10 minutes denatures the tertiary structure of fibrils, a process which is reversed following treatment with recombinant HSP47. Cellix Vena8 Fluoro+ channels were coated with 100µg/mL T1 Collagen which had been heated to RT, 40°C or 60°C in the presence of rHSP47 for one hour at room temperature. Whole blood stained with DiOC6 was then perfused over the channel at 1000^{s-1} at 37°C for 6 minutes and imaged using a Nikon A1 Confocal using a 20X objective. Microscope images were then analysed to determine the fluorescence intensity of the image and a thresholding method was used to determine the area of surface covered by adhered thrombi. A) Average fluorescence intensity of all coatings. B) Maximum fluorescence intensity. C) Average surface coverage of all coatings. D) Maximum surface coverage. Data presented as mean ±SD. One-way Anova with Sidak's multiple comparisons, ns = non-significant, * = P<0.5, ** = P<0.01, N=3.

3.3.8 HSP47 binds to denatured type I collagen, but not type II or III

We previously showed that HSP47 was able to restore denatured type I collagen to a state where platelets are able to bind and form thrombi. This then opened the question as to the ability of recombinant HSP47 to bind to different collagens in their native and denatured state. Firstly, this would help to understand whether the effect of rHSP47 on denatured collagen in thrombus formation was due to the ability of HSP47 to bind to collagen itself or if HSP47 is altering the ability of the platelet to respond to the denatured collagen. Secondly, this would allow us to test how HSP47 binds to a number of different types of collagen, particularly important as there are a range of collagen types present within the blood vessel wall.

A protein binding assay was used to investigate this. Briefly, collagens were denatured at RT (Native), 40°C and 60°C before 100µg/mL was coated on a 96 well flat bottom clear plate before being blocked with 5% (w/v) BSA, then 1µg His tagged rHSP47 added. Unbound protein was removed after one hour, then protein bound was measured using HRP-anti-His antibodies, TMB substrate was allowed to develop for 150 seconds before being stopped using stop solution and absorbance was measured at 450nm using a FlexStation2 (Molecular Devices, Winnersh, UK). A more in-depth protocol is provided in Section 2.2.6.

rHSP47 is able to bind to TI collagen, with no difference in the amount of protein bound following denaturing at 40°C ($P>0.05$) and 60°C ($P>0.05$) (Figure 17, A), confirming that the results presented previously, where rHSP47 was able to reverse the impact of denatured collagen on thrombus formation (Figure 16).

rHSP47, however, is not able to bind TII or TII collagen after denaturation at 60°C, with a 75% reduction in binding to TII collagen ($P<0.005$) (Figure 17, B) and a 59% reduction in binding to TIII collagen ($P<0.01$) (Figure 17, C). rHSP47 binding to TII and TIII collagen after denaturation at 60°C was equivalent to that of a negative control, BSA ($P>0.05$). This suggests that HSP47 is able to bind and modulate TI collagen, but not TII and TII and that if we repeated the thrombus formation experiment performed previously in sections 3.3.5 and 3.3.6 with thermally denatured TII and TIII collagen in the presence of HSP47 there would be no restoration in thrombus formation.

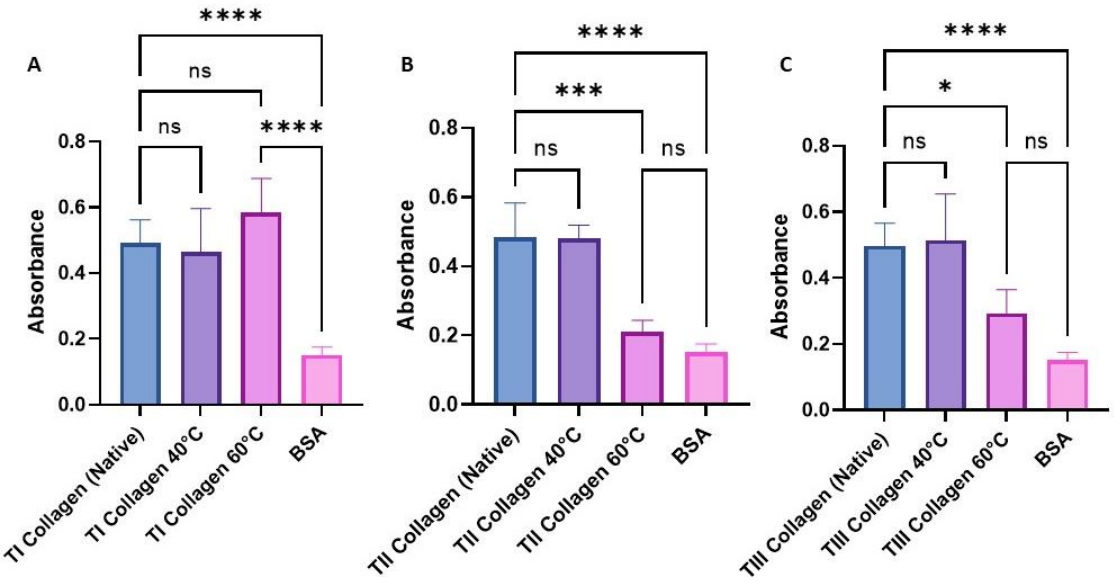

Figure 17. HSP47 binds to denatured Coll I, but not denatured Coll II or Coll III
Type I, II and III collagens were heated to RT (Native), 40 and 60°C then added to a 96 well plate for one hour. Samples were then blocked with 5% (w/v) BSA for one hour before washing 3x then 100µL 10ug/mL His tagged recombinant HSP47 was added to collagen coated wells for one hour. Unbound protein was removed then samples washed 3x again. Bound his-tagged protein was detected using HRP anti-His antibody, then HRP was detected by TMB Elisa substrate binding and stop solutions and absorbance (450nm) measured using a FlexStation2 (Molecular Devices, Winnersh, UK). A, B, and C) Type I, II and III collagens, respectively. Data presented as mean ±SD. One way Anova with Sidaks multiple comparisons, ns = non significant, P>0.05, ** = P<0.01, *** and **** = P<0.005, N=3.

3.4 Discussion

In this chapter, we gained a further understanding of the role HSP47 plays in regulating collagen. Previous work identified that cellular HSP47 binds to nascent procollagen chains in the ER and remains bound to these chains during their transport to the Golgi. HSP47 is then recycled back to the ER. HSP47 was also identified to be important for platelet function, with Sasikumar *et al.* presenting data suggesting that HSP47 plays a role in collagen, but not thrombin stimulated aggregation, thrombus formation and extending tail bleeding times (Sasikumar et al., 2018).

We have identified, using megakaryocyte lineage specific knock out mice, that in the absence of HSP47 collagen synthesis is reduced. In the bone marrow, where haematopoiesis works to maintain our red and white blood cell population, the extracellular matrix plays an essential role in maintaining the environment for these populations to be regulated. Megakaryocytes play a vital role in regulating the maintenance of the bone marrow environment, producing TIV collagen, fibronectin and laminin in order to support the environment and assist in haematopoiesis (Malara et al., 2014). Blood counts from megakaryocyte-specific HSP47 deficient mice suggest haematopoiesis is unaltered (Figure 11) suggesting that the reduction in collagen production has no effect on the differentiation and maturation of blood cells from HSCs. We can not, however, rule out the possibility that throughout development the mice have come to a state of “normal” over time and in response to a challenge such as experimentally induced thrombocytopenia or haemorrhage, would be able to regain this state.

Megakaryocytes from HSP47-deficicient (KO) mice were determined to become polyploidy at a similar rate to those from control (WT) mice, suggesting that MK maturation occurs independently of HSP47 (Figure 12). Pallotta *et al* found that HSCs, in the osteoblastic niche (ON), deposit Collagen I, and though and interaction with α2β1 on the MK, support MK differentiation but not maturation or proplatelet formation (Arai and Suda, 2007, Pallotta et al., 2009, Sabri et al., 2004, Sabri et al., 2006, Zou et al., 2009). Supporting this, we identified that MKs from HSP47 deficient mice still form proplatelets (Figure 13) suggesting that collagen is not required for this process. Proplatelet production begins after MKs have migrated to the vascular niche (VN), an area rich in Collagen IV, fibronectin and fibrinogen (Machlus and Italiano, 2013). The presence of collagen I here may result in platelet activation, so its absence is not a surprise.

We have identified that megakaryocytes isolated from KO mice produce less collagen than those from WT (Figure 14). The assay used measures total, newly synthesized soluble collagen,

so further investigation is required to determine if this is a reduction in total collagen or a specific type. These results support our hypothesis that HSP47 may act as a therapeutic target for myelofibrosis. Recently, it has been suggested that there are two populations of megakaryocytes in the bone marrow – those that secret growth factors and support the bone marrow environment, and those that migrate through the bone marrow to produce proplatelets. We did not attempt to differentiate between these populations in this study, however if we were able to specifically target HSP47 in the regulatory population of MKs, it would further encourage the use of HSP47 as a therapeutic target for myelofibrosis, though not ET as our results suggest no differences in proplatelet production.

We have also identified that HSP47 is able to bind to thermally denatured type I, but not type II or III collagen (Figure 17). In binding to TI collagen, HSP47 is able to reverse the impact that thermal denaturing of TI collagen to 60°C has on thrombus formation, though the mechanism of this is not understood. We suggest two different explanations of this result: HSP47 is able to bind and interact with denatured collagen, returning TI collagen to its native state and supporting platelet adhesion and thrombus formation. The alternative mechanism involves regulation of the platelet collagen interaction, and that the additional HSP47 present in the chip supports platelet adhesion to collagen. This second option supports previous work from the Gibbins lab on HSP47, where AlOuda *et al* identified that HSP47 colocalises with, and supports GPVI dimerization and signalling (AlOuda *et al.*, Under review). It would be interesting to understand the impact of denatured TII and TIII collagen on thrombus formation. TII collagen, a homotrimeric molecule composed of three identical αI(II) chains mainly expressed in the cartilage, has been shown to support platelet adhesion mediated by α2β1 as efficiently as TI, but there is very little other data regarding TII collagen-platelet interactions (Guidetti et al., 2003). TIII collagen, also found in the blood vessels as well as in the skin and lungs, is also able to support adhesion and aggregation like TI, so it is surprising the HSP47 is able to bind to thermally denatured TI but not TIII collagen (Morton et al., 1989) (Monnet and Fauvel-Lafève, 2000)

These results suggest that HSP47 is able to regulate megakaryocytic collagen synthesis, and is also able to support TI collagen -platelet responses, even in the occurrence of thermal denaturation.

Chapter 4-HSP47 has dual functionality within platelets

4.1 Introduction

Platelet receptors play an instrumental role in the initiation of platelet-platelet aggregation and thereby thrombus formation, but also allow for interactions between platelets and leukocytes, endothelial cells and coagulation factors with functions including antimicrobial activity, angiogenesis, tumour growth and metastasis (Muller, 2003, Yeaman, 1997, Klement et al., 2009, Labelle et al., 2011). Platelet disorders generally fall into two groups (Palma-Barqueros et al., 2021):

1) Inherited thrombocytopenias, where patients present with low numbers of platelets ranging from small to large in size and include Grey platelet syndrome where patients present with grey-ish coloured platelets and lack α granules resulting in a lack of vWF; and Wiskott-Aldrich syndrome where patients present with severe thrombocytopenia, immunodeficiency and autoimmune disorders due to a mutation in WAS gene and the resulting lack of any functional WASP protein, essential for cellular surface-actin cytoskeleton communication (Kirchhausen and Rosen, 1996).
2) Inherited platelet function disorders, characterised by dysfunctional platelets as a result of defects in receptors, granules or elements involved in signal transduction/cellular machinery, include Bernard-Soulier syndrome, where mutations in GPIb-IX-V subunits, result in prolonged bleeding and large platelets and Glanzmann Thrombasthenia in which platelet aggregation is severely reduced and clot retraction is reduced due to absence or functional loss of αIIbβ3 (Berndt and Andrews, 2011) (Nurden and Pillois, 2018).

The first disorders of platelet receptors were first described by Glanzmann and Bernard, after which structure and function of receptors was extensively studied, since identifying pathologies related to mutations in CalDAG-GEF1, $P2Y_{12}$, GPVI, and others (Canault et al., 2014, Cattaneo et al., 1992, Moroi et al., 1989, Nurden et al., 2021). Platelets contain a wide variety of receptors, including integrins, leucine-rich repeats, selectins, tetraspanins, transmembrane, prostaglandin, lipid, immunoglobulin superfamily and tyrosine kinase receptors providing a large number of proteins in which mutations may lead to bleeding disorders (Saboor et al., 2013).

Collagen is the most abundant protein in the body, with its multiple family members making up the major constituents of the ECM of blood vessels and are extremely thrombogenic. There

are a number of collagen receptors on the platelet surface, including integrin α2β1 and GPVI. These receptors are often involved in the initial stages of platelet activation, stimulated in platelets at the base of a thrombus and their downstream signalling cascades result in release of ADP and TxA_2, resulting in increased platelet accumulation, activation and aggregation.

HSP47 has been shown to bind to collagen, and inhibition of HSP47 in platelets results in a collagen specific inhibition of activation, a process which may be mediated through interactions with the platelet specific collagen receptor, GPVI (Sasikumar et al., 2018)(AlOuda *et al.*, Under review). In the previous chapter we demonstrated that HSP47 deficiency results in reduced megakaryocyte collagen synthesis and is able to bind to and modulate platelet responses to denatured collagen, however we have not investigated the possibility that HSP47 itself may act as a collagen receptor.

In order to understand this, we will use HSP47 binding sequences identified within collagen II and III as agonists, and test different aspects of platelet function to determine if HSP47 alone is able to initiate platelet activation/aggregation. The HSP47 binding sequences within collagen have been identified from the collagen toolkits (Cai et al., 2021). These are a bank of peptides, developed by Prof. Farndale (Cambcol, Ely) that have been used to elucidate the role of specific sequences within collagen II and III. An example of this, is the identification of the GPO and GFOGER sequences, the binding/activation sites of GPVI and integrin α2β1 respectively (Morton et al., 1995, Knight et al., 1999, Knight et al., 2000). Multiple GPO repeats, flanked by GPC which gives collagen its triple helical structure, are able to specifically activate GPVI and is known as collagen-related peptide (CRP, when crosslinked CRP-XL). We use a number of toolkit peptides in this study, chosen for either their ability to bind HSP47 to further understand the role HSP47 plays on platelet function; or those which do not bind HSP47 as controls to ensure any responses observed are due to the guest sequence and not the flanking sequence, included to maintain a triple helical structure. These sequences are presented in

Table ***7***.

We have shown that HSP47 is able to bind to a number of sequences within the collagen toolkits, and proposed that further investigation will help us to understand the importance of these sequences and the mechanisms of HSP47 function.

Table 7. Collagen toolkit peptides used in this study, the guest sequence of the peptide and mean absorbance to HSP47

Collagen II		
Peptide	**Guest sequence**	**Mean A_{450}**
13	GAKGSAGAOGIAGAOGFOGPRGPOGPQ	>1.5
14	GPRGPOGPQGATGPLGPKGQTGEOGIA	>2
20	GANGDOGROGEOGLOGARGLTGROGDA	>2
26	GERGEQGAOGPSGFQGLOGPOGPOGEG	>1.5
33	GAOGKDGGRGLTGPIGPOGPAGANGEK	<0.5
Collagen III		
Peptide	**Guest sequence**	**Mean A_{450}**
5a	GERGLOGPOGIKGPAGIO	>1.5

4.2 Results

4.2.1 HSP47 binding sequences are unable to directly stimulate platelet aggregation

Within haemostasis, platelets play a vital role in the maintenance of the circulatory system and respond to stimuli in order to plug a break within blood vessels. To do this, platelets accumulate resulting in the formation of a platelet thrombus. Measurement of platelet aggregation is often the first step in platelet function tests, so to identify whether HSP47 acts as a receptor on the platelet surface we used peptides from the collagen toolkits that are known HSP47 binding sequences as a stimuli. Of the 113 toolkit peptides, 12 were identified to be HSP47 binders: Coll II 14 and Coll II 20 bound recombinant HSP47 with the highest affinity, followed by Coll II 13, Coll II 26 and Coll III 5, then Coll II 11 and finally Coll II 10,17 24, 39, Coll III 14 and Coll III 30 (Cai et al., 2021). It was also identified that HSP47 bound extremely well to the integrin α2β1 binding sequence, GFOGER.

Light transmission aggregometry (LTA) has been used to measure platelet activation and aggregation since the development of the first aggregometer in the early 1960's (Born, 1962). After the preparation of platelet rich plasma (PRP) or washed platelets (WP) and the addition of a platelet agonist in stirring conditions, as platelet aggregates form, platelets fall out of suspension and light transmitted through the sample increases. It is also possible to measure aggregation in a plate-based (plate-based aggregation, PBA) assay, which requires fewer platelets, a reduced volume of agonists and allows for higher throughput, measuring aggregation in 96 samples within seconds. We wanted to identify whether HSP47 binding sequences were able to initiate platelet aggregation, using a PBA approach in order to measure a range of concentrations of different toolkits simultaneously. This would allow us to measure platelet responses to the HSP47 binding sequences without platelets "aging" and responses going off over time.

Washed human platelets were incubated with a 10μg/mL of toolkit peptides Coll II 13, 14,20 26 and Coll III 5a (Coll III 5 is unstable at 37°C, even after crosslinking, an effect that is reduced upon truncation of the peptide). These peptides were chosen as they were the sequences that showed the highest affinity to rHSP47. WP and HSP47 binding sequences were incubated in wells of a 96well half area flat bottom plate at 37°C and shaken at 1200rpm for 5 minutes using a plate shaker. Absorbance was read at 405nm and values adjusted to % aggregation using washed platelets and Tyrodes to calibrate 0% and 100% aggregation, respectively.

All five HSP47 binding sequences were unable to initiate aggregation at 10µg/mL. This was compared to platelets incubated with T1 collagen, to ensure platelets are responsive ($P<0.005$) (Figure 18 A). To determine if HSP47 required an increased level of binding site saturation to initiate aggregation, the assay was repeated using 30µg/mL of toolkit peptides. Again, these sequences were unable to initiate aggregation when compared to the response of T1 collagen ($P<0.005$) (Figure 18 B).

Platelet aggregation requires the initiation of a sequence of signalling events that in turn initiate further platelet recruitment and activation in a paracrine mechanism for an aggregate to occur, so to determine if HSP47 binding sequences were able to activate platelets but are unable to initiate aggregation we measured two key steps in platelet activation: granule secretion, measured by the increased presence of P-selectin on the platelet surface and integrin αIIbβ3 activation, measured by fibrinogen binding to the platelet.

Washed human platelets were stimulated with 10µg/mL toolkit peptides in the presence of an anti- CD62P antibody and an anti-fibrinogen antibody before being analysed using a BD-Accuri C6plus flow cytometer. CRP-XL was used as a positive control, to ensure that platelets used in this assay were responsive to activation, and Tyrodes as a negative control to ensure that platelets were indeed resting before exposure to agonists/HSP47 binding sequences.

Quantification of the MFI of these samples identified that exposure of washed platelets to HSP47 binding sequences did not result in granule secretion (Figure 18 C) or integrin αIIbβ3 activation (Figure 18 D). For all HSP47 binding sequences, both P-selectin exposure and fibrinogen binding identified no increase following exposure to HSP47 binding sequences from the resting sample ($P>0.05$) and significantly lower than the MFI measured from platelets exposed to CRP-XL ($P<0.005$).

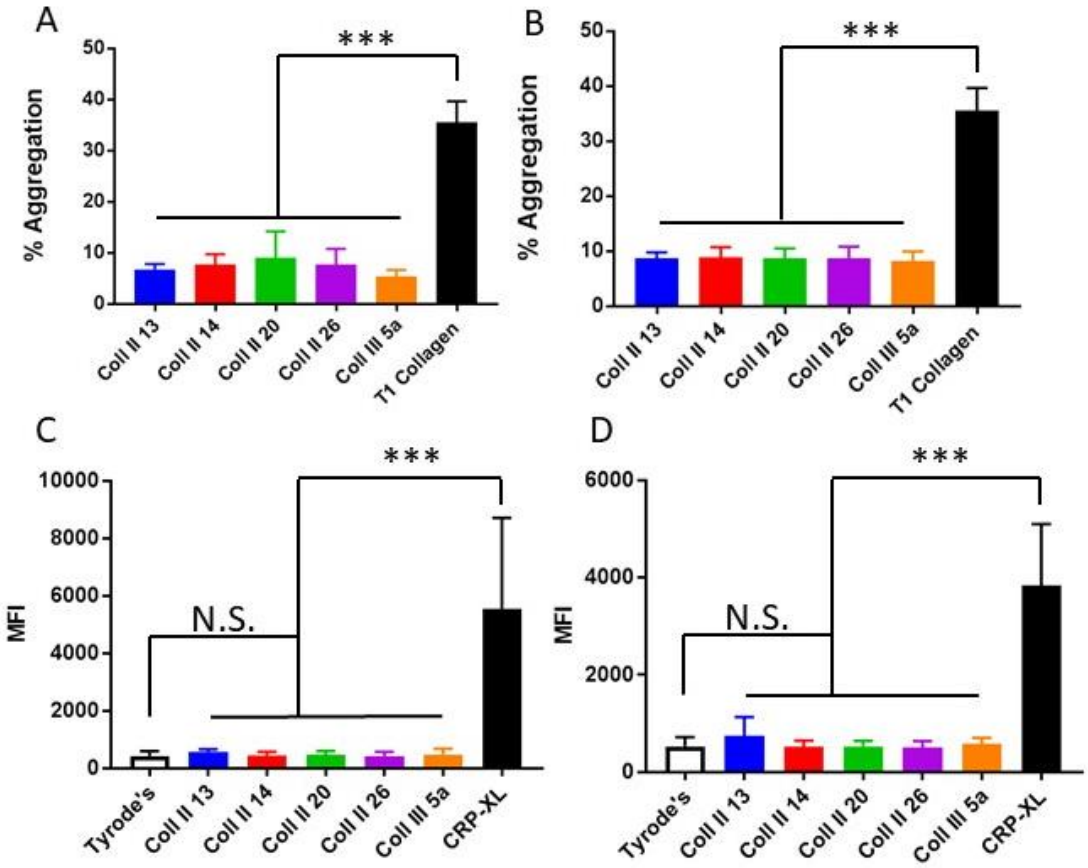

Figure 18. Platelets do not to aggregate or activate in response to HSP47 binding sequences
A,B) Washed platelets (4x10^8 cells/mL) were incubated with A)10 µg/mL or B) 30 µg/mL peptide in a flat bottom, half area 96-well plate at 37°C and stirred at 1200RPM using a plate shaker. Washed platelets were also incubated with 1µg/mL TI collagen as a positive control. Absorbance was measured at 405nm using FlexStation2 (Molecular Devices, Winnersh) and converted to percentage aggregation. C,D) Washed platelets (4x10^7cells/mL) were incubated with Tyrodes buffer, 10µg/mL peptide, or 1µg/mL CRP-XL in the presence of anti P-Selectin © and anti-Fibrinogen (D) antibody for 20 minutes at room temperature before fixing and fluorescence was analysed using a BD-Accuri C6Plus flow cytometer (BD, Winnersh). Platelets were incubated with Tyrodes to identify a measure of fluorescence when resting, and TI collagen to ensure platelet responsiveness to the assay. One-way Anova with Dunnett's multiple comparison of peptide treatment compared to Tyrode's/Collagen/CRP-XL. Data presented as mean ± SD, n=3, *** indicates P<0.005, N.S. = non-significant, P>0.05.

4.2.2 HSP47 binding sequences support platelet adhesion and shape change

The ability of platelets to change shape and spread their cellular contents into a larger, thinner cell, and therefore increase their surface area is also an essential process that allows platelets to interact with a larger area following vascular trauma and form a haemostatic plug (Furie and Furie, 2008). α2β1, a collagen receptor found on the platelet surface supports adhesion and shape change following interaction with collagen but does not initiate aggregation (Jarvis et al., 2004). This observation, that it is possible for some collagen receptors to support some platelet functional responses without initiating aggregation, led us to question whether HSP47 might have a similar effect, and that platelets would adhere and change shape in response to HSP47 binding sequences.

To investigate this, glass coverslips were coated with 10µg/mL toolkit peptides or 100µg/mL TI collagen and coated overnight for 1 hour at 4°C. Coverslips were then blocked with heat deactivated BSA to prevent any unspecific binding, with additional wells blocked with the same BSA to act as a negative control. $2x10^7$ cells/mL washed platelets were allowed to adhere/spread onto the coverslips for 45 minutes at 37°C. Samples were then fixed, permeabilised then stained using fluorophore labelled Phalloidin to allow identification of the platelet cytoskeleton. Samples were imaged on a Nikon A1 Confocal using a 100x oil objective. Three randomly chosen fields of view per coverslip were taken and images analysed to determine the number of platelets adhered to each coverslip.

The number of platelets per field of view allows quantification of adherence to the surface. Using this method, we were able to identify that platelets were able to adhere to all HSP47 binding sequences significantly more than they do to the negative surface control (BSA) ($P<0.05$) (Figure 19 A). Platelet adherence to TI collagen was also measured to ensure functional platelet responses and identified an increase in platelet adherence when compared to that in response to HSP47 binding sequences ($P<0.05$) (Figure 19 B). This suggests that platelets are able to adhere to HSP47 binding sites.

The ability of a platelet to change shape is an import process in platelet activation. Using the same images as used to analyse the number of platelets adhered, platelets were classified into four different groups:

1) Resting, discoid platelets
2) Presence of filopodia – individual cytoskeletal projections only
3) Presence of lamellipodia – cytoskeletal projections had been joined forming a web like

structure

4) Fully spread platelets, 'fried egg shape'

The percentage of platelets per field of view in each group was calculated to identify if there was a difference between the ability of platelets to spread on TI collagen or HSP47 binding sequences. No difference was identified suggesting that adhesion to HSP47 binding sequences supports full shape change ($P>0.05$).

After identifying that platelets are able to adhere to HSP47 binding sequences, we wanted to ensure this was a process mediated through HSP47.

To investigate this, washed platelets were pre-incubated with a small molecule inhibitor of HSP47 (SMIH) or an inhibitory HSP47 antibody (αHSP47) which blocks its function. Platelets were then allowed to spread on HSP47 binding sequences before being fixed, permeabilised, stained using fluorophore labelled Phalloidin and imaged, as mentioned previously.

The number of platelets adhered to Coll II 13 was reduced by 34% following preincubation with SMIH ($P<0.01$) and 68% following pre-incubation with αHSP47 ($P<0.05$) (Figure 20, A, F, K and P). SMIH and αHSP47 reduced platelet adherence on Coll II 14, SMIH by 53% and αHSP47 by 67% though only αHSP47 resulted in a significant reduction ($P<0.05$) (Figure 20, B, G, L and Q). Both SMIH and αHSP47 resulted in a reduction in platelet adherence to Coll II 20, with adherence reducing by 54% in the presence of SMIH and 45% in the presence of αHSP47 ($P<0.01$) (Figure 20, C, H, M and R). Adherence to Coll II 26, like that of Coll II 14, was reduced in the presence of αHSP47 (33%) ($P<0.01$) however a 22% reduction in the presence of SMIH was not deemed significant ($P>0.05$) (Figure 20, D, I, N and S). Platelet adherence to Coll III 5a was not altered in the presence of either SMIH or αHSP47 (Figure 20, E, J, O and T).

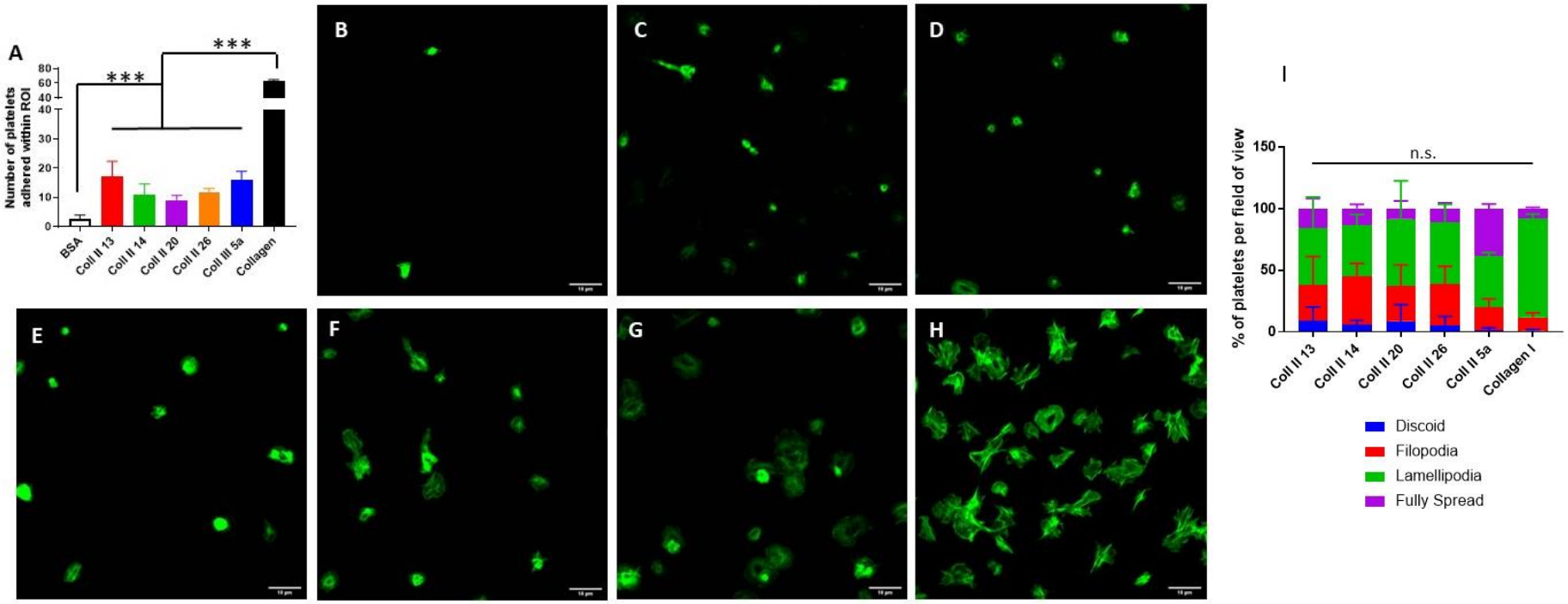
A
***
***
Number of platelets adhered within ROI
80
60
40
40
30
20
10
0
BSA
Coll II 13
Coll II 14
Coll II 20
Coll II 26
Coll III 5a
Collagen
B
C
D
E
F
G
H
I
n.s.
% of platelets per field of view
150
100
50
0
Coll II 13
Coll II 14
Coll II 20
Coll II 26
Coll II 5a
Collagen I
Discoid
Filopodia
Lamellipodia
Fully Spread

Figure 19.Platelets spread on HSP47 binding sequences
Glass coverslips were coated with 10µg/mL toolkit peptides or 100µg/mL collagen overnight at 4°C. Coverslips were then blocked with BSA with additional wells coated to act as negative controls for one hour at RT before washed platelets ($2x10^7$ cells/mL) were allowed to adhere and spread for 45 minutes at 37°C. Platelets were then fixed, permeabilised, stained using Alexa-488 conjugated Phalloidin (1:750 in PBS) and mounted onto slides. Images were acquired using 100x Nikon A1 confocal microscope X100 oil immersion lens and analysed using ImageJ. A) Number of platelets adhered and spread on toolkit peptides per field of view. B-H) Representative images of samples from B) BSA, C) Coll II 13, D) Coll II 14, E) Coll II 20, F) Coll II 26, G) Coll III 5a, and H) Collagen. One-way Anova with Dunnetts multiple comparisons of number of platelets adhered on peptides compared to BSA or Collagen; *** = P<0.005.I) Two-way Anova with Dunnetts multiple comparisons of percentage of platelets per field of view, in each classification, on different surface coatings. n.s. = non-significant, P>0.05. Images shown are representative of three random images taken per condition from four independent experiments. Scale bar = 10µM, n=4.

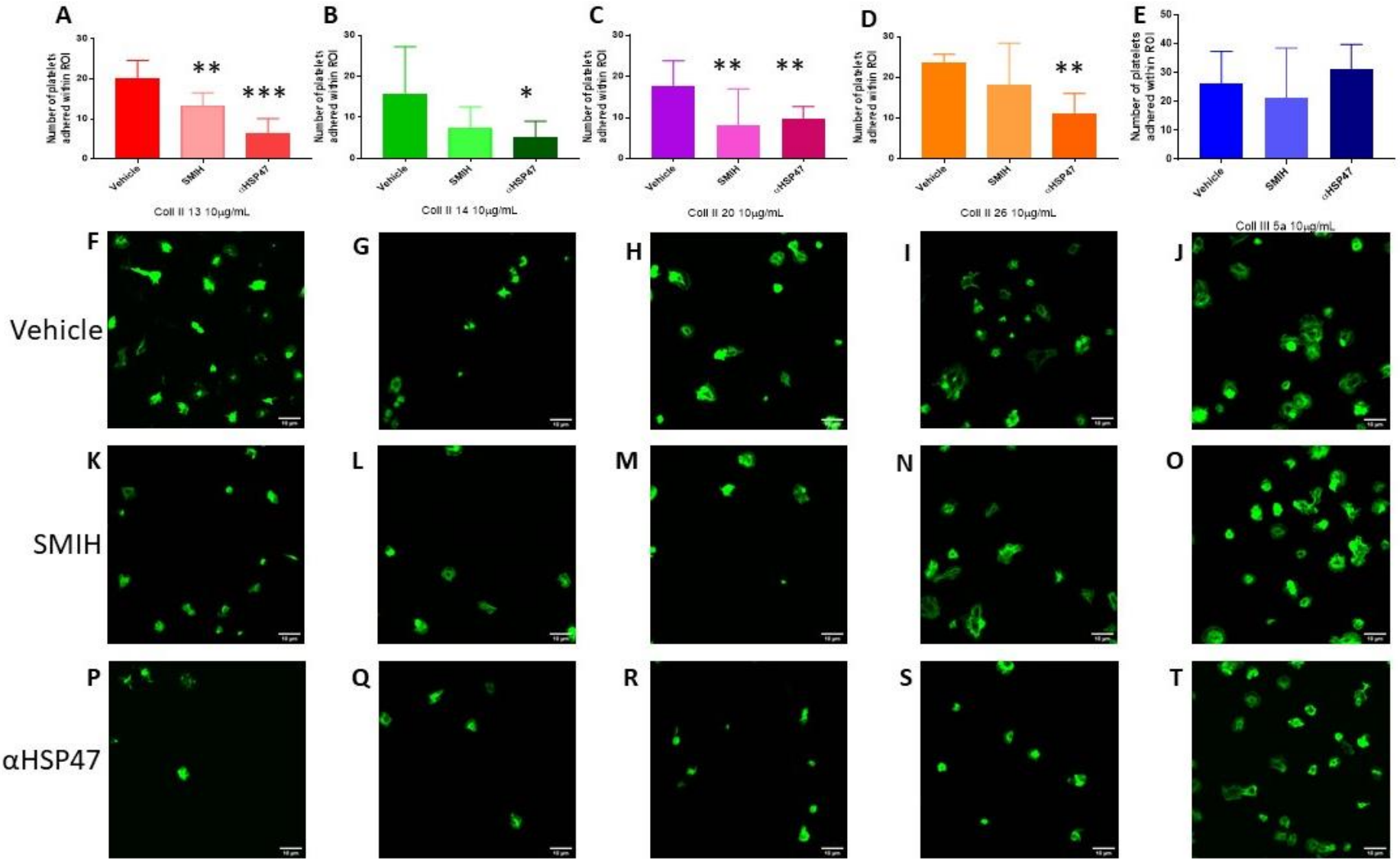
A
B
C
D
E
Number of platelets adhered within ROI
Vehicle
SMIH
αHSP47
**
***
*
Coll II 13 10μg/mL
Coll II 14 10μg/mL
Coll II 20 10μg/mL
Coll II 26 10μg/mL
Coll III 5a 10μg/mL
F
G
H
I
J
K
L
M
N
O
P
Q
R
S
T
Vehicle
SMIH
αHSP47

Figure 20. Platelet adherence to HSP47 binding sequences is HSP47 dependent
Platelets ($2x10^7$) were incubated with Vehicle (1% (v/v) DMSO), 10µg/mL SMIH or 10µg/mL αHSP47 for 15 minutes prior to platelets being left to adhere and spread on coverslips for 45 minutes at 37°C. Samples were then fixed, permeabilised, stained and imaged and analysed as above. A-E) Number of platelets adhered per field of view on Coll II 13, 14, 20, 26, and Coll II 5a; ± vehicle, SMIH or αHSP47. F-T) Representative images for all conditions, scale bar = 10µm. One-way Anova with Dunnetts multiple comparisons of SMIH/αHSP47 compared to vehicle; $P<0.05$, 0.01, 0.005: *, **, *** respectively. Results are mean ± SD, n=4 with three random images taken per condition.

4.2.3 HSP47 binding sequences are unable to support thrombus formation at arterial shear

Platelets, within the circulation, are able to respond to stimuli under high shear rates such as those found in arteries. Arterial thrombosis, following the rupture of an atherosclerotic plaque, leads to platelet aggregation and eventually thrombus formation where platelets, RBCs and fibrin all come together to form a clot.

To determine if HSP47 binding sequences were able to support thrombus formation, Cellix Vena8fluro+ chips were coated with 100µg/mL Coll II 13, Coll II 14, Coll II 20 or Coll II 33. Peptides 13, 14, and 20 were chosen as these were the sequences that supported platelet adhesion and spreading in a static assay, in a HSP47 dependent manner as indicated with the use of inhibitors (Figure 19 and Figure 20). We introduced Coll II 33, as this was a peptide identified not to bind HSP47 in the initial peptide screen, and therefore acts as a control (Cai et al., 2021). One channel was also coated with GPP, a toolkit control consisting of the flanking sequence to form the triple helical structure, but no "active" sequence in between. Channels coated with 100µg/mL T1 collagen or 100µg/mL GFOGER were used as controls. Channels were coated for one hour at RT before whole citrated blood stained with DiOC6 was perfused over at a rate of 1000^{s-1}. This was carried out at 37°C while mounted above a Nikon A1 Confocal system using a 20X objective. Images were captured every 2 seconds for 8 minutes, and captured at the base of the thrombi, identified by focusing the camera on the collagen fibres before flow was initiated. Images were then analysed using ImageJ to determine median fluorescence intensity and surface coverage of the field of view using a thresholding technique.

Collagen supports thrombus formation (Figure 21 panel A) consistent with previous reports , however HSP47 binding sequences (Toolkit Coll II 13 is shown here as a representative image) (Unsworth et al., 2019, Sahli et al., 2021) (Figure 21 B) do not support thrombi formation. These visualisations were confirmed by plotting the both median fluorescence intensity (Figure 21 C) and percent surface coverage (Figure 21 D) over time, where T1 collagen supports thrombus formation but there is no response to any of the HSP47 binding sequences or control sequences suggesting that at arterial flow rates, binding of HSP47 is not able to initiate thrombus formation, growth or stability.

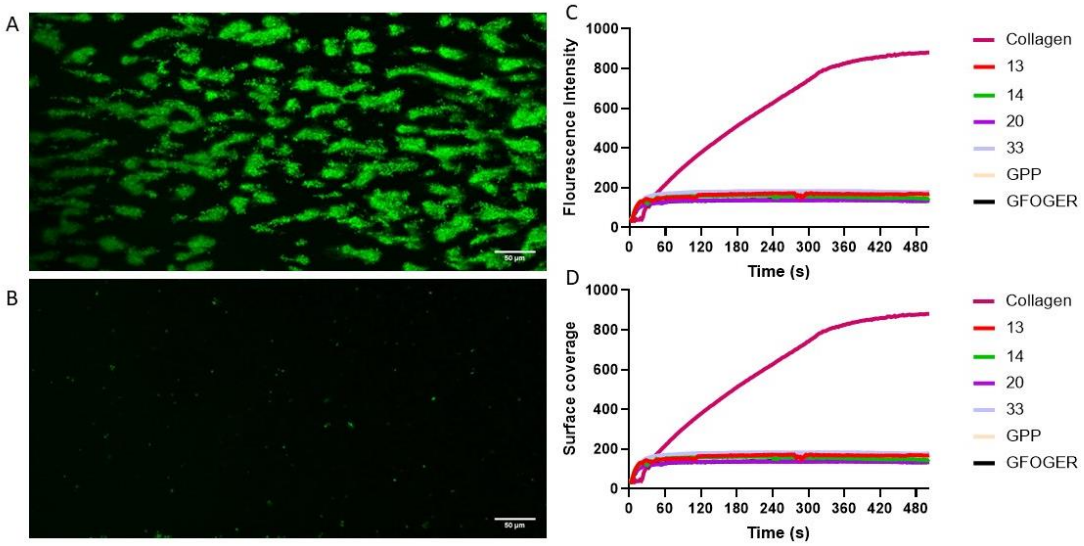

Figure 21. HSP47 binding sequences are unable to support thrombus formation at arterial shear.

Cellix Vena8 Fluoro+ channels were coated with 100µg/mL T1 Collagen, toolkit peptides and GFOGER for one hour at room temperature. Whole blood stained with DiOC6 was then perfused over the channel at 1000^{s-1} at 37°C for 8 minutes and imaged using a Nikon A1 Confocal using a 20X objective. Microscope images were then analysed to determine the fluorescence intensity of the image and a thresholding method was used to determine the area of surface covered by adhered thrombi. A&B) Representative images of thrombi formed on collagen (A) and toolkit peptide 13 (B), scale bar = 100µm. C) Average fluorescence intensity of all coatings. D) Average surface coverage of all coatings. Representative of 3 separate experiments.

4.2.3 HSP47 binding sequences influence collagen-stimulated platelet aggregation.

HSP47 has been shown to influence collagen-stimulated aggregation since inhibition or genetic deletion of HSP47 reduces platelet responses to collagen (Sasikumar, 2015). We hypothesised that HSP47 may act as an additional platelet surface collagen receptor however HSP47 binding sequences have been unable to support platelet aggregation and thrombus formation. We did however identify that HSP47 binding sequences are able to support static platelet adhesion. Previous work, both from the previous chapter and currently unpublished data, suggests that HSP47 influences platelet-collagen interactions leading us to question if we could use HSP47 binding sequences to identify the specific regions within collagen that HSP47 interacts with the modulate responses. In order to do this, we pre-incubated HSP47 binding sequences with platelets before initiating platelet aggregation.

Platelets ($4x10^8$ cells/mL) were incubated with 10µg/mL toolkit peptides or vehicle for 10 minutes in a 96-well, half area, flat bottom plate at RT. Platelets were then incubated with increasing concentrations of TI collagen at 37°C on a plate shaker and shaken at 1200rpm for 5 minutes using a plate shaker. Absorbance was read at 405nm and values adjusted to % aggregation using washed platelets and Tyrodes to calibrate 0% and 100% aggregation, respectively.

Upon stimulation with collagen at 0.3 and 1µg/mL HSP47 binding sequences had no effect (Figure 22 A, B, C), however stimulation with collagen at 3µg/mL was reduced by 41% in the presence of Coll II 13 and 45% Coll II 14 ($P<0.005$) and Coll II 20 reduced collagen stimulated aggregation by 20% ($P<0.01$) when compared to vehicle, however Coll II 26 and Coll III 5a had no impact on collagen stimulated aggregation ($P>0.05$) (Figure 22 D).

HSP47 binding sequences consist of a 27 amino acid sequence flanked by GPP repeats, and by binding to HSP47 Coll II 13, 14 and 20 may be obstructing or competing with collagen binding to HSP47 thereby reducing a platelets ability to aggregate.

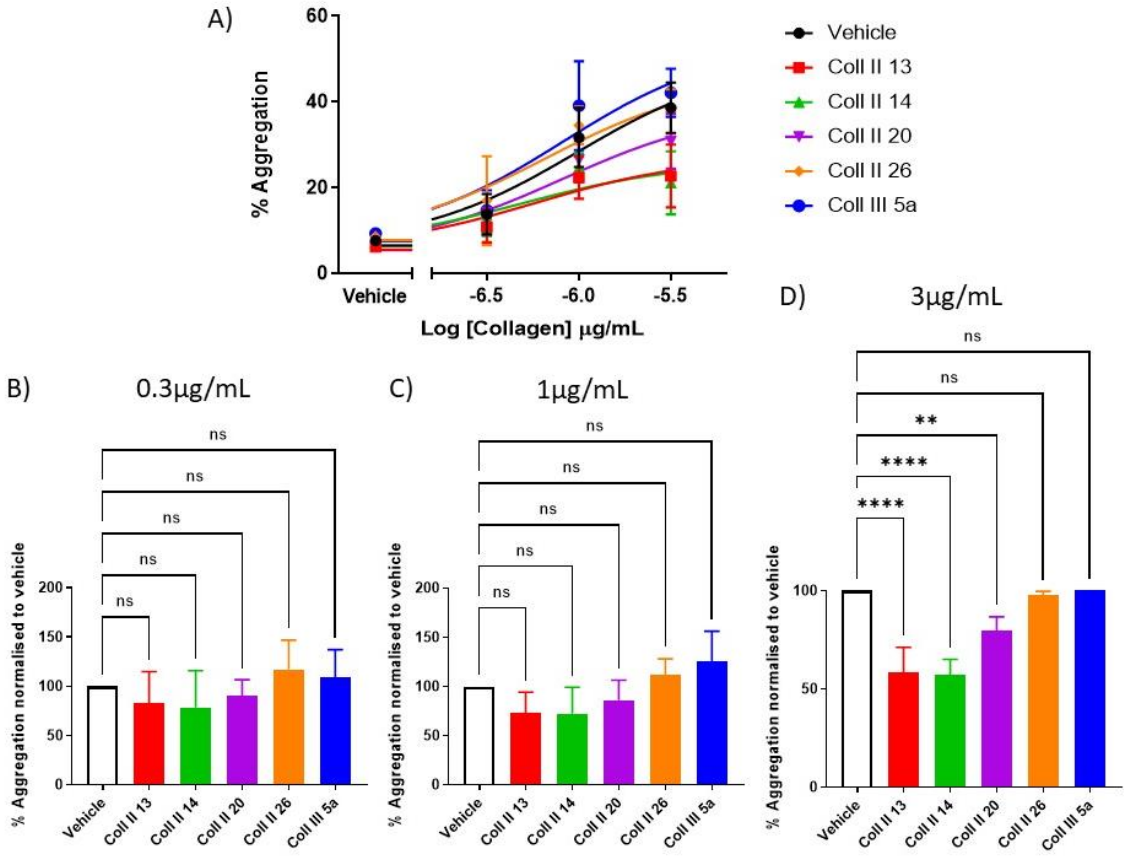

Figure 22. HSP47 binding sequences inhibit Collagen stimulated aggregation
HSP47 binding sequences (10µg/mL), or vehicle (Tyrodes) were pre-incubated with washed platelets ($4x10^8$ cells/mL) for 10 minutes before stimulating in a high-throughput plate-based aggregation assay as described previously with T1 Collagen for 5 minutes at 37°C and stirred at 1200RPM using a plate shaker. Absorbance was measured at 405nm using FlexStation2 (Molecular Devices, Winnersh) and converted to light transmittance then percentage aggregation. A) Percent aggregation. B-D) Aggregation presented as a percentage of vehicle for 0.3, 1 and 3µg/mL T1 collagen, respectively. One-way Anova with Dunnett's multiple comparison of peptide treatment compared to Tyrode's in the presence of Collagen. Results are mean ± SD, n=3. ** = P<0.01, **** = P<0.005, n.s. = non-significant: P>0.05

4.2.4 HSP47 binding sequences modulate collagen receptor stimulated activation

We have established that pre-treatment of platelets with HSP47 binding sequences reduced collagen stimulated aggregation, so therefore it was important to determine whether this extended to other platelet functional responses. This may help to identify the mechanism in which the HSP47 binding sequences are reducing functional responses to platelet agonists.

The effect of collagen tool kit peptides on CRP-XL stimulated alpha granule secretion and integrin activation was therefore determined using flow cytometry. Washed platelets ($4x10^8$ cells/mL) were incubated with peptides (10µg/mL) or vehicle for 10 minutes in the presence of 0.5µL PE-Cy5 mouse anti-human CD62P antibody and 0.5µL FITC rabbit anti-human anti-fibrinogen antibody before stimulating with 1µg/mL CRP-XL for 20 minutes at room temperature in the dark. Samples were then fixed and analysed using a BD-Accuri C6 Plus Flow Cytometer (BD, Winnersh) as described previously. Median fluorescence intensity (MFI) was used to determine whether there was a change in antibody binding following pre-incubation with HSP47 binding sequences before stimulation, compared to vehicle.

Pre-incubation of HSP47 binding sequences with platelets before stimulation identified a reduction in CRP-XL stimulated granule release (Figure 23 A) and fibrinogen binding (Figure 23 B). Coll II 20 caused the greatest reduction in P-selectin exposure (89%) ($P<0.01$), followed by Coll II 14 (81%) ($P<0.05$) and Coll II 13 (59%) ($P<0.05$) however Coll II 26 and Coll III 5a had no effect ($P>0.05$) (Figure 23 A). As seen with P-Selectin exposure, Coll II 20 also caused greatest reduction in fibrinogen binding (91%) ($P<0.01$), followed by Coll II 14 (87%) ($P<0.05$) and Coll II 13 (58%) ($P<0.05$) however Coll II 26 and Coll III 5a had no effect ($P>0.05$) (Figure 23 B).

These results suggest that the interaction between Coll II 20 and HSP47 on the platelet surface is able to module platelet responses to CRP-XL more efficiently than that of Coll II 13 and 14. This is unlike the inhibition seen previously in aggregation, where Coll II 13 and Coll II 14 were observed to reduce collagen stimulation to a greater extent than Coll II 20 (Figure 22 A, B). These inconsistencies may be due to the conditions of the specific assays, for example the high throughput aggregation assay was carried out in stirring conditions, and flow cytometry samples were prepared under static conditions on the bench and then fixed. This may suggest that Coll II 13 and Coll II 14 have a greater affinity to HSP47 under stirring conditions however in static conditions, Coll II 20 has a greater affinity.

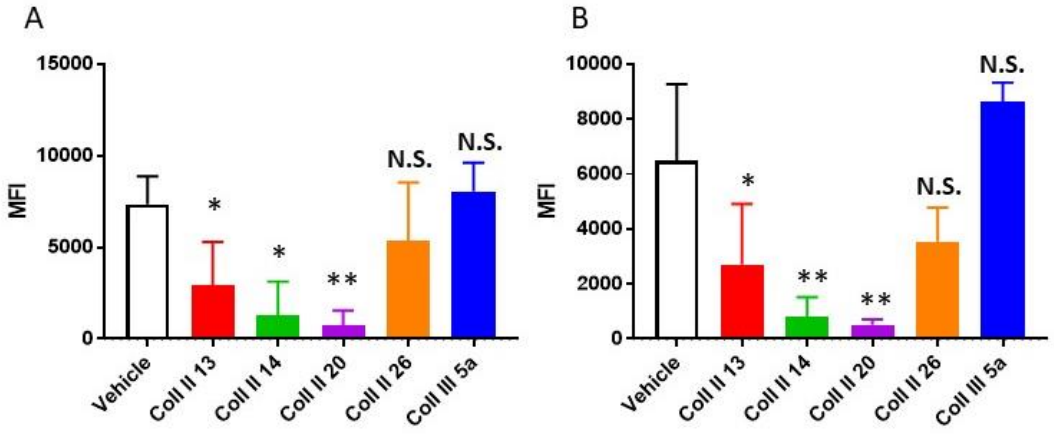

Figure 23. Coll II 13, 14 and 20 inhibit CRP-XL stimulated activation
A) P-selectin exposure and B) fibrinogen binding were measured when platelets were incubated with 10µg/mL Coll II 13, 14, 20 and Coll III 5a/vehicle (tyrodes) and fluorophore bound antibodies against P-selectin and fibrinogen and then stimulated with 1µg/mL CRP-XL for 20 minutes at room temperature in the dark before fixing and analysed via flow cytometry to detect amount of antibody bound, calculated by median fluroescence intensity (MFI). One-way Anova with Dunnett's multiple comparisons of pre-incubation with peptides compared to vehicle,* = $P<0.05$, ** = $P<0.01$, n.s = non significant, $P>0.05$ Data presented as mean ± SD, n=3.

4.2.5 HSP47 binding collagen toolkit peptides do not influence collagen-stimulated thrombus formation

Following the identification that HSP47 binding collagen toolkit peptides Coll II 13, 14 and Coll II 20 have an inhibitory effect on both collagen stimulated aggregation and activation, and the identification that HSP47 is able to modulate denatured T1 collagen to support thrombus formation, we sought to determine whether these peptides would influence T1 collagen stimulated thrombus formation.

To investigate this, Cellix Vena8Fluoro+ channels were coated with 100µg/mL T1 collagen for 1 hour at RT. Whole citrated blood, stained with DiOC6 was incubated with 10µg/mL Coll II 13, 14 and 20 for 10 minutes at RT. Blood was also incubated with the control peptides Coll II 33, GPP and GFOGER before being perfused over the collagen coated channel at 1000^{s-1} at 37°C and visualised using a 20X objective lens on a Nikon A1 confocal microscope. Images were analysed to determine the median fluorescence intensity, and the percent surface coverage covered by the thrombi.

Incubating whole blood with HSP47 binding sequences resulted in no change in the ability of thrombi to form on collagen, represented by both the fluorescence intensity of the field measured (Figure 24 A-C) and percentage surface coverage (Figure 24 D-E) showing no significant differences following the pre-incubation of the HSP47 binding sequences on responses (Figure 24 C&F) ($P>0.05$).

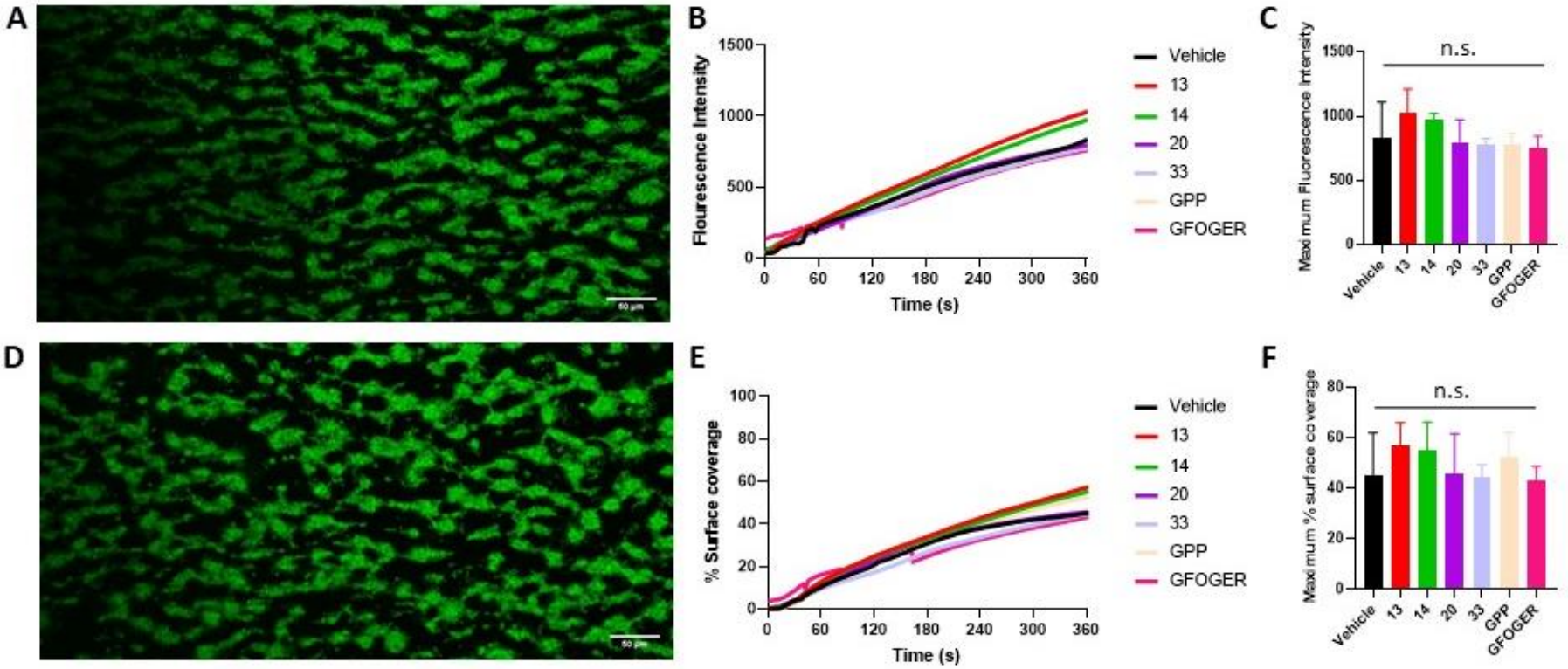
A
B
C
D
E
F
Flourescence Intensity
Time (s)
Vehicle
13
14
20
33
GPP
GFOGER
Maximum Fluorescence Intensity
n.s.
% Surface coverage
Maximum % surface coverage

Figure 24. HSP47 binding sequences do not influence collagen stimulated thrombus formation
Cellix Vena8 Fluoro+ channels were coated with 100µg/mL T1 Collagen for one hour at room temperature. Whole blood stained with DiOC6 was incubated with 10µg/mL toolkit peptides for 10 minutes at RT and then perfused over the channel at 1000^{s-1} at 37°C for 8 minutes and imaged using a Nikon A1 Confocal using a 20X objective. Microscope images were then analysed to determine the fluorescence intensity of the image and a thresholding method was used to determine the area of surface covered by adhered thrombi. A&D) Representative images of thrombi formed on collagen in the presence of vehicle (A) and collagen in the presence of toolkit peptide 13 (D), scale bar = 100µm. B) Average fluorescence intensity of all coatings. C) Maximum fluorescence intensity. D) Average surface coverage and F) Maximum percent surface coverage. B,D: Data presented as Mean. C, E Data presented as Mean ±SD. One-way Anova with Dunnett's multiple comparisons comparing vehicle to samples treated with HSP47 binding toolkit peptides. n.s. = non-significant, P>0.05. N=3

4. 3 Discussion

Collagen toolkit peptides have been used to investigate the role of specific collagen sequences for over twenty years, and led to the identification of GFOGER, the α2β1 binding site within the collagen 1α1 chain (Raynal et al., 2006, Morton et al., 1989). Collagen-like peptides have been used in platelet research for years following the identification of what became a vital platelet agonist, CRP. Collagen like synthetic peptides were shown to be potent platelet agonists, more so than individual collagen fibres and induced granule secretion, arachidonic acid release from membrane lipids and αIIbβ3 activation, resulting in platelet aggregation (Morton et al., 1995). Since then, toolkit peptides have contributed to the understanding of platelet-collagen interactions via vWF and GPIb (Lisman et al., 2006) Toolkit peptides have also been used to investigate collagen interactions with other cell types, including leukocyte LAIR-1, where Gly-Pro-Hyp repeats bind LAIR-1 and directly inhibit immune cell activation *in vitro* (Lebbink et al., 2006).

Previously, we have shown that HSP47 binds to a number of the collagen toolkit peptides, in particular Coll II 13, Coll II 14, Coll II 20, Coll II 26 and Coll III 5a (Cai et al., 2021) Molecular modelling identified that residues flanking key Arg residues within the sequence allow for the high affinity of these peptides with HSP47.

We aimed to explore if HSP47 was able to act as a receptor on the platelet surface, using the HSP47 binding sequences from the collagen toolkits as a ligand. We identified that HSP47 binding sequences do not support aggregation, but do support platelet adhesion and shape change in a static assay. It was previously reported that there are different sites within collagen for adhesion and aggregation (Morton et al., 1989) which lead to the identification of independent integrin roles on the platelet surface. Integrin α2β1 supports platelet adhesion but not aggregation, and the work we have presented here suggests HSP47 may be able to mimic this interaction. The ability of platelets to adhere and spread on HSP47 toolkit peptides was further investigated to be HSP47 specific through the use of a small molecule inhibitor (SMIH) and an inhibitory HSP47 antibody. Adhesion to Coll II 13 and Coll II 20 was reduced by both of these inhibitors, suggesting the sequences these peptides contain may play a vital role in the Collagen-HSP47 interaction and further confirmation of the importance of HSP47 in megakaryocyte-collagen interactions. We observed a greater reduction in platelet adhesion when platelets are treated with the inhibitory antibody than the SMIH, which may be due to the size of the SMIH and therefore being less able to displace the peptides. αHSP47 is targeted at the C-terminal end of HSP47, binding a 28 amino acid sequence including the RDEL

sequence, therefore suggesting that this region of HSP47 is key for modulating the collagen/HSP47 interaction.

Following the identification that HSP47 is able to modulate collagen synthesis and function in the previous chapter, we aimed to use the HSP47 binding sequences to identify whether we could identify specific regions of collagen that HSP47 modulates. Coll II 13, Coll II 14 and Coll II 20 were able to interfere with the platelet-TI collagen interaction and resulted in a reduction in aggregation, up to ~50%. This response was not seen in response to stimulation with CRP and TRAP6 suggesting it is not due to an interference with GPVI. These same binding sequences also reduced granule release and fibrinogen binding in response to CRP. These results suggest that HSP47 is able to module platelet responses to collagen and that the addition of these peptides before stimulation have bound HSP47 and therefore prevented the ability of HSP47 to modulate the response.

HSP47 binding sequences had no impact on the ability of platelets to form thrombi in the response to T1 collagen at arterial flow. This may suggest that HSP47 does not modulate the platelet-collagen response in these circumstance, although it has been previously reported that inhibition of HSP47, and knockout of HSP47 result in reduced thrombus formation, both *in vivo* and *in vitro* (Sasikumar, 2015). One explanation for why there was no effect of the HSP47 binding sequences in this assay compared to the aggregation and activation assays may be that the collagen concentration used to coat the chip was 10X higher than the maximum concentration used previously, suggesting that at higher concentrations of collagen, HSP47 does not regulate the collagen – platelet interaction.

The ability of platelets to adhere and spread in a HSP47 dependent manner on peptides Coll II 13, Coll II 14, Coll II 20 and Coll II 26 suggest that there is a sequence within these peptides that supports this response. Coll II 13 and Coll II 14 share nine amino acids, with the final 9 residues in Coll II 13 being the first 9 in Coll II 14 so may contain the sequence supporting platelet adhesion in a HSP47 dependent manner. Both these peptides contain Gly-Pro-Arg residues which have been confirmed to the preferential binding sequence of HSP47 within collagen (Koide et al., 2002, Koide et al., 2006, Tasab et al., 2002).Coll II 26 contains both GPS and GPO repeats, with O representing hydroxyproline. Serine, like Arginine is also a polar amino acid which may give an explanation of the ability of platelet to bind this sequence.

Coll II 13 and Coll II 14 were also able to inhibit collagen stimulated aggregation and activation (granule release and integrin activation) suggesting that HSP47 is able to modulate collagen responses through the Gly-Pro-Arg sequence.

In conclusion, these studies identify that HSP47 may have dual functionalities within the platelet, both as a receptor functioning similar to α2β1 to support platelet adhesion, and also modulating platelet responses to collagen through Gly-Pro-Arg sequences. Further research to understand how HSP47 is anchored on the platelet surface and the mechanism in which it is able to support platelet adhesion whilst modulating platelet responses is needed.

Chapter 5 – KDEL proteins: ER chaperone proteins within the platelet play a role in platelet function

5.1 Introduction

Following the identification that platelets release PDI in 1992, a number of chaperone proteins have been identified within the platelet proteome including HSP47 and a number of thiol isomerases. Of those investigated, it seems these proteins are found within the platelet DTS and are released to the platelet surface following activation (Crescente et al., 2016). A number of these proteins are thought to regulate platelet function, identified through multiple *in vivo* and *in vitro* assays, further supported via the study of genetically modified animal models (Cho et al., 2008, Reinhardt et al., 2008, Holbrook et al., 2010, Holbrook et al., 2012, Cho et al., 2012, Kim et al., 2013a, Holbrook et al., 2018).

PDI mediates integrin-dependent adhesion, specifically αIIbβ3, and therefore regulates platelet aggregation and secretion (Lahav et al., 2000, Essex and Li, 1999). PDI also supports thrombus formation *in vivo*. Subsequent thiol isomerases identified and investigated include ERp57, ERp5 and ERp72 and have been found to also mediate platelet accumulation and fibrin generation in vivo. (Holbrook et al., 2012, Passam et al., 2015, Holbrook et al., 2018). Work is currently ongoing in order to establish precise mechanisms and interdependence between these thiol isomerases.

In addition to the thiol isomerases and HSP47, other chaperone proteins which contain KDEL (or similar) have also been identified within the human platelet proteome such as Calreticulin (CALR), Endoplasmin (Grp94), Ig heavy chain-binding protein (BiP/Grp78) and Grp170, with copy numbers ranging from 20,300 (Calreticulin) to 3,800 (HSP47) (Burkhart et al., 2012). Whilst these proteins have been shown to exist within the platelet proteome there is very little in the literature about the potential role these proteins may play in platelet function.

5.1.1 BiP

Binding immunoglobulin protein (BiP) is a member of the HSP70 family, that resides in the lumen of the ER and chaperones both non-glycosylated and glycosylated proteins (Brocchieri et al., 2008). In addition to chaperoning nascent proteins, BiP maintains the permeability barrier of the ER during translocation and identifies misfolded proteins and targets them for degradation (Little et al., 1994, Pfaffenbach and Lee, 2011, Wang et al., 2009, Ibrahim et al., 2019). BiP contributes to the activation mechanism of the unfolded protein response (UPR) and is therefore involved in the cellular response to stress. During cellular homeostasis, BiP is complexed with UPR stress sensors including Activating Transcription Factor 6 (AFT6) and Inositol-Requiring Enzyme 1 (IRE1) (Pfaffenbach and Lee, 2011). When the cell is exposed to

unfolded proteins, BiP is released from the UPR sensors, decreases protein translation and enhances folding.

BiP consists of a highly conserved N-terminal nucleotide binding domain (NBD), a substrate-binding domain (SBD) containing eight β-strands with a helical lid, and a linker controlling the interaction between these two domains (Lindquist and Craig, 1988). Like other members of the HSP70 family, BiP interactivity with other proteins is regulated by its nucleotide bound state: when bound to ATP, the SBD is docked on the NBD allowing for a high on/off rate interaction with other proteins. ATP hydrolysis changes the confirmation, closes the SBD lid and allows proteins to bind with higher affinity due to a slower on/off rate.

Dysfunction of BiP is associated with multiple pathologies including cancers, neurodegenerative disorders and the development of virus envelope proteins – a vital step for viruses to survive in their host environment (Kuroda et al., 2011, Zhang et al., 2006, Wu et al., 2014, Ellgaard and Helenius, 2003, Choukhi et al., 1998, Wang et al., 2009).

BiP was first reported to be found on the platelet surface in 2010 by *Molins et. al* who showed that surface exposure was altered by changes in shear stress (Molins et al., 2010). BiP levels, along with those of PDI, have also been shown to be upregulated in the platelets of diabetic animals resulting in an increase in active tissue factor and therefore has been proposed to contribute to an increased thrombotic risk (Vera et al., 2012).

5.1.2 Endoplasmin

Endoplasmin, also known as Grp94 and gp96, belongs to the HSP90 family, is constitutively expressed in all metazoans and is essential for development, with various effects in knockdown/knock out models including embryonic lethality in mice (Wanderling et al., 2007). Unlike other ubiquitous molecular chaperones such as Calreticulin and BiP, which have a large number of clients, Endoplasmin is required for the folding of only a small number of proteins including MHC class II, Toll-like Receptors, integrins and collagen (Schaiff et al., 1992, Yang et al., 2007). It is also essential for the assembly of the GPIb-V-IX complex in megakaryocytes and platelets, with gene deficient mice exhibiting a complete loss in surface GPIb-V-IX due to enhanced ER associated protein degradation (Staron et al., 2011). The reduced expression of the complex is due to a specific interaction between Endoplasmin and the GPIb subunit, not the entire complex. Additionally, Endoplasmin acts as a major ER Ca^{2+} buffer and has a range of low- and high-affinity Ca^{2+} binding sites (Nigam et al., 1994, Van et al., 1989).

5.1.3 Calreticulin

Calreticulin's major function is to bind, buffer and regulate intracellular Ca^{2+} however it also associates with many ER proteins, newly synthesized glycoproteins and also some mRNAs (Wang et al., 2012, Peterson et al., 1995, High et al., 2000, Michalak et al., 2009). Calreticulin (CALR) has been identified to interact with a number of other chaperone proteins including ERp57 and is part of the eukaryotic Initiation Factor 2 (eIF2) complex which also includes Endoplasmin and BiP, amongst a number of other proteins and is critically important for initiation of translation (Panaretakis et al., 2008, Timchenko et al., 2006, Adomavicius et al., 2019). CALR, a 46kDa protein consists of an N-domain and a P-domain which support the chaperone function of the protein, and at the C terminus a C-domain which is essential for calcium buffering (Michalak et al., 1999, Varricchio et al., 2017). Also found at the c terminus is the KDEL sequence commonly seen in ER chaperone proteins required for ER/Golgi retention (Michalak et al., 2009).

5.1.4 Grp170

Glucose regulated protein 170 (GRP170) is an endoplasmic reticulum chaperone induced by major stresses including hypoxia and ischemia and calcium depletion (Lin et al., 1993, Cai et al., 1993). Grp170 has been identified to be co-ordinately induced with BiP and Endoplasmin and also plays a role in immunoglobulin processing (Lin et al., 1993).

Therefore, a number of molecular chaperone proteins have been recognised within the platelet, and an ever increasing number of these chaperones are suggested to play a role in thrombosis and haemostasis (Cho et al., 2008, Holbrook et al., 2010, Kim et al., 2013a, Crescente et al., 2016, Sasikumar et al., 2018). BiP, Endoplasmin, Calreticulin and Grp170 are additional chaperone proteins that the literature surrounding their presence and function in platelets is limited or currently unreported. Therefore, we sought to investigate to understand if these proteins may identify therapeutic targets leading to the development of anti-thrombotic therapies, but also targets for treatments for a number of other conditions that these proteins are implicated in.

We hypothesised that we will find these KDEL-containing proteins in the platelet, and will be able to use inhibitors of these proteins to further understand the role that KDEL-containing proteins play on platelet function.

5.2 Results

5.2.1 KDEL proteins are present in the platelet proteome

Proteomic methodologies are becoming more and more important in understanding cellular contents and their functions, and can be used to compare protein expression, identification of post-translational modifications (PTMs) and the study of protein-protein interactions. The human genome contains ~30,000 genes, resulting in around 1 million protein products after splice variants and PTMs are taken into account (Chandramouli and Qian, 2009, Baltimore, 2001, Wilkins et al., 1999).

To identify if KDEL-containing proteins un-reported in the literature were present in the platelet proteome, we used two published data sources. Haematlas was curated using gene expression data within differentiated blood cells and endothelial cells to further understand haematopoiesis (Watkins et al., 2009). This data was compiled focussing on transcription factors, immunoglobulin superfamily members and lineage specific transcripts. Burkhart *et. al.* compiled the first comprehensive quantitative human platelet proteome to understand dysfunction of anucleate platelets, hypothesizing that dysfunction is due to PTMs and protein expression changes/abnormalities (Burkhart et al., 2012). To confirm the presence of these KDEL proteins within the platelet, we western blotted for these proteins using resting washed platelet samples. $4x10^8$/mL washed platelets were lysed in Lamelli sample buffer then proteins were separated using a 10% SDS-Page gel. Proteins were then transferred onto a PVDF membrane before immunoblotting for Grp170, Endoplasmin and BiP.

Haematlas identified mRNA for both Endoplasmin and Calreticulin present at notable levels in megakaryocytes, with 12.5(A.U.) copies of Endoplasmin and 12 (A.U.) copies of CALR, though it is worth noting that mRNA levels do not always correlate with protein levels (Figure 25, A, MKs highlighted in red). Grp170, and HSP47 mRNAs were present in MKs, but at much lower numbers (9.3 and 9.2 (A.U.) respectively).These results were further confirmed using the Burkhart database, suggesting that platelets contain 14,000 and 20,300 copies of Endoplasmin and Calreticulin, respectively and GRp170 and HSP47 are present at considerably lower expression levels (4,500 and 3,800, respectively) (Figure 25, B). The Burkhart database also identified BiP within the platelet proteome, with 27,900 copies however its gene, HSPA5 was not identified using Haematlas. Immunoblot analysis confirmed the presence of Grp170, Endoplasmin and BiP from four individual donors within the platelet proteome (Figure 25 C).

A)

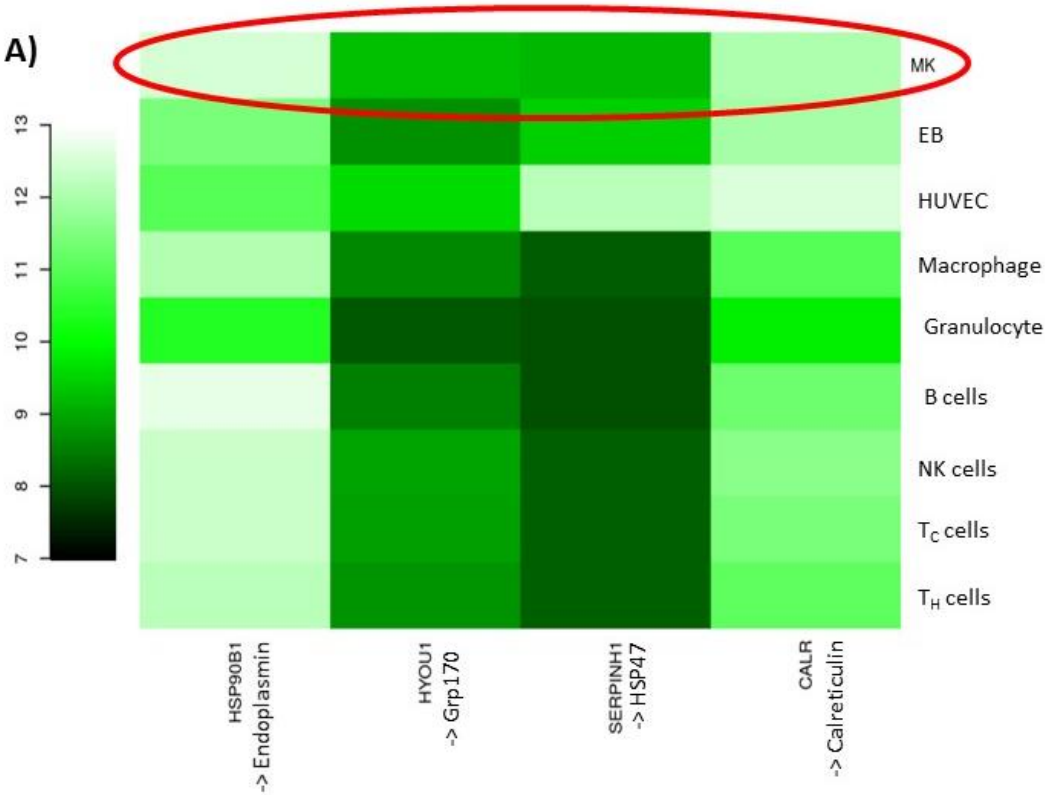

B)

Gene	HSP90B1	HYOU1	SERPINH1	CALR	HSPA5
Protein	Endoplasmin	Grp170	HSP47	Calreticulin	BiP
Copy numer	14,000	4,500	3,800	20,300	27,900

C)

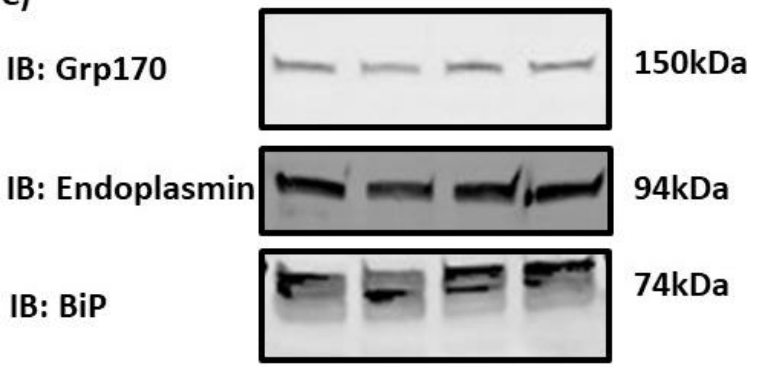

Figure 25. Endoplasmin, Grp170 Calreticulin and BiP are within the MK/platelet transcriptome/proteome
A) Gene expression heatmap of HSPB1 (Endoplasmin),HYOU1 (Grp170), SERPINH1 (HSP47) and CALR (Calreticulin) in precursors for number of differentiated blood cells: MK = megakaryocytes, EB = erythroblasts, HUVEC = human umbilical vein endothelial cells, macrophages, granulocytes, B cells, natural killer (NK) cells, cytotoxic T cells (T_C) and helper T cells (T_H). MKs are shown at the top of the image in the red circle.(Watkins et al., 2009). B) Copy numbers of HSP90B1, HYOU1, SERPINH1, CALR and HSPA5 from (Burkhart et al., 2012). C) 4x 10^8 cells/mL washed platelets were lysed in Lamelli sample buffer then separated on a 10% gel by SDS-Page under reducing conditions before being transferred to PVDF membrane. Immunoblot analysis of proteins on PVDF membrane was performed by incubating with primary antibodies to Grp170, Endoplasmin and BiP. Alexa 488 labelled specific secondary antibodies were added and bands detected by fluorescence detection using a Typhoon fluroimager (GE Healthcare). Each blot shows platelets from four donors.

5.2.2 Endoplasmin, Grp170, BiP and Calreticulin are detectable at the platelet surface but only Endoplasmin increases in surface exposure upon activation

It has previously been reported that KDEL containing proteins, including HSP47, PDI and other thiol isomerases translocate to the platelet surface following activation (Crescente et al., 2016, Sasikumar et al., 2018, Holbrook et al., 2010). These proteins have also been identified to play a role in platelet function and modulating platelet receptors, so their detection at the surface during/following stimulation is not surprising. Therefore, we sought to determine whether this happened to Endoplasmin, Grp170, BiP and Calreticulin during platelet activation.

To identify if Endoplasmin, GRp170, BiP and Calreticulin increase in surface exposure, washed platelets were incubated with primary and species specific secondary antibodies (for concentrations see Table 1 and Table 3) in the presence of 3µM thrombin receptor activating peptide (TRAP6) or 3µg/mL CRP-XL for 20 minutes at RT before being fixed with 0.2% FS and analysed using a BDAccuri C6Plus flow cytometer.

There was no change in Endoplasmin surface binding following TRAP6 stimulation ($P>0.05$) , however there was a 163% increase in antibody binding following CRP stimulation (Figure 26 A) ($P<0.05$) suggesting that Endoplasmin may play a role in collagen signalling, particularly after stimulation of GPVI. Grp170, BiP or Calreticulin exposure was not changed following CRP-XL or TRAP6 stimulation ($P>0.05$) (Figure 26 B, C, D).

We expected to identify an increase in surface exposure of these KDL- containing proteins, in accordance with other ER chaperone proteins identified within the platelet, however this was only identified with Endoplasmin. Additionally, there was a large amount of variation in surface exposure, particularly following activation using CRP-XL.

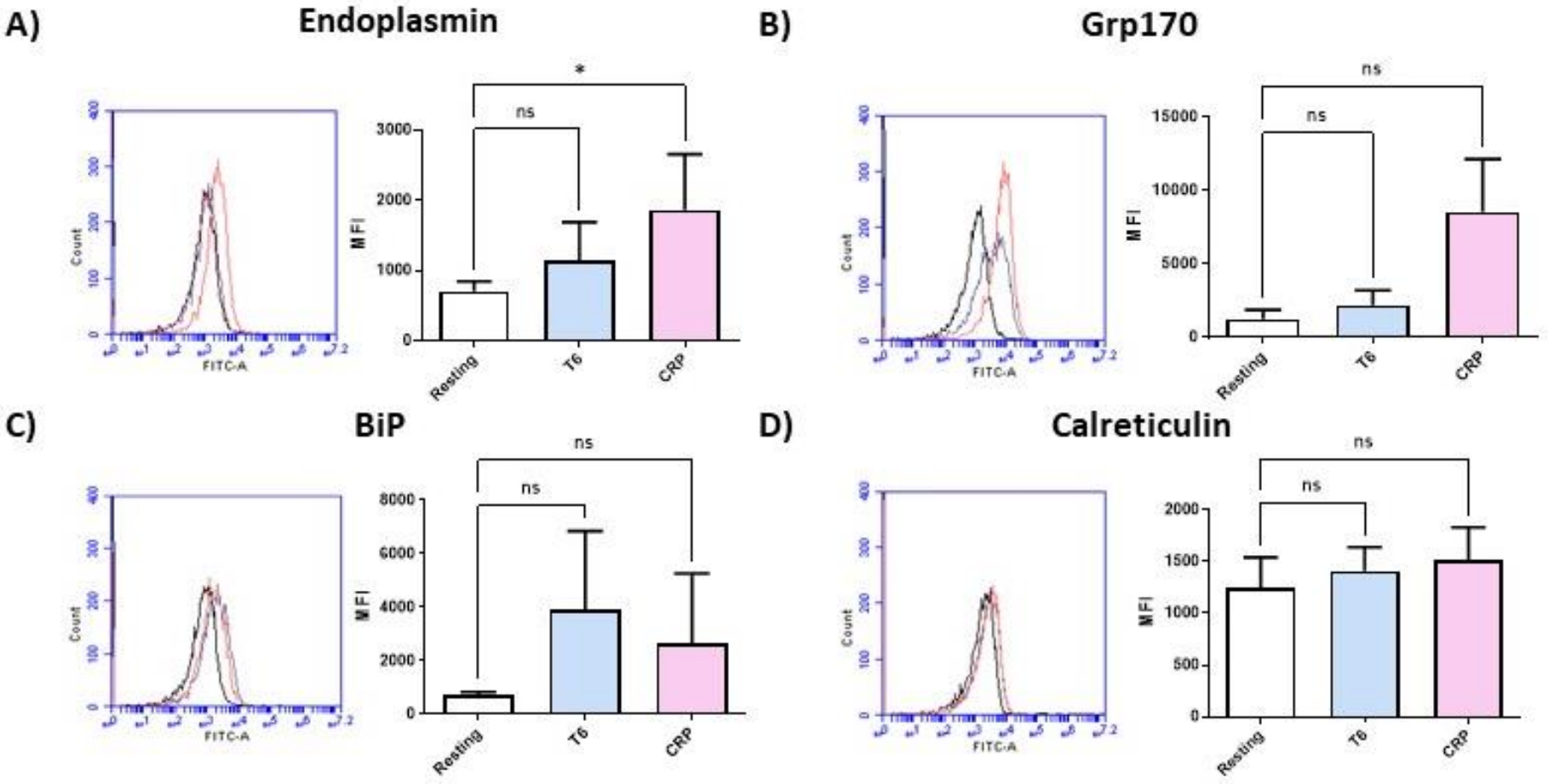
A)
Endoplasmin
Count
FITC-A
MFI
ns
*
Resting
T6
CRP
B)
Grp170
ns
ns
C)
BiP
ns
ns
D)
Calreticulin
ns
ns

Figure 26.Endoplasmin increases in surface expression upon CRP stimulation
Washed platelets were incubated with primary and secondary antibodies for Endoplasmin (A), Grp170 (B) BiP (C) and Calreticulin (D) in the presence of both TRAP6 and CRP for 20 minutes at 37°C before being fixed and analysed using a BDAccuri C6Plus Flow cytometer (Winnersh, UK). A) Endoplasmin was significantly increased following stimulation by CRP but not TRAP ($P<0.05$). B) Though a visible increase, Grp170 is not significantly increased following both TRAP or CRP stimulation. There was no statistical increase of BiP (C) or Calreticulin (D) following TRAP or CRP stimulation. Data presented as Mean ±SD, One way Anova with Dunnetts multiple comparisons, Resting compared to TRAP and CRP. * = $P<0.05$, n.s = non-significant. N=4.

5.2.3 KDEL proteins are distributed through the platelet and are colocalised with integrin αIIbβ3

We have previously reported that PDI Erp5, Erp57 and Erp72 translocate to the platelet surface following stimulation (Holbrook et al., 2010, Crescente et al., 2016). We have identified that Endoplasmin, BiP, Grp170 and Calreticulin are present in the platelet, and it is possible to detect an increase in Endoplasmin on the surface through flow cytometry however we found no significant change in surface expression of BiP Grp170, or Calreticulin following stimulation with TRAP6 or CRP.

A confocal microscopy approach was taken to confirm the location of these chaperone proteins and determine whether their location changes upon stimulation, as is seen with PDI , Erp5, Erp57 and Erp72. To do this, an immunocytochemistry approach was taken. PRP, in the presence of 4µg/mL eptifibatide, to prevent platelet aggregation, was either fixed with 4% (w/v) PFA (final concentration) whilst resting, or fixed with 4% (w/v) PFA (final concentration) following activation with 10µM TRAP6. Fixed samples were washed and platelets allowed to adhere to poly-l-lysine coated coverslips, as described in section 2.2.4.4. After blocking, samples were stained using primary and species specific Alexa fluorophore tagged secondary antibodies at concentrations specified in Table 1 and Table 3 before imaging on a Nikon A1 Confocal microscope using a 100X oil objective. To determine Pearson's Coefficient, JACoP – an ImageJ plugin was used (Bolte and CordeliÈRes, 2006). The maximum median fluorescence intensity of 10 platelets per field of view were calculated using ImageJ to determine if there was a change in the amount of antibody bound, and therefore the amount of protein in the cell, before and after activation.

Endoplasmin was distributed throughout the resting platelet, colocalised with integrin αIIbβ3, as identified by a mean Pearson's Coefficient of 0.88 (Figure 27). In the activated platelet, there is a clear ring of αIIbβ3 around the edge of the platelet and Endoplasmin appears to remain distributed throughout the platelet, with a 2.5% decrease in colocalization to integrin αIIbβ3 ($P<0.01$). This is inconsistent with data obtained via flow cytometry, that identified Endoplasmin increased in surface exposure following stimulation with CRP-XL, however this difference may be partially explained by the use of different agonists. Calculation of MFI of Endoplasmin in resting (1749±976) and activated (1890±576) platelets suggests that there is no change in total amount of Endoplasmin following stimulation.

BiP is also distributed throughout the resting platelet, however it appears that in some platelets it is in clusters, potentially suggesting BiP may be present in granules (Figure 28). In

these platelets, Pearson's Coefficient was identified to be 0.77 suggesting a degree of BiP and integrin αIIbβ3 colocalization. Following activation, BiP appears to be more evenly distributed throughout the platelet, with a brighter section on one of the platelets suggesting there is one area it has preferentially located to. Calculation of MFI of BiP in these samples support the visualisation of a brighter section on activated platelets as a statistically significant increase in MFI was calculated between resting platelets (1586 ±522) and activated platelets (1986±627) ($P<0.01$). There is no difference identified in corelation between integrin αIIbβ3 and BiP following activation with CRP-XL ($P<0.05$), supporting flow cytometry data presented previously (Figure 26)**.**

Grp170 appears to remain distributed throughout the platelet when resting and following stimulation. Pearson's Coefficient determined a 32% increase following stimulation, suggesting that Grp170 is more colocalised with integrin αIIbβ3 when platelets are active ($P<0.01$), however this does not support flow cytometry data measuring Grp170 surface exposure, suggesting that potentially Grp170 may be found underneath the platelet surface and therefore inaccessible to antibody binding in non-permeabilised samples. This is supported by the increase in MFI of Grp170 calculated, that identified a statistically significant increase following activation, from 2016±496 to 2610±456 ($P<0.05$).

Calreticulin appears to be distributed through the platelet, with some platelets showing a clear ring structure following stimulation (Figure 30). In resting platelets, visually there appears to be colocalization with integrin αIIbβ3 however this is not visible on every platelet suggesting it may be a transient event. This is supported by calculation of Pearson's coefficient, which identified no change in integrin αIIbβ3 colocalization following activation ($P>0.05$), calculation of MFI also identified no change in antibody binding following activation ($P>0.05$), and flow cytometry surface exposure data which also identified no difference following TRAP6 or CRP-XL exposure.

We have identified a reduction in Endoplasmin colocalization with integrin αIIbβ3, and an increase in colocalization following Grp170 after quantification of Pearson's coefficient, suggesting that not all KDEL- containing proteins within the platelet are found at the surface following activation

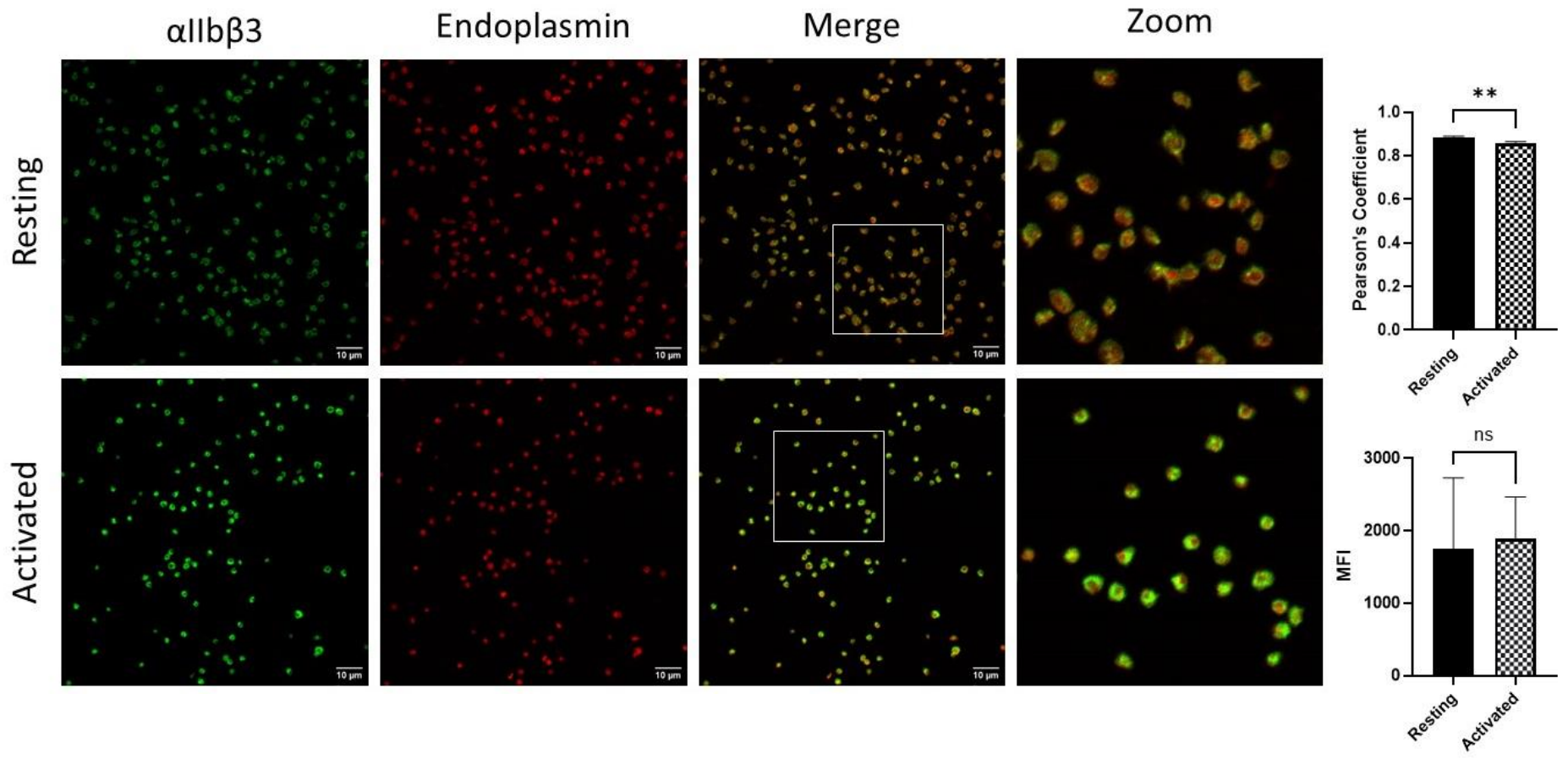
αIIbβ3
Endoplasmin
Merge
Zoom
Resting
Activated
10 µm
**
Pearson's Coefficient
1.0
0.8
0.6
0.4
0.2
0.0
Resting
Activated
ns
MFI
3000
2000
1000
0
Resting
Activated

Figure 27. Endoplasmin is distributed through both resting and activated platelets
Immunofluorescence microscopy imaging of resting or activated platelets (10µM TRAP6 in the presence of 4µg/ml eptifibatide) adhered to poly-L-lysine coated coverslips, stained for integrin αIIbβ3 and Endoplasmin and acquired using 100x Nikon A1 confocal microscope X100 oil immersion lens. In the resting sample, it appears Endoplasmin is colocalised with αIIbβ3 due to the presence of the orange/yellow colour however in the activated sample there is a clear outer ring of αIIbβ3 and Endoplasmin remains distributed throughout the platelet. Scale bar = 10µM, white boxes show region zoomed in. Images are representative of three independent experiments with platelets from different donors. Pearson's coefficient was determined using JACoP, an ImageJ plugin, and presented as mean ±SD, paired T-test. ** = $P<0.01$, n=3. MFI was calculated from 10 platelets, from three random fields of view, and data presented mean ±SD, paired T-test. ns = $P>0.05$, n=3

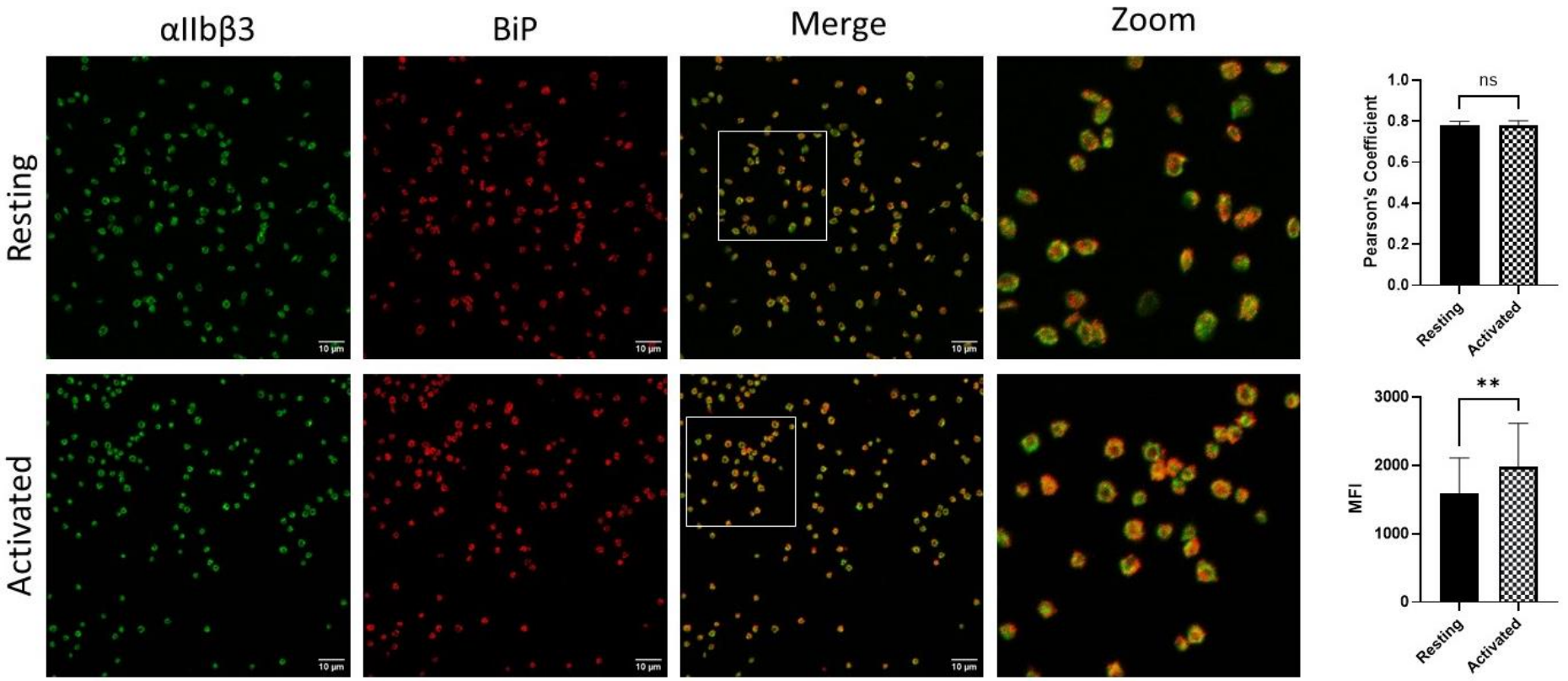
αIIbβ3
BiP
Merge
Zoom
Resting
Activated
10 µm
Pearson's Coefficient
1.0
0.8
0.6
0.4
0.2
0.0
ns
Resting
Activated
MFI
3000
2000
1000
0
**
Resting
Activated

Figure 28. BiP is found in clusters in resting platelets, but not following activation
Immunofluorescence microscopy imaging of resting or activated platelets (10µM TRAP6 in the presence of 4µg/ml eptifibatide) adhered to poly-L-lysine coated coverslips, stained for integrin αIIbβ3 and BiP and acquired using 100x Nikon A1 confocal microscope X100 oil immersion lens. In the resting sample, BiP appears to be in clusters through the platelet, however following stimulation becomes more evenly distributed throughout the sample. There is also some colocalization of BiP and αIIbβ3 following activation which appears to be on one side of the platelet, not the entire surface. Scale bar = 10µM, white boxes show region zoomed in. Images are representative of three independent experiments with platelets from different donors. Pearson's coefficient was determined using JACoP, an ImageJ plugin, and presented as mean ±SD, paired T-test, ns = $P>0.05$, n=3. MFI was calculated from 10 platelets, from three random fields of view, and data presented mean ±SD, paired T-test. ** = $P<0.01$, n=3

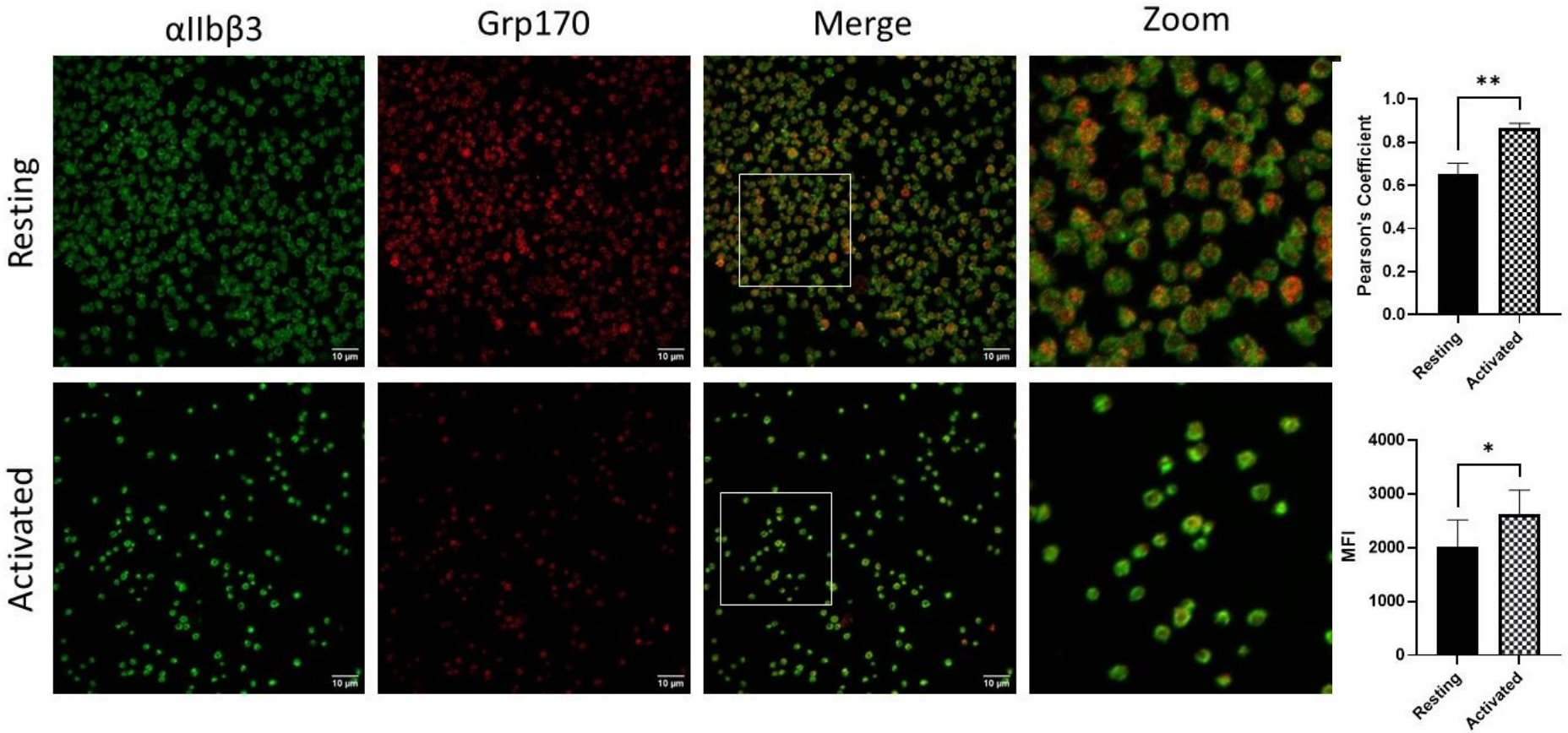
αIIbβ3
Grp170
Merge
Zoom
Resting
Activated
10 µm
Pearson's Coefficient
1.0
0.8
0.6
0.4
0.2
0.0
**
Resting
Activated
MFI
4000
3000
2000
1000
0
*
Resting
Activated

Figure 29. Grp170 remains distributed throughout the platelet following stimulation
Immunofluorescence microscopy imaging of resting or activated platelets (10μM TRAP6 in the presence of 4μg/ml eptifibatide) adhered to poly-L-lysine coated coverslips, stained for integrin αIIbβ3 and Grp170 and acquired using 100x Nikon A1 confocal microscope X100 oil immersion lens.Grp170 appears to be distributed throughout the platelet in both resting and activated samples, however the resting samples are a lot brighter. Scale bar = 10μM, white boxes show region zoomed in. Images are representative of three independent experiments with platelets from different donors. Pearson's coefficient was determined using JACoP, an ImageJ plugin, and presented as mean ±SD, paired T-test, ** = $P<0.01$, n=3. MFI was calculated from 10 platelets, from three random fields of view, and data presented mean ±SD, paired T-test. * = $P<0.05$, n=3

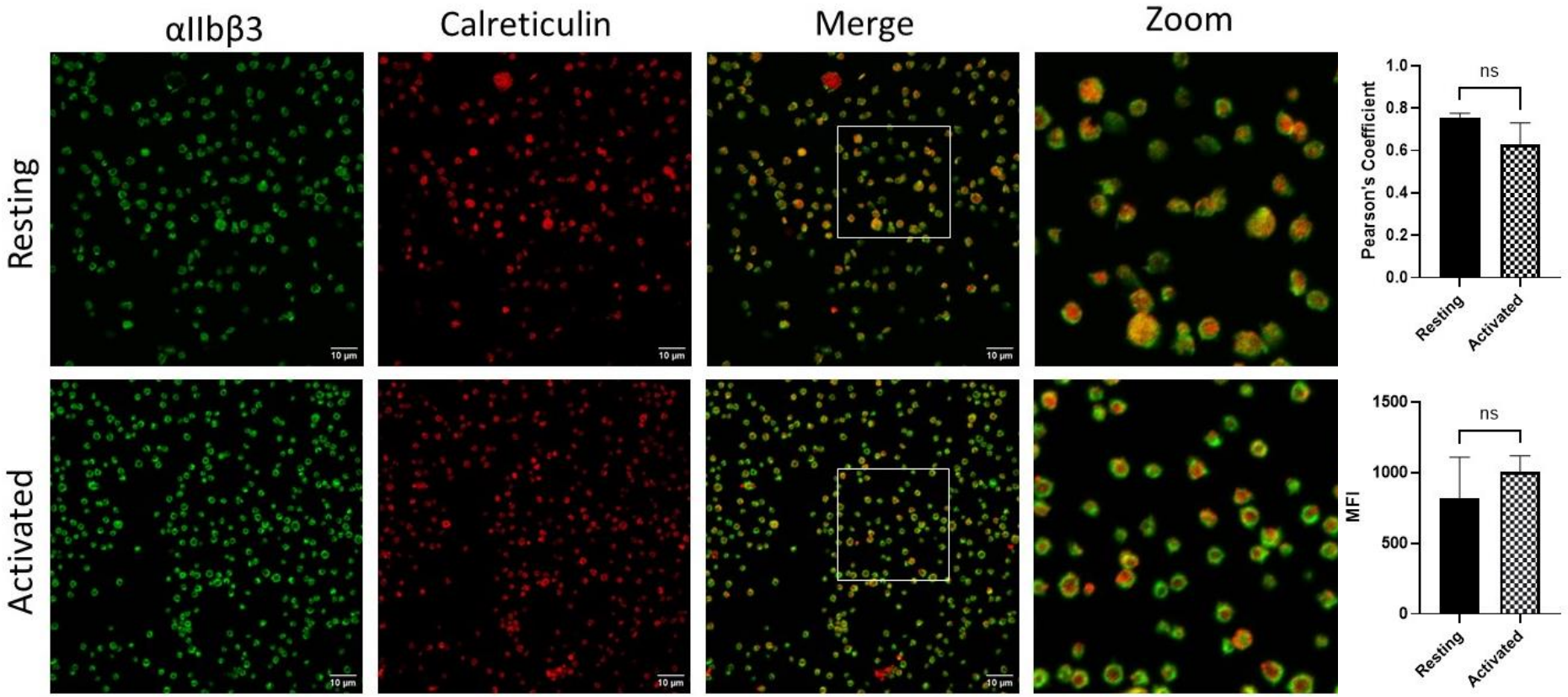
αIIbβ3
Calreticulin
Merge
Zoom
Resting
Activated
10 µm
Pearson's Coefficient
1.0
0.8
0.6
0.4
0.2
0.0
ns
Resting
Activated
MFI
1500
1000
500
0
ns
Resting
Activated

Figure 30. Calreticulin moves to the platelet surface following stimulation
Immunofluorescence microscopy imaging of resting or activated platelets (10μM TRAP6 in the presence of 4μg/ml eptifibatide) adhered to poly-L-lysine coated coverslips, stained for integrin αIIbβ3 and Calreticulin and acquired using 100x Nikon A1 confocal microscope X100 oil immersion lens. Calreticulin appears to be distributed throughout the platelet, with some activated platelets showing a clear ring like structure following stimulation which colocalises with αIIbβ3. Scale bar = 10μM, white boxes show region zoomed in. Images are representative of three independent experiments with platelets from different donors. Pearson's coefficient was determined using JACoP, an ImageJ plugin, and presented as mean ±SD, paired T-test, ns=P>0.05, n=3. MFI was calculated from 10 platelets, from three random fields of view, and data presented mean ±SD, paired T-test. ns=P>0.05, n=3.

5.2.4 Role of Endoplasmin on platelet function

5.2.4.1 P13 modulates the kinetics but not the scale of platelet aggregation

PU-WS 13 (P13), an inhibitor of Endoplasmin, has previously been used to investigate the role of Endoplasmin in multiple myeloma and integrin chaperoning (Hua et al., 2013, Hong et al., 2013). As an integrin chaperone, we hypothesised that it would play a role in platelet function, due to the range of integrins on the platelet surface.

Here we investigated the effect of Endoplasmin inhibition on platelet aggregation. Using a high-throughput plate-based assay, as described previously, we screened a range of concentrations of P13 (1µM to 100µM) against a range of concentrations of CRP-XL and TRAP6.

At all concentrations of TRAP6 measured, P13 did not induce a statistically significant effect on aggregation in PRP, although a 60% reduction was seen at 1µM TRAP following incubation with 100µM P13 (Figure 31 A&B). At the lowest concentration of CRP (0.1µg/mL), P13 had no effect on aggregation in PRP, however at 0.3µg/mL pre-incubation with 100µM P13 was able to significantly reduce aggregation ($P<0.01$) (Figure 31 C&D). An increase in CRP to 3µg/mL was able to overcome this inhibition. These results suggest Endoplasmin may play in a role in the regulation of collagen, specifically GPVI stimulated activation, a role which we could assume is through the regulation of platelet integrins.

Following the identification that P13 inhibits platelet aggregation in a plate-based assay, we sought to confirm the effect of P13 on light-transmittance aggregometry.

PRP was incubated with vehicle or 10, 30, or 100µM P13 for 20 minutes at RT before being stimulated with 0.3µg/mL or 1µg/mL CRP in an aggregometer at 37°C stirring at 1200RPM.

PRP was seen to aggregate fully to both concentrations of CRP measured regardless of the presence of P13 (Figure 32 A, C), however a lag was detected in aggregation following 100µM P13 treatment before being stimulated with 0.3µg/mL CRP. Time to 50% aggregation was calculated and shown to increase by 32% ($P<0.01$) (Figure 32 B). An increase in CRP concentration overcame this lag, and there was no visible increase in time to 50% aggregation ($P>0.05$) (Figure 32 D).

These results suggest that Endoplasmin may play a role in platelet activation and aggregation, but when stimulating with higher concentrations of agonist the effect of inhibition is overcome and the platelet is able to overcome this effect.

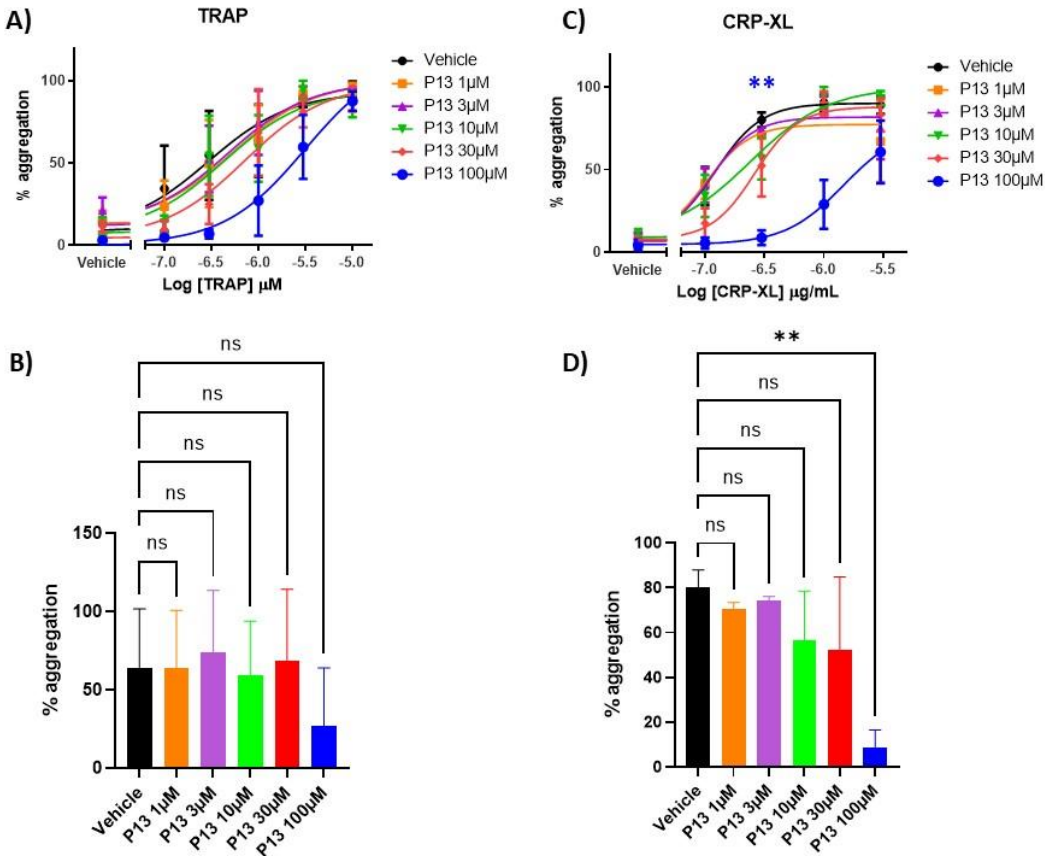

Figure 31.Determination of the inhibitory concentrations of an Endoplasmin inhibitor
Plate-based aggregation assay was used to determine the IC50 of P13 on platelets. PRP was incubated with P13 or vehicle (0.1% DMSO) for 20 minutes at 30°C in a 96 well, flat bottom half area plate. Agonists were then added and the plate was shaken at 1200RPM for 5 minutes at 37°C. Samples were read at 405nm on a FlexStation2 (Molecular devices, Winnersh, UK) and absorbance was converted to % aggregation by using the absorbance values with PRP as 0% aggregation and PPP as 100% aggregation. A) Dose response curve of P13 (1-100µM) in response to 0.1-10µM TRAP6. B) Percent aggregation at 1µM TRAP6. C) Dose response curve of P13 (1-100µM) in response to 0.1-3µg/mL CRP. D) Percent aggregation at 0.3µg/mL CRP Data presented as mean ±SD. B&D) One-way Anova with Dunnetts multiple comparisons, vehicle compared to all concentrations of P13. ** = P<0.01; n.s. = nonsignificant. N=4.

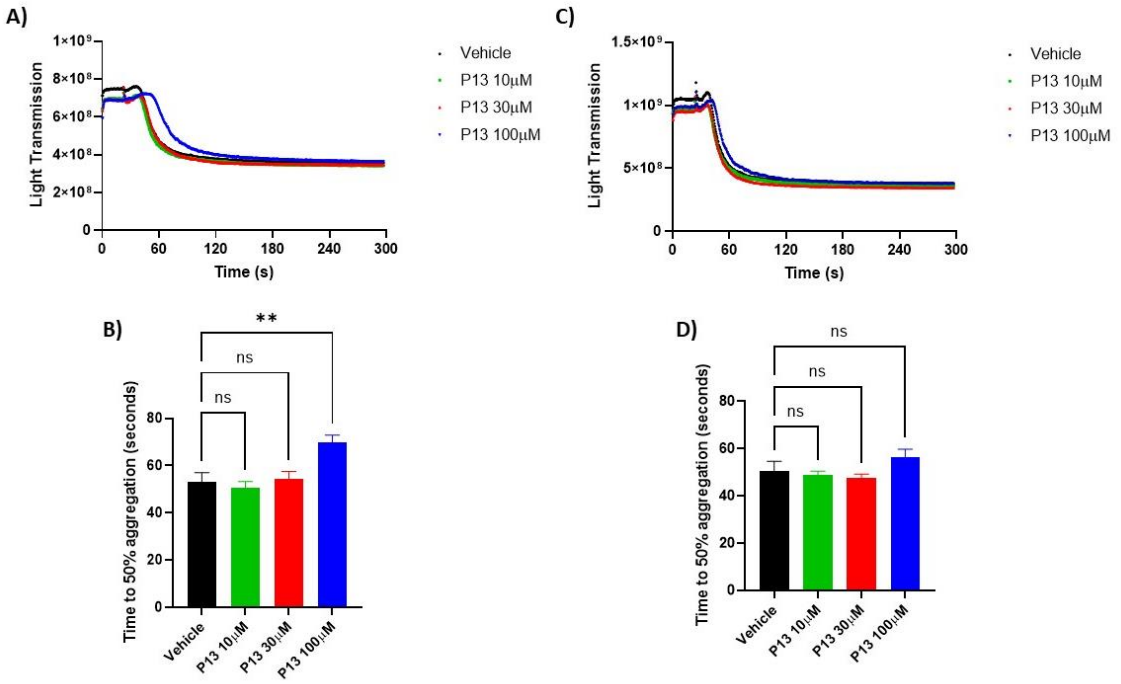

Figure 32. P13 slows but does not inhibit aggregation
PRP was incubated with vehicle (0.1% (v/v) DMSO) or varying concentrations of P13 for 20 minutes before being stimulated with 0.3μg/mL (A) and 1μg/mL (B) CRP for 5 minutes at 1200RPM. Time to reach 50% aggregation was determined for both 0.3μg/mL (B) and 1μg/mL (D) CRP. Data presented as Mean ± SD, One way ANOVA with Dunnett's multiple comparisons between vehicle and inhibitors. N.s. = non-significant, ** = P<0.01. N=3.

5.2.4.2 P13 reduces granule release and integrin activation

P13 was shown to reduce platelet aggregation in response to CRP stimulation. Endoplasmin chaperone the folding of nascent integrin proteins, of which platelets contain several different types, the most abundant being αIIbβ3. αIIbβ3 is activated in a multi-step process, where platelet agonists result in an increase in Ca^{2+}, activating CalDAG-GEFI and resulting in the replacement of RAP1-GDP by RAP1-GTP. This in turn activates the Talin/Kindlin complex and allows for a confirmational change in αIIbβ3. This change allows αIIbβ3 to bind its ligand, fibrinogen, and signal back into the platelet to release factors to activate other local platelets and form a platelet aggregate. As P13 was able to inhibit CRP stimulated aggregation, we explored whether Endoplasmin alters the state of αIIbβ3 and therefore its ability to bind fibrinogen or platelet aggregation was altered due to an alternative mechanism which resulted in a total reduction in platelet aggregation.

To investigate this, we used anti-Human P-Selectin and anti-Human anti-Fibrinogen antibodies detected using flow cytometry to begin to understand the mechanism of P13 action within the platelet. Using an anti-fibrinogen antibody allowed quantification of fibrinogen bound to the platelet surface, and P-selectin exposure identified by antibody binding allowed us to confirm that granule release was being initiated, or inhibited, following CRP stimulation.

Fibrinogen binding was shown to be unaltered in the presence of P13 at all concentrations of CRP-XL measured ($P>0.05$)(Figure 33 A, B). P-selectin exposure was also unaltered in the presence of P13 at all concentrations of CRP-XL measured ($P>0.05$)(Figure 33 C, D). These results may however be due to the large variation in MFI values detected in these samples and may require further investigation before a conclusion can be made.

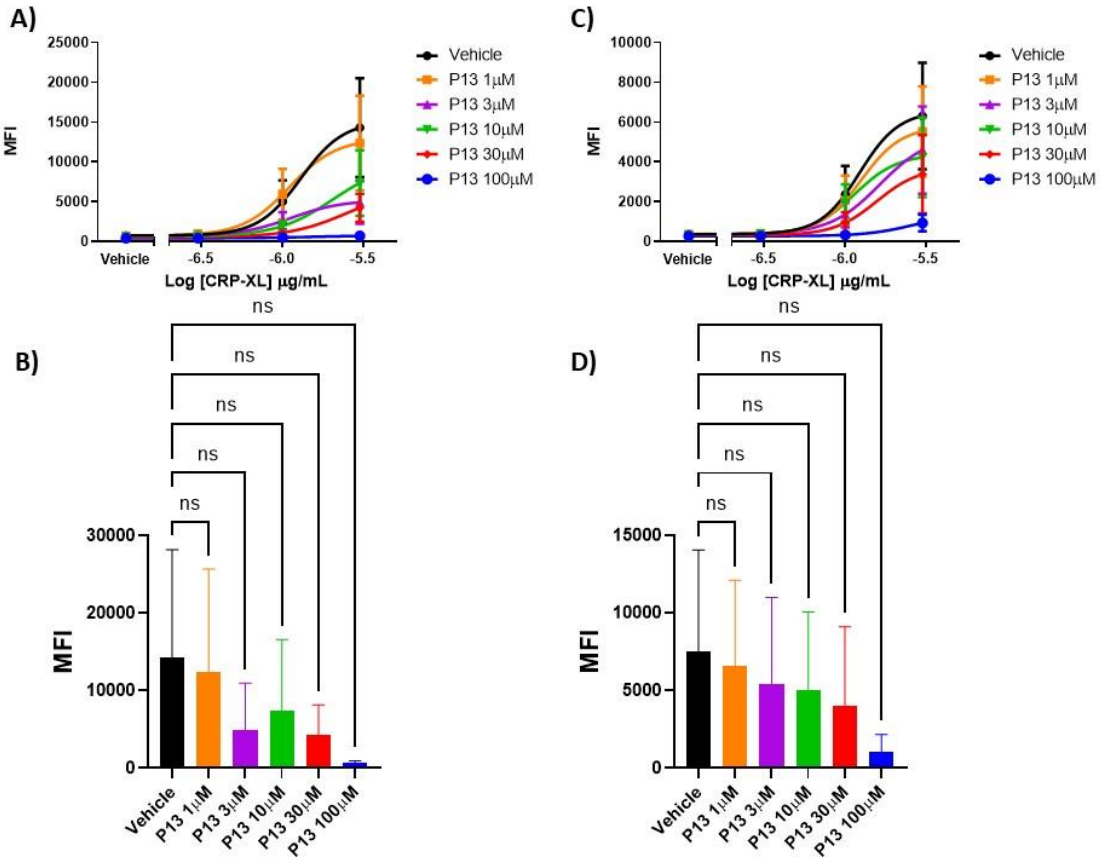

Figure 33. P13 reduces fibrinogen binding and granule secretion
PRP was incubated with increasing concentrations of P13 in the presence of anti-P selectin and anti-fibrinogen antibodies. Samples were then stimulated with increasing concentrations of CRP for 20 minutes at RT before being fixed and analysed using a BDAccuri C6Plus flow cytometer. A) Median fluorescence intensity (MFI) of anti-fibrinogen antibody of all concentrations of P13 after stimulation by 0, 0.3, 1 and 3μg/mL CRP. B) MFI of anti-fibrinogen antibody of all concentrations of P13 after stimulation by 3μg/mL CRP. C) Median fluorescence intensity (MFI) of anti-P-selectin antibody of all concentrations of P13 after stimulation by 0, 0.3, 1 and 3μg/mL CRP. D) MFI of anti-P-selectin antibody of all concentrations of P13 after stimulation by 3μg/mL CRP. All data presented as mean ± SD. B&D) One way ANOVA with Dunnetts multiple comparisons, vehicle compared to each concentration of inhibitor. N.s. = non-significant, P>0.05. N=5.

5.2.4.3 P13 inhibits thrombus formation on collagen

The ability of a platelet to form a clot is vital in order to maintain haemostasis. In arteries, platelets respond to stimuli under high shear and form stable thrombi containing platelets, red blood cells and fibrin to plug any breakages in the vessel wall. We have shown that surface expression levels of Endoplasmin increase following stimulation, and that inhibition of Endoplasmin using P13 slows aggregation, and reduces granule release and fibrinogen binding. We therefore sought to determine the role P13 may play on thrombus formation at high shear rates.

To investigate this, Cellix Vena8fluro+ chips were coated with 100µg/mL T1 collagen for one hour at RT. Citrated whole blood, stained with DiOC6, was incubated with vehicle, 10, or 30µM P13 for 20 minutes at RT before being perfused over the collagen coated chip at a rate of 1000^{s-1}. This was carried out at 37°C and imaged using a 20X objective lens on a Nikon A1 Confocal microscope. Images were captured every 2 seconds for 8 minutes. Images were then analysed using ImageJ to determine median fluorescence intensity and surface coverage of the field of view using a thresholding technique.

Median fluorescence intensity (FI) was measured over 8 minutes (Figure 34 C). Maximum FI, when calculated, identified a 43% decrease in FI following incubation with 30µM P13 ($P<0.05$) (Figure 34 D). Percentage surface coverage was measured over 8 minutes (Figure 34 E) however this did not reach statistical significance ($P>0.05$) (Figure 34 F).

The difference in the two results may be due to a number of factors. FI is a measure of fluorescence, which is affected by the laser power of the microscope and the ability of the fluorescent stain to emit. Fluorescent compounds are often light sensitive, so it may be that the significant reduction in fluorescence is an artefact. Surface coverage of the thrombi requires transformation of the image into a binary image, a process which requires a level of manual manipulation and therefore may not be a true representation of the thrombi.

Taking this into consideration, Endoplasmin may play a role in thrombus formation as identified with the reduction in fluorescence however this requires further investigation.

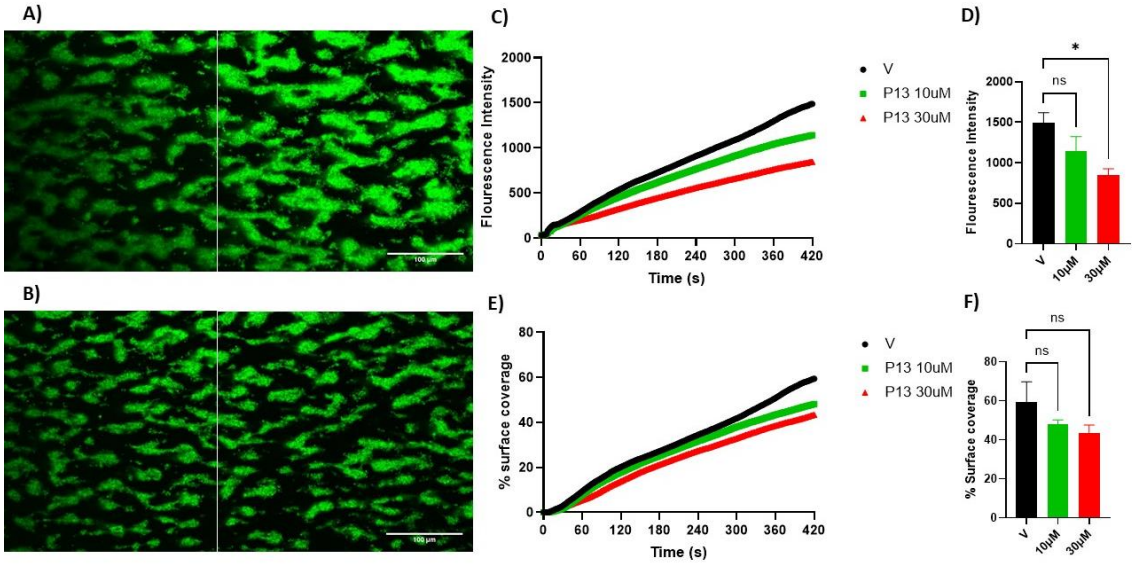

Figure 34. Endoplasmin regulates thrombus formation on collagen
Cellix Vena8 Fluoro+ channels were coated with 100µg/mL T1 Collagen for one hour at room temperature. Whole blood stained with DiOC6 was incubated with 10µM and 30µM P13 for 20 minutes at RT and then perfused over the channel at 1000^{s-1} at 37°C for 8 minutes and imaged using a Nikon A1 Confocal using a 20X objective. Microscope images were then analysed to determine the fluorescence intensity of the image and a thresholding method was used to determine the area of surface covered by adhered thrombi. A&B) Representative images of thrombi formed on collagen in the presence of vehicle (A) and 30µM P13 (B), scale bar = 100µm. Where chips were not completely flat, field of view was not 100% in focus so analysis was only carried out on the in-focus ROI, identified to the right of the white line. C) Average fluorescence intensity of all coatings over 8 minutes. D) Maximum fluorescence intensity. E) Average percent surface coverage of all coatings over 8 minutes. F) Maximum percent surface coverage. Data presented as Mean ± SD, One way ANOVA with Dunnett's multiple comparisons, vehicle compared to inhibitor. N.s. = non-significant, * = P<0.05. N=3.

5.2.5 Role of BiP on platelet function

5.2.5.1 Pifithrin, an inhibitor of BiP, reduces aggregation in a plate-based assay but not in LTA

In addition to the confirmation of Endoplasmin presence, BiP was also confirmed to be within the platelet. Pifithrin-μ (Pft), an inhibitor of BiP, has previously been used to investigate the role of BiP in tumour cell death related to unfolded protein responses. Here we investigated the effect of this inhibitor on platelet aggregation. Using a high-throughput plate-based assay, as described previously, we screened a range of concentrations of Pifithrin-μ (1μM to 100μM) and its ability to inhibit platelet aggregation in PRP using a range of concentrations of CRP-XL and TRAP6.

PRP was incubated with Pft or vehicle (0.1% (v/v) DMSO) for 20 minutes at 30°C in a 96 well, flat bottom half area plate. Agonists were then added and the plate shaken at 1200RPM for 5 minutes at 37°C. Samples were then read at 405nm on a Flexstation 2 fluorescence plate reader (Molecular devices, Winnersh, UK). Absorbance was converted to % aggregation by using the absorbance values for PRP as 0% aggregation and platelet rich plasma (PPP) as 100% aggregation.

Pft exhibited no effect on aggregation at lower concentrations of TRAP6 ($P>0.05$). At 1μM of TRAP6, 100μM Pft resulted in a 67% reduction in aggregation ($P<0.05$). This effect was overcome with 3μM of TRAP6 (Figure 35 A&B).

At lower concentrations of CRP-XL (0.1 and 0.3μg/mL) Pft had no effect on aggregation, however at 1μg/mL there was a trend similar to that seen in response to TRAP6 ($P>0.05$). An increase in CRP-XL concentration to 3μg/mL was able to overcome the inhibition of PFT and near 100% aggregation was observed.

Following the identification that Pft inhibits aggregation to TRAP6 in a plate-based assay, we wanted to confirm the effects of this inhibitor using light-transmittance aggregometry.

To do this, PRP was incubated with vehicle or 10, 30, and 100μM Pft for 20 minutes at RT before being stimulated with 1μM in an aggregometer at 37°C stirring at 1200RPM.

PRP fully aggregated in response to TRAP6 regardless of the addition of up to 100μM Pft (Figure 36). This was an unexpected result as we previously identified a 67% reduction in a plate-based aggregation assay (Figure 35)

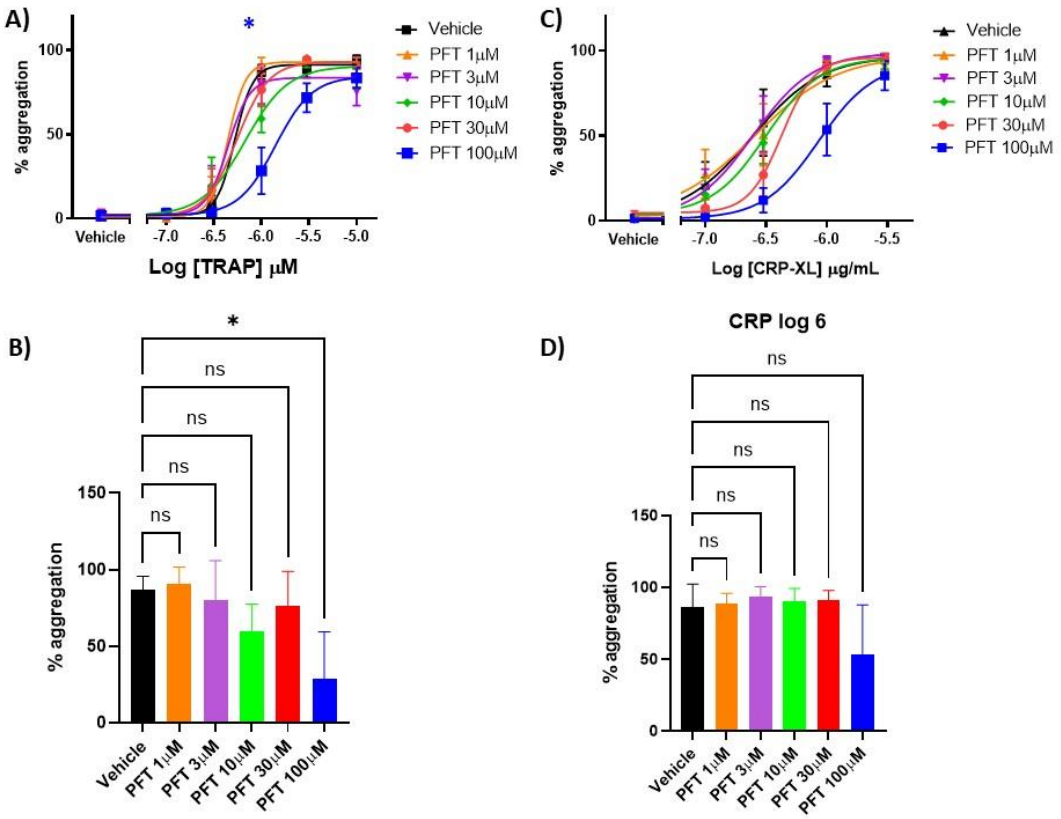

Figure 35. Identification of inhibitory concentrations of a BiP inhibitor
Plate-based aggregation assay was used to determine the IC50 of Pft on platelets. PRP was incubated with Pft or vehicle (0.1% DMSO) for 20 minutes at 30°C in a 96 well, flat bottom half area plate. Agonists were then added and the plate was shaken at 1200RPM for 5 minutes at 37°C. Samples were read at 405nm on a FlexStation2 (Molecular devices, Winnersh, UK) and absorbance was converted to % aggregation by using the absorbance values with PRP as 0% aggregation and PPP as 100% aggregation. A) Dose response curve of Pft (1-100µM) in response to 0.1-10µM TRAP6. B) Percent aggregation at 1µM TRAP6. C) Dose response curve of Pft (1-100µM) in response to 0.1-3µg/mL CRP. D) Percent aggregation at 0.3µg/mL CRP Data presented as mean ±SD. B&D) One-way Anova with Dunnetts multiple comparisons, V compared to all concentrations of Pft. * = P<0.05; n.s. = nonsignificant. N=4.

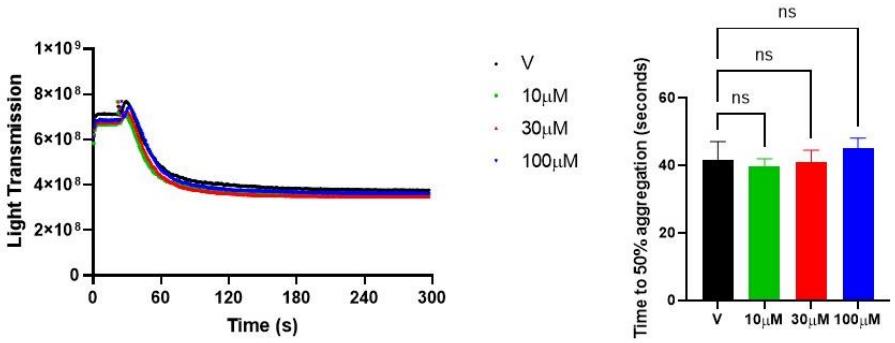

Figure 36. Pft has no effect on TRAP6 stimulated aggregation

PRP was incubated with vehicle or varying concentrations of PFT for 20 minutes before being stimulated with 1μM TRAP6 for 5 minutes at 1200RPM. All samples reached 100% aggregation, with no difference in the time it took to reach this point. Data presented as Mean ± SD, One way ANOVA with Dunnett's multiple comparisons between vehicle and inhibitors. N.s. = non-significant, P>0.05. N=3.

5.2.5.3 Pft reduces fibrinogen binding and granule release

Pft was unable to inhibit aggregation in a cuvette, however we had seen a reduction of aggregation in a plate-based aggregation assay. This led us to investigate whether any other aspects of platelet activation were modulated in the presence of this inhibitor.

To investigate this, we used anti-human P-selectin and anti-human anti-fibrinogen antibodies detected using flow cytometry to determine if there was a change in fibrinogen binding, mediated by an alteration in integrin αIIbβ3 activation, or if granule secretion was altered. PRP was incubated with P-selectin and fibrinogen antibodies in the presence of vehicle (0.1% (v/v) DMSO) or increasing concentrations of Pft for 20 minutes at RT before being stimulated with TRAP6 for 20 minutes at RT. Samples were then fixed using 0.2% formal saline and analysed using a BD Accuri C6Plus flow cytometer.

Flow cytometry analysis identified a trend towards a reduction in both fibrinogen binding (Figure 37 A, B) and P-selectin exposure (Figure 37 C, D) in the presence on 100μM Pft after stimulation with both 3μM TRAP6 ($P>0.05$) (Figure 37 B, D).

These results suggest Pft may have an effect on granule release and integrin αIIbβ3 activation at lower concentrations of inhibitor, however large amounts of variation in particularly in resting samples meant that no differences were identified.

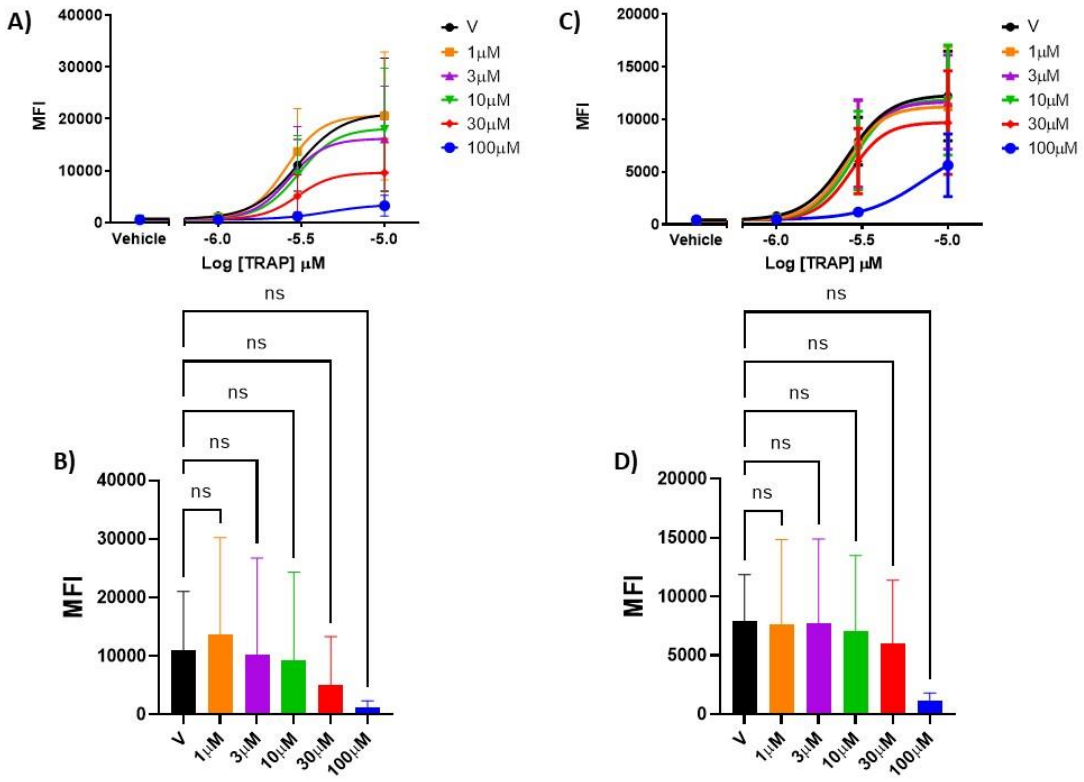

Figure 37.Pft reduces fibrinogen binding and granule release
PRP was incubated with increasing concentrations of Pft in the presence of anti-P selectin and anti-fibrinogen antibodies. Samples were then stimulated with increasing concentrations of CRP for 20 minutes at RT before being fixed and analysed using a BDAccuri C6Plus flow cytometer. A) Median fluorescence intensity (MFI) of anti-fibrinogen antibody of all concentrations of Pft after stimulation by 0, 1, 3, and 10µM TRAP6. B) MFI of anti-fibrinogen antibody of all concentrations of Pft after stimulation by 3µM TRAP6. C) Median fluorescence intensity (MFI) of anti-P-selectin antibody of all concentrations of Pft after stimulation by 0, 1, 3, and 10µm trap6. D) MFI of anti-P-selectin antibody of all concentrations of PFT after stimulation by 3µm TRAP6. All data presented as mean ± SD. B&D) One way ANOVA with Dunnetts multiple comparisons, vehicle compared to each concentration of inhibitor. N.s. = non-significant, P>0.05. N=5.

5.2.5.4 Pft reduces the ability of platelets to form thrombi in response to collagen

The ability of platelets to form a thrombus is vital in order to maintain haemostasis. In the arteries, platelets respond to stimuli under high shear and form a stable thrombi containing platelets, red blood cells and fibrin to plug any breakages in the vessel wall.

We have shown that BiP increases in surface expression following stimulation, and that inhibition of BiP using Pft reduces granule release and fibrinogen binding. We therefore wanted to explore whether BIP is likely to play a role on thrombus formation at high shear rates.

To investigate this, Cellix Vena8fluoro+ chips were coated with 100µg/mL T1 collagen for one hour at RT before whole citrated blood stained with DiOC6 was incubated with vehicle or 10 and 30µM Pft for 20 minutes at RT before being perfused over the collagen coated chip at a rate of 1000^{s-1}. This was carried out at 37°C above a 20X objective on a Nikon A1 Confocal system. Images were captured every 2 seconds for 8 minutes. Images were then analysed using ImageJ to determine median fluorescence intensity and surface coverage of the field of view using a thresholding technique.

Median fluorescence intensity (FI) was measured over 8 minutes (Figure 38 B). Maximum FI, when calculated, identified a % decrease in FI following incubation with 30µM Pft ($P<0.01$) (Figure 38 C). Percent surface coverage was measured over 8 minutes (Figure 38 E) however when maximum percent surface coverage was calculated no significant difference was identified ($P>0.05$) (Figure 38 E).

These results are similar to those seen after incubation with the Endoplasmin inhibitor, P13, and they suggest that BiP may play a role in thrombus formation however this requires further investigation.

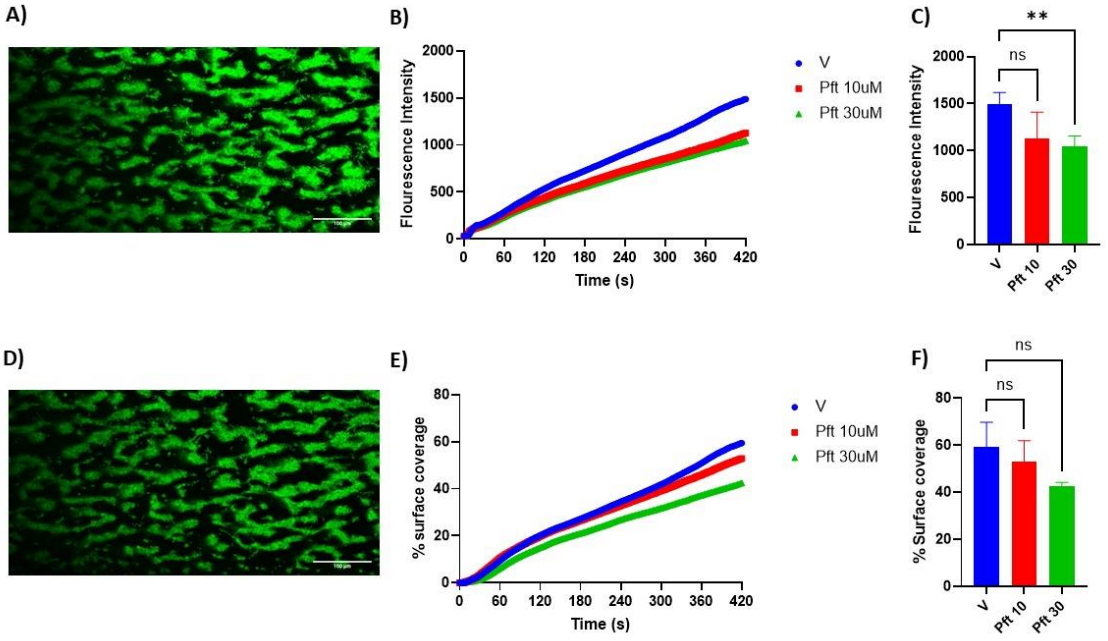

Figure 38. BiP regulates collagen stimulated thrombus formation

Cellix Vena8 Fluoro+ channels were coated with 100µg/mL T1 Collagen for one hour at room temperature. Whole blood stained with DiOC6 was incubated with 10µM and 30µM Pft for 20 minutes at RT and then perfused over the channel at 1000^{s-1} at 37°C for 8 minutes and imaged using a Nikon A1 Confocal using a 20X objective. Microscope images were then analysed to determine the fluorescence intensity of the image and a thresholding method was used to determine the area of surface covered by adhered thrombi. A&D) Representative images of thrombi formed on collagen in the presence of vehicle (A) and 30µM Pft (D), scale bar = 100µm. B) Average fluorescence intensity. C) Maximum fluorescence intensity. E) Average percent surface coverage. F) Maximum percent surface coverage. Data presented as Mean ± SD, One way ANOVA with Dunnett's multiple comparisons, vehicle compared to inhibitor. n.s. = non-significant, * = P<0.05. N=3

5.3 Discussion

Chaperone proteins exist within cells to aid with protein expression, binding to nascent proteins and assisting their folding into tertiary and quaternary structures (Kim et al., 2013b, Kerner et al., 2005, Hartl, 1996). Chaperone proteins also bind to mis-folded proteins in order to prevent protein aggregates leaving the ER or Golgi (Kim et al., 2013b). Since the identification of the KDEL- ER retention sequence over 30 years ago, the function of KDEL-containing proteins has been further understood (Munro and Pelham, 1987). Chaperones bind to nascent proteins and transport them from the ER to the Golgi. Upon release in the Golgi, KDEL proteins containing a KDEL- or KDEL-like structure, in a pathway mediated by the KDEL-receptor, are trafficked back to the ER in order to continue this role (Wilson et al., 1993, Aoe et al., 1997, Cabrera et al., 2003). Platelets, cells without a nucleus, produce only small amounts of proteins, so the presence of these KDEL- containing proteins within the platelet seems counterintuitive, however we are regularly learning about the presence and vital role these proteins play in platelet physiology. HSP47 is an example of this, and though HSP47 contains an RDEL-sequence instead of KDEL-, also plays a role in platelet function in addition to its role chaperoning procollagen and assisting its formation into its triple helical structure (Hirayoshi et al., 1991, Sasikumar et al., 2018, Lamande and Bateman, 1999, Hendershot and Bulleid, 2000). Within resting platelets HSP47 has been identified in the DTS with PDI and has also shown to be increased in surface exposure following stimulation (AlOuda et al., Under review)*(Sasikumar et al., 2018).*

The identification and further understanding of the roles in platelet function of PDI, the thiol isomerases Erp5, Erp57 and Erp72, and HSP47 led us to question if this was not an exhaustive list of chaperone proteins that function within the platelet. After searching the literature for known chaperone proteins, we then found a number of these within MK, the platelet precursor, and platelet proteomic and transcriptome datasets (Figure 25 A&B). Immunoblotting of whole platelet lysates confirmed the presence of BiP, Endoplasmin and Grp170 within the platelet proteome (Figure 25 C).

It has been widely reported that platelet chaperone proteins increase in surface exposure following platelet activation, so we aimed to identify if these newly identified proteins also exhibited the same characteristics (Holbrook et al., 2010, Crescente et al., 2016, Sasikumar et al., 2018). Flow cytometry analysis identified that platelet activation resulted in increased antibody binding to Endoplasmin following both stimulation with TRAP6 and CRP (Figure 26 A). We also identified a trend towards an increase in Grp170 surface exposure following CRP-XL

stimulation (Figure 26 B) , and BiP following TRAP6 (Figure 26 C) exposure however the large variability on the stimulated samples suggest that this is highly dependent on the donor and this study was under-powered, however the trend may suggest that translocation of Grp170 occurs as a result of the GPVI-FcRγ platelet activation pathway and BiP is downstream of TRAP6 activation. Calreticulin binding was not altered following TRAP6 or CRP stimulation (Figure 26 D).

Integrin αIIbβ3 is the most abundant receptor on the platelet surface, with around 80,000 copies within the platelet (Moebius et al., 2005). The identification that these newly confirmed proteins within the platelet increase in surface expression following stimulation led us to question whether these proteins colocalise with αIIbβ3 at the platelet surface. Pearson's coefficient, a measurement of colocalization within a dual colour microscopy image where 1 is when pixels in two different colours are completely colocalised, 0 is not colocalized and -1 suggests the pixels in each colour are completely opposite from each other and the proteins being imaged may repel each other (Bolte and CordeliÈRes, 2006). Immunocytochemistry observations (ICC) of resting and stimulated platelets suggested that Endoplasmin appears to remain distributed throughout the platelet following TRAP6 stimulation (Figure 27), results which support flow cytometry data about surface expression that showed surface expression increased following stimulation with CRP but not with TRAP6 (Figure 26 A) and we may see differences in the location of Endoplasmin following CRP stimulation for ICC samples. In resting samples, Pearson's coefficient comparing Endoplasmin and αIIbβ3 was calculated to be 0.88, reducing upon activation potentially due to the appearance that Endoplasmin remains distributed throughout the platelet and αIIbβ3 translocates to the surface to provide addition binding sites to form a stable thrombi.

ICC suggests that BiP is found in clusters in resting platelets, but following stimulation is found distributed around the platelet and appears to form a platelet "cap" on one side of the platelet (Figure 28). In resting platelets, Pearson's coefficient was determined to be 0.77 and there was no change quantified after stimulation confirming the observation that BiP changes in its location and remains co-localised to αIIbβ3. Visualisation of Grp170 shows distribution throughout the resting platelet (Figure 29), but no distinct change following stimulation which again, like that seen of Endoplasmin, may be due to ICC samples being stimulated using TRAP6. Analysis by flow cytometry identified a significant increase in Grp170 expression following CRP stimulation but not TRAP6 (Figure 26). Pearson's coefficient, however, calculated a 32% increase following stimulation suggesting that Grp170 is more likely to be found at the platelet surface colocalised with αIIbβ3 following stimulation. In resting platelets,

Calreticulin appears to be distributed throughout the platelet when resting, but upon stimulation forms a ring like structure and colocalises with αIIbβ3 (Figure 30). This is supported by the calculation of Pearson's coefficient, where no difference was found between resting and stimulated samples suggesting a similar level of colocalization of Calreticulin and αIIbβ3 in both states.

Further investigation of the localisation of these proteins may suggest that they are found within similar regions of the platelet, as Grp170 has been identified in a complex with BiP, Endoplasmin, thyroglobulin and the thiol isomerase Erp72 (Kuznetsov et al., 1997, Olden et al., 1978). This interaction was identified in thyroid epithelial cells taken from a rat however it may be that this interaction occurs in all cell types and that we will find these proteins co-localised within the platelet.

Inhibitors of KDEL- proteins have been used to elucidate the role of these proteins within the platelet. We used PU-WS 13 (P13), an inhibitor of Endoplasmin, and Pifithrin (Pft), and an inhibitor of BiP, to identify the roles these proteins played in platelet function. These inhibitors were selected based on their selectivity to the proteins in question and their availability. We first tested these inhibitors on their ability to inhibit platelet aggregation for two reasons: 1) to identify if P13 and Pft targeted proteins identified in platelets and 2) to identify an inhibitory concentration effective in platelet function. Both P13 and Pft were most effective at the higher range of the concentrations tested (30μM – 100μM) however these effects were overcome in the presence of higher concentrations of agonist (Figure 31 and Figure 35). 100μM P13 resulted in a 60% reduction in CRP stimulated aggregation, and 100μM Pft resulted in a 67% reduction in TRAP6 stimulated aggregation, both identified in a plate-based aggregation (PBA) assay. PBA assays, while allowing for a large number of variations in agonist/inhibitor concentrations measured, are only end point assays and do not identify the differences in the kinetics of aggregation. Light transmittance aggregometry (LTA) tracks light transmittance through a stirring sample and allows for the identification of kinetics during aggregation, and identified that a lag at 1μg/mL CRP in the presence of 100μM P13, but total aggregation was reached in the end. The lag was calculated to identify at 32% increase in time to 50% aggregation. Pft had no effect on TRAP6 stimulated aggregation in the LTA assay.

In order for platelets to aggregate a number of activatory steps are initiated, including granule release and integrin activation. Endoplasmin is an integrin chaperone, so we hypothesised that the reduction in aggregation was due to an effect on integrin activation. Anti-fibrinogen antibodies quantify the amount of fibrinogen bound to the platelet surface, a marker of

integrin activation as αIIbβ3 will only bind to fibrinogen when in its fully active state. P-selectin antibodies quantify whether P-selectin, contained in α granules within the resting platelet, is released following signalling pathways stimulation and increase of intracellular Ca^{2+} resulting in an increase in availability of P-selectin. Both P13 and Pft suggested that they may reduce both fibrinogen binding and P-selectin exposure, though these results were not significant due to the large amount of variation particularly in the resting samples and may be under-powered (Figure 33 and Figure 37).

The ability of a platelet to form thrombi in a vessel in response to exposed collagens is vital in haemostasis and the maintenance of the circulatory system. Both P13 and Pft resulted in a reduction in thrombi formation in response to collagen at arterial shear rates (1000^{-s-1}) suggesting that both Endoplasmin and BiP are required for thrombi formation to occur.

We have identified that inhibitors of Endoplasmin and BiP both result in the inhibition of functional platelet responses, and these proteins join other KDEL- containing proteins known to have an impact on platelet biology, however we haven't taken any steps to ensure the impacts seen following pre-incubation with P13 and Pft are due to inhibition of the proteins in question. The concentrations of both P13 and Pft used in this study were high (30-100µM) compared to when used in previous studies. Murillo-Solana *et al.* used P13 from 100nM to 10µM and Zhu *et al.* used Pft at 0.2-1.6µM suggesting that the concentrations used in this study may have resulted in off-target effects (Murillo-Solano et al., 2017, Zhu et al., 2020). Further understanding of the role Endoplasmin and BiP may play on platelet function, and the mechanism of their inhibitors would potentially provide new therapeutic targets in the platelet field.

Previously, we mentioned that several chaperone proteins were identified within a complex. A recent analysis of the platelet proteome following cancer-related biochemical changes identified Calreticulin, BiP and PDI were all found to be upregulated in patients with brain cancer (Ercan et al., 2021). Our understanding of the role of platelets in systems outside of the circulation is rapidly improving, and it may be that these chaperone proteins, which are known cellular stress responders, are implicated in the platelet response to pathological conditions. Mutations in exon 9 of CALR, the gene which produces Calreticulin and that we identified to be distributed throughout the platelet proteome, results in the onset of Philadelphia-negative myeloproliferative neoplasms (MPN) essential thrombocythemia (ET) and primary myelofibrosis (PMF) (Klampfl et al., 2013, Nangalia et al., 2013, Nunes et al., 2015). Both ET and PMF are commonly the result of a JAK2V617F mutation, (but CALR mutations are the next

most common cause) and patients with CALR mutations respond to treatment with JAK inhibitors (Cervantes et al., 2013). We previously suggested that HSP47, an ER-chaperone protein with a KDEL-like sequence that also plays a role in platelet function, may play a role in MPNs and present a newly suggested therapeutic target for these conditions.

Chapter 6 – Discussion

6.1 General

Megakaryocytes are the rarest cell type found within the bone marrow, accounting for ~0.01% of nucleated cells in this environment (Nakeff and Maat, 1974). Differentiation of a haematopoietic stem cell into a MK, and MK maturation is driven by thrombopoietin (TPO) binding its receptor, c-Mpl (Kaushansky et al., 1994). MKs undergo endomitosis, progressing through the cell cycle without cell division resulting in cells containing multiple copies of DNA in a single nucleus, calculated to be 64 n or larger (Kuter et al., 1994, Zimmet and Ravid, 2000). Upon maturation and the formation of sufficient internal membranes and organelles, MKs migrate to the vascular niche, the area of the bone marrow closest to the sinusoidal blood vessels. Once they are in this location, a process previously inhibited through the presence of collagen in the osteoblastic niche is initiated and MKs are able to extend proplatelets into the sinusoidal space and from which platelets are released into circulation (Sabri et al., 2004, Tablin et al., 1990, Italiano et al., 1999). Each MK produces $1x10^4$ platelet per day, an extremely efficient process which as yet, has not been replicated *in vivo (Long, 1998)*. MK dysfunction, as seen in myeloproliferative neoplasms (MPNs), can result in overproduction of MKs and therefore platelets, overwhelming the bone marrow environment and also resulting in the loss of other blood cells in circulation. Megakaryocytes have been shown to also play a role in maintaining the BM environment, secreting ECM proteins for cellular support (Malara et al., 2018). The BM environment is altered in the case of myelofibrosis, where increased collagen results in scarring making it difficult for HSCs to differentiate and blood cells to mature (Zahr et al., 2016).

Upon release into the circulation, platelets remain in a resting state as a result of NO and PGI_2 release from endothelial cells (de Nucci et al., 1988). In the event of endothelial damage following injury or atherosclerotic plaque rupture, haemostatic mechanisms are triggered to maintain the integrity of the circulatory system and prevent bleeding out. Platelets have a variety of receptors on their surface in order to respond to stressors that initiate signalling cascades, including multiple collagen receptors (Jackson et al., 2003). GPIb-V-IX binds to exposed collagen in the basement membrane or tissue ECM via vWF within the circulation in a process which slows, but does not stop platelet movement (Ruggeri, 1997, Vasudevan et al., 2000). This allows integrin α2β1 and GPVI to bind to collagen, which results in the initiation of intracellular signalling leading to the release of intracellular calcium stores and platelet granules containing additional surface receptors, vWF, and secondary activators including ADP (Geue et al., 2017, Suzuki-Inoue et al., 2003, Varga-Szabo et al., 2009) .The increase in intracellular calcium results in a confirmational change in integrin αIIbβ3 on the platelet to

support binding of its ligands. Fibrinogen binding to integrin αIIbβ3 results in outside-in signalling which leads to irreversible activation of platelets, recruitment of localised activated platelets and therefore the formation of a thrombus (Staatz et al., 1989). Thrombi can be used as a plug to fix damaged vessels, however when formation is triggered inappropriately, they can also result in circulating thrombi which can have a catastrophic effect if they reach the lungs or brain, demonstrating the importance of the balance between haemostasis and pathological formation of clots. The formation of thrombi within coronary arteries, often due to pre-existing atherosclerotic plaques, is also extremely dangerous as these can result in arterial blockage leading to hypoxia, and eventually myocardial infarction. Understanding of the regulatory mechanisms controlling receptors and signalling cascades which control both platelet inhibition and stimulation have led to the development of a number of anti-platelet therapeutic targets.

A number of chaperone proteins, normally found within the ER of protein producing cells have been identified within the platelet, and contribute to function at the cell surface. HSP47, a collagen chaperone protein, is one example of this and has been shown to play a role in collagen mediated platelet function although how and why is not properly understood (Kaiser et al., 2009, Sasikumar et al., 2018). In this study, we gained a further understanding of the role of HSP47 in both MKs and platelets.

6.2 HSP47 as a regulator of MK collagen synthesis

HSP47 upregulation has been identified in a number of conditions including osteogenesis imperfecta and liver, intestinal, kidney and pulmonary fibrosis (Essawi et al., 2018, Masuda et al., 1994, Honzawa et al., 2014, Razzaque et al., 1998b). Targeting HSP47 using siRNA has ameliorated the effects of fibrotic conditions in the skin, eyes, and lungs, and has also been used prophylactically to prevent onset of pulmonary fibrosis (Yamakawa et al., 2018, Ohigashi et al., 2019, Kishimoto et al., 2019, Otsuka et al., 2017, Liu et al., 2021). HSP47 has been identified in the megakaryocyte MEG01 cell line, which led us to question whether HSP47 may be a target for MPNs and fibrosis (Sasikumar et al., 2018). HSP47 is a highly conserved protein found in zebrafish to homo sapiens with few sequence differences, so we used a murine model to further understand the role of HSP on MKs (Lele and Krone, 1997, Ikegawa et al., 1995). We used a PF4-Cre dependent gene deletion murine model as HSP47 is embryonically lethal at 11.5 days post coitus (Nagai et al., 2000). The PF4 promoter is stimulated during megakaryopoesis therefore resulting in the production of mice with megakaryocyte lineage HSP47 gene deficiency, however stimulation of the PF4 promoter has also been detected in HSCs, lymphoid- and myeloid- derived cells suggesting that the gene deletion may be leaky,

and not MK specific as previously thought (Pertuy et al., 2015, Calaminus et al., 2012). We did not investigate HSP47 expression, or lack of, in cells other than MKs however quantification of full blood counts identified no changes following PF4-Cre-HSP47$^{flox/flox}$ mutation suggesting this genetic alteration has no major effect on other cell types. An alternative Cre recombinase model using the GPIbα locus has been developed, with Cre inserted into the exon containing the open reading for GPIbα (Nagy et al., 2019). GPIbα is singularly expressed in the MK lineage reducing the off-target effects however it is thought that the GPIbα-Cre construct would not result in high Cre levels and therefore inactivation of the protein of choice would not be 100% efficient (Gollomp and Poncz, 2019).

Using the PF4-Cre HSP47$^{flox/flox}$ mice, we identified that there was no identifiable difference in ploidy in MKs from HSP47 deficient mice and control mice, suggesting that MKs are able to undergo endomitosis as normal and that HSP47 is unlikely to have a role in this process. Ploidy of MKs isolated from HSP47 deficient and control mice was determined to be between 4 and 8N, a value lower than Heib *et al.* identified when isolating MKs using a similar isolation method (Heib et al., 2021). Following isolation from the bone marrow, cells were passed through a cell strainer to remove any debris from the sample. In this study we used a 70µm strainer where Heib *et al.* used a 100µm strainer so there is a chance that some of the larger, higher ploidy MKs that are 32 and 64N were caught here and not analysed in these samples but might be identified if a larger cell strainer was used in further studies.

Proplatelet formation was also determined to be unaltered in HSP47 deficient cells, suggesting that HSP47 does not play a role in MK maturation and platelet production. Following 24-hour imaging of proplatelet formation, it would have been useful to confirm that the cells identified as proplatelets were as thought. Processing the supernatant from the microscopy slides through a flow cytometer, in the presence of platelet markers such as antibodies against αIIbβ3, would allow us to confirm the identity of these objects. In the bone marrow, megakaryocytes are surrounded by numerous other cell types and a microenvironment that has previously been reported to be important for the production of proplatelets. In this assay, there was a small number of cells due to difficulties with cell numbers and needing to provide experimental repeats. From the images presented, as was the case in all samples, the number of megakaryocytes that were near, or in contact with other megakaryocytes during this process was also limited. These factors may have resulted in these experiments not being a true representation of the impact that deletion of HSP47 in megakaryocytes has on proplatelet formation and should be repeated with larger cell numbers to further confirm these results. Previously, platelet production in the lungs has been identified but the role of HSP47 in this

process was not assessed in this study. It would however, be interesting to determine if there is a role of HSP47 in those additional populations of megakaryocytes that have differentiated from cells outside of the bone marrow. Whilst we did not identify a difference in proplatelet formation, we did identify a reduction in collagen production from HSP47 deficient MKs, leading us to hypothesise that HSP47 may be a suitable target for myelofibrosis. Current myelofibrosis treatments such as Ruxolitinib, a selective Janus kinase (JAK) 1 and JAK2 inhibitor which modulates cytokine-stimulates intracellular signalling, result in the onset of anaemia and thrombocytopenia, and chronic use results in increased risk of infection, skin cancer and secondary malignant tumours (Galli et al., 2014, Barbui et al., 2019, Ostojic et al., 2012). We hypothesise that by targeting megakaryocytic HSP47, collagen synthesis in the bone marrow would be reduced whilst other MK functions remain resulting in patients not presenting with the off-target effects of treatments such as Ruxolitinib.

6.3 HSP47 as a platelet receptor

Platelet receptors have been researched widely, however the identification of HSP47 on the platelet surface and its ability to regulate collagen stimulated responses led us to question whether HSP47 itself acts as a receptor on the surface (Kaiser et al., 2009, Sasikumar et al., 2018). Collagen toolkit peptides contain 27 amino acids in a flanking sequence which gives the peptide a triple helical structure. We previously identified that a number of these peptides bind to HSP47 with a range of affinities (Cai et al., 2021). Those which bound with the highest affinity were Coll II 14 and 26, followed by Coll II 13 and Coll II 26. Testing a number of platelet function assays identified that platelets are able to adhere to and spread on these peptides in an HSP47-dependent manner by using a small molecule inhibitor. We did not however, test whether the effect of this molecule is specifically impacting HSP47 by using platelets from HSP47 deficient mice, or an alternative small compound that does not inhibit HSP47, both of which would allow us to further understand the interaction between the HSP47 binding sequences within collagen and HSP47 itself.

Though HSP47 binding sequences are able to support adherence and shape change, they are not able to initiate platelet activation, determined by analysis of granule release, fibrinogen binding as a measure of integrin αIIbβ3 activation or platelet aggregation. These results suggest HSP47 may function in a similar mechanism to integrin α2β1, supporting adhesion and signalling that promotes platelet spreading. HSP47 is able to bind to the integrin α2β1 collagen binding sequence, GFOGER identified through a protein binding assay. AlOuda *et al.* however identified that when washed platelets are treated with a HSP47 inhibitor, SMIH, there is no

change in the response to adhesion and shape change to GFOGER suggesting that HSP47 does not modulate α2β1 and its interaction with GFOGER (AlOuda et al., Under review). Investigation of active motifs within collagen toolkit sequences from previous work identify the amino acid sequence GPR in Coll II 13 and Coll II 14, GAR in Coll II 20 and GER in Coll II 26 suggesting that GXR, where X is a non-specific amino acid, is essential for this response. Proline is the only amino acid where the side chain is connected to the backbone twice, forming a ring containing nitrogen, and has been suggested to be the unspecified residue in the GXR sequence, with GPR essential for HSP47 interactions (Koide et al., 2002, Koide et al., 2006). Alanine and Glutamic acid both have charged side chains, although Arginine is positively charged and glutamic acid is negatively charged so it is possible that the ability of platelets to adhere and change shape in a HSP47-dependent manner is due to chance.

We hypothesise that HSP47 does act as a receptor on the platelet surface, although the mechanism for this has not been investigated. HSP47 is not a transmembrane protein, so it cannot be a traditional cell surface receptor, however we suggest it binds to an unknown protein on the cell surface, in addition to interacting with GPR/GAR/GER sequences within collagen. We hypothesise that these interactions result in adhesion and shape change in a mechanism that involves actin fragmentation, as HSP47 has been previously reported to be involved in cytoskeletal rearrangement of actin filaments, identified in interstitial and epithelial cells in addition to chronic diabetic renal cells (Razzaque et al., 1998c, Liu et al., 2001). We have also previously demonstrated that release of HSP47 from the DTS to the platelet surface occurs in an actin dependent mechanism, similar to that seen in the translocation of PDI following activation further supporting this hypothesis (AlOuda *et al.,* Under review)(Crescente et al., 2016).

6.4 HSP47- a modulator of collagen-platelet interactions

AlOuda *et al* previously identified that HSP47 supports GPVI dimerization and GPVI signalling by supporting Syk, LAT and PLCγ2 phosphorylation and this signalling in response to GPVI agonists following HSP47 suggests that HSP47 modulates platelet responses to collagen (AlOuda et al., Under review). We aimed to use Collagen toolkit peptides to identify if these responses were due to specific regions of collagen. After pre-incubating platelets with HSP47 binding sequences, we then attempted to initiate functional platelet responses to collagen and identified that 10µg/mL collagen toolkit sequences Coll II 13, Coll II 14, and Coll II 20 resulted in an inhibition in granule release, integrin activation and platelet aggregation . Again, Coll II 13, 14 and 20 present as the sequences that have the greatest regulatory role further

suggesting that the GPR/GAR motifs are the key HSP47 modulatory sequences, however we did not include controls in these experiments to determine if the GPP flanking sequence, or non-HSP47 binding sequences were able to interrupt platelet activation and aggregation. We hypothesise that pre-treatment of platelets with peptides containing these motifs bind HSP47 and therefore result in a reduction of HSP47 availability for collagen stimulation. We also investigated the ability of platelets to form thrombi on collagen after pre-incubation of whole citrated blood with toolkit sequences however peptides were found to have no effect. This however may be due to the set-up of the assay, with channels coated with up to 10X more collagen than used in the other assays suggesting that at greater concentrations of collagen platelets are able to overcome the reduced availability of HSP47. Alternatively, thrombus formation was carried out at arterial shear, and it may suggest that the interaction of HSP47 with these peptides is a relatively weak one in these circumstances. Overall, we suggest that HSP47 interacts with GPR and GAR motifs within collagen and modulates collagen receptors on the platelet surface.

6.5 Role of KDEL proteins in platelets and their ability to modulate function

Chaperone proteins assist the folding of nascent proteins into their correct structure, and many contain a c-terminal KDEL- retention sequence (or similar) which retains these proteins within the ER, or supports their trafficking from the golgi back to ER (Kerner et al., 2005, Kelly, 1990). PDI, a thiol isomerase, was identified within the platelet and its role in regulating platelet function is continuing to be understood (Chen et al., 1992, Chen et al., 1995, Essex et al., 1995, Kim et al., 2013a). Other thiol isomerases have also been identified within the platelet and shown to play a role in thrombosis including Erp5, Erp57 and Erp72, in addition to HSP47, leading us to question the presence of other chaperones within the platelet proteome that are involved in the regulation of platelet function at the cell surface (Holbrook et al., 2010, Passam et al., 2015, Holbrook et al., 2012, Crescente et al., 2016, Holbrook et al., 2018, Kaiser et al., 2009, Sasikumar et al., 2018). Using proteomic and transcriptomic approaches, we confirmed the presence of addition KDEL- containing proteins Endoplasmin, BiP, Grp170 and Calreticulin within a platelet (Watkins et al., 2009, Burkhart et al., 2012). It is no surprise that these proteins are all found in the platelet, as previously Grp170 has identified to be co-ordinately induced with BiP and Endoplasmin and in a complex with BiP, Endoplasmin and Erp72 (Cervantes et al., 2013, Kuznetsov et al., 1997, Olden et al., 1978).

Using a flow cytometry approach, we then confirmed that these proteins were detectable at the platelet surface, and surface levels of Endoplasmin were increased following stimulation

with CRP-XL. Previous reports suggest that the thiol isomerases and HSP47 increase in surface exposure following stimulation, however this was not the case we identified with Grp170, BiP and Calreticulin (Holbrook et al., 2010). We also used immunocytochemistry to determine the location of these proteins in both resting and stimulated platelets. Co-staining with integrin αIIbβ3 as a marker of granules and the platelet surface for reference, allowed us to determine that Grp170 colocalization increases upon stimulation but Endoplasmin-αIIbβ3 colocalization decreases. This may suggest that Grp170 is stored independently of αIIbβ3 in resting platelets but is found at the surface following stimulation, and Endoplasmin is stored in α-granules in resting platelets. We identified no change in BiP or Calreticulin colocalization with αIIbβ3 suggesting that as αIIbβ3 is trafficked from α-granules to the surface during activation, as are BiP and Calreticulin however we were unable to quantify this using flow cytometry. We investigated the role of an Endoplasmin inhibitor, P13, on platelet function and identified that CRP-XL stimulated platelet aggregation was reduced suggesting P13 has an impact on the collagen-GPVI signalling pathway and is also able to reduce thrombus formation at arterial shear rates. Previously, P13 has been shown to both inhibit growth and induce apoptosis in human multiple myeloma cells and a number of similar inhibitors are in clinical trials for treatment of cancer and neurodegenerative diseases, so understanding the role these inhibitors play on platelet function is important if they are to be introduced as treatments (Hua et al., 2013). Whilst investigating the role of P13 on platelet function, we identified a reduction to platelet aggregation in a plate-based assay that was not seen in the light transmittance assay. We are not the first group to report differences between the two assays, with Chan *et. al.* suggesting that the two assays are not interchangeable, and should be used as complementary tests to investigate platelet function (Chan et al., 2018).

We also investigated the role of a BiP inhibitor, Pft, on platelet function and identified that TRAP6 stimulated platelet aggregation was reduced in a plate-based assay. Pft also reduced the ability of platelets to form thrombi on collagen at arterial shear. In order to identify a reduction in function however, these inhibitors were used at high concentrations (30-100μM) so we are unable to rule out that these inhibitors may have had off-target effects.

In separate experiments investigating the role of P13 and Pft on thrombus formation, we analysed data using two different methods that resulted in differing results with one method showing statistically significant differences and the other showing no differences. Firstly, we calculated the fluorescence intensity of the field of view, per frame, over eight minutes. Thrombi, in the presence of both inhibitors, were shown to be reduced as calculated by the reduction in fluorescence suggesting that less platelets had adhered. Secondly, the same

image was converted to a binary image using a thresholding technique and was used to determine the percent surface coverage, however this method identified no differences between conditions (vehicle and following drug treatment). Both of these calculations however only measure thrombi in one plane and therefore does not give a true representation of the total system as it has been reported that measurements at the extremities of flow chambers are less reproducible (Pugh et al., 2012). Post flow, collection of z-stacks of a set location in the chamber and calculation of the surface coverage throughout the entire thrombi would ensure that data produced is reproducible.

Systemic deletion of the Endoplasmin gene, like that of HSP47, is embryonically lethal around day 7 therefore Mao *et al.* created a transgenic model targeting exon 2 of the Endoplasmin allele allowing conditional deletion, also using a cre-recombinase approach (Wanderling et al., 2007) (Mao et al., 2010). Systemic knock out of BiP is also embryonically lethal, earlier than both Endoplasmin and HSP47 at 3.5 days post coitus compared to 7 and 11.5, respectively (Luo et al., 2006, Wanderling et al., 2007, Nagai et al., 2000). Again, like Endoplasmin and HSP47, a conditional knockout using a Cre-recombinase approach targeting exons 5 and 8 has been produced (Luo et al., 2006). Generation of a PF4-Cre/Endoplasmin $^{flox/flox}$ or BiP $^{flox/flox}$ transgenic would allow further exploration of the role Endoplasmin and BiP play in platelet function, in addition to providing further insight into the specificities of the effects of P13 and Pft.

6.6 Future work

With the current lack of targeted treatments for myelofibrosis, there is a need for alternative options for these patients. We have identified that HSP47 may be a target for treatment, and there are no differences in haematopoiesis between megakaryocytic HSP47 deficient mice and controls however it would be beneficial to understand if there is still no difference following challenge to the bone marrow. There is also a need to further investigate the reduction in collagen production from HSP47 deficient MKs. The assay used in this study identified total newly synthesised collagen, it would therefore be reasonable to further investigate the specific types of collagen that MKs synthesise and if HSP47 deficiency impacts synthesis of all collagens, or specific types as types I and III form reticulin and collagen fibres, characteristics of bone marrow fibrosis (Kuter et al., 2007, Malara et al., 2018).

We identified that HSP47 binding sequences are able to support platelet adhesion and shape change in a mechanism that we have suggested involves cytoskeletal reorganisation, potentially mediated via actin fragmentation. Further investigation of how HSP47 is anchored

to the cell surface would provide a greater understanding in this mechanism and would allow determination of whether HSP47 acts as a receptor. Synthesis of shorter or scrambled peptides would confirm the motif which supports this response, and repeated spreading assays in the presence of an actin inhibitor such as latrunculin would confirm the mechanism. Shorter/scrambled peptides would also provide additional insight regarding the HSP47 regulatory motif identified within collagens.

We confirmed the presence of additional KDEL proteins within the platelet. Reports that these KDEL- proteins are found in a complex in other cell types lead us to wonder if they are present in complex in platelets as well. This could be investigated using immunoprecipitation techniques to determine if these proteins are in complexes, or super resolution microscopy to determine if proteins are colocalised with each other or other chaperone proteins such as PDI. We believe we used inhibitors of Endoplasmin and BiP in platelets for the first time, however the concentrations of these required to illicit a response were high and therefore may result in off target effects which we did not investigate. Assays were carried out in PRP, so it may be that plasma proteins bound these inhibitors reducing the availability to platelets. Generation of megakaryocyte specific Endoplasmin and BiP deficient mice would provide further insight into the involvement of these proteins on platelet function, and determination of the specificity of the inhibitors used in this study.

Conclusions

The work presented in this study revealed that HSP47 deficiency has no impact on haematopoiesis or MK maturation even though synthesis of collagen, an ECM protein essential for the BM environment is reduced. In platelets, we identified that HSP47 is involved in cytoskeletal changes as presence of HSP47 binding sequences within collagen support adhesion and shape change. The same binding sequences are also able to modulate platelet-collagen interactions, suggesting that HSP47 has dual functionality within the platelet, as demonstrated in Figure 39.

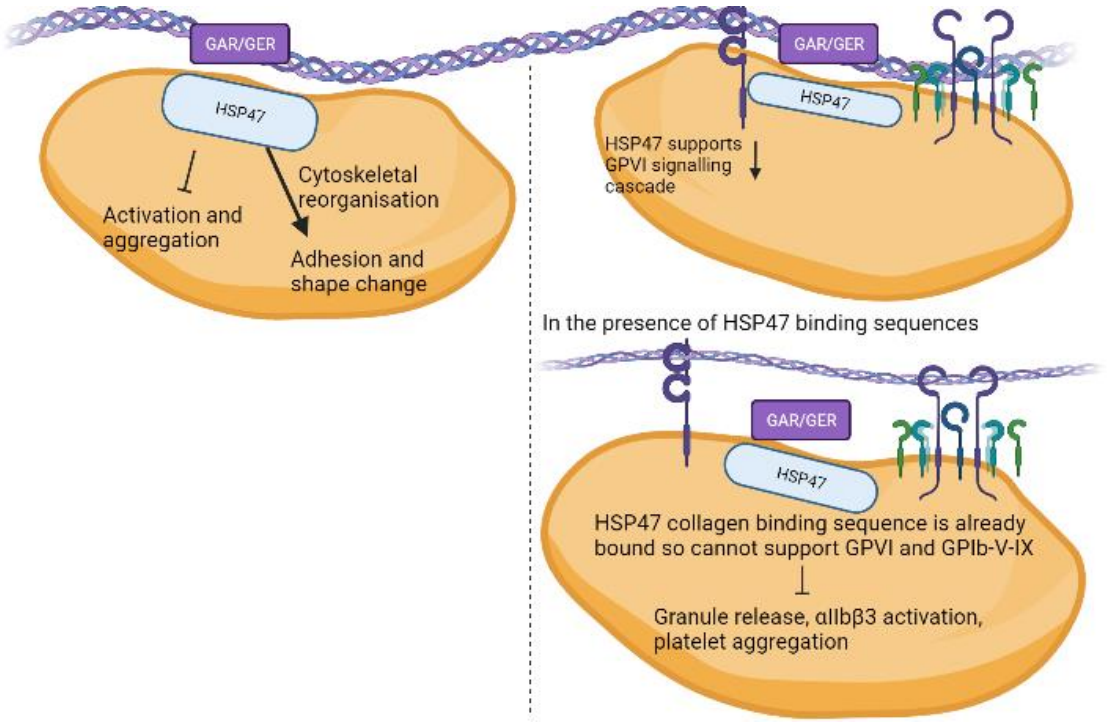

Figure 39. HSP47 has dual functionality in platelets
HSP47, through GAR/GER sequences within collagen, mediates platelet adhesion and shape change in a process involving cytoskeletal reorganisation. HSP47 also supports collagen-platelet interactions and signalling. When HSP47 is bound to GAR/GER, it is unable to support collagen receptors on the platelet surface reducing functional responses to collagen. Created in BioRender.com.

References

2002. Collaborative meta-analysis of randomised trials of antiplatelet therapy for prevention of death, myocardial infarction, and stroke in high risk patients. *BMJ,* 324**,** 71.

AARTS, P. A., VAN DEN BROEK, S. A., PRINS, G. W., KUIKEN, G. D., SIXMA, J. J. & HEETHAAR, R. M. 1988. Blood platelets are concentrated near the wall and red blood cells, in the center in flowing blood. *Arteriosclerosis,* 8**,** 819-24.

ADOMAVICIUS, T., GUAITA, M., ZHOU, Y., JENNINGS, M. D., LATIF, Z., ROSEMAN, A. M. & PAVITT, G. D. 2019. The structural basis of translational control by eIF2 phosphorylation. *Nature Communications,* 10**,** 2136.

AGUILAR, A., PERTUY, F., ECKLY, A., STRASSEL, C., COLLIN, D., GACHET, C., LANZA, F. & LÉON, C. 2016. Importance of environmental stiffness for megakaryocyte differentiation and proplatelet formation. *Blood,* 128**,** 2022-2032.

AOE, T., CUKIERMAN, E., LEE, A., CASSEL, D., PETERS, P. J. & HSU, V. W. 1997. The KDEL receptor, ERD2, regulates intracellular traffic by recruiting a GTPase-activating protein for ARF1. *The EMBO journal,* 16**,** 7305-7316.

ARAI, F. & SUDA, T. 2007. Maintenance of Quiescent Hematopoietic Stem Cells in the Osteoblastic Niche. *Annals of the New York Academy of Sciences,* 1106**,** 41-53.

AVECILLA, S. T., HATTORI, K., HEISSIG, B., TEJADA, R., LIAO, F., SHIDO, K., JIN, D. K., DIAS, S., ZHANG, F., HARTMAN, T. E., HACKETT, N. R., CRYSTAL, R. G., WITTE, L., HICKLIN, D. J., BOHLEN, P., EATON, D., LYDEN, D., DE SAUVAGE, F. & RAFII, S. 2004. Chemokine-mediated interaction of hematopoietic progenitors with the bone marrow vascular niche is required for thrombopoiesis. *Nat Med,* 10**,** 64-71.

BADIMON, L., PADRÓ, T. & VILAHUR, G. 2012. Atherosclerosis, platelets and thrombosis in acute ischaemic heart disease. *European heart journal. Acute cardiovascular care,* 1**,** 60-74.

BALDUINI, A., PALLOTTA, I., MALARA, A., LOVA, P., PECCI, A., VIARENGO, G., BALDUINI, C. L. & TORTI, M. 2008. Adhesive receptors, extracellular proteins and myosin IIA orchestrate proplatelet formation by human megakaryocytes. *J Thromb Haemost,* 6**,** 1900-7.

BALTIMORE, D. 2001. Our genome unveiled. *Nature,* 409**,** 814-6.

BARBUI, T., GHIRARDI, A., MASCIULLI, A., CAROBBIO, A., PALANDRI, F., VIANELLI, N., DE STEFANO, V., BETTI, S., DI VEROLI, A., IURLO, A., CATTANEO, D., DELAINI, F., BONIFACIO, M., SCAFFIDI, L., PATRIARCA, A., RUMI, E., CASETTI, I. C., STEPHENSON, C., GUGLIELMELLI, P., ELLI, E. M., PALOVA, M., BERTOLOTTI, L., EREZ, D., GOMEZ, M., WILLE, K., PEREZ-ENCINAS, M., LUNGHI, F., ANGONA, A., FOX, M. L., BEGGIATO, E., BENEVOLO, G., CARLI, G., CACCIOLA, R., MCMULLIN, M. F., TIEGHI, A., RECASENS, V., MARCHETTI, M., GRIESSHAMMER, M., ALVAREZ-LARRAN, A., VANNUCCHI, A. M. & FINAZZI, G. 2019. Second cancer in Philadelphia negative myeloproliferative neoplasms (MPN-K). A nested case-control study. *Leukemia,* 33**,** 1996-2005.

BARBUI, T., TEFFERI, A., VANNUCCHI, A. M., PASSAMONTI, F., SILVER, R. T., HOFFMAN, R., VERSTOVSEK, S., MESA, R., KILADJIAN, J. J., HEHLMANN, R., REITER, A., CERVANTES, F., HARRISON, C., MC MULLIN, M. F., HASSELBALCH, H. C., KOSCHMIEDER, S., MARCHETTI, M., BACIGALUPO, A., FINAZZI, G., KROEGER, N., GRIESSHAMMER, M., BIRGEGARD, G. & BAROSI, G. 2018. Philadelphia chromosome-negative classical myeloproliferative neoplasms: revised management recommendations from European LeukemiaNet. *Leukemia,* 32**,** 1057-1069.

BEARER, E. L., PRAKASH, J. M. & LI, Z. 2002. Actin dynamics in platelets. *International review of cytology,* 217**,** 137-182.

BECK, K., CHAN, V. C., SHENOY, N., KIRKPATRICK, A., RAMSHAW, J. A. & BRODSKY, B. 2000. Destabilization of osteogenesis imperfecta collagen-like model peptides correlates with the identity of the residue replacing glycine. *Proc Natl Acad Sci U S A,* 97**,** 4273-8.

BEHNKE, O. 1967. Electron microscopic observations on the membrane systems of the rat blood platelet. *Anat Rec,* 158**,** 121-37.

BEHNKE, O. 1968. An electron microscope study of the megacaryocyte of the rat bone marrow. I. The development of the demarcation membrane system and the platelet surface coat. *J Ultrastruct Res,* 24**,** 412-33.

BERNDT, M. C. & ANDREWS, R. K. 2011. Bernard-Soulier syndrome. *Haematologica,* 96**,** 355-9.

BERTOZZI, C. C., SCHMAIER, A. A., MERICKO, P., HESS, P. R., ZOU, Z., CHEN, M., CHEN, C. Y., XU, B., LU, M. M., ZHOU, D., SEBZDA, E., SANTORE, M. T., MERIANOS, D. J., STADTFELD, M., FLAKE, A. W., GRAF, T., SKODA, R., MALTZMAN, J. S., KORETZKY, G. A. & KAHN, M. L. 2010. Platelets regulate lymphatic vascular development through CLEC-2-SLP-76 signaling. *Blood,* 116**,** 661-70.

BLANN, A. D. & DUNMORE, S. 2011. Arterial and venous thrombosis in cancer patients. *Cardiol Res Pract,* 2011**,** 394740.

BOLTE, S. & CORDELIÈRES, F. P. 2006. A guided tour into subcellular colocalization analysis in light microscopy. *Journal of Microscopy,* 224**,** 213-232.

BORN, G. V. 1962. Aggregation of blood platelets by adenosine diphosphate and its reversal. *Nature,* 194**,** 927-9.

BOSE, D. & CHAKRABARTI, A. 2017. Substrate specificity in the context of molecular chaperones. *IUBMB Life,* 69**,** 647-659.

BRANEHÖG, I., RIDELL, B., SWOLIN, B. & WEINFELD, A. 1975. Megakaryocyte quantifications in relation to thrombokinetics in primary thrombocythaemia and allied diseases. *Scand J Haematol,* 15**,** 321-32.

BRETON-GORIUS, J. 1975. Development of two distinct membrane systems associated in giant complexes in pathological megakaryocytes. *Ser Haematol,* 8**,** 49-67.

BROCCHIERI, L., CONWAY DE MACARIO, E. & MACARIO, A. J. 2008. hsp70 genes in the human genome: Conservation and differentiation patterns predict a wide array of overlapping and specialized functions. *BMC Evol Biol,* 8**,** 19.

BROEKMAN, M. J., HANDIN, R. I. & COHEN, P. 1975. Distribution of fibrinogen, and platelet factors 4 and XIII in subcellular fractions of human platelets. *Br J Haematol,* 31**,** 51-5.

BUCHAN, J. R. & PARKER, R. 2009. Eukaryotic stress granules: the ins and outs of translation. *Mol Cell,* 36**,** 932-41.

BURKHART, J. M., VAUDEL, M., GAMBARYAN, S., RADAU, S., WALTER, U., MARTENS, L., GEIGER, J., SICKMANN, A. & ZAHEDI, R. P. 2012. The first comprehensive and quantitative analysis of human platelet protein composition allows the comparative analysis of structural and functional pathways. *Blood,* 120**,** e73-82.

BYE, A. P., HOEPEL, W., MITCHELL, J. L., JÉGOUIC, S., LOUREIRO, S., SAGE, T., VIDARSSON, G., NOUTA, J., WUHRER, M., DE TAEYE, S., VAN GILS, M., KRIEK, N., COOPER, N., JONES, I., DEN DUNNEN, J. & GIBBINS, J. M. 2021. Aberrant glycosylation of anti-SARS-CoV-2 spike IgG is a prothrombotic stimulus for platelets. *Blood,* 138**,** 1481-1489.

BYE, A. P., UNSWORTH, A. J. & GIBBINS, J. M. 2016. Platelet signaling: a complex interplay between inhibitory and activatory networks. *J Thromb Haemost,* 14**,** 918-30.

CABRERA, M., MUÑIZ, M., HIDALGO, J., VEGA, L., MARTÍN, M. E. & VELASCO, A. 2003. The retrieval function of the KDEL receptor requires PKA phosphorylation of its C-terminus. *Molecular biology of the cell,* 14**,** 4114-4125.

CAI, H., SASIKUMAR, P., LITTLE, G., BIHAN, D., HAMAIA, S. W., ZHOU, A., GIBBINS, J. M. & FARNDALE, R. W. 2021. Identification of HSP47 Binding Site on Native Collagen and Its Implications for the Development of HSP47 Inhibitors. *Biomolecules,* 11**,** 983.

CAI, J. W., HENDERSON, B. W., SHEN, J. W. & SUBJECK, J. R. 1993. Induction of glucose regulated proteins during growth of a murine tumor. *J Cell Physiol,* 154**,** 229-37.

CALAMINUS, S. D., GUITART, A. V., SINCLAIR, A., SCHACHTNER, H., WATSON, S. P., HOLYOAKE, T. L., KRANC, K. R. & MACHESKY, L. M. 2012. Lineage tracing of Pf4-Cre marks hematopoietic stem cells and their progeny. *PLoS One,* 7**,** e51361.

CAMPBELL, I. D. & HUMPHRIES, M. J. 2011. Integrin structure, activation, and interactions. *Cold Spring Harb Perspect Biol,* 3.

CANAULT, M., GHALLOUSSI, D., GROSDIDIER, C., GUINIER, M., PERRET, C., CHELGHOUM, N., GERMAIN, M., RASLOVA, H., PEIRETTI, F., MORANGE, P. E., SAUT, N., PILLOIS, X., NURDEN, A. T., CAMBIEN, F., PIERRES, A., VAN DEN BERG, T. K., KUIJPERS, T. W., ALESSI, M. C. & TREGOUET, D. A. 2014. Human CalDAG-GEFI gene (RASGRP2) mutation affects platelet function and causes severe bleeding. *J Exp Med,* 211**,** 1349-62.

CAPITANI, M. & SALLESE, M. 2009. The KDEL receptor: New functions for an old protein. *FEBS Letters,* 583**,** 3863-3871.

CATRICALA, S., TORTI, M. & RICEVUTI, G. 2012. Alzheimer disease and platelets: how's that relevant. *Immunity & ageing : I & A,* 9**,** 20-20.

CATTANEO, M., LECCHI, A., RANDI, A. M., MCGREGOR, J. L. & MANNUCCI, P. M. 1992. Identification of a new congenital defect of platelet function characterized by severe impairment of platelet responses to adenosine diphosphate. *Blood,* 80**,** 2787-96.

CERVANTES, F., VANNUCCHI, A. M., KILADJIAN, J. J., AL-ALI, H. K., SIRULNIK, A., STALBOVSKAYA, V., MCQUITTY, M., HUNTER, D. S., LEVY, R. S., PASSAMONTI, F., BARBUI, T., BAROSI, G., HARRISON, C. N., KNOOPS, L. & GISSLINGER, H. 2013. Three-year efficacy, safety, and survival findings from COMFORT-II, a phase 3 study comparing ruxolitinib with best available therapy for myelofibrosis. *Blood,* 122**,** 4047-53.

CHAN, M. V., LEADBEATER, P. D., WATSON, S. P. & WARNER, T. D. 2018. Not all light transmission aggregation assays are created equal: qualitative differences between light transmission and 96-well plate aggregometry. *Platelets,* 29**,** 686-689.

CHANDRAMOULI, K. & QIAN, P.-Y. 2009. Proteomics: challenges, techniques and possibilities to overcome biological sample complexity. *Human genomics and proteomics : HGP,* 2009**,** 239204.

CHEN, J., WANG, S., ZHANG, Z., RICHARDS, C. I. & XU, R. 2019. Heat shock protein 47 (HSP47) binds to discoidin domain-containing receptor 2 (DDR2) and regulates its protein stability. *J Biol Chem,* 294**,** 16846-16854.

CHEN, K., DETWILER, T. C. & ESSEX, D. W. 1995. Characterization of protein disulphide isomerase released from activated platelets. *Br J Haematol,* 90**,** 425-31.

CHEN, K., LIN, Y. & DETWILER, T. C. 1992. Protein disulfide isomerase activity is released by activated platelets. *Blood,* 79**,** 2226-8.

CHO, J., FURIE, B. C., COUGHLIN, S. R. & FURIE, B. 2008. A critical role for extracellular protein disulfide isomerase during thrombus formation in mice. *J Clin Invest,* 118**,** 1123-31.

CHO, J., KENNEDY, D. R., LIN, L., HUANG, M., MERRILL-SKOLOFF, G., FURIE, B. C. & FURIE, B. 2012. Protein disulfide isomerase capture during thrombus formation in vivo depends on the presence of β3 integrins. *Blood,* 120**,** 647-55.

CHOUKHI, A., UNG, S., WYCHOWSKI, C. & DUBUISSON, J. 1998. Involvement of endoplasmic reticulum chaperones in the folding of hepatitis C virus glycoproteins. *J Virol,* 72**,** 3851-8.

CHRISTIANSEN, H. E., SCHWARZE, U., PYOTT, S. M., ALSWAID, A., AL BALWI, M., ALRASHEED, S., PEPIN, M. G., WEIS, M. A., EYRE, D. R. & BYERS, P. H. 2010. Homozygosity for a missense mutation in SERPINH1, which encodes the collagen chaperone protein HSP47, results in severe recessive osteogenesis imperfecta. *Am J Hum Genet,* 86**,** 389-98.

CIFERRI, S., EMILIANI, C., GUGLIELMINI, G., ORLACCHIO, A., NENCI, G. G. & GRESELE, P. 2000. Platelets release their lysosomal content in vivo in humans upon activation. *Thromb Haemost,* 83**,** 157-64.

CIFUNI, S. M., WAGNER, D. D. & BERGMEIER, W. 2008. CalDAG-GEFI and protein kinase C represent alternative pathways leading to activation of integrin alphaIIbbeta3 in platelets. *Blood,* 112**,** 1696-703.

CLARKE, E. P. & SANWAL, B. D. 1992. Cloning of a human collagen-binding protein, and its homology with rat gp46, chick hsp47 and mouse J6 proteins. *Biochim Biophys Acta,* 1129**,** 246-8.

CLEMETSON, J. M., POLGAR, J., MAGNENAT, E., WELLS, T. N. & CLEMETSON, K. J. 1999. The platelet collagen receptor glycoprotein VI is a member of the immunoglobulin superfamily closely related to FcalphaR and the natural killer receptors. *J Biol Chem,* 274**,** 29019-24.

COOTE, P. J., COLE, M. B. & JONES, M. V. 1991. Induction of increased thermotolerance in Saccharomyces cerevisiae may be triggered by a mechanism involving intracellular pH. *J Gen Microbiol,* 137**,** 1701-8.

COURGEON, A. M., MAISONHAUTE, C. & BEST-BELPOMME, M. 1984. Heat shock proteins are induced by cadmium in Drosophila cells. *Exp Cell Res,* 153**,** 515-21.

CRESCENTE, M., PLUTHERO, F. G., LI, L., LO, R. W., WALSH, T. G., SCHENK, M. P., HOLBROOK, L. M., LOURIERO, S., ALI, M. S., VAIYAPURI, S., FALET, H., JONES, I. M., POOLE, A. W., KAHR, W. H. A. & GIBBINS, J. M. 2016. Intracellular Trafficking, Localization, and Mobilization of Platelet-Borne Thiol Isomerases. *Arteriosclerosis, thrombosis, and vascular biology,* 36**,** 1164-1173.

DE NUCCI, G., GRYGLEWSKI, R. J., WARNER, T. D. & VANE, J. R. 1988. Receptor-mediated release of endothelium-derived relaxing factor and prostacyclin from bovine aortic endothelial cells is coupled. *Proc Natl Acad Sci U S A,* 85**,** 2334-8.

DOPHEIDE, S. M., MAXWELL, M. J. & JACKSON, S. P. 2002. Shear-dependent tether formation during platelet translocation on von Willebrand factor. *Blood,* 99**,** 159-67.

DUTTA-ROY, A. K. & SINHA, A. K. 1987. Purification and properties of prostaglandin E1/prostacyclin receptor of human blood platelets. *J Biol Chem,* 262**,** 12685-91.

EBBE, S. 1976. Biology of megakaryocytes. *Prog Hemost Thromb,* 3**,** 211-29.

ELLGAARD, L. & HELENIUS, A. 2003. Quality control in the endoplasmic reticulum. *Nat Rev Mol Cell Biol,* 4**,** 181-91.

ELLIS, R. J., VAN DER VIES, S. M. & HEMMINGSEN, S. M. 1989. The molecular chaperone concept. *Biochem Soc Symp,* 55**,** 145-53.

ERCAN, H., MAURACHER, L. M., GRILZ, E., HELL, L., HELLINGER, R., SCHMID, J. A., MOIK, F., AY, C., PABINGER, I. & ZELLNER, M. 2021. Alterations of the Platelet Proteome in Lung Cancer: Accelerated F13A1 and ER Processing as New Actors in Hypercoagulability. *Cancers (Basel),* 13.

ESCOLAR, G., LEISTIKOW, E. & WHITE, J. G. 1989. The fate of the open canalicular system in surface and suspension-activated platelets. *Blood,* 74**,** 1983-8.

ESSAWI, O., SYMOENS, S., FANNANA, M., DARWISH, M., FARRAJ, M., WILLAERT, A., ESSAWI, T., CALLEWAERT, B., DE PAEPE, A., MALFAIT, F. & COUCKE, P. J. 2018. Genetic analysis of osteogenesis imperfecta in the Palestinian population: molecular screening of 49 affected families. *Mol Genet Genomic Med,* 6**,** 15-26.

ESSEX, D. W., CHEN, K. & SWIATKOWSKA, M. 1995. Localization of protein disulfide isomerase to the external surface of the platelet plasma membrane. *Blood,* 86**,** 2168-73.

ESSEX, D. W. & LI, M. 1999. Protein disulphide isomerase mediates platelet aggregation and secretion. *Br J Haematol,* 104**,** 448-54.

EZUMI, Y., SHINDOH, K., TSUJI, M. & TAKAYAMA, H. 1998. Physical and functional association of the Src family kinases Fyn and Lyn with the collagen receptor glycoprotein VI-Fc receptor gamma chain complex on human platelets. *J Exp Med,* 188**,** 267-76.

FOGELSON, A. L. & WANG, N. T. 1996. Platelet dense-granule centralization and the persistence of ADP secretion. *Am J Physiol,* 270**,** H1131-40.

FRANCO, A. T., CORKEN, A. & WARE, J. 2015. Platelets at the interface of thrombosis, inflammation, and cancer. *Blood,* 126**,** 582.

FURIE, B. & FURIE, B. C. 2008. Mechanisms of thrombus formation. *N Engl J Med,* 359**,** 938-49.

GALLI, S., MCLORNAN, D. & HARRISON, C. 2014. Safety evaluation of ruxolitinib for treating myelofibrosis. *Expert Opin Drug Saf,* 13**,** 967-76.

GARG, N., GUPTA, R. J. & KUMAR, S. 2019. Megakaryocytes in Peripheral Blood Smears. *Turk J Haematol.*

GEUE, S., WALKER-ALLGAIER, B., EIßLER, D., TEGTMEYER, R., SCHAUB, M., LANG, F., GAWAZ, M., BORST, O. & MÜNZER, P. 2017. Doxepin inhibits GPVI-dependent platelet Ca(2+) signaling and collagen-dependent thrombus formation. *Am J Physiol Cell Physiol,* 312**,** C765-c774.

GIBBINS, J. M., OKUMA, M., FARNDALE, R., BARNES, M. & WATSON, S. P. 1997. Glycoprotein VI is the collagen receptor in platelets which underlies tyrosine phosphorylation of the Fc receptor gamma-chain. *FEBS Lett,* 413**,** 255-9.

GOLLOMP, K. & PONCZ, M. 2019. Gp1ba-Cre or Pf4-Cre: pick your poison. *Blood,* 133**,** 287-288.

GORDON, M. Y., BEARPARK, A. D., CLARKE, D. & DOWDING, C. R. 1990. Haemopoietic stem cell subpopulations in mouse and man: discrimination by differential adherence and marrow repopulating ability. *Bone Marrow Transplant,* 5 Suppl 1**,** 6-8.

GRAGEROV, A. I., MARTIN, E. S., KRUPENKO, M. A., KASHLEV, M. V. & NIKIFOROV, V. G. 1991. Protein aggregation and inclusion body formation in Escherichia coli rpoH mutant defective in heat shock protein induction. *FEBS Lett,* 291**,** 222-4.

GROSS, B. S., LEE, J. R., CLEMENTS, J. L., TURNER, M., TYBULEWICZ, V. L., FINDELL, P. R., KORETZKY, G. A. & WATSON, S. P. 1999. Tyrosine phosphorylation of SLP-76 is downstream of Syk following stimulation of the collagen receptor in platelets. *J Biol Chem,* 274**,** 5963-71.

GUIDETTI, G. F., GRECO, F., BERTONI, A., GIUDICI, C., VIOLA, M., TENNI, R., TIRA, E. M., BALDUINI, C. & TORTI, M. 2003. Platelet interaction with CNBr peptides from type II collagen via integrin alpha2beta1. *Biochim Biophys Acta,* 1640**,** 43-51.

GURNEY, A. L., CARVER-MOORE, K., DE SAUVAGE, F. J. & MOORE, M. W. 1994. Thrombocytopenia in c-mpl-deficient mice. *Science,* 265**,** 1445-7.

HANAFY, K. A., KRUMENACKER, J. S. & MURAD, F. 2001. NO, nitrotyrosine, and cyclic GMP in signal transduction. *Med Sci Monit,* 7**,** 801-19.

HARPER, M. T. & POOLE, A. W. 2010. Diverse functions of protein kinase C isoforms in platelet activation and thrombus formation. *J Thromb Haemost,* 8**,** 454-62.

HARTL, F. U. 1996. Molecular chaperones in cellular protein folding. *Nature,* 381**,** 571-9.

HARTWIG, J. H. & ITALIANO, J. E., JR. 2006. Cytoskeletal mechanisms for platelet production. *Blood Cells Mol Dis,* 36**,** 99-103.

HATAHET, F. & RUDDOCK, L. W. 2009. Protein disulfide isomerase: a critical evaluation of its function in disulfide bond formation. *Antioxid Redox Signal,* 11**,** 2807-50.

HAYASHI, T., TANAKA, S., HORI, Y., HIRAYAMA, F., SATO, E. F. & INOUE, M. 2011. Role of mitochondria in the maintenance of platelet function during in vitro storage. *Transfus Med,* 21**,** 166-74.

HEIB, T., GROSS, C., MÜLLER, M. L., STEGNER, D. & PLEINES, I. 2021. Isolation of murine bone marrow by centrifugation or flushing for the analysis of hematopoietic cells - a comparative study. *Platelets,* 32**,** 601-607.

HENDERSHOT, L. M. & BULLEID, N. J. 2000. Protein-specific chaperones: The role of hsp47 begins to gel. *Current Biology,* 10**,** R912-R915.

HIGH, S., LECOMTE, F. J., RUSSELL, S. J., ABELL, B. M. & OLIVER, J. D. 2000. Glycoprotein folding in the endoplasmic reticulum: a tale of three chaperones? *FEBS Lett,* 476**,** 38-41.

HIRATA, H., YAMAMURA, I., YASUDA, K., KOBAYASHI, A., TADA, N., SUZUKI, M., HIRAYOSHI, K., HOSOKAWA, N. & NAGATA, K. 1999. Separate cis-acting DNA elements control cell type- and tissue-specific expression of collagen binding molecular chaperone HSP47. *J Biol Chem,* 274**,** 35703-10.

HIRAYOSHI, K., KUDO, H., TAKECHI, H., NAKAI, A., IWAMATSU, A., YAMADA, K. M. & NAGATA, K. 1991. HSP47: a tissue-specific, transformation-sensitive, collagen-binding heat shock protein of chicken embryo fibroblasts. *Mol Cell Biol,* 11**,** 4036-44.

HO, M. S., MEDCALF, R. L., LIVESEY, S. A. & TRAIANEDES, K. 2015. The dynamics of adult haematopoiesis in the bone and bone marrow environment. *Br J Haematol,* 170**,** 472-86.

HOLBROOK, L. M., SANDHAR, G. K., SASIKUMAR, P., SCHENK, M. P., STAINER, A. R., SAHLI, K. A., FLORA, G. D., BICKNELL, A. B. & GIBBINS, J. M. 2018. A humanized monoclonal antibody that inhibits platelet-surface ERp72 reveals a role for ERp72 in thrombosis. *J Thromb Haemost,* 16**,** 367-377.

HOLBROOK, L. M., SASIKUMAR, P., STANLEY, R. G., SIMMONDS, A. D., BICKNELL, A. B. & GIBBINS, J. M. 2012. The platelet-surface thiol isomerase enzyme ERp57 modulates platelet function. *J Thromb Haemost,* 10**,** 278-88.

HOLBROOK, L. M., WATKINS, N. A., SIMMONDS, A. D., JONES, C. I., OUWEHAND, W. H. & GIBBINS, J. M. 2010. Platelets release novel thiol isomerase enzymes which are recruited to the cell surface following activation. *Br J Haematol,* 148**,** 627-37.

HONG, F., LIU, B., CHIOSIS, G., GEWIRTH, D. T. & LI, Z. 2013. α7 Helix Region of αI Domain Is Crucial for Integrin Binding to Endoplasmic Reticulum Chaperone gp96: A POTENTIAL THERAPEUTIC TARGET FOR CANCER METASTASIS. *Journal of Biological Chemistry,* 288**,** 18243-18248.

HONZAWA, Y., NAKASE, H., SHIOKAWA, M., YOSHINO, T., IMAEDA, H., MATSUURA, M., KODAMA, Y., IKEUCHI, H., ANDOH, A., SAKAI, Y., NAGATA, K. & CHIBA, T. 2014. Involvement of interleukin-17A-induced expression of heat shock protein 47 in intestinal fibrosis in Crohn's disease. *Gut,* 63**,** 1902-12.

HOSOKAWA, N., TAKECHI, H., YOKOTA, S., HIRAYOSHI, K. & NAGATA, K. 1993. Structure of the gene encoding the mouse 47-kDa heat-shock protein (HSP47). *Gene,* 126**,** 187-93.

HSU-LIN, S., BERMAN, C. L., FURIE, B. C., AUGUST, D. & FURIE, B. 1984. A platelet membrane protein expressed during platelet activation and secretion. Studies using a monoclonal antibody specific for thrombin-activated platelets. *Journal of Biological Chemistry,* 259**,** 9121-9126.

HUA, Y., WHITE-GILBERTSON, S., KELLNER, J., RACHIDI, S., USMANI, S. Z., CHIOSIS, G., DEPINHO, R. A., LI, Z. & LIU, B. 2013. Molecular chaperone gp96 is a novel therapeutic target of multiple myeloma. *Clinical Cancer Research***,** clincanres.2083.2013.

HUANG, J., LI, X., SHI, X., ZHU, M., WANG, J., HUANG, S., HUANG, X., WANG, H., LI, L., DENG, H., ZHOU, Y., MAO, J., LONG, Z., MA, Z., YE, W., PAN, J., XI, X. & JIN, J. 2019. Platelet integrin αIIbβ3: signal transduction, regulation, and its therapeutic targeting. *Journal of Hematology & Oncology,* 12**,** 26.

HUO, Y., SCHOBER, A., FORLOW, S. B., SMITH, D. F., HYMAN, M. C., JUNG, S., LITTMAN, D. R., WEBER, C. & LEY, K. 2003. Circulating activated platelets exacerbate atherosclerosis in mice deficient in apolipoprotein E. *Nat Med,* 9**,** 61-7.

HYNES, R. O. 2002. Integrins: bidirectional, allosteric signaling machines. *Cell,* 110**,** 673-87.

IBRAHIM, I. M., ABDELMALEK, D. H. & ELFIKY, A. A. 2019. GRP78: A cell's response to stress. *Life Sci,* 226**,** 156-163.

IKEGAWA, S., SUDO, K., OKUI, K. & NAKAMURA, Y. 1995. Isolation, characterization and chromosomal assignment of human colligin-2 gene (CBP2). *Cytogenet Cell Genet,* 71**,** 182-6.

ILL, C. R., ENGVALL, E. & RUOSLAHTI, E. 1984. Adhesion of platelets to laminin in the absence of activation. *J Cell Biol,* 99**,** 2140-5.

ISHIDA, Y. & NAGATA, K. 2011. Hsp47 as a collagen-specific molecular chaperone. *Methods Enzymol,* 499**,** 167-82.

ITALIANO, J. E., JR., LECINE, P., SHIVDASANI, R. A. & HARTWIG, J. H. 1999. Blood platelets are assembled principally at the ends of proplatelet processes produced by differentiated megakaryocytes. *J Cell Biol,* 147**,** 1299-312.

ITO, S. & NAGATA, K. 2019. Roles of the endoplasmic reticulum-resident, collagen-specific molecular chaperone Hsp47 in vertebrate cells and human disease. *J Biol Chem,* 294**,** 2133-2141.

ITO, S., OGAWA, K., TAKEUCHI, K., TAKAGI, M., YOSHIDA, M., HIROKAWA, T., HIRAYAMA, S., SHIN-YA, K., SHIMADA, I., DOI, T., GOSHIMA, N., NATSUME, T. & NAGATA, K. 2017. A small-molecule compound inhibits a collagen-specific molecular chaperone and could represent a potential remedy for fibrosis. *J Biol Chem,* 292**,** 20076-20085.

JACKSON, S. P., NESBITT, W. S. & KULKARNI, S. 2003. Signaling events underlying thrombus formation. *J Thromb Haemost,* 1**,** 1602-12.

JARVIS, G. E., BEST, D. & WATSON, S. P. 2004. Differential roles of integrins alpha2beta1 and alphaIIbbeta3 in collagen and CRP-induced platelet activation. *Platelets,* 15**,** 303-13.

JOBE, S. M., WILSON, K. M., LEO, L., RAIMONDI, A., MOLKENTIN, J. D., LENTZ, S. R. & DI PAOLA, J. 2008. Critical role for the mitochondrial permeability transition pore and cyclophilin D in platelet activation and thrombosis. *Blood,* 111**,** 1257-65.

KAISER, W. J., HOLBROOK, L. M., TUCKER, K. L., STANLEY, R. G. & GIBBINS, J. M. 2009. A functional proteomic method for the enrichment of peripheral membrane proteins reveals the collagen binding protein Hsp47 is exposed on the surface of activated human platelets. *J Proteome Res,* 8**,** 2903-14.

KARACHALIOU, N., PILOTTO, S., BRIA, E. & ROSELL, R. 2015. Platelets and their role in cancer evolution and immune system. *Translational lung cancer research,* 4**,** 713-720.

KAUFMAN, R. M., AIRO, R., POLLACK, S. & CROSBY, W. H. 1965. Circulating megakaryocytes and platelet release in the lung. *Blood,* 26**,** 720-31.

KAUSHANSKY, K., LOK, S., HOLLY, R. D., BROUDY, V. C., LIN, N., BAILEY, M. C., FORSTROM, J. W., BUDDLE, M. M., OORT, P. J., HAGEN, F. S. & ET AL. 1994. Promotion of megakaryocyte progenitor expansion and differentiation by the c-Mpl ligand thrombopoietin. *Nature,* 369**,** 568-71.

KELLEY, P. M. & SCHLESINGER, M. J. 1978. The effect of amino acid analogues and heat shock on gene expression in chicken embryo fibroblasts. *Cell,* 15**,** 1277-86.

KELLY, R. B. 1990. Cell biology. Tracking an elusive receptor. *Nature,* 345**,** 480-1.

KERNER, M. J., NAYLOR, D. J., ISHIHAMA, Y., MAIER, T., CHANG, H. C., STINES, A. P., GEORGOPOULOS, C., FRISHMAN, D., HAYER-HARTL, M., MANN, M. & HARTL, F. U. 2005. Proteome-wide analysis of chaperonin-dependent protein folding in Escherichia coli. *Cell,* 122**,** 209-20.

KHAN, E. S., SANKARAN, S., LLONTOP, L. & DEL CAMPO, A. 2020. Exogenous supply of Hsp47 triggers fibrillar collagen deposition in skin cell cultures in vitro. *BMC Mol Cell Biol,* 21**,** 22.

KHAN, E. S., SANKARAN, S., PAEZ, J. I., MUTH, C., HAN, M. K. L. & DEL CAMPO, A. 2019. Photoactivatable Hsp47: A Tool to Regulate Collagen Secretion and Assembly. *Adv Sci (Weinh),* 6**,** 1801982.

KHOLMUKHAMEDOV, A. & JOBE, S. 2019. Platelet respiration. *Blood Adv,* 3**,** 599-602.

KIM, C. H. 2010. Homeostatic and pathogenic extramedullary hematopoiesis. *J Blood Med,* 1**,** 13-9.

KIM, K., HAHM, E., LI, J., HOLBROOK, L. M., SASIKUMAR, P., STANLEY, R. G., USHIO-FUKAI, M., GIBBINS, J. M. & CHO, J. 2013a. Platelet protein disulfide isomerase is required for thrombus formation but not for hemostasis in mice. *Blood,* 122**,** 1052-61.

KIM, Y. E., HIPP, M. S., BRACHER, A., HAYER-HARTL, M. & HARTL, F. U. 2013b. Molecular chaperone functions in protein folding and proteostasis. *Annu Rev Biochem,* 82**,** 323-55.

KIRCHHAUSEN, T. & ROSEN, F. S. 1996. Disease mechanism: Unravelling Wiskott–Aldrich syndrome. *Current Biology,* 6**,** 676-678.

KISHIMOTO, Y., YAMASHITA, M., WEI, A., TOYA, Y., YE, S., KENDZIORSKI, C. & WELHAM, N. V. 2019. Reversal of Vocal Fold Mucosal Fibrosis Using siRNA against the Collagen-Specific Chaperone Serpinh1. *Mol Ther Nucleic Acids,* 16**,** 616-625.

KLAMPFL, T., GISSLINGER, H., HARUTYUNYAN, A. S., NIVARTHI, H., RUMI, E., MILOSEVIC, J. D., THEM, N. C., BERG, T., GISSLINGER, B., PIETRA, D., CHEN, D., VLADIMER, G. I., BAGIENSKI, K., MILANESI, C., CASETTI, I. C., SANT'ANTONIO, E., FERRETTI, V., ELENA, C., SCHISCHLIK, F., CLEARY, C., SIX, M., SCHALLING, M., SCHONEGGER, A., BOCK, C., MALCOVATI, L., PASCUTTO, C., SUPERTI-FURGA, G., CAZZOLA, M. & KRALOVICS, R. 2013. Somatic mutations of calreticulin in myeloproliferative neoplasms. *N Engl J Med,* 369**,** 2379-90.

KLEMENT, G. L., YIP, T. T., CASSIOLA, F., KIKUCHI, L., CERVI, D., PODUST, V., ITALIANO, J. E., WHEATLEY, E., ABOU-SLAYBI, A., BENDER, E., ALMOG, N., KIERAN, M. W. & FOLKMAN, J. 2009. Platelets actively sequester angiogenesis regulators. *Blood,* 113**,** 2835-42.

KLOK, F. A., KRUIP, M., VAN DER MEER, N. J. M., ARBOUS, M. S., GOMMERS, D., KANT, K. M., KAPTEIN, F. H. J., VAN PAASSEN, J., STALS, M. A. M., HUISMAN, M. V. & ENDEMAN, H. 2020. Incidence of thrombotic complications in critically ill ICU patients with COVID-19. *Thromb Res,* 191**,** 145-147.

KNIGHT, C. G., MORTON, L. F., ONLEY, D. J., PEACHEY, A. R., ICHINOHE, T., OKUMA, M., FARNDALE, R. W. & BARNES, M. J. 1999. Collagen-platelet interaction: Gly-Pro-Hyp is uniquely specific for platelet Gp VI and mediates platelet activation by collagen. *Cardiovasc Res,* 41**,** 450-7.

KNIGHT, C. G., MORTON, L. F., PEACHEY, A. R., TUCKWELL, D. S., FARNDALE, R. W. & BARNES, M. J. 2000. The collagen-binding A-domains of integrins alpha(1)beta(1) and alpha(2)beta(1) recognize the same specific amino acid sequence, GFOGER, in native (triple-helical) collagens. *J Biol Chem,* 275**,** 35-40.

KOIDE, T., NISHIKAWA, Y., ASADA, S., YAMAZAKI, C. M., TAKAHARA, Y., HOMMA, D. L., OTAKA, A., OHTANI, K., WAKAMIYA, N., NAGATA, K. & KITAGAWA, K. 2006. Specific recognition of the collagen triple helix by chaperone HSP47. II. The HSP47-binding structural motif in collagens and related proteins. *J Biol Chem,* 281**,** 11177-85.

KOIDE, T., TAKAHARA, Y., ASADA, S. & NAGATA, K. 2002. Xaa-Arg-Gly triplets in the collagen triple helix are dominant binding sites for the molecular chaperone HSP47. *J Biol Chem,* 277**,** 6178-82.

KRUUV, J., GLOFCHESKI, D., CHENG, K. H., CAMPBELL, S. D., AL-QYSI, H. M., NOLAN, W. T. & LEPOCK, J. R. 1983. Factors influencing survival and growth of mammalian cells exposed to hypothermia. I. Effects of temperature and membrane lipid perturbers. *J Cell Physiol,* 115**,** 179-85.

KUIVANIEMI, H., TROMP, G. & PROCKOP, D. J. 1991. Mutations in collagen genes: causes of rare and some common diseases in humans. *Faseb j,* 5**,** 2052-60.

KURODA, K., HORIGUCHI, A., ASANO, T., ITO, K., ASAKUMA, J., SATO, A., YOSHII, H., HAYAKAWA, M., SUMITOMO, M. & ASANO, T. 2011. Glucose-regulated protein 78

positivity as a predictor of poor survival in patients with renal cell carcinoma. *Urol Int,* 87**,** 450-6.

KUTER, D. J., BAIN, B., MUFTI, G., BAGG, A. & HASSERJIAN, R. P. 2007. Bone marrow fibrosis: pathophysiology and clinical significance of increased bone marrow stromal fibres. *Br J Haematol,* 139**,** 351-62.

KUTER, D. J., BEELER, D. L. & ROSENBERG, R. D. 1994. The purification of megapoietin: a physiological regulator of megakaryocyte growth and platelet production. *Proceedings of the National Academy of Sciences,* 91**,** 11104.

KUZNETSOV, G., CHEN, L. B. & NIGAM, S. K. 1997. Multiple molecular chaperones complex with misfolded large oligomeric glycoproteins in the endoplasmic reticulum. *J Biol Chem,* 272**,** 3057-63.

LABELLE, M., BEGUM, S. & HYNES, R. O. 2011. Direct signaling between platelets and cancer cells induces an epithelial-mesenchymal-like transition and promotes metastasis. *Cancer Cell,* 20**,** 576-90.

LAEMMLI, U. K. 1970. Cleavage of structural proteins during the assembly of the head of bacteriophage T4. *Nature,* 227**,** 680-5.

LAHAV, J., GOFER-DADOSH, N., LUBOSHITZ, J., HESS, O. & SHAKLAI, M. 2000. Protein disulfide isomerase mediates integrin-dependent adhesion. *FEBS Lett,* 475**,** 89-92.

LAMANDE, S. R. & BATEMAN, J. F. 1999. Procollagen folding and assembly: The role of endoplasmic reticulum enzymes and molecular chaperones. *Seminars in Cell & Developmental Biology,* 10**,** 455-464.

LEBBINK, R. J., DE RUITER, T., ADELMEIJER, J., BRENKMAN, A. B., VAN HELVOORT, J. M., KOCH, M., FARNDALE, R. W., LISMAN, T., SONNENBERG, A., LENTING, P. J. & MEYAARD, L. 2006. Collagens are functional, high affinity ligands for the inhibitory immune receptor LAIR-1. *J Exp Med,* 203**,** 1419-25.

LEE, H. S., LIM, C. J., PUZON-MCLAUGHLIN, W., SHATTIL, S. J. & GINSBERG, M. H. 2009. RIAM activates integrins by linking talin to ras GTPase membrane-targeting sequences. *J Biol Chem,* 284**,** 5119-27.

LEFRANÇAIS, E., ORTIZ-MUÑOZ, G., CAUDRILLIER, A., MALLAVIA, B., LIU, F., SAYAH, D. M., THORNTON, E. E., HEADLEY, M. B., DAVID, T., COUGHLIN, S. R., KRUMMEL, M. F., LEAVITT, A. D., PASSEGUÉ, E. & LOONEY, M. R. 2017. The lung is a site of platelet biogenesis and a reservoir for haematopoietic progenitors. *Nature,* 544**,** 105-109.

LELE, Z. & KRONE, P. H. 1997. Expression of genes encoding the collagen-binding heat shock protein (Hsp47) and type II collagen in developing zebrafish embryos. *Mech Dev,* 61**,** 89-98.

LEMAUX, P. G., HERENDEEN, S. L., BLOCH, P. L. & NEIDHARDT, F. C. 1978. Transient rates of synthesis of individual polypeptides in E. coli following temperature shifts. *Cell,* 13**,** 427-34.

LI, C. H. & LEE, C. K. 1993. Minimum cross entropy thresholding. *Pattern Recognition,* 26**,** 617-625.

LI, C. H. & TAM, P. K. S. 1998. An iterative algorithm for minimum cross entropy thresholding. *Pattern Recognition Letters,* 19**,** 771-776.

LI, Z., DELANEY, M. K., O'BRIEN, K. A. & DU, X. 2010. Signaling during platelet adhesion and activation. *Arterioscler Thromb Vasc Biol,* 30**,** 2341-9.

LIBBY, P. 2002. Inflammation in atherosclerosis. *Nature,* 420**,** 868-74.

LIN, H. Y., MASSO-WELCH, P., DI, Y. P., CAI, J. W., SHEN, J. W. & SUBJECK, J. R. 1993. The 170-kDa glucose-regulated stress protein is an endoplasmic reticulum protein that binds immunoglobulin. *Mol Biol Cell,* 4**,** 1109-19.

LINDQUIST, S. & CRAIG, E. A. 1988. The heat-shock proteins. *Annu Rev Genet,* 22**,** 631-77.

LISMAN, T., RAYNAL, N., GROENEVELD, D., MADDOX, B., PEACHEY, A. R., HUIZINGA, E. G., DE GROOT, P. G. & FARNDALE, R. W. 2006. A single high-affinity binding site for von

Willebrand factor in collagen III, identified using synthetic triple-helical peptides. *Blood,* 108**,** 3753-6.

LITTLE, E., RAMAKRISHNAN, M., ROY, B., GAZIT, G. & LEE, A. S. 1994. The glucose-regulated proteins (GRP78 and GRP94): functions, gene regulation, and applications. *Crit Rev Eukaryot Gene Expr,* 4**,** 1-18.

LIU, D., RAZZAQUE, M. S., CHENG, M. & TAGUCHI, T. 2001. The renal expression of heat shock protein 47 and collagens in acute and chronic experimental diabetes in rats. *Histochem J,* 33**,** 621-8.

LIU, Y., LIU, J., QUIMBO, A., XIA, F., YAO, J., CLAMME, J. P., ZABLUDOFF, S., ZHANG, J. & YING, W. 2021. Anti-HSP47 siRNA lipid nanoparticle ND-L02-s0201 reverses interstitial pulmonary fibrosis in preclinical rat models. *ERJ Open Res,* 7.

LONG, M. W. 1998. Megakaryocyte differentiation events. *Semin Hematol,* 35**,** 192-9.

LONG, M. W., WILLIAMS, N. & EBBE, S. 1982. Immature megakaryocytes in the mouse: physical characteristics, cell cycle status, and in vitro responsiveness to thrombopoietic stimulatory factor. *Blood,* 59**,** 569-75.

LU, S. J., LI, F., YIN, H., FENG, Q., KIMBREL, E. A., HAHM, E., THON, J. N., WANG, W., ITALIANO, J. E., CHO, J. & LANZA, R. 2011. Platelets generated from human embryonic stem cells are functional in vitro and in the microcirculation of living mice. *Cell Res,* 21**,** 530-45.

LUO, S., MAO, C., LEE, B. & LEE, A. S. 2006. GRP78/BiP is required for cell proliferation and protecting the inner cell mass from apoptosis during early mouse embryonic development. *Mol Cell Biol,* 26**,** 5688-97.

MA, W., OU, T., CUI, X., WU, K., LI, H., LI, Y., PENG, G., XIA, W. & WU, S. 2021. HSP47 contributes to angiogenesis by induction of CCL2 in bladder cancer. *Cell Signal,* 85**,** 110044.

MACHLUS, K. R. & ITALIANO, J. E., JR. 2013. The incredible journey: From megakaryocyte development to platelet formation. *Journal of Cell Biology,* 201**,** 785-796.

MALARA, A., ABBONANTE, V., ZINGARIELLO, M., MIGLIACCIO, A. & BALDUINI, A. 2018. Megakaryocyte Contribution to Bone Marrow Fibrosis: many Arrows in the Quiver. *Mediterranean journal of hematology and infectious diseases,* 10**,** e2018068-e2018068.

MALARA, A., CURRAO, M., GRUPPI, C., CELESTI, G., VIARENGO, G., BURACCHI, C., LAGHI, L., KAPLAN, D. L. & BALDUINI, A. 2014. Megakaryocytes contribute to the bone marrow-matrix environment by expressing fibronectin, type IV collagen, and laminin. *Stem Cells,* 32**,** 926-37.

MAO, C., WANG, M., LUO, B., WEY, S., DONG, D., WESSELSCHMIDT, R., RAWLINGS, S. & LEE, A. S. 2010. Targeted mutation of the mouse Grp94 gene disrupts development and perturbs endoplasmic reticulum stress signaling. *PLoS One,* 5**,** e10852.

MARSHALL, C., LOPEZ, J., CROOKES, L., POLLITT, R. C. & BALASUBRAMANIAN, M. 2016. A novel homozygous variant in SERPINH1 associated with a severe, lethal presentation of osteogenesis imperfecta with hydranencephaly. *Gene,* 595**,** 49-52.

MASUDA, H., FUKUMOTO, M., HIRAYOSHI, K. & NAGATA, K. 1994. Coexpression of the collagen-binding stress protein HSP47 gene and the alpha 1(I) and alpha 1(III) collagen genes in carbon tetrachloride-induced rat liver fibrosis. *J Clin Invest,* 94**,** 2481-8.

MAXIMILIAN, G. G., OĞUZHAN, A., KATHERINA, H., VANESSA, K., DAVID, S. & KATRIN, G. H. 2020. Megakaryocyte volume modulates bone marrow niche properties and cell migration dynamics. *Haematologica,* 105**,** 895-904.

MAYNARD, D. M., HEIJNEN, H. F., HORNE, M. K., WHITE, J. G. & GAHL, W. A. 2007. Proteomic analysis of platelet alpha-granules using mass spectrometry. *J Thromb Haemost,* 5**,** 1945-55.

MCALISTER, L. & FINKELSTEIN, D. B. 1980. Heat shock proteins and thermal resistance in yeast. *Biochem Biophys Res Commun,* 93**,** 819-24.

MEHTA, P. R., APAP MANGION, S., BENGER, M., STANTON, B. R., CZUPRYNSKA, J., ARYA, R. & SZTRIHA, L. K. 2021. Cerebral venous sinus thrombosis and thrombocytopenia after COVID-19 vaccination - A report of two UK cases. *Brain Behav Immun,* 95**,** 514-517.

MELLION, B. T., IGNARRO, L. J., OHLSTEIN, E. H., PONTECORVO, E. G., HYMAN, A. L. & KADOWITZ, P. J. 1981. Evidence for the inhibitory role of guanosine 3', 5'-monophosphate in ADP-induced human platelet aggregation in the presence of nitric oxide and related vasodilators. *Blood,* 57**,** 946-55.

MICHALAK, M., CORBETT, E. F., MESAELI, N., NAKAMURA, K. & OPAS, M. 1999. Calreticulin: one protein, one gene, many functions. *Biochem J,* 344 Pt 2**,** 281-92.

MICHALAK, M., GROENENDYK, J., SZABO, E., GOLD, L. I. & OPAS, M. 2009. Calreticulin, a multi-process calcium-buffering chaperone of the endoplasmic reticulum. *Biochem J,* 417**,** 651-66.

MIDDELDORP, S., COPPENS, M., VAN HAAPS, T. F., FOPPEN, M., VLAAR, A. P., MÜLLER, M. C. A., BOUMAN, C. C. S., BEENEN, L. F. M., KOOTTE, R. S., HEIJMANS, J., SMITS, L. P., BONTA, P. I. & VAN ES, N. 2020. Incidence of venous thromboembolism in hospitalized patients with COVID-19. *J Thromb Haemost,* 18**,** 1995-2002.

MOEBIUS, J., ZAHEDI, R. P., LEWANDROWSKI, U., BERGER, C., WALTER, U. & SICKMANN, A. 2005. The human platelet membrane proteome reveals several new potential membrane proteins. *Mol Cell Proteomics,* 4**,** 1754-61.

MOLINS, B., PEÑA, E., PADRO, T., CASANI, L., MENDIETA, C. & BADIMON, L. 2010. Glucose-Regulated Protein 78 and Platelet Deposition. *Arteriosclerosis, Thrombosis, and Vascular Biology,* 30**,** 1246-1252.

MONNET, E. & FAUVEL-LAFÈVE, F. 2000. A New Platelet Receptor Specific to Type III Collagen: TYPE III COLLAGEN-BINDING PROTEIN *. *Journal of Biological Chemistry,* 275**,** 10912-10917.

MORITA, Y., ISEKI, A., OKAMURA, S., SUZUKI, S., NAKAUCHI, H. & EMA, H. 2011. Functional characterization of hematopoietic stem cells in the spleen. *Exp Hematol,* 39**,** 351-359.e3.

MOROI, M. & JUNG, S. M. 2004. Platelet glycoprotein VI: its structure and function. *Thromb Res,* 114**,** 221-33.

MOROI, M., JUNG, S. M., OKUMA, M. & SHINMYOZU, K. 1989. A patient with platelets deficient in glycoprotein VI that lack both collagen-induced aggregation and adhesion. *J Clin Invest,* 84**,** 1440-5.

MORTON, L. F., HARGREAVES, P. G., FARNDALE, R. W., YOUNG, R. D. & BARNES, M. J. 1995. Integrin alpha 2 beta 1-independent activation of platelets by simple collagen-like peptides: collagen tertiary (triple-helical) and quaternary (polymeric) structures are sufficient alone for alpha 2 beta 1-independent platelet reactivity. *Biochem J,* 306 (Pt 2)**,** 337-44.

MORTON, L. F., PEACHEY, A. R. & BARNES, M. J. 1989. Platelet-reactive sites in collagens type I and type III. Evidence for separate adhesion and aggregatory sites. *The Biochemical journal,* 258**,** 157-163.

MULLER, W. A. 2003. Leukocyte-endothelial-cell interactions in leukocyte transmigration and the inflammatory response. *Trends Immunol,* 24**,** 327-34.

MUNRO, S. & PELHAM, H. R. 1987. A C-terminal signal prevents secretion of luminal ER proteins. *Cell,* 48**,** 899-907.

MURILLO-SOLANO, C., DONG, C., SANCHEZ, C. G. & PIZARRO, J. C. 2017. Identification and characterization of the antiplasmodial activity of Hsp90 inhibitors. *Malaria journal,* 16**,** 292-292.

MYLLYHARJU, J. 2003. Prolyl 4-hydroxylases, the key enzymes of collagen biosynthesis. *Matrix Biol,* 22**,** 15-24.

NAGAI, N., HOSOKAWA, M., ITOHARA, S., ADACHI, E., MATSUSHITA, T., HOSOKAWA, N. & NAGATA, K. 2000. Embryonic lethality of molecular chaperone hsp47 knockout mice is associated with defects in collagen biosynthesis. *J Cell Biol,* 150**,** 1499-506.

NAGATA, K. 2003. HSP47 as a collagen-specific molecular chaperone: function and expression in normal mouse development. *Seminars in Cell & Developmental Biology,* 14**,** 275-282.

NAGATA, K., SAGA, S. & YAMADA, K. M. 1986. A major collagen-binding protein of chick embryo fibroblasts is a novel heat shock protein. *J Cell Biol,* 103**,** 223-9.

NAGY, Z., VÖGTLE, T., GEER, M. J., MORI, J., HEISING, S., DI NUNZIO, G., GAREUS, R., TARAKHOVSKY, A., WEISS, A., NEEL, B. G., DESANTI, G. E., MAZHARIAN, A. & SENIS, Y. A. 2019. The Gp1ba-Cre transgenic mouse: a new model to delineate platelet and leukocyte functions. *Blood,* 133**,** 331-343.

NAKEFF, A. & MAAT, B. 1974. Separation of megakaryocytes from mouse bone marrow by velocity sedimentation. *Blood,* 43**,** 591-5.

NANGALIA, J., MASSIE, C. E., BAXTER, E. J., NICE, F. L., GUNDEM, G., WEDGE, D. C., AVEZOV, E., LI, J., KOLLMANN, K., KENT, D. G., AZIZ, A., GODFREY, A. L., HINTON, J., MARTINCORENA, I., VAN LOO, P., JONES, A. V., GUGLIELMELLI, P., TARPEY, P., HARDING, H. P., FITZPATRICK, J. D., GOUDIE, C. T., ORTMANN, C. A., LOUGHRAN, S. J., RAINE, K., JONES, D. R., BUTLER, A. P., TEAGUE, J. W., O'MEARA, S., MCLAREN, S., BIANCHI, M., SILBER, Y., DIMITROPOULOU, D., BLOXHAM, D., MUDIE, L., MADDISON, M., ROBINSON, B., KEOHANE, C., MACLEAN, C., HILL, K., ORCHARD, K., TAURO, S., DU, M. Q., GREAVES, M., BOWEN, D., HUNTLY, B. J. P., HARRISON, C. N., CROSS, N. C. P., RON, D., VANNUCCHI, A. M., PAPAEMMANUIL, E., CAMPBELL, P. J. & GREEN, A. R. 2013. Somatic CALR mutations in myeloproliferative neoplasms with nonmutated JAK2. *N Engl J Med,* 369**,** 2391-2405.

NARUMIYA, S., SUGIMOTO, Y. & USHIKUBI, F. 1999. Prostanoid receptors: structures, properties, and functions. *Physiol Rev,* 79**,** 1193-226.

NAVI, B. B., REINER, A. S., KAMEL, H., IADECOLA, C., OKIN, P. M., ELKIND, M. S. V., PANAGEAS, K. S. & DEANGELIS, L. M. 2017. Risk of Arterial Thromboembolism in Patients With Cancer. *J Am Coll Cardiol,* 70**,** 926-938.

NEUMAN, R. E. & LOGAN, M. A. 1950. The determination of collagen and elastin in tissues. *J Biol Chem,* 186**,** 549-56.

NI, H., DENIS, C. V., SUBBARAO, S., DEGEN, J. L., SATO, T. N., HYNES, R. O. & WAGNER, D. D. 2000. Persistence of platelet thrombus formation in arterioles of mice lacking both von Willebrand factor and fibrinogen. *J Clin Invest,* 106**,** 385-92.

NIESWANDT, B., MOSER, M., PLEINES, I., VARGA-SZABO, D., MONKLEY, S., CRITCHLEY, D. & FASSLER, R. 2007. Loss of talin1 in platelets abrogates integrin activation, platelet aggregation, and thrombus formation in vitro and in vivo. *J Exp Med,* 204**,** 3113-8.

NIEUWENHUIS, H. K., AKKERMAN, J. W., HOUDIJK, W. P. & SIXMA, J. J. 1985. Human blood platelets showing no response to collagen fail to express surface glycoprotein Ia. *Nature,* 318**,** 470-2.

NIGAM, S. K., GOLDBERG, A. L., HO, S., ROHDE, M. F., BUSH, K. T. & SHERMAN, M. 1994. A set of endoplasmic reticulum proteins possessing properties of molecular chaperones includes Ca(2+)-binding proteins and members of the thioredoxin superfamily. *J Biol Chem,* 269**,** 1744-9.

NIIYA, K., HODSON, E., BADER, R., BYERS-WARD, V., KOZIOL, J. A., PLOW, E. F. & RUGGERI, Z. M. 1987. Increased surface expression of the membrane glycoprotein IIb/IIIa complex induced by platelet activation. Relationship to the binding of fibrinogen and platelet aggregation. *Blood,* 70**,** 475-83.

NUNES, D. P., LIMA, L. T., CHAUFFAILLE MDE, L., MITNE-NETO, M., SANTOS, M. T., CLIQUET, M. G. & GUERRA-SHINOHARA, E. M. 2015. CALR mutations screening in wild type

JAK2(V617F) and MPL(W515K/L) Brazilian myeloproliferative neoplasm patients. *Blood Cells Mol Dis,* 55**,** 236-40.

NURDEN, A. T. & PILLOIS, X. 2018. ITGA2B and ITGB3 gene mutations associated with Glanzmann thrombasthenia. *Platelets,* 29**,** 98-101.

NURDEN, P., STRITT, S., FAVIER, R. & NURDEN, A. T. 2021. Inherited platelet diseases with normal platelet count: phenotypes, genotypes and diagnostic strategy. *Haematologica,* 106**,** 337-350.

OHIGASHI, H., HASHIMOTO, D., HAYASE, E., TAKAHASHI, S., ARA, T., YAMAKAWA, T., SUGITA, J., ONOZAWA, M., NAKAGAWA, M. & TESHIMA, T. 2019. Ocular instillation of vitamin A-coupled liposomes containing HSP47 siRNA ameliorates dry eye syndrome in chronic GVHD. *Blood Adv,* 3**,** 1003-1010.

OLDEN, K., PRATT, R. M. & YAMADA, K. M. 1978. Role of carbohydrates in protein secretion and turnover: effects of tunicamycin on the major cell surface glycoprotein of chick embryo fibroblasts. *Cell,* 13**,** 461-73.

ONO, Y., WANG, Y., SUZUKI, H., OKAMOTO, S., IKEDA, Y., MURATA, M., PONCZ, M. & MATSUBARA, Y. 2012. Induction of functional platelets from mouse and human fibroblasts by p45NF-E2/Maf. *Blood,* 120**,** 3812-21.

ORCI, L., STAMNES, M., RAVAZZOLA, M., AMHERDT, M., PERRELET, A., SOLLNER, T. H. & ROTHMAN, J. E. 1997. Bidirectional transport by distinct populations of COPI-coated vesicles. *Cell,* 90**,** 335-49.

OSTOJIC, A., VRHOVAC, R. & VERSTOVSEK, S. 2012. Ruxolitinib for the treatment of myelofibrosis: its clinical potential. *Ther Clin Risk Manag,* 8**,** 95-103.

OTSUKA, M., SHIRATORI, M., CHIBA, H., KURONUMA, K., SATO, Y., NIITSU, Y. & TAKAHASHI, H. 2017. Treatment of pulmonary fibrosis with siRNA against a collagen-specific chaperone HSP47 in vitamin A-coupled liposomes. *Exp Lung Res,* 43**,** 271-282.

PALLOTTA, I., LOVETT, M., RICE, W., KAPLAN, D. L. & BALDUINI, A. 2009. Bone marrow osteoblastic niche: a new model to study physiological regulation of megakaryopoiesis. *PLoS One,* 4**,** e8359.

PALMA-BARQUEROS, V., REVILLA, N., SÁNCHEZ, A., ZAMORA CÁNOVAS, A., RODRIGUEZ-ALÉN, A., MARÍN-QUÍLEZ, A., GONZÁLEZ-PORRAS, J. R., VICENTE, V., LOZANO, M. L., BASTIDA, J. M. & RIVERA, J. 2021. Inherited Platelet Disorders: An Updated Overview. *International journal of molecular sciences,* 22**,** 4521.

PANARETAKIS, T., JOZA, N., MODJTAHEDI, N., TESNIERE, A., VITALE, I., DURCHSCHLAG, M., FIMIA, G. M., KEPP, O., PIACENTINI, M., FROEHLICH, K. U., VAN ENDERT, P., ZITVOGEL, L., MADEO, F. & KROEMER, G. 2008. The co-translocation of ERp57 and calreticulin determines the immunogenicity of cell death. *Cell Death & Differentiation,* 15**,** 1499-1509.

PAROUTIS, P., TOURET, N. & GRINSTEIN, S. 2004. The pH of the secretory pathway: measurement, determinants, and regulation. *Physiology (Bethesda),* 19**,** 207-15.

PASQUET, J. M., GROSS, B., QUEK, L., ASAZUMA, N., ZHANG, W., SOMMERS, C. L., SCHWEIGHOFFER, E., TYBULEWICZ, V., JUDD, B., LEE, J. R., KORETZKY, G., LOVE, P. E., SAMELSON, L. E. & WATSON, S. P. 1999. LAT is required for tyrosine phosphorylation of phospholipase cgamma2 and platelet activation by the collagen receptor GPVI. *Mol Cell Biol,* 19**,** 8326-34.

PASSAM, F. H., LIN, L., GOPAL, S., STOPA, J. D., BELLIDO-MARTIN, L., HUANG, M., FURIE, B. C. & FURIE, B. 2015. Both platelet- and endothelial cell-derived ERp5 support thrombus formation in a laser-induced mouse model of thrombosis. *Blood,* 125**,** 2276-85.

PATRONO, C., ROCCA, B. & DE STEFANO, V. 2013. Platelet activation and inhibition in polycythemia vera and essential thrombocythemia. *Blood,* 121**,** 1701-11.

PEARSON, D. S., KULYK, W. M., KELLY, G. M. & KRONE, P. H. 1996. Cloning and characterization of a cDNA encoding the collagen-binding stress protein hsp47 in zebrafish. *DNA Cell Biol,* 15**,** 263-72.

PERTUY, F., AGUILAR, A., STRASSEL, C., ECKLY, A., FREUND, J. N., DULUC, I., GACHET, C., LANZA, F. & LÉON, C. 2015. Broader expression of the mouse platelet factor 4-cre transgene beyond the megakaryocyte lineage. *J Thromb Haemost,* 13**,** 115-25.

PETERSON, J. R., ORA, A., VAN, P. N. & HELENIUS, A. 1995. Transient, lectin-like association of calreticulin with folding intermediates of cellular and viral glycoproteins. *Molecular biology of the cell,* 6**,** 1173-1184.

PETERSON, N. S., MOLLER, G. & MITCHELL, H. K. 1979. Genetic mapping of the coding regions for three heat-shock proteins in Drosophila melanogaster. *Genetics,* 92**,** 891-902.

PETRICH, B. G., MARCHESE, P., RUGGERI, Z. M., SPIESS, S., WEICHERT, R. A., YE, F., TIEDT, R., SKODA, R. C., MONKLEY, S. J., CRITCHLEY, D. R. & GINSBERG, M. H. 2007. Talin is required for integrin-mediated platelet function in hemostasis and thrombosis. *J Exp Med,* 204**,** 3103-11.

PFAFFENBACH, K. T. & LEE, A. S. 2011. The critical role of GRP78 in physiologic and pathologic stress. *Curr Opin Cell Biol,* 23**,** 150-6.

PIOTROWICZ, R. S., ORCHEKOWSKI, R. P., NUGENT, D. J., YAMADA, K. Y. & KUNICKI, T. J. 1988. Glycoprotein Ic-IIa functions as an activation-independent fibronectin receptor on human platelets. *J Cell Biol,* 106**,** 1359-64.

PIPER, P. W., MILLSON, S. H., MOLLAPOUR, M., PANARETOU, B., SILIGARDI, G., PEARL, L. H. & PRODROMOU, C. 2003. Sensitivity to Hsp90-targeting drugs can arise with mutation to the Hsp90 chaperone, cochaperones and plasma membrane ATP binding cassette transporters of yeast. *Eur J Biochem,* 270**,** 4689-95.

PUGH, N., JARVIS, G. E., KOCH, A., SAKARIASSEN, K. S., DAVIS, B. & FARNDALE, R. W. 2012. The impact of factor Xa inhibition on axial dependent arterial thrombus formation triggered by a tissue factor rich surface. *J Thromb Thrombolysis,* 33**,** 6-15.

QI, Y., ZHANG, Y., PENG, Z., WANG, L., WANG, K., FENG, D., HE, J. & ZHENG, J. 2018. SERPINH1 overexpression in clear cell renal cell carcinoma: association with poor clinical outcome and its potential as a novel prognostic marker. *J Cell Mol Med,* 22**,** 1224-1235.

RAYNAL, N., HAMAIA, S. W., SILJANDER, P. R. M., MADDOX, B., PEACHEY, A. R., FERNANDEZ, R., FOLEY, L. J., SLATTER, D. A., JARVIS, G. E. & FARNDALE, R. W. 2006. Use of Synthetic Peptides to Locate Novel Integrin α₂β₁-binding Motifs in Human Collagen III *. *Journal of Biological Chemistry,* 281**,** 3821-3831.

RAZZAQUE, M. S., HOSSAIN, M. A., KOHNO, S. & TAGUCHI, T. 1998a. Bleomycin-induced pulmonary fibrosis in rat is associated with increased expression of collagen-binding heat shock protein (HSP) 47. *Virchows Arch,* 432**,** 455-60.

RAZZAQUE, M. S., NAZNEEN, A. & TAGUCHI, T. 1998b. Immunolocalization of collagen and collagen-binding heat shock protein 47 in fibrotic lung diseases. *Mod Pathol,* 11**,** 1183-8.

RAZZAQUE, M. S., SHIMOKAWA, I., NAZNEEN, A., HIGAMI, Y. & TAGUCHI, T. 1998c. Age-related nephropathy in the Fischer 344 rat is associated with overexpression of collagens and collagen-binding heat shock protein 47. *Cell Tissue Res,* 293**,** 471-8.

REDDI, A. H., GAY, R., GAY, S. & MILLER, E. J. 1977. Transitions in collagen types during matrix-induced cartilage, bone, and bone marrow formation. *Proceedings of the National Academy of Sciences,* 74**,** 5589.

REINHARDT, C., VON BRÜHL, M. L., MANUKYAN, D., GRAHL, L., LORENZ, M., ALTMANN, B., DLUGAI, S., HESS, S., KONRAD, I., ORSCHIEDT, L., MACKMAN, N., RUDDOCK, L., MASSBERG, S. & ENGELMANN, B. 2008. Protein disulfide isomerase acts as an injury

response signal that enhances fibrin generation via tissue factor activation. *J Clin Invest,* 118**,** 1110-22.

ROBINSON, B. E., MCGRATH, H. E. & QUESENBERRY, P. J. 1987. Recombinant murine granulocyte macrophage colony-stimulating factor has megakaryocyte colony-stimulating activity and augments megakaryocyte colony stimulation by interleukin 3. *J Clin Invest,* 79**,** 1648-52.

RUGGERI, Z. M. 1997. Mechanisms initiating platelet thrombus formation. *Thromb Haemost,* 78**,** 611-6.

SABOOR, M., AYUB, Q., ILYAS, S. & MOINUDDIN 2013. Platelet receptors; an instrumental of platelet physiology. *Pakistan journal of medical sciences,* 29**,** 891-896.

SABRI, S., FOUDI, A., BOUKOUR, S., FRANC, B., CHARRIER, S., JANDROT-PERRUS, M., FARNDALE, R. W., JALIL, A., BLUNDELL, M. P., CRAMER, E. M., LOUACHE, F., DEBILI, N., THRASHER, A. J. & VAINCHENKER, W. 2006. Deficiency in the Wiskott-Aldrich protein induces premature proplatelet formation and platelet production in the bone marrow compartment. *Blood,* 108**,** 134-40.

SABRI, S., JANDROT-PERRUS, M., BERTOGLIO, J., FARNDALE, R. W., MAS, V. M., DEBILI, N. & VAINCHENKER, W. 2004. Differential regulation of actin stress fiber assembly and proplatelet formation by alpha2beta1 integrin and GPVI in human megakaryocytes. *Blood,* 104**,** 3117-25.

SAHLI, K. A., FLORA, G. D., SASIKUMAR, P., MAGHRABI, A. H., HOLBROOK, L. M., ALOUDA, S. K., ELGHEZNAWY, A., SAGE, T., STAINER, A. R., ADIYAMAN, R., ABOHASSAN, M., CRESCENTE, M., KRIEK, N., VAIYAPURI, S., BYE, A. P., UNSWORTH, A. J., JONES, C. I., MCGUFFIN, L. J. & GIBBINS, J. M. 2021. Structural, functional, and mechanistic insights uncover the fundamental role of orphan connexin-62 in platelets. *Blood,* 137**,** 830-843.

SAM, J. E. & DHARMALINGAM, M. 2017. Osteogenesis Imperfecta. *Indian journal of endocrinology and metabolism,* 21**,** 903-908.

SANTILLI, F., SIMEONE, P., LIANI, R. & DAVI, G. 2015. Platelets and diabetes mellitus. *Prostaglandins Other Lipid Mediat,* 120**,** 28-39.

SANTORO, S. A. 1986. Identification of a 160,000 dalton platelet membrane protein that mediates the initial divalent cation-dependent adhesion of platelets to collagen. *Cell,* 46**,** 913-20.

SASIKUMAR, P. 2015. *The Chaperone Protein HSP47: A Platelet Collagen Binding Protein that Contributes to Thrombosis and Haemostasis.* Doctor of Philosophy, University of Reading.

SASIKUMAR, P., ALOUDA, K. S., KAISER, W. J., HOLBROOK, L. M., KRIEK, N., UNSWORTH, J. A., BYE, A. P., SAGE, T., USHIODA, R., NAGATA, K., FARNDALE, R. W. & GIBBINS, J. M. 2018. The Chaperone Protein HSP47: A Platelet Collagen Binding Protein that Contributes to Thrombosis and Haemostasis. *J Thromb Haemost*.

SATOH, M., HIRAYOSHI, K., YOKOTA, S., HOSOKAWA, N. & NAGATA, K. 1996. Intracellular interaction of collagen-specific stress protein HSP47 with newly synthesized procollagen. *J Cell Biol,* 133**,** 469-83.

SCHAIFF, W. T., HRUSKA, K. A., JR., MCCOURT, D. W., GREEN, M. & SCHWARTZ, B. D. 1992. HLA-DR associates with specific stress proteins and is retained in the endoplasmic reticulum in invariant chain negative cells. *J Exp Med,* 176**,** 657-66.

SCHARF, R. E. 2018. Platelet Signaling in Primary Haemostasis and Arterial Thrombus Formation: Part 1. *Hamostaseologie,* 38**,** 203-210.

SCULLY, M., SINGH, D., LOWN, R., POLES, A., SOLOMON, T., LEVI, M., GOLDBLATT, D., KOTOUCEK, P., THOMAS, W. & LESTER, W. 2021. Pathologic Antibodies to Platelet Factor 4 after ChAdOx1 nCoV-19 Vaccination. *N Engl J Med,* 384**,** 2202-2211.

SENIS, Y. A., MAZHARIAN, A. & MORI, J. 2014. Src family kinases: at the forefront of platelet activation. *Blood,* 124**,** 2013-24.

SHIRAVI, A. A., ARDEKANI, A., SHEIKHBAHAEI, E. & HESHMAT-GHAHDARIJANI, K. 2021. Cardiovascular Complications of SARS-CoV-2 Vaccines: An Overview. *Cardiol Ther*, 1-9.

SIXMA, J. J., SLOT, J. W. & GEUZE, H. J. 1989. Immunocytochemical localization of platelet granule proteins. *Methods Enzymol,* 169**,** 301-11.

SMYTH, S. S., WHITEHEART, S., ITALIANO, J. E., BRAY, P. & COLLER, B. S. 2015. Platelet Morphology, Biochemistry, and Function. *In:* KAUSHANSKY, K., LICHTMAN, M. A., PRCHAL, J. T., LEVI, M. M., PRESS, O. W., BURNS, L. J. & CALIGIURI, M. (eds.) *Williams Hematology, 9e.* New York, NY: McGraw-Hill Education.

SOLAR, G. P., KERR, W. G., ZEIGLER, F. C., HESS, D., DONAHUE, C., DE SAUVAGE, F. J. & EATON, D. L. 1998. Role of c-mpl in early hematopoiesis. *Blood,* 92**,** 4-10.

SONG, X., LIAO, Z., ZHOU, C., LIN, R., LU, J., CAI, L., TAN, X., ZENG, W., LU, X., ZHENG, W., CHEN, J. & SU, Z. 2017. HSP47 is associated with the prognosis of laryngeal squamous cell carcinoma by inhibiting cell viability and invasion and promoting apoptosis. *Oncol Rep,* 38**,** 2444-2452.

SPANGRUDE, G. J., HEIMFELD, S. & WEISSMAN, I. L. 1988. Purification and characterization of mouse hematopoietic stem cells. *Science,* 241**,** 58-62.

STAATZ, W. D., RAJPARA, S. M., WAYNER, E. A., CARTER, W. G. & SANTORO, S. A. 1989. The membrane glycoprotein Ia-IIa (VLA-2) complex mediates the Mg++-dependent adhesion of platelets to collagen. *J Cell Biol,* 108**,** 1917-24.

STARON, M., WU, S., HONG, F., STOJANOVIC, A., DU, X., BONA, R., LIU, B. & LI, Z. 2011. Heat-shock protein gp96/grp94 is an essential chaperone for the platelet glycoprotein Ib-IX-V complex. *Blood,* 117**,** 7136-44.

STRASSEL, C., ECKLY, A., LÉON, C., MOOG, S., CAZENAVE, J. P., GACHET, C. & LANZA, F. 2012. Hirudin and heparin enable efficient megakaryocyte differentiation of mouse bone marrow progenitors. *Exp Cell Res,* 318**,** 25-32.

STRITT, S., WOLF, K., LORENZ, V., VÖGTLE, T., GUPTA, S., BÖSL, M. R. & NIESWANDT, B. 2015. Rap1-GTP-interacting adaptor molecule (RIAM) is dispensable for platelet integrin activation and function in mice. *Blood,* 125**,** 219-22.

SUN, Y., CHEN, W.-L., LIN, S.-J., JEE, S.-H., CHEN, Y.-F., LIN, L.-C., SO, P. T. C. & DONG, C.-Y. 2006. Investigating Mechanisms of Collagen Thermal Denaturation by High Resolution Second-Harmonic Generation Imaging. *Biophysical Journal,* 91**,** 2620-2625.

SUZUKI-INOUE, K., INOUE, O., FRAMPTON, J. & WATSON, S. P. 2003. Murine GPVI stimulates weak integrin activation in PLCgamma2-/- platelets: involvement of PLCgamma1 and PI3-kinase. *Blood,* 102**,** 1367-73.

SUZUKI-INOUE, K., TULASNE, D., SHEN, Y., BORI-SANZ, T., INOUE, O., JUNG, S. M., MOROI, M., ANDREWS, R. K., BERNDT, M. C. & WATSON, S. P. 2002. Association of Fyn and Lyn with the proline-rich domain of glycoprotein VI regulates intracellular signaling. *J Biol Chem,* 277**,** 21561-6.

SUZUKI-INOUE, K., YATOMI, Y., ASAZUMA, N., KAINOH, M., TANAKA, T., SATOH, K. & OZAKI, Y. 2001. Rac, a small guanosine triphosphate-binding protein, and p21-activated kinase are activated during platelet spreading on collagen-coated surfaces: roles of integrin alpha(2)beta(1). *Blood,* 98**,** 3708-16.

SZALAI, G., LARUE, A. C. & WATSON, D. K. 2006. Molecular mechanisms of megakaryopoiesis. *Cellular and Molecular Life Sciences CMLS,* 63**,** 2460-2476.

TABAS, I., WILLIAMS, K. J. & BORÉN, J. 2007. Subendothelial lipoprotein retention as the initiating process in atherosclerosis: update and therapeutic implications. *Circulation,* 116**,** 1832-44.

TABLIN, F., CASTRO, M. & LEVEN, R. M. 1990. Blood platelet formation in vitro. The role of the cytoskeleton in megakaryocyte fragmentation. *J Cell Sci,* 97 (Pt 1)**,** 59-70.

TAKAYAMA, N., NISHIKII, H., USUI, J., TSUKUI, H., SAWAGUCHI, A., HIROYAMA, T., ETO, K. & NAKAUCHI, H. 2008. Generation of functional platelets from human embryonic stem

cells in vitro via ES-sacs, VEGF-promoted structures that concentrate hematopoietic progenitors. *Blood,* 111**,** 5298-306.

TANG, N., LI, D., WANG, X. & SUN, Z. 2020. Abnormal coagulation parameters are associated with poor prognosis in patients with novel coronavirus pneumonia. *J Thromb Haemost,* 18**,** 844-847.

TASAB, M., JENKINSON, L. & BULLEID, N. J. 2002. Sequence-specific recognition of collagen triple helices by the collagen-specific molecular chaperone HSP47. *J Biol Chem,* 277**,** 35007-12.

THON, J. N. & ITALIANO, J. E. 2012. Platelets: production, morphology and ultrastructure. *Handb Exp Pharmacol***,** 3-22.

THON, J. N., MONTALVO, A., PATEL-HETT, S., DEVINE, M. T., RICHARDSON, J. L., EHRLICHER, A., LARSON, M. K., HOFFMEISTER, K., HARTWIG, J. H. & ITALIANO, J. E., JR. 2010. Cytoskeletal mechanics of proplatelet maturation and platelet release. *J Cell Biol,* 191**,** 861-74.

THON, J. N., PETERS, C. G., MACHLUS, K. R., ASLAM, R., ROWLEY, J., MACLEOD, H., DEVINE, M. T., FUCHS, T. A., WEYRICH, A. S., SEMPLE, J. W., FLAUMENHAFT, R. & ITALIANO, J. E., JR. 2012. T granules in human platelets function in TLR9 organization and signaling. *J Cell Biol,* 198**,** 561-74.

TIEDT, R., SCHOMBER, T., HAO-SHEN, H. & SKODA, R. C. 2006. Pf4-Cre transgenic mice allow the generation of lineage-restricted gene knockouts for studying megakaryocyte and platelet function in vivo. *Blood,* 109**,** 1503-1506.

TIMCHENKO, L. T., SALISBURY, E., WANG, G. L., NGUYEN, H., ALBRECHT, J. H., HERSHEY, J. W. & TIMCHENKO, N. A. 2006. Age-specific CUGBP1-eIF2 complex increases translation of CCAAT/enhancer-binding protein beta in old liver. *J Biol Chem,* 281**,** 32806-19.

TRAVLOS, G. S. 2006. Normal structure, function, and histology of the bone marrow. *Toxicol Pathol,* 34**,** 548-65.

UNSWORTH, A. J., BYE, A. P., KRIEK, N., SAGE, T., OSBORNE, A. A., DONAGHY, D. & GIBBINS, J. M. 2019. Cobimetinib and trametinib inhibit platelet MEK but do not cause platelet dysfunction. *Platelets,* 30**,** 762-772.

VAN, P. N., PETER, F. & SOLING, H. D. 1989. Four intracisternal calcium-binding glycoproteins from rat liver microsomes with high affinity for calcium. No indication for calsequestrin-like proteins in inositol 1,4,5-trisphosphate-sensitive calcium sequestering rat liver vesicles. *J Biol Chem,* 264**,** 17494-501.

VARGA-SZABO, D., BRAUN, A. & NIESWANDT, B. 2009. Calcium signaling in platelets. *J Thromb Haemost,* 7**,** 1057-66.

VARRICCHIO, L., FALCHI, M., DALL'ORA, M., DE BENEDITTIS, C., RUGGERI, A., UVERSKY, V. N. & MIGLIACCIO, A. R. 2017. Calreticulin: Challenges Posed by the Intrinsically Disordered Nature of Calreticulin to the Study of Its Function. *Frontiers in Cell and Developmental Biology,* 5.

VASUDEVAN, S., ROBERTS, J. R., MCCLINTOCK, R. A., DENT, J. A., CELIKEL, R., WARE, J., VARUGHESE, K. I. & RUGGERI, Z. M. 2000. Modeling and functional analysis of the interaction between von Willebrand factor A1 domain and glycoprotein Ibalpha. *J Biol Chem,* 275**,** 12763-8.

VERA, R. H., VILAHUR, G., FERRER-LORENTE, R., PEÑA, E. & BADIMON, L. 2012. Platelets Derived From the Bone Marrow of Diabetic Animals Show Dysregulated Endoplasmic Reticulum Stress Proteins That Contribute to Increased Thrombosis. *Arteriosclerosis, Thrombosis, and Vascular Biology,* 32**,** 2141-2148.

VIGH, L., NAKAMOTO, H., LANDRY, J., GOMEZ-MUNOZ, A., HARWOOD, J. L. & HORVATH, I. 2007. Membrane regulation of the stress response from prokaryotic models to mammalian cells. *Ann N Y Acad Sci,* 1113**,** 40-51.

VON HUNDELSHAUSEN, P., LORENZ, R., SIESS, W. & WEBER, C. 2021. Vaccine-Induced Immune Thrombotic Thrombocytopenia (VITT): Targeting Pathomechanisms with Bruton Tyrosine Kinase Inhibitors. *Thromb Haemost,* 121**,** 1395-1399.

VON HUNDELSHAUSEN, P. & WEBER, C. 2007. Platelets as immune cells: bridging inflammation and cardiovascular disease. *Circ Res,* 100**,** 27-40.

VOYSEY, M., CLEMENS, S. A. C., MADHI, S. A., WECKX, L. Y., FOLEGATTI, P. M., ALEY, P. K., ANGUS, B., BAILLIE, V. L., BARNABAS, S. L., BHORAT, Q. E., BIBI, S., BRINER, C., CICCONI, P., COLLINS, A. M., COLIN-JONES, R., CUTLAND, C. L., DARTON, T. C., DHEDA, K., DUNCAN, C. J. A., EMARY, K. R. W., EWER, K. J., FAIRLIE, L., FAUST, S. N., FENG, S., FERREIRA, D. M., FINN, A., GOODMAN, A. L., GREEN, C. M., GREEN, C. A., HEATH, P. T., HILL, C., HILL, H., HIRSCH, I., HODGSON, S. H. C., IZU, A., JACKSON, S., JENKIN, D., JOE, C. C. D., KERRIDGE, S., KOEN, A., KWATRA, G., LAZARUS, R., LAWRIE, A. M., LELLIOTT, A., LIBRI, V., LILLIE, P. J., MALLORY, R., MENDES, A. V. A., MILAN, E. P., MINASSIAN, A. M., MCGREGOR, A., MORRISON, H., MUJADIDI, Y. F., NANA, A., O'REILLY, P. J., PADAYACHEE, S. D., PITTELLA, A., PLESTED, E., POLLOCK, K. M., RAMASAMY, M. N., RHEAD, S., SCHWARZBOLD, A. V., SINGH, N., SMITH, A., SONG, R., SNAPE, M. D., SPRINZ, E., SUTHERLAND, R. K., TARRANT, R., THOMSON, E. C., TÖRÖK, M. E., TOSHNER, M., TURNER, D. P. J., VEKEMANS, J., VILLAFANA, T. L., WATSON, M. E. E., WILLIAMS, C. J., DOUGLAS, A. D., HILL, A. V. S., LAMBE, T., GILBERT, S. C. & POLLARD, A. J. 2021. Safety and efficacy of the ChAdOx1 nCoV-19 vaccine (AZD1222) against SARS-CoV-2: an interim analysis of four randomised controlled trials in Brazil, South Africa, and the UK. *Lancet,* 397**,** 99-111.

WANDERLING, S., SIMEN, B. B., OSTROVSKY, O., AHMED, N. T., VOGEN, S. M., GIDALEVITZ, T. & ARGON, Y. 2007. GRP94 is essential for mesoderm induction and muscle development because it regulates insulin-like growth factor secretion. *Mol Biol Cell,* 18**,** 3764-75.

WANG, M., WEY, S., ZHANG, Y., YE, R. & LEE, A. S. 2009. Role of the unfolded protein response regulator GRP78/BiP in development, cancer, and neurological disorders. *Antioxid Redox Signal,* 11**,** 2307-16.

WANG, W. A., GROENENDYK, J. & MICHALAK, M. 2012. Calreticulin signaling in health and disease. *Int J Biochem Cell Biol,* 44**,** 842-6.

WATKINS, N. A., GUSNANTO, A., DE BONO, B., DE, S., MIRANDA-SAAVEDRA, D., HARDIE, D. L., ANGENENT, W. G., ATTWOOD, A. P., ELLIS, P. D., ERBER, W., FOAD, N. S., GARNER, S. F., ISACKE, C. M., JOLLEY, J., KOCH, K., MACAULAY, I. C., MORLEY, S. L., RENDON, A., RICE, K. M., TAYLOR, N., THIJSSEN-TIMMER, D. C., TIJSSEN, M. R., VAN DER SCHOOT, C. E., WERNISCH, L., WINZER, T., DUDBRIDGE, F., BUCKLEY, C. D., LANGFORD, C. F., TEICHMANN, S., GÖTTGENS, B. & OUWEHAND, W. H. 2009. A HaemAtlas: characterizing gene expression in differentiated human blood cells. *Blood,* 113**,** e1-9.

WATSON, S. P., AUGER, J. M., MCCARTY, O. J. & PEARCE, A. C. 2005. GPVI and integrin alphaIIb beta3 signaling in platelets. *J Thromb Haemost,* 3**,** 1752-62.

WEISS, L. & GEDULDIG, U. 1991. Barrier cells: stromal regulation of hematopoiesis and blood cell release in normal and stressed murine bone marrow. *Blood,* 78**,** 975-90.

WELCH, W. J. & SUHAN, J. P. 1985. Morphological study of the mammalian stress response: characterization of changes in cytoplasmic organelles, cytoskeleton, and nucleoli, and appearance of intranuclear actin filaments in rat fibroblasts after heat-shock treatment. *J Cell Biol,* 101**,** 1198-211.

WHITE, J. G. 1969. The submembrane filaments of blood platelets. *Am J Pathol,* 56**,** 267-77.

WHITE, J. G. 2005. Platelets are covercytes, not phagocytes: uptake of bacteria involves channels of the open canalicular system. *Platelets,* 16**,** 121-31.

WHITE, J. G. 2008. Electron opaque structures in human platelets: which are or are not dense bodies? *Platelets,* 19**,** 455-66.

WHITE, J. G. & KRUMWIEDE, M. 1987. Further studies of the secretory pathway in thrombin-stimulated human platelets. *Blood,* 69**,** 1196-203.

WHITE, J. G., KRUMWIEDE, M. D., JOHNSON, D. K. & ESCOLAR, G. 1995. Localization of GPIb/IX and GPIIb/IIIa on Discoid Platelets. *Platelets,* 6**,** 233-41.

WILKINS, B. S., ERBER, W. N., BAREFORD, D., BUCK, G., WHEATLEY, K., EAST, C. L., PAUL, B., HARRISON, C. N., GREEN, A. R. & CAMPBELL, P. J. 2008. Bone marrow pathology in essential thrombocythemia: interobserver reliability and utility for identifying disease subtypes. *Blood,* 111**,** 60-70.

WILKINS, M. R., GASTEIGER, E., GOOLEY, A. A., HERBERT, B. R., MOLLOY, M. P., BINZ, P. A., OU, K., SANCHEZ, J. C., BAIROCH, A., WILLIAMS, K. L. & HOCHSTRASSER, D. F. 1999. High-throughput mass spectrometric discovery of protein post-translational modifications. *J Mol Biol,* 289**,** 645-57.

WILSON, D. W., LEWIS, M. J. & PELHAM, H. R. 1993. pH-dependent binding of KDEL to its receptor in vitro. *J Biol Chem,* 268**,** 7465-8.

WILSON, R., LEES, J. F. & BULLEID, N. J. 1998. Protein disulfide isomerase acts as a molecular chaperone during the assembly of procollagen. *J Biol Chem,* 273**,** 9637-43.

WRIGHT, N. T. & HUMPHREY, J. D. 2002. Denaturation of Collagen Via Heating: An Irreversible Rate Process. *Annual Review of Biomedical Engineering,* 4**,** 109-128.

WU, C. T., WANG, W. C., CHEN, M. F., SU, H. Y., CHEN, W. Y., WU, C. H., CHANG, Y. J. & LIU, H. H. 2014. Glucose-regulated protein 78 mediates hormone-independent prostate cancer progression and metastasis through maspin and COX-2 expression. *Tumour Biol,* 35**,** 195-204.

WU, Y., AHMAD, S. S., ZHOU, J., WANG, L., CULLY, M. P. & ESSEX, D. W. 2012a. The disulfide isomerase ERp57 mediates platelet aggregation, hemostasis, and thrombosis. *Blood,* 119**,** 1737-46.

WU, Y., AHMAD, S. S., ZHOU, J., WANG, L., CULLY, M. P. & ESSEX, D. W. 2012b. The disulfide isomerase ERp57 mediates platelet aggregation, hemostasis, and thrombosis. *Blood.* Washington, DC.

XIE, S. Y., WU, Q. Q., LIU, C., DENG, W. & TANG, Q. Z. 2020. [The effect and mechanism of heat shock protein 47 on streptozotocin-induced diabetic cardiomyopathy]. *Zhonghua Yi Xue Za Zhi,* 100**,** 430-436.

XIONG, G., CHEN, J., ZHANG, G., WANG, S., KAWASAKI, K., ZHU, J., ZHANG, Y., NAGATA, K., LI, Z., ZHOU, B. P. & XU, R. 2020. Hsp47 promotes cancer metastasis by enhancing collagen-dependent cancer cell-platelet interaction. *Proc Natl Acad Sci U S A,* 117**,** 3748-3758.

YAMADA, Y., SUGAWARA, S., ARAI, T., KOJIMA, S., KATO, M., OKATO, A., YAMAZAKI, K., NAYA, Y., ICHIKAWA, T. & SEKI, N. 2018. Molecular pathogenesis of renal cell carcinoma: Impact of the anti-tumor miR-29 family on gene regulation. *Int J Urol,* 25**,** 953-965.

YAMAKAWA, T., OHIGASHI, H., HASHIMOTO, D., HAYASE, E., TAKAHASHI, S., MIYAZAKI, M., MINOMI, K., ONOZAWA, M., NIITSU, Y. & TESHIMA, T. 2018. Vitamin A-coupled liposomes containing siRNA against HSP47 ameliorate skin fibrosis in chronic graft-versus-host disease. *Blood,* 131**,** 1476-1485.

YAMANE, M., OGAWA, Y., MUKAI, S., YAGUCHI, S., KAMIJUKU, H., INABA, T., ASAI, K., MORIKAWA, S., KAWAKAMI, Y., SHIMMURA, S. & TSUBOTA, K. 2018. Functional Role of Lacrimal Gland Fibroblasts in a Mouse Model of Chronic Graft-Versus-Host Disease. *Cornea,* 37**,** 102-108.

YANG, Y., LIU, B., DAI, J., SRIVASTAVA, P. K., ZAMMIT, D. J., LEFRANCOIS, L. & LI, Z. 2007. Heat shock protein gp96 is a master chaperone for toll-like receptors and is important in the innate function of macrophages. *Immunity,* 26**,** 215-26.

YEAMAN, M. R. 1997. The role of platelets in antimicrobial host defense. *Clin Infect Dis,* 25**,** 951-68; quiz 969-70.

YONEDA, A., SAKAI-SAWADA, K., MINOMI, K. & TAMURA, Y. 2020. Heat Shock Protein 47 Maintains Cancer Cell Growth by Inhibiting the Unfolded Protein Response Transducer IRE1alpha. *Mol Cancer Res*.

YUE, B. 2014. Biology of the extracellular matrix: an overview. *Journal of glaucoma,* 23**,** S20-S23.

ZAHR, A. A., SALAMA, M. E., CARREAU, N., TREMBLAY, D., VERSTOVSEK, S., MESA, R., HOFFMAN, R. & MASCARENHAS, J. 2016. Bone marrow fibrosis in myelofibrosis: pathogenesis, prognosis and targeted strategies. *Haematologica,* 101**,** 660-671.

ZHANG, J., JIANG, Y., JIA, Z., LI, Q., GONG, W., WANG, L., WEI, D., YAO, J., FANG, S. & XIE, K. 2006. Association of elevated GRP78 expression with increased lymph node metastasis and poor prognosis in patients with gastric cancer. *Clin Exp Metastasis,* 23**,** 401-10.

ZHU, H., CAO, X., CAI, X., TIAN, Y., WANG, D., QI, J., TENG, Z., LU, G., NI, Q., WANG, S. & ZHANG, L. 2020. Pifithrin-μ incorporated in gold nanoparticle amplifies pro-apoptotic unfolded protein response cascades to potentiate synergistic glioblastoma therapy. *Biomaterials,* 232**,** 119677.

ZIMMET, J. & RAVID, K. 2000. Polyploidy: occurrence in nature, mechanisms, and significance for the megakaryocyte-platelet system. *Exp Hematol,* 28**,** 3-16.

ZOU, Z., SCHMAIER, A. A., CHENG, L., MERICKO, P., DICKESON, S. K., STRICKER, T. P., SANTORO, S. A. & KAHN, M. L. 2009. Negative regulation of activated alpha-2 integrins during thrombopoiesis. *Blood,* 113**,** 6428-39.

ZUTTER, M. M. & SANTORO, S. A. 1990. Widespread histologic distribution of the alpha 2 beta 1 integrin cell-surface collagen receptor. *Am J Pathol,* 137**,** 113-20.